

# Molecular dissection of Pax6 DNA-binding domains and their roles in mouse cerebral cortex development

Dissertation der Fakultät für Biologie der  
Ludwig-Maximilian-Universität München



Angefertigt in der Arbeitsgruppe von Prof. Dr. Magdalena  
Götz am Institut für Stammzellforschung, Helmholtz Zentrum  
München

Tessa Walcher  
05.09.2012

Einreichung der Dissertation bei der Fakultät für Biologie: 05. September 2012

Tag der mündlichen Prüfung (Disputation): 31. Januar 2013

1. Gutachter: Prof. Heinrich Leonhardt
2. Gutachter: PD. Dr. Mario Wullimann
3. Gutachter: Prof. Barbara Conradt
4. Gutachter: PD Dr. Katrin Philippar (Protokoll)
5. Gast: Prof. Magdalena Götz

## Eidesstattliche Erklärung

Ich versichere hiermit an Eides statt, dass die vorgelegte Dissertation von mir selbständig und ohne unerlaubte Hilfe angefertigt ist.

München, den .....

.....  
(Unterschrift)



## Table of Contents

Table of Contents.....	I
Abstract.....	1
Zusammenfassung.....	3
<b>1 Introduction.....</b>	<b>5</b>
1.1 Early brain development – generation of the cerebral cortex.....	6
1.2 Generation of cell diversity in the cerebral cortex.....	10
1.2.1 Neural stem and progenitor cells in the developing telencephalon.....	10
1.2.2 Neuronal cell diversity forming the six layers of the cerebral cortex.....	14
1.2.3 Molecular fate determinants in cortical development.....	15
1.2.3.1 <i>Extrinsic cues</i> .....	16
1.2.3.2 <i>Intrinsic cues</i> .....	11
1.3 The transcription factor Pax6 – a master regulator.....	20
1.3.1 Pax6 Expression.....	20
1.3.2 The role of Pax6 in forebrain development.....	22
1.3.2.1 <i>Pax6 function in dorso-ventral patterning</i> .....	22
1.3.2.2 <i>Pax6 function in area patterning</i> .....	23
1.3.2.3 <i>Pax6 function in the olfactory system</i> .....	24
1.3.2.4 <i>Pax6 function in proliferation and neurogenesis</i> .....	25
1.3.3 Complexity of Pax6 – structure and isoforms.....	27
1.3.4 Molecular mechanisms underlying the multiple functions of Pax6.....	31
1.4 A fate determinant from the RNA world: the microRNA.....	33
1.4.1 The microRNA pathway.....	33
1.4.2 The role of microRNAs in the developing nervous system.....	34
1.4.3 MicroRNAs in embryonic stem cells.....	37
1.5 Aim of the thesis.....	38
<b>2 Results.....</b>	<b>39</b>
2.1 Relevance of the Pax6 homeodomain during cortical development.....	39
2.1.1 Gene expression analysis of the homeodomain mutant Pax6 <sup>4NEU</sup> during forebrain development.....	39
2.2 Functional dissection of the paired-domain of Pax6 during cortical development.....	42
2.2.1 Gross phenotypical differences of Pax6 <sup>Leca4</sup> (PAI-domain) and Pax6 <sup>Leca2</sup> (RED-domain) mutant mice.....	42

2.2.1.3	<i>Pax6<sup>Leca2</sup>, but not Pax6<sup>Leca4</sup> mice survive into adulthood.....</i>	44
2.2.1.2	<i>Pax6<sup>Leca4</sup> and Pax6<sup>Leca2</sup> mice exhibit no ‘olfactory bulb-like structure (OBLS)’.....</i>	45
2.2.1.3	<i>Pax6<sup>Leca2</sup> mutants lack TH+ interneurons in the adult olfactory bulb... </i>	45
<b>2.2.2</b>	<b>Telencephalic development in Pax6<sup>Leca4</sup> (PAI-domain) and Pax6<sup>Leca2</sup> (RED-domain) mutant mice.....</b>	<b>48</b>
<b>2.2.3</b>	<b>Progenitor proliferation is differently affected in the cerebral cortex of Pax6<sup>Leca4</sup> (PAI domain) and Pax6<sup>Leca2</sup> (RED domain) mutant mice.....</b>	<b>51</b>
2.2.3.1	<i>Progenitor identity in Pax6<sup>Leca4</sup> and Pax6<sup>Leca2</sup> mutant mice.....</i>	54
<b>2.2.4</b>	<b>The role of the PAI and the RED subdomain in dorso-ventral patterning of the telencephalon.....</b>	<b>56</b>
2.2.4.1	<i>Molecular specification in Pax6<sup>Sey</sup>/Gsx2 double mutants.....</i>	63
<b>2.2.5</b>	<b>The role of the PAI and the RED subdomain in the regulation of neurogenesis.....</b>	<b>65</b>
2.2.5.1	<i>Effect of Pax6<sup>Leca4</sup> and Pax6<sup>Leca2</sup> mutation on neurogenesis in-vitro....</i>	68
<b>2.2.6</b>	<b>Cell death analysis in the Pax6<sup>Leca2</sup> and Pax6<sup>Leca4</sup> mutant cortex at midneurogenesis .....</b>	<b>72</b>
<b>2.2.7</b>	<b>Genome-wide expression analysis in the Pax6<sup>Leca4</sup> (PAI domain) and Pax6<sup>Leca2</sup> (RED domain) mutant cerebral cortex.....</b>	<b>74</b>
2.2.7.1	<i>Differentially expressed genes in the Pax6<sup>Leca4</sup> mutant cortex.....</i>	76
2.2.7.2	<i>Differentially expressed genes in the Pax6<sup>Leca2</sup> mutant cortex.....</i>	77
2.2.7.3	<i>Comparison of differentially expressed genes between the Pax6<sup>Leca4</sup> and Pax6<sup>Leca2</sup> mutant cortex.....</i>	77
2.2.7.4	<i>Comparison of differentially expressed genes between the Pax6 Leca mutant cortices and the functional Pax6 null mutant Pax6<sup>Sey</sup>.....</i>	78
2.2.7.5	<i>Comparison of the differentially expressed genes in the Pax6 Leca mutant cortices and Pax6-Chip data</i>	
<b>2.2.8</b>	<b>Superactivation by the RED domain mutation of Pax6.....</b>	<b>80</b>
<b>2.3</b>	<b>Fate determinants at post-transcriptional level: microRNA expression during neuronal differentiation.....</b>	<b>82</b>
<b>2.3.1</b>	<b>The screening system: in-vitro differentiation from ESC to glutamatergic neurons.....</b>	<b>82</b>
<b>2.3.2</b>	<b>Differentially expressed microRNAs during differentiation.....</b>	<b>84</b>

---

<b>3</b>	<b>Discussion.....</b>	<b>87</b>
3.1	Summary.....	87
3.2	The paired subdomains - PAI and RED - of Pax6 are crucial for Pax6 function and show selective roles during cortical development.....	88
3.2.1	The PAI and the RED subdomain of Pax6 regulate dorso-ventral patterning in a redundant manner.....	88
3.2.2	The PAI and the RED subdomains of Pax6 exert distinct and opposing functions on progenitor proliferation.....	90
3.2.3	The PAI subdomain of Pax6 is responsible for its neurogenic function....	93
3.2.4	The Leca mutations in the PAI and the RED subdomain of Pax6 affect its function through distinct binding sites.....	96
3.2.5	The Leca mutation in the RED subdomain of Pax6 leads to enhanced transcriptional activation in vitro.....	99
3.3	The role of the homeodomain and region-specific differences of the function of the different DNA-binding domains of Pax6.....	100
3.4	Identification of new microRNA candidates during neuronal differentiation..	102
<b>4</b>	<b>Material and Methods.....</b>	<b>104</b>
4.1	Materials.....	104
4.1.1	Chemicals.....	104
4.1.2	Kits.....	105
4.1.3	Culture reagents and media.....	105
4.1.3.1	General tissue culture reagents.....	105
4.1.3.2	Embryonic stem cell culture reagents.....	106
4.1.4	Cell lines.....	108
4.1.5	Cloning and expression plasmids.....	108
4.1.6	Primary antibodies.....	109
4.1.7	Primers used for q-PCR analysis.....	110
4.1.8	General Buffers and Solutions.....	111
4.2	Methods.....	112
4.2.1	Animals and genotyping.....	112
4.2.1.1	Animals.....	112
4.2.1.2	Mouse tail DNA extraction.....	112
4.2.1.3	PCR Genotyping.....	113

4.2.1.4	<i>Sequencing</i> .....	114
4.2.1.5	<i>Fixation of mouse brains and cryosectioning</i> .....	114
<b>4.2.2</b>	<b>Immunostainings</b> .....	<b>115</b>
<b>4.2.3</b>	<b>In situ hybridization - mRNA</b> .....	<b>116</b>
<b>4.2.4</b>	<b>In situ hybridization - microRNA</b> .....	<b>117</b>
<b>4.2.5</b>	<b>Molecular Biology</b> .....	<b>118</b>
4.2.5.1	<i>Cloning of constructs</i> .....	118
4.2.5.2	<i>Transformation into chemically competent E.coli</i> .....	118
4.2.5.3	<i>Bacterial liquid cultures and DNA purification</i> .....	118
4.2.5.4	<i>Restriction digestion of DNA</i> .....	119
4.2.5.5	<i>Ligation</i> .....	119
<b>4.2.6</b>	<b>Cell Culture</b> .....	<b>119</b>
4.2.6.1	<i>Preparation of primary embryonic cerebral cortical cell culture</i> .....	119
4.2.6.2	<i>Clonal analysis in primary culture</i> .....	120
4.2.6.3	<i>Dual-luciferase reporter assay</i> .....	120
<b>4.2.7</b>	<b>Embryonic stem cell differentiation culture protocol</b> .....	<b>120</b>
<b>4.2.8</b>	<b>RNA isolation and microarray analysis</b> .....	<b>121</b>
<b>4.2.9</b>	<b>MicroRNA extraction and miRNA-array analysis</b> .....	<b>122</b>
<b>4.2.10</b>	<b>CDNA synthesis and quantative pcr analysis</b> .....	<b>123</b>
<b>4.2.11</b>	<b>Data analysis</b> .....	<b>123</b>
4.2.11.1	<i>Statistics</i> .....	124
<b>5</b>	<b>Appendix</b> .....	<b>125</b>
5.1	<b>Abbreviations</b> .....	<b>125</b>
5.2	<b>Tables</b> .....	<b>126</b>
<b>6</b>	<b>References</b> .....	<b>146</b>
<b>7</b>	<b>Acknowledgments</b> .....	<b>166</b>
	<b>Publications</b> .....	<b>167</b>

## Abstract

Generation of the brain depends on proper regulation of progenitor proliferation and differentiation during development. Many such factors known to affect proliferation and differentiation are transcription factors. In particular, the transcription factor Pax6 has received much attention because of its potency to control various aspects of brain development. During development of the telencephalon Pax6 regulates patterning, cell proliferation and neurogenesis, but how Pax6 mediates and coordinates these diverse functions at the molecular level is not well understood. It has previously been demonstrated that the homeodomain of Pax6 plays a role in establishing the pallial-subpallial boundary. However it is not involved in other processes during telencephalic development as shown by the analysis of Pax6<sup>4NEU</sup> mice, which are characterized by a point-mutation in the DNA-binding helix of the homeodomain. In order to gain more insights into the molecular network underlying the mild homeodomain function in the developing telencephalon, transcriptome analysis with Pax6<sup>4NEU</sup> mice was performed. Almost no transcriptional changes were detected, suggesting that transcriptional regulation by the homeodomain of Pax6 has no major impact on forebrain development. Additionally, these results implied that the majority of effects exerted through Pax6 during telencephalic development are mediated by the bipartite paired-domain (PD). Therefore the main focus of this thesis was to examine the specific roles of the Pax6 paired-domain and its individual DNA-binding subdomains (PAI and RED) during forebrain development. The role of these DNA-binding domains was examined using mice with point-mutations in the PAI (Pax6<sup>Leca4</sup>, N50K) and RED (Pax6<sup>Leca2</sup> R128C) subdomains and showed that the mutations in these subdomains exert opposing roles regulating proliferation in the developing cortex. While the mutated PAI domain resulted in reduced proliferation of both apical and basal progenitors, the mutated RED domain provoked increased proliferation. However, the PAI domain largely mediates the neurogenic function of Pax6. Additionally, genome-wide transcriptome analysis was able to unravel the key signatures mediated by the distinct domains. In summary, Pax6 exerts its key roles during forebrain development by use of distinct subdomains to regulate proliferation and differentiation. Thus Pax6 is able to coordinate and fine tune patterning, neurogenesis and proliferation in a simultaneous manner in different radial glial subpopulations.

The transcriptional regulation through Pax6 may not only be restricted to protein coding genes, but may also include control of microRNA (miRNA) expression. Such small RNA molecules have recently been implicated in proliferation and differentiation during development, however expression and the role of single microRNAs is still poorly understood.

Towards this end, miRNA expression profiling was performed using an embryonic stem cell differentiation system at different stages of neuronal differentiation in order to identify new miRNAs involved in radial glia specification and differentiation. This analysis revealed a number of microRNAs induced during differentiation from neural progenitors to neurons. Most strikingly only four miRNA candidates were found with exclusively high expression in progenitor cells. These data suggest that also Pax6 may play a role in transcriptional regulation beyond mRNAs.

## Zusammenfassung

Während der Entwicklung des Gehirns regulieren und koordinieren verschiedene Mechanismen die Proliferation von Vorläuferzellen und deren Differenzierung so dass sich das Gehirn letztlich normal entwickelt. Zu den Faktoren welche diese beiden Mechanismen beeinflussen gehören viele Transkriptionsfaktoren. Einer dieser Faktoren ist der Transkriptionsfaktor Pax6, welcher eine besondere Stellung einnimmt, da er ein wichtiger Regulator für viele verschiedener Aspekte der Gehirnentwicklung ist. Während der Entwicklung des Vorderhirns besitzt Pax6 verschiedene Funktionen wie die Kontrolle Zellproliferation und Neurogenese oder die korrekte Regionalisierung verschiedener Gehirndomänen. Aber bis heute ist unklar wie Pax6 diese unterschiedlichen Aufgaben auf molekularer Ebene kontrolliert. Es wurde kürzlich gezeigt dass die Homeodomäne von Pax6 eine Funktion in der Etablierung der Pallialen-Subpallialen Grenze ausübt, aber an anderen Prozessen während der Entwicklung des Vorderhirns nicht beteiligt ist. Dies wurde mithilfe einer Mauslinie untersucht, die eine Punktmutation in der Homeodomäne (HD) besitzt wodurch die DNA bindende Helix zerstört ist (Pax6<sup>4NEU</sup>). Um aber die mögliche molekulare Regulation der spezifischen HD-Funktion im sich entwickelnden Vorderhirn zu untersuchen, wurde eine Transkriptomanalyse der Pax6<sup>4NEU</sup> Mauslinie durchgeführt. Diese zeigte fast keine Veränderungen des Transkriptoms, was zur Schlussfolgerung führte, dass die HD von Pax6 keine Regulation auf transkriptioneller Ebene im sich entwickelnden Vorderhirn ausübt. Dieses Ergebnis impliziert, dass die meisten von Pax6 ausgeübten Funktionen im sich entwickelnden Vorderhirn von der zweiten DNA bindenden Domäne – der PAIRED Domäne – ausgeübt wird. Diese Domäne besitzt eine zweiteilige Struktur und kann demnach also in zwei Subeinheiten (genannt PAI und RED) unterteilt werden. Die verschiedenen Rollen dieser beiden Subdomänen wurden mithilfe zweier Mauslinien untersucht. Diese Mauslinien besitzen jeweils eine Punktmutation innerhalb der PAI-Subdomäne (N50K in der Pax6<sup>Leca4</sup> Mauslinie) bzw. der RED-Subdomäne (R128C in der Pax6<sup>Leca2</sup> Mauslinie). Es konnte gezeigt werden, dass diese Mutationen eine gegensätzliche Rolle in der Kontrolle der Zellproliferation ausüben. Während die Mutation in der PAI-Subdomäne zu einer verminderten Proliferation der apikal und basal gelegenen Vorläuferzellen führte, resultierte die Mutation in der RED-Subdomäne hingegen in verstärkter Proliferation. Im Gegensatz dazu konnte gezeigt werden dass die neurogene Funktion von Pax6 nur abhängig von der PAI-Subdomäne ist und dass beide Subdomänen die Regionalisierung in einem überwiegend redundanten Maß kontrollieren. Diese Ergebnisse wurden untermauert durch eine Genomanalyse der beiden Mutanten, die es auch erlaubte wichtige Regulationskandidaten

der beiden Subdomänen zu identifizieren. Abschließend lässt sich sagen, dass Pax6 im sich entwickelnden Vorderhirn seine unterschiedlichen Funktionen durch die differenzielle Verwendung der einzelnen Subdomänen ausübt und somit Zellproliferation, Neurogenese und Regionalisierung kontrolliert.

Pax6 übt seine transkriptionelle Kontrolle möglicherweise nicht nur auf Protein-kodierende Gene aus, sondern auch auf die Expression von microRNA (miRNA) Molekülen. Diese kleinen RNA Moleküle spielen ebenfalls eine Rolle in der Regulation von Proliferation und Differenzierung während der Entwicklung. Jedoch ist die Expression und spezifische Funktion einzelner miRNAs noch nicht gut verstanden. Um neue miRNA Moleküle zu identifizieren die eine Rolle in der Spezifizierung und Differenzierung von Pax6+ Vorläuferzellen spielen wurde mithilfe eines auf embryonalen Stammzellen beruhenden Differenzierungssystems ein miRNA Expressionprofil zu verschiedenen Stadien der Differenzierung erstellt. Das verwendete System spiegelt die Pax6 abhängige Neurogenese - ähnlich wie sie im sich entwickelnden Vorderhirn abläuft - wieder. Diese Analyse deckte miRNAs auf deren Expression während der Differenzierung von Vorläuferzellen zu Neuronen induziert wird. Im Besonderen, konnten vier miRNA Moleküle identifiziert werden die spezifisch nur im Stadium der neuronalen Vorläuferzellen -in denen die Pax6 Expression am stärksten ist - expremiert werden. Diese Daten zeigen dass Pax6 ein wichtiger Regulator in der Gehirnentwicklung ist und möglicherweise auch eine Rolle in der transkriptionellen Kontrolle jenseits von mRNA kodierenden Genen spielt.

## 1 Introduction

The adult mammalian brain consists of an enormous variety of cell types. At first glance, the two main cell types found are neurons and glial cells. Amongst neurons, there are different types, i.e. excitatory and inhibitory neurons - which can be even further classified by the different neurotransmitters they manufacture such as glutamate, GABA, Dopamine and many others. Accordingly, many different glial cells exist such as astrocytes, oligodendrocytes and ependymal cells.

Considering this plethora of different cell types in an adult brain, one major question is how these cell types arise from pluripotent stem cells during development. For a long time it had been believed that neurons and glia originate from distinct progenitor pools (Virchow et al., 1846; Jacobson et al., 1991; Kriegstein and Alvarez-Buylla, 2009). However, in the late 20th century a common origin for glia and neurons could be demonstrated in the rodent brain (Malatesta et al., 2000; Miyata et al., 2001; Noctor et al., 2001a). As both cell types share a common origin there certainly need to be different factors that determine the distinct fate of these stem cells during development. Indeed, today many different factors including extrinsic and intrinsic cues have been shown to influence the neuronal and glial output of progenitors during development. The accurate combination of these factors interplaying to form the correct number of each specific cell type at the right time and in the right place is the key for proper brain development (Guillemot et al., 2006; Johansson et al., 2010; Lui et al., 2011; Tiberi et al., 2012). Therefore elucidating the molecular mechanisms controlling forebrain development is crucial to understand the distinctive output from originally one multipotent stem cell pool. The present thesis has looked in detail on molecular fate determinants regulating embryonic neurogenesis. In particular, the transcription factor Pax6 and its molecular characteristics in regulating multiple functions during forebrain development were main focus of this thesis. Furthermore, on transcriptional level Pax6 may not only regulate expression of mRNAs, but also of miRNA genes. Therefore as a second part, a screen for miRNA expression during neuronal differentiation was performed.

Before describing Pax6, as well as miRNAs as fate determinants in more detail, the following sections will guide through and describe broad concepts of telencephalic development.

## 1.1 Early brain development – generation of the cerebral cortex

Early development of the nervous system comprises three key steps: (i) induction, (ii) neurulation and (iii) formation of the brain vesicles. After the three germ layers have formed, the first step - the conversion of naive ectoderm into neuroectoderm - is induced (Fig.1-1A). Many studies between the 1920s and 1980s have revealed that a region within the mesoderm, known as “Spemann’s organizer” in amphibians or the “node” in mice, secretes neuralization and regionalization signals (Spemann and Mangold, 1924; Mangold, 1933, Nakamura und Toivonen, 1978). These signals between mesoderm and ectoderm together with signals within the ectoderm are important for neural induction (Ruiz I Altaba, 1993). However, until more recently, the nature of these signals had remained un-identified. Several studies have now shown that inhibitors of the bone morphogenic protein (BMP) signaling pathway represent the neuralizing factors that allow the ectoderm to acquire neural properties. In contrast, the BMP molecules act as epidermal inducers within the ectoderm (Sasai and DeRobertis, 1997; Wilson and Hemmati-Brivanlou, 1997). After the neuroectoderm has transformed into the neural plate, neurulation begins. A groove forms in the neural plate which then wraps in on itself and finally constricts to form the neural tube (Fig.1-1B). In humans this process takes place around the fourth post-ovulatory week, which corresponds to embryonic days 7-9 in mice. The anterior part of the neural tube then gives rise to the brain, while the posterior part develops into the spinal cord. For brain development, the neural tube differentiates into three primary brain vesicles: the forebrain vesicle (prosencephalon), the midbrain vesicle (mesencephalon) and the hindbrain vesicle (rhombencephalon) (Fig1-1C). These then give rise to five secondary brain vesicles that - as the vertebrate grows - differentiate into various adult structures. Hereby, the hindbrain vesicle further divides into the metencephalon (forming the pons and cerebellum) and the myelencephalon (forming the medulla) (Melton et al., 2004). The forebrain vesicle gives rise to the diencephalon (forming amongst others, the thalamus, the retina and the optic nerve) and to the telencephalon. The telencephalon is again subdivided into the cerebral cortex (ctx; pallium) located dorsally and into the ganglionic eminences (GE; subpallium) located ventrally with the pallial-subpallial boundary sharply separating both regions. The pallium can be further separated into ventral, lateral, medial and dorsal domains as depicted within Fig.1-2. The GE forms bulges into the ventricle and thus is subdivided into the lateral-, medial- and caudal ganglionic eminence (LGE, MGE, CGE respectively) that finally give rise to the striatum and pallidum in the adult forebrain. The cerebral cortex itself can be subdivided into three regions in the adult: the archicortex (includes amongst others the hippocampus), the paleocortex (olfactory cortex)

and the neocortex (being positioned in-between the other two structures). The neocortex represents the part of the brain that accounts most for the increase in overall brain size and complexity found in more advanced mammals (Krubitzer and Kaas, 2005).

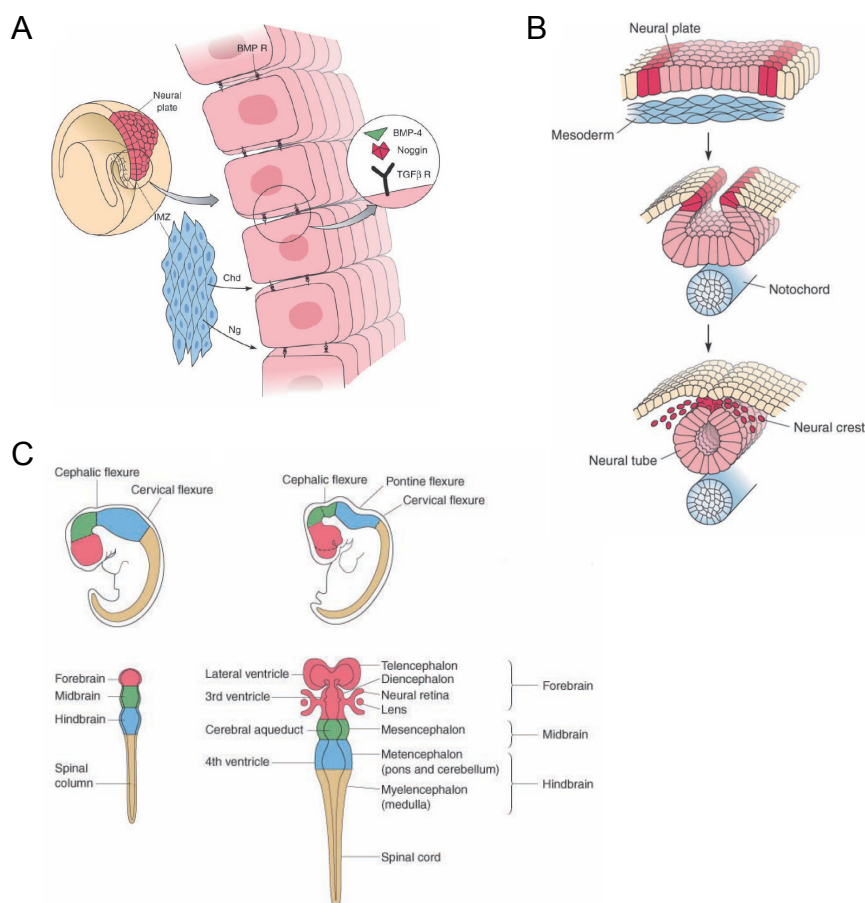


**Figure 1-1 Schematic depictions of the three key steps in early nervous system development: from induction to neurulation followed by formation of the brain vesicles (taken from Sanes, Reh and Harris; *Development of the Nervous System*; Second edition)**

(A) Model of neuroectoderm induction in *Xenopus laevis* (as example). The release of BMP-antagonists, such as noggin, from the Spemann organiser induces the neuroectoderm.

(B) When the neuroectoderm has formed the neural plate (light red) it rolls up forming a tube that delaminates from the rest of the ectoderm. At the same time, the organiser differentiates into the notochord and also into some somite- and head-mesodermal tissue. At the point where the neural tube fuses, a group of cells, known as the neural crest cells (bright red) arise. These generate the peripheral nervous system, while the central nervous system emanates from the neural tube.

(C) Schematic depicting the generation of the primary and secondary brain vesicles using the example of a human embryo (lateral view: top panels; dorsal view: bottom panels). First, the three primary brain vesicles develop, known as: forebrain (prosencephalon), midbrain (mesencephalon) and hindbrain (rhombencephalon). As development proceeds, the forebrain further divides and generates the paired telencephalic vesicles, the diencephalon and the rhombencephalon. The latter furthermore splits into the metencephalon and the myelencephalon.

Abbreviation: BMP, bone morphogenic protein; BMP R, bone morphogenetic protein receptor; Chd, chordin; IMZ, involuting marginal zone; Ng, noggin.

During early development, the identities of the dorsal and the ventral telencephalon are specified by signaling molecules that are expressed from early patterning centers. Amongst these the Wingless-Int protein (Wnt), the Bone morphogenic protein (BMP), Sonic hedgehog (Shh) and Fibroblast growth factor families (Fgf) (Lumsden and Krumlauf, 1996; Rubenstein et al., 1998; Takahashi and Liu, 2006; Rash and Grove, 2007). These signals act by regulating the expression of a specific set of transcription factors that establish the molecular identities and characteristics of the locally generated cell types. Transcription factors important for dorsal fate specification comprise the empty spiracle homologs (Emx) 1 and 2 and the paired-box transcription factor Pax6. Besides specifying dorsal precursors both also act antagonistically to further pattern distinct area identities and thus are expressed in opposing gradients (Bishop et al., 2000; Bishop et al., 2002; Muzio et al., 2002b; Muzio and Mallamaci, 2003). The gradient of Pax6 in the cortex is defined as rostral high to caudal low and laterally high to medial low. However, its expression is found already at the neural plate stage throughout the telencephalic anlagen, but is then down-regulated at the neural tube stage in the region that will give rise to the ventral telencephalon (Inoue et al., 2000; Hebert and Fishell, 2008). The down regulation of Pax6 in the region that will later become the ventral forebrain goes along with the up-regulation of the transcription factor Nkx2.1 in the same region that determines ventral fate (Corbin et al., 2003; Hebert and Fishell, 2008). As a result, the boundary between both transcription factors represents the initial dorsal-ventral border (Hebert and Fishell, 2008). Slightly later, the transcription factor Gsx2 starts to be expressed in a domain between Nkx2.1 and Pax6 (Hebert and Fishell, 2008). This ultimately leads to the formation of the pallial-subpallial boundary (PSB). At this stage the Gsx2 and Pax6 expression domains slightly overlap, but become separated later during development (Hebert and Fishell, 2008). Structurally, this boundary lies at the interface of the dorsal most region of the LGE with the ventral pallium (Hebert and Fishell, 2008). As development proceeds the regionalization becomes more defined, including structural and expression refinements of important transcription factors. For a better understanding, important transcription factors and their genetic interactions underlying the regionalization of the telencephalon are depicted in Fig.1-2.

Boundary fascicles at the PSB furthermore restrict the migration of cells across the border and loss of Pax6 function results in a disturbed PSB with an increased migration of cells between the GE and the cortex (Stoykova et al., 1997; Gotz et al., 1998; Chapouton et al., 1999). Moreover, Pax6 expression in progenitors of the PSB plays an important role in the generation of different neuronal subtypes later populating the olfactory bulb and amygdala (Cocas et al., 2011). In addition, Pax6 is expressed in the largest pallial regions – the medial

and dorsal pallium – and is crucial for the establishment of a correct glutamatergic phenotype (Schuurmans and Guillemot, 2002; Kroll and O'Leary, 2005).

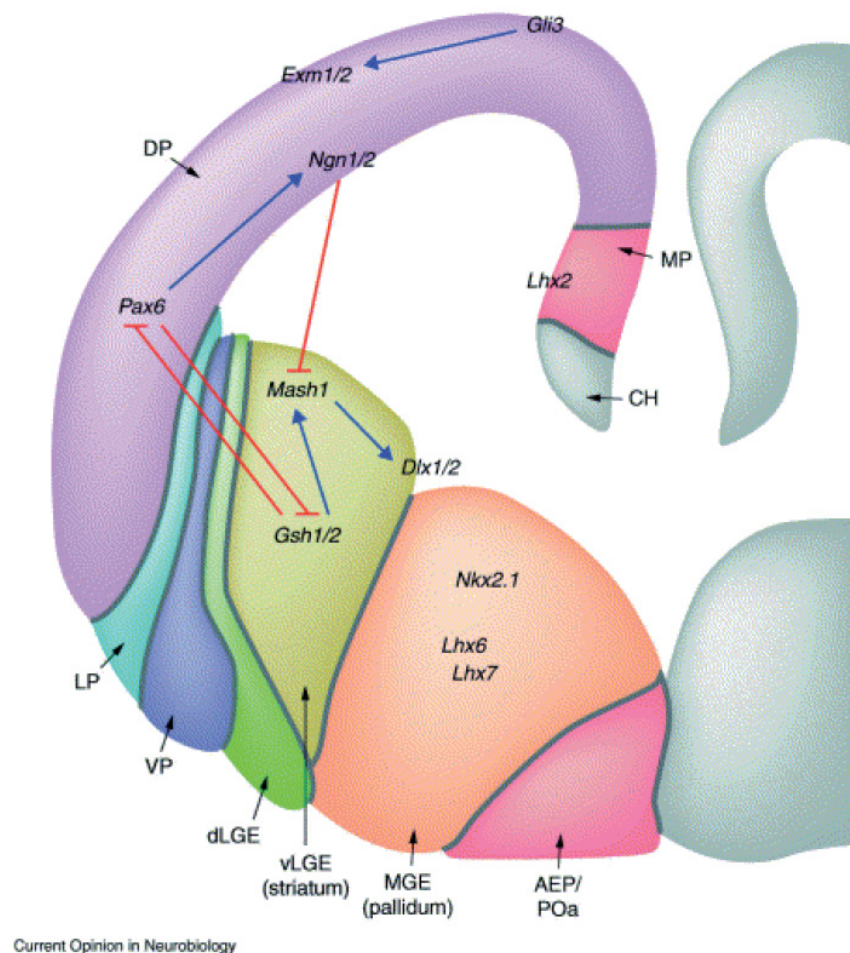


**Figure 1-2 Summary of regionalized transcription factors and their genetic interactions in the developing telencephalon (taken from Schuurmans and Guillemot et al., 2002)**

Schematic drawing of a coronal section through the telencephalon of an E12.5 mouse brain, showing dorsal and ventral subdomains, as defined by their unique patterns of gene expression. The dorsal telencephalon shows high expression levels of Pax6, Ngn1/2, Emx1, Emx2 and Lhx2. In contrast, high expression of Mash1, Gsh1/2 (Gsx1/2), Dlx1/2/5/6 is found in the lateral ganglionic eminence (LGE) of the ventral telencephalon. Whereas Lhx6, Lhx7 and Nkx2.1 are only found in the medial ganglionic eminence (MGE). The dorsal telencephalon can be further subdivided into different domains: medial pallium (MP), dorsal pallium (DP), lateral pallium (LP) and ventral pallium (VP). The LGE can be further subdivided into the dorsal LGE (dLGE) and ventral LGE (vLGE) compartments on the basis of higher levels of Pax6, Gsx2, Mash1 and Dlx2 in the dLGE and exclusive expression of Gsx1 in the vLGE.

## **1.2 Generation of cell diversity in the cerebral cortex**

The cerebral cortex is the most complex structure in the mammalian brain, composed of hundreds of different neuronal subtypes (Tiberi et al., 2012). The generation of this neuronal cell diversity is a complex process which involves a number of tightly coordinated steps (Guillemot et al., 2006). These include the generation of different progenitor types that show distinct proliferation behaviors, their commitment to a neuronal fate, the migration away from the progenitor zones towards a particular laminar position building up the complex six-layered structure of the cerebral cortex and the acquisition of differentiated features (Guillemot et al., 2006). All of these steps require distinct molecular regulatory mechanisms, some of which will be discussed after introduction of the distinct progenitor types and neurons present and produced during development of the cerebral cortex.

### **1.2.1 Neural stem and progenitor cells in the developing telencephalon**

The first neural stem cell type which is specified during the induction of the neuroectoderm, is the neuroepithelial cell. The morphology of this progenitor is characterized by a prominent bipolar polarity, spanning the wall of the neural tube from apical (ventricular) to basal (pial). During cell-cycle, their nuclei move along their entire axis - from apical-to-basal in G1 phase and from basal-to-apical in G2 phase, followed by mitosis exclusively at the ventricular surface. This process is known as interkinetic nuclear migration (INM) and leads to a pseud-stratified appearance of the neuroepithelium (Takahashi et al., 1996). Before the onset of neurogenesis, the neuroepithelial cell population undergoes symmetric divisions to expand the progenitor pool and thereby also increases the surface area of the tissue (lateral expansion) (Murciano et al., 2002). With the onset of neurogenesis (around E10.5 in the mouse) they switch to an asymmetric mode of division, generating a neuroepithelial cell that stays in the ventricular zone (VZ) and one daughter cell that differentiates and migrates outwards along the radial process (Fig.1-3). These are the first neurons generated in the developing cortex and are designated to settle in the preplate (Casanova and Trippe, 2006; Pinto and Gotz, 2007). Now, the tissue also starts to grow in thickness (radial expansion), which is accompanied by the lengthening of the radial processes. This goes along with some molecular changes resulting in the transformation of neuroepithelial cells to radial glial cells. These include the expression of glial markers such as the astrocyte specific glutamate transporter (GLAST) or the brain-lipid binding protein (BLBP) but also expression of intermediate filament proteins like nestin, vimentin and the RC1 and RC2 epitopes has been

described (Hartfuss et al., 2001; Malatesta et al., 2003b; Mori et al., 2005; Pinto and Gotz, 2007; Alvarez-Buylla et al., 2009). Radial glial cells maintain the bipolar polarity of neuroepithelial cells with a basal end-foot at the pial surface and a single ciliated apical end-foot lining the ventricle. But, compared to neuroepithelial cells that are connected at the apical-most end of their plasma membrane via tight junctions (TJ), adherens junctions (AJ) and gap junctions, radial glial cells lose the tight junctional connections (Shoukimas and Hinds, 1978; Astrom and Webster, 1991; Aaku-Saraste et al., 1996; Gotz and Huttner, 2005). On the other hand they form specialized contacts with endothelial cells of the developing cerebral vasculature (Takahashi et al., 1990; Misson et al., 1991). Another change appears in regard to INM. Radial glial cells still undergo INM, however the movement of their nuclei becomes restricted to the VZ due to the thickening of the tissue and the arising neuronal layer on top of the progenitor zone (Gotz and Huttner, 2005). It has been shown that RG cells undergo self-renewing divisions, expanding the progenitor pool, but also producing all remaining neurons that originate from the cerebral cortex (Fig.1-3) (Malatesta et al., 2003a). The predominant mode of division is asymmetric with about 30% of the radial glial cells that still undergo symmetric self-renewing divisions around midneurogenesis (Konno et al., 2008). The asymmetric self-renewing divisions of radial glial cells produce a progenitor and a daughter cell that is either a neuron or a second type of neural progenitor with more restricted potential (Noctor et al., 2001a; Huttner and Kosodo, 2005). In rodents, the most abundant progenitor type, originating from RG in the telencephalon is the basal progenitor (BP or intermediate progenitor IPC). These progenitors delaminate from the apical surface and translocate their nucleus to the basal site of the ventricular zone and this way form a second germinal layer, the subventricular zone (SVZ) (Farkas et al., 2008). Before mitosis, they have also retracted both their apical and basal processes. Frequently they possess multipolar processes, but these are too short to contact the ventricle or the pial surface. Time-lapse imaging studies have shown that in contrast to RG, the majority of BPs in the cerebral cortex divides in a symmetric mode of division. In terms of daughter cell fate, these symmetric divisions predominantly produce two neurons and much less frequently (~10% of the divisions) produce two additional BPs (Haubensak et al., 2004; Miyata et al., 2004; Noctor et al., 2004; Huttner and Kosodo, 2005; Wu et al., 2005; Fietz et al., 2010). A recent description has raised the possibility that proliferation behaviour and fate of basal progenitors may be influenced by signals from the developing vasculature as it was shown that BPs localize preferentially close to the blood vessels during cortical neurogenesis (Javaherian and Kriegstein, 2009; Stubbs et al., 2009).

As described above, the majority of secondary progenitors derived from radial glial cells are the basal progenitors. Recent work has identified additional progenitors – radial glia-like (oRG) progenitor cells and short neural precursors (SNP) - present in the developing rodent cortex. While imaging studies have proven that oRGs derive from radial glial cells (Shitamukai et al., 2011; Wang et al., 2011b), the RG-ancestry of SNPs has just been hypothesized (Gal et al., 2006). Short neural precursors exhibit apical polarity but in contrast to RG their basal process is not reaching the pial surface and is retracted during mitosis. They have been identified by GFP expression driven by the tubulin alpha1 promoter (Fietz et al., 2010), which is solely active in the SNPs and were found in substantial numbers between E13.5-E16.5 – the major birth period of neurons in the developing cerebral cortex. Moreover, genetic fate mapping has revealed that SNPs produce rather neurons than BPs (Gal et al., 2006; Stancik et al., 2010). Short neural precursors and oRGs have one feature in common– the expression of the transcription factor Pax6. But, in contrast to SNPs, oRGs possess only basal polarity inherited from their radial glial mother cell. Elegant imaging studies have furthermore shown that these progenitors undergo asymmetric self-renewing divisions located basally of the SVZ (Shitamukai et al., 2011; Wang et al., 2011b). In mice oRGs are present in low numbers (~5% at E14), which is in contrast to humans and primates that are populated by a large number of the corresponding outer-subventricular zone (OSVZ) progenitors contributing to the cortical expansion in higher mammals (Lui et al., 2011). Taken together, within the developing cerebral cortex diversity in progenitor populations exist – NE cells, RG cells, SNP cells, BP cells, oRG cells – all contributing to the generation of distinct neuronal subtypes.

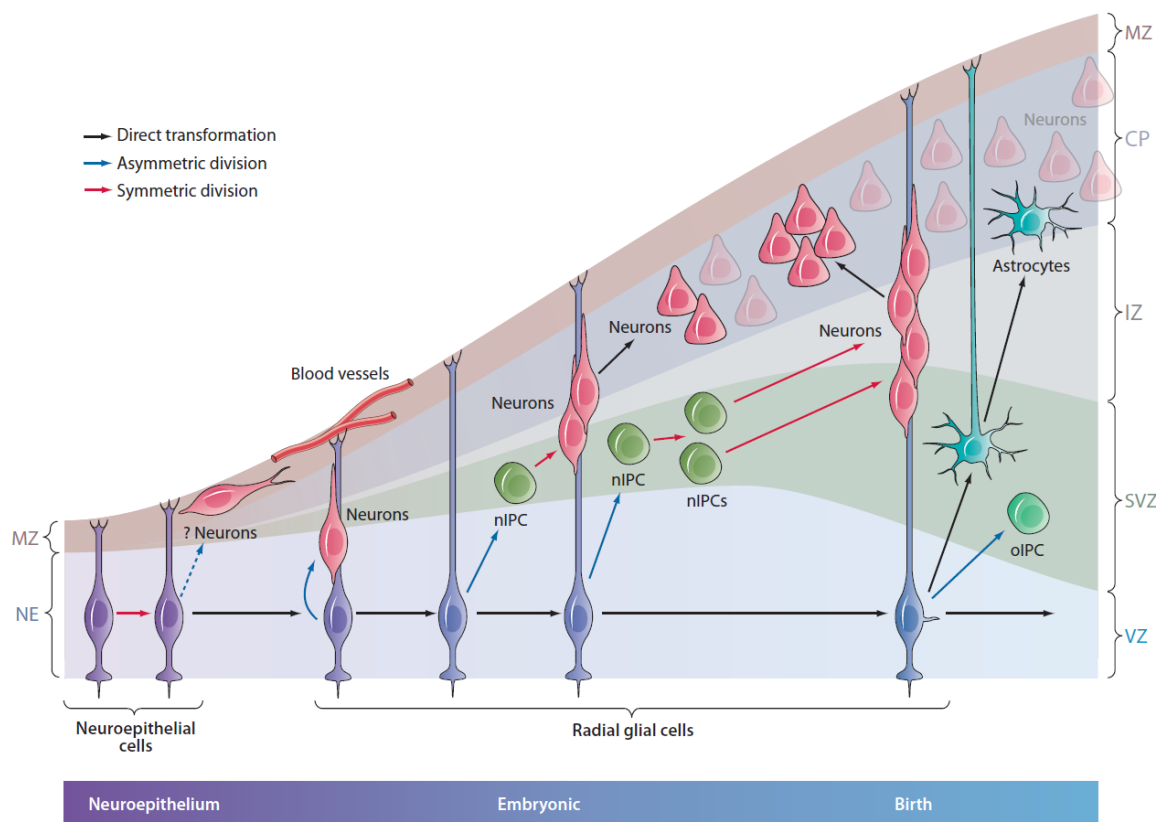


**Figure 1-3 Generation of cell diversity in the brain: different subtypes of progenitors contribute to cortical neurogenesis (taken from Kriegstein and Alvarez-Buylla et al., 2009)**

Early in development, neuroepithelial cells (NEC) expand by symmetric divisions. As development proceeds, the NECs elongate and convert into radial glial cells (RG). RGs divide mainly asymmetric, generating neurons directly or indirectly through intermediate progenitors (IPC; also known as basal progenitors). The progeny of RG and IPC migrates basally for differentiation. The brain gains in thickness and RG cells further elongate their process. RG cells possess an apical (down) to basal (up) polarity and contact the ventricle, where they project a single primary cilium. On the basal side, RG cells contact the basal lamina at the meninges and blood vessels. At the end of embryonic development most RG start to detach from the apical surface and then either convert into astrocytes or continue with oligodendrocyte production (oPC).

Abbreviations: CP, cortical plate; IPC, intermediate progenitor cell; IZ, intermediate zone; MA, mantle; MZ, marginal zone; NE, neuroepithelium; nIPC, neurogenic progenitor cell; oIPC, oligodendrocytic progenitor cell; RG, radial glia; SVZ, subventricular zone; VZ, ventricular zone.

### 1.2.2 Neuronal cell diversity forming the six layers of the cerebral cortex

The cerebral cortex is organized radially into six layers and tangentially into distinct areas. Each layer contains pyramidal neurons of a specific subtype with distinct morphology, projection pattern, function and gene-expression profile and are generated from the progenitor populations described above in a tightly controlled temporal order (Casanova and Trippe, 2006; Molyneaux et al., 2007). In mouse the birth period of these neurons takes place between E10.5 to E17.5 and the postmitotic neurons position themselves in an inside-out manner (Fig.1-4) (Molyneaux et al., 2007). That is, later born neurons migrate radially past early born neurons settling on top of them. The earliest born neurons that appear in the dorsal cortex form a transient structure called the preplate, which then splits into the upper marginal zone and the lower subplate. The neurons of the marginal zone are termed Cajal-Retzius cells and noteworthy, they not only originate from cortical neuroepithelial progenitors (Shen et al., 2006) but also from other region including the cortical hem (Garcia-Moreno et al., 2007). Cajal-Retzius cells secrete the molecule Reelin, which is important for the correct positioning of the postmitotic neurons within the six-layered structure (D'Arcangelo et al., 1995; Ogawa et al., 1995; D'Arcangelo et al., 1997; Schiffmann et al., 1997). Proceeding in development, the cortical plate develops in between the marginal zone and subplate and subsequently gives rise to the multilayered cortex. Its different neuronal subtypes are generated in overlapping temporal waves that begin a bit earlier rostro-laterally: neurons of the deeper layers 6 and 5 are generated around E12.5 and E13.5 respectively and neurons of the upper layers 4 and 3/2 are born around E14.5 and E15.5 respectively (Molyneaux et al., 2007). Neurogenesis caudo-medially slightly lags behind (Molyneaux et al., 2007). As mentioned before, the cortical layers can be distinguished by a specific gene expression pattern of their neurons. For example, deep layer neurons 6 and 5 can be distinguished by the expression of *Foxp2* and *Er81* respectively (Molyneaux et al., 2007). Another marker gene present in both deep-layers is *Ctip2* - which is expressed at high levels in the lower portion of layer 5 neurons (5b; subcerebral neurons) and with lower levels in layer 6 neurons (Molyneaux et al., 2007). The neurons of the upper layers 2, 3 and 4 express many genes in common such as *Cux1* and *Cux2* or *Svet1* (Molyneaux et al., 2007). However, they also possess some individual marker gene expression like *Rorb*, which is restricted to layer 4 neurons. Moreover expression of some genes is found in both upper and deep layers, such as *Tbr1* (Molyneaux et al., 2007). Besides their different gene expressions and other complexities, such as the brain region they project to, all these subtypes of neurons have two things in common - they originate from cortical progenitors and are all pyramidal shaped

excitatory projection neurons using glutamate for neuronal transmission (Molyneaux et al., 2007).

In contrast, a second class of cortical neurons – inhibitory interneurons – is generated primarily from ventral telencephalic progenitors and uses gamma-aminobutyric acid (GABA) as neurotransmitter (Gotz and Sommer, 2005). These neurons migrate via distinct roots tangentially into the cortex and finally form local connections with the excitatory projection neurons (Gotz and Sommer, 2005; Wonders and Anderson, 2006). Taken together, the cerebral cortex possesses a unique six-layered structure consisting of diverse neuronal subtypes all generated during embryonic neurogenesis.

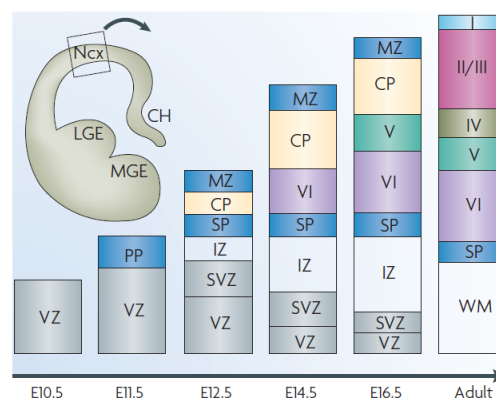


**Figure 1-4 Schematic depicting the generation of the six-layered structure of the cortex (adapted from Molyneaux et al., 2007)**

The earliest born neurons from VZ progenitors form the preplate (PP), which is later split into the upper -marginal zone (MZ) and the deeper located subplate (SP). As a next step, the cortical plate (CP) develops in between the MZ and SP. As development proceeds, the cortical plate gives rise to the layered cortex; neurons born at later stages migrate past early born neurons, settle on top of them and this way generate the multilayered structure of the cortex via an inside-out mechanism. Different classes of projection neurons are born in overlapping temporal waves between E10.5-E16.5 in the mouse.

Abbreviations: CH, cortical hem; E, embryonic day; Ncx, neocortex; IZ, intermediate zone; LGE, lateral ganglionic eminence; MGE, medial ganglionic eminence; SVZ, subventricular zone; VZ, ventricular zone; WM, white matter.

### 1.2.3 Molecular fate determinants in cortical development

The generation of pyramidal neurons in the developing cerebral cortex requires tight control of proliferation, cell fate specification and differentiation of the cortical progenitors. One important question then is – what are the molecular determinants involved? Two classes of regulators have emerged: extrinsic and intrinsic factors that interplay to control cortical neurogenesis (Guillemot et al., 2006; Johansson et al., 2010; Tiberi et al., 2012).

### 1.2.3.1 *Extrinsic cues*

A number of extracellular factors have been described, such as retinoic acid (RA), bone morphogenic proteins (BMPs), sonic hedgehog (Shh), fibroblast growth factors (FGFs), and Wingless-Int proteins (Wnts). In addition to cortical neurogenesis, the roles of these classical morphogen families have been best studied in regional patterning as briefly mentioned before. The family of Wnts are secreted signalling molecules and expression of distinct Wnts and their receptors or antagonists are found in different compartments in the developing cortex (Chenn, 2008). For example, several Wnts (including Wnt3a, 5a, 2b, 7b and 8b) originate from a caudomedial structure called the cortical hem (Grove et al., 1998). In contrast, the laterally located anti-hem expresses Wnt antagonists, like the secreted frizzled related protein 2 (Sfrp2). The dorsal pallium has a high abundance of Wnt-ligands and  $\beta$ -catenin (a major component of the canonical Wnt-signalling pathway) as well as of the frizzled family receptors. Interestingly, they are found in different cortical compartments. While the ventricular zone expresses Wnt-receptors (mFz-5, mFz-8), Wnt7a and  $\beta$ -catenin, the ligand Wnt7b is absent from the VZ and instead is found in the subventricular zone and developing cortical plate (Grove et al., 1998; Rubenstein et al., 1999; Kim et al., 2001; Chenn and Walsh, 2002; Funatsu et al., 2004). Wnt proteins activate different intracellular signaling pathways including the  $\beta$ -catenin/TCF pathway (known as the canonical Wnt pathway) (Wodarz and Nusse, 1998; Brantjes et al., 2002) and non-canonical pathways, like the planar cell polarity pathway mediated by Jun N-terminal kinase (JNK) or the Wnt/Ca<sup>2+</sup> pathway (Kuhl et al., 2000; Huelsken and Birchmeier, 2001; Habas et al., 2003; Hirabayashi et al., 2004). Their effects during cortical development are diverse and appear to depend on the progenitor state and developmental time. It has been reported that the canonical Wnt pathway promotes self-renewal of progenitor cells during early neurogenesis; expression of stabilized  $\beta$ -catenin has been shown to result in an increased number of progenitors and suppression of neuronal differentiation (Chenn and Walsh, 2002). Conversely, loss of Wnt signalling lead to a decrease in cortical neuronal production (Woodhead et al., 2006; Zhou et al., 2006). On the contrary, recent reports have shown that Wnt-ligands can exert pro-neurogenic effects during mid-neurogenesis (Hirabayashi et al., 2004; Israsena et al., 2004; Kuwahara et al., 2010). For example, the ligand Wnt7a promotes neuronal differentiation in part by direct regulation of the proneuronal factor Ngn1 (Hirabayashi et al., 2004). Most recently, a comparison of activating or inhibiting Wnt-ligands demonstrated a dual role of Wnt-signalling in cortical neurogenesis (Munji et al., 2011). While Wnt-signalling regulates self-renewal in radial glial cells, its activation in basal progenitors is required for neuronal

production at mid and late stages of neurogenesis. Thus Wnt regulators are an important extrinsic cue during cortical neurogenesis.

The morphogen retinoic acid is a hormone derived from vitamin A (retinol) (Chambon, 1996). During cortical neurogenesis, RA is released from a neural crest derived structure – the meninges, which overlays the neuroectoderm (Siegenthaler et al., 2009). This structure in addition expresses the proteins that bind and chaperone RA (e.g. CRABP I, II and CRBP1) and are implicated in titrating the RA exposure to the radial glial endfeet (Ruberte et al., 1993; Napoli, 1999; Siegenthaler et al., 2009). Furthermore, CRABP II is also expressed in the ventricular zone, where it is suggested to aid in the intracellular transport of RA through the cytoplasm of the radial glial fiber up to the nucleus (Ruberte et al., 1993; Siegenthaler et al., 2009). Moreover a recent report identified another transport protein (of the RA precursors retinol and retinaldehyde) in the ventricular zone - CRALBP (also known as Rlbp1) and showed that CRALBP expression is directly controlled by the transcription factor Pax6 (Boppana et al., 2012). The role of RA in cortical neurogenesis was investigated in a recent study and unraveled an impact of RA on basal progenitor specification (Siegenthaler et al., 2009). This was revealed examining *Foxc1* mutants, which displayed defects in the formation of the meninges accompanied by lack of secreted retinoic acid (Tiberi et al., 2012). Loss of meningeal cell derived RA resulted in a decreased generation of basal progenitors from radial glial cells (Siegenthaler et al., 2009). This finding is especially interesting as for many years retinoic acid has been used to induce neural differentiation from pluripotent embryonic stem cells (Bain et al., 1995; Bain et al., 1996; Guan et al., 2001; Bibel et al., 2004; Bibel et al., 2007).

Taken together, various extracellular cues, like the morphogens Wnt or RA (or others see for example (Johansson et al., 2010) play an important role in cortical neurogenesis and furthermore cooperate with different intrinsic factors to regulate cortical development.

#### 1.2.3.2 *Intrinsic cues*

Intrinsic factors that control cortical differentiation involve many transcription factors, post-transcriptional regulators like miRNAs as well as regulators of cell-polarity and mitosis. All these different intrinsic factors act at the level of at least one type of progenitor to control cortical neurogenesis (Gotz and Huttner, 2005; Pinto and Gotz, 2007; Kriegstein and Alvarez-Buylla, 2009; Fietz and Huttner, 2011; Tiberi et al., 2012). Interestingly, however within the lineage of progenitors, many aspects of cortical neurogenesis seem to be programmed (Tiberi et al., 2012). This notion of an intrinsic programme is supported by lineage studies

of isolated progenitors. When cultured, the progenitors were able to generate the different subtypes of neurons in an order that resembled the one observed in-vivo (Qian et al., 2000; Shen et al., 2006). However, while earlier transplantation experiments support the presence of such a cell-intrinsic programme, they also imply that extrinsic factors cooperate to determine neuronal fate, in particular by influencing final mitosis. When early progenitors (isolated when deep-layer neurons were generated) were transplanted into a developmentally more progressed environment, they only switched to the generation of upper-layer neurons when the progenitor was in its S-phase of the cell cycle (Desai and McConnell, 2000). Conversely, early progenitors transplanted late in their cell-cycle state (G2-phase) were not able to switch (McConnell and Kaznowski, 1991; Frantz and McConnell, 1996; Desai and McConnell, 2000). In contrast, progenitors of a later stage (determined to generate upper-layer neurons) were restricted to an upper-layer fate (Desai and McConnell, 2000). Thus, as the developmental programme unfolds, progenitors lose their capacity to generate deep layer neurons.

As mentioned above one large class of intrinsic factors regulating the developmental programme are transcription factors. In the mammalian brain, commitment to a neuronal fate involves the expression of proneural basic helix-loop-helix (bHLH) transcription factors such as Neurogenin1 and Neurogenin2 (Neurog1&2) as well as the mammalian achaete-scute homolog1 (Mash1) (Fode et al., 2000; Nieto et al., 2001). Their expression patterns are largely complementary within the telencephalon and important for the specification of distinct neuronal fates (Guillemot et al., 2006). Expression of Neurogenins is restricted solely to the dorsal telencephalon and induce a regional character by promoting the expression of differentiation genes such as NeuroD1/2, Math2/3 and Nsc1 that are sequentially expressed during neuronal differentiation (Schuurmans et al., 2004; Guillemot et al., 2006). In addition, both Neurogenins are important for activating a program that provides neurons with a glutamatergic phenotype in the dorsal telencephalon (Guillemot et al., 2006). In contrast, high Mash1 expression is confined to the progenitors of the ventral telencephalon that produce mainly GABAergic neurons. The specification of neuron identity has been demonstrated by loss- and gain-of function experiments. Intriguingly, loss of Neurog1&2 results in ectopic expression of ventral and GABAergic genes, while these remain low in the cerebral cortex of Neurog2/Mash1 double mutants (Guillemot et al., 2006). This suggests that Neurog1&2 may specify cortical neuron identity by repression of Mash1 expression (Fode et al., 2000; Schuurmans et al., 2004; Guillemot et al., 2006).

Another regulatory gene that depends on the function of Ngn1/2 is the T-box gene Tbr2

(Englund et al., 2005). Tbr2 is abundantly expressed in basal progenitors and promotes their generation from radial glial cells (Englund et al., 2005). Moreover, recent studies have identified additional transcription factors that add to the specification of basal progenitors. Amongst them Ap2gamma and Fezf1/2, which both are expressed in radial glial cells (Fietz et al., 2010). While Ap2gamma promotes BP specification by directly activating Tbr2, Fezf1/2 drives Tbr2 expression indirectly by a mechanism that involves derepression of Ngn2 (Pinto et al., 2009; Fietz et al., 2010; Shimizu et al., 2010). As mentioned before, BPs form the SVZ which can be recognized as a distinct compartment during mid and late stages of neurogenesis - the time when upper layer neurons are produced. However, several studies including time-lapse imaging have revealed that BPs are abundant during all cortical stages of neurogenesis and do generate neurons of all cortical layers including the earliest born preplate neurons (Arnold et al., 2008; Sessa et al., 2008; Kowalczyk et al., 2009). However, the precise contribution of BPs to each layer remains to be defined (Pontius et al., 2008). In addition to transcription factors that promote their fate, basal progenitors express several molecular factors of upper-layer neurons, such as the cut-like homeobox transcription factors 1 and 2 (Cux1/2). Their expression is detected at or before the onset of upper layer neurogenesis and it has been shown that Cux2 regulates the cell-cycle exit rate of basal progenitors and thereby controls in particular the number of upper cortical neurons generated (Nieto et al., 2004; Cubelos et al., 2008).

Another important transcription factor expressed in radial glia cells and involved in BP specification through directly activating Ngn2 and Tbr2 is Pax6 (Scardigli et al., 2003; Sansom et al., 2009). Pax6 is one of the most intensely studied transcription factors during brain development (Osumi et al., 2008; Georgala et al., 2011a) and has been shown to play multiple roles in the development of the cerebral cortex. Although many functions of Pax6 have been reported and recent advances in identifying Pax6 target genes have been made, the mechanisms of how Pax6 can exert these functions on the molecular level are poorly characterized. Therefore the main part of this thesis work concentrated on dissecting the role of distinct DNA-binding domains of Pax6 in cortical development. Hence, the next chapter describes the transcription factor Pax6 and its various functions during cortical development.

## **1.3 The transcription factor Pax6 – a master regulator**

### **1.3.1 Pax6 Expression**

The expression of Pax6 in mammals has been observed in the pancreas, the gut, the pituitary, in nasal structures, the brain and the spinal cord (Walther and Gruss, 1991). Pax6 expression is important for survival and loss of functional Pax6 in mice leads to death immediately after birth (Hogan et al., 1986). In the developing nervous system of the mouse embryo, Pax6 expression starts as early as E8 in regions of the anterior neural plate that will give rise to the telencephalon, the eyes and the diencephalon as well as in neuroepithelium of the presumptive spinal cord and hindbrain (Fig1-5) (Walther et al., 1991; Stoykova and Gruss, 1994). Within the developing telencephalon Pax6 expression becomes restricted to the radial glial cells that mask the ventricular zone of the dorsal telencephalon and occurs in a gradient with rostral high to caudal low and lateral high to medial low expression (Bishop et al., 2000; Bishop et al., 2002; Muzio et al., 2002b; Muzio and Mallamaci, 2003). During embryonic neurogenesis, Pax6 expression remains in the VZ that gradually becomes thinner as development proceeds. In contrast, Pax6 expression is down-regulated during transition of radial glial cells to the second major progenitor population in the dorsal telencephalon - the basal progenitors (Gotz et al., 1998; Englund et al., 2005). The high expression of Pax6 in the dorsal VZ extends to the border between the dorsal and ventral telencephalon, where Pax6 expression is found in a small stripe of cells along this pallial-subpallial boundary (PSB) (Stoykova and Gruss, 1994; Stoykova et al., 1996). Within the ventral telencephalon low expression of Pax6 is detected in the ventricular zone of the lateral ganglionic eminence (LGE) but is absent in the medial ganglionic eminence (MGE) (Fig.1-5). On cellular level, Pax6 protein in the mouse telencephalon has so far been detected exclusively in the nucleus of radial glial cells. Interestingly, a recent report determined extracellular expression of Pax6 in the embryonic chick spinal cord with paracrine activity (Di Lullo et al., 2011).

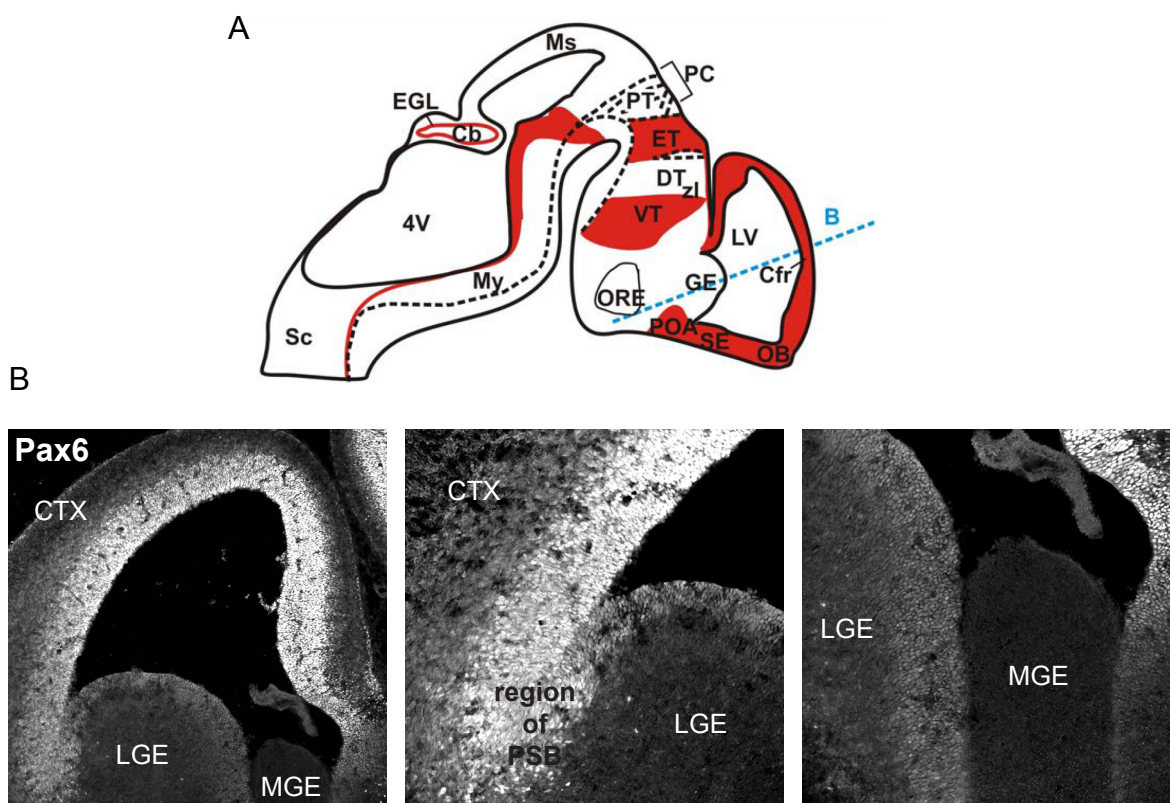


### Figure 1-5 Expression of Pax6 in the developing mouse brain

(A) Schematic drawing of an E13.5 mouse brain (sagittal view), showing the regions of Pax6 expression in red; (taken from PhD-thesis of Nicole Haubst 2005; modified from Stoykova and Gruss 1994).

(B) Micrographs depicting Pax6 expression in one hemisphere of a dorsal section of an E14 mouse telencephalon (coronal view; corresponding to the level indicated by the blue line in A). The border between the dorsal telencephalon (cortex; pallium) and the ventral telencephalon (ganglionic eminences; subpallium) is delineated by the pallial-subpallial boundary (PSB). The ventral telencephalon is further subdivided into the lateral ganglionic eminence (LGE) and medial ganglionic eminence (MGE). High expression of Pax6 is found in the dorsal telencephalon and low levels in the progenitor zone of the LGE. In contrast, Pax6 expression is absent from the MGE. In the dorsal telencephalon Pax6 is expressed in a gradient, showing rostral high to caudal low and laterally high to medial low expression.

Abbreviations: Cb (cerebellum), Cfr (frontal cortex), DT (dorsal thalamus), egl (external granular layer of the cerebellum), ET (epithalamus), GE (ganglionic eminence), LV (lateral ventricle), Ms (mesencephalon), My (myelencephalon), OB (olfactory bulb), ORE (optic recess), PC (posterior commissure), Pn (pons), POA (Anterior preoptic area), PT (pretegmentum), SE (septum), 4V (fourth ventricle).

### 1.3.2 The role of Pax6 in forebrain development

The activity of Pax6 is very complex and most knowledge about Pax6 function comes from studies examining the phenotypes of mutant lines of mice and rats with a mutation in the Pax6 gene that leads to loss of Pax6 function. In mice the Small eye mouse strain (Sey or SeyNeu; termed Pax6<sup>Sey</sup> in this study) is characterized by a natural occurring point mutation that truncates the C-terminal half of Pax6 and creates a truncated protein considered functionally inactive (Hill et al., 1991). In addition, more recent studies either conditionally deleting Pax6 in the cortex (Pinon et al., 2008; Tuoc et al., 2009) or using a gain-of function mouse line have confirmed and revealed more detailed phenotypes (Manuel et al., 2007; Georgala et al., 2011a).

In the developing eye, gross morphological analyses of heterozygote Pax6<sup>Sey</sup> mutants have shown that these mutants possess a small eye phenotype, while homozygous Pax6 mutants completely lack their eyes (Hogan et al., 1986; Osumi et al., 2008). Furthermore detailed analyses have shown that Pax6 function is essential for proper development of the lens and retina (Ashery-Padan et al., 2000; Ashery-Padan and Gruss, 2001; Kozmik, 2005; Graw, 2010). In the developing telencephalon, the gross morphological phenotype after loss of full Pax6 function is a smaller and shorter cerebral cortex with a thinner cortical plate (Schmahl et al., 1993; Heins et al., 2002; Asami et al., 2011). In fact, Pax6 function in the developing telencephalon is essential for various processes such as cell proliferation, neurogenesis, cortical arealization and regionalization of the telencephalon which is in turn coupled to the establishment of the pallial-subpallial boundary (Georgala et al., 2011b). Therefore in the following sections some of these Pax6 functions will be explained in more detail.

#### 1.3.2.1 Pax6 function in dorso-ventral patterning

As described before, the subdivision of the dorsal (pallial) and ventral (subpallial) telencephalon, including the establishment of the pallial-subpallial boundary involves Pax6 function. The PSB itself is molecularly defined with high or restricted expression of factors like Ngn2, Tbr2, Dbx and Pax6 on the dorsal side and factors such as Gsx2, Nkx2.2, Olig2 or Mash1 on the ventral side (Toresson et al., 2000; Yun et al., 2001; Campbell, 2003). In addition also a physical boundary in form of radial glial fascicles develops (Neyt et al., 1997; Stoykova et al., 1997). Loss of functional Pax6 leads to disruption of this molecular and also physical boundary (Stoykova et al., 1997). In particular, the expression of Ngn2 and Tbr2 in the dorsal telencephalon is lost (Stoykova et al., 2000; Toresson et al., 2000; Yun et al., 2001; Haubst et al., 2004), whereas many transcription factors of the ventral telencephalon

such as *Gsx1/2*, *Mash1*, *Dlx1/2* or *Olig2* are misexpressed into the *Pax6<sup>Sey</sup>* mutant cortex (Stoykova and Gruss, 1994; Stoykova et al., 1996; Stoykova et al., 1997; Toresson et al., 2000; Yun et al., 2001; Heins et al., 2002). Moreover an increase in dorsally migrating cells has been reported (Chapouton et al., 1999). Some of these ventral genes such as *Gsx2*, play complementary roles to that of *Pax6* in establishing the boundary. Indeed in functional *Gsx2* null-mutants an opposite phenotype, with ectopic expression of dorsal markers ventrally has been described (Toresson et al., 2000; Yun et al., 2001). *Gsx2* itself is important for the maintenance of molecular identity of early striatal progenitors and loss of *Gsx2* not only results in ectopic expression of dorsal genes ventrally, but also to the loss of other ventral regulatory genes such as *Mash1* or *Dlx* (Toresson et al., 2000). Accordingly, some phenotypes of the *Pax6* or *Gsx2* single mutants are improved in *Gsx2/Pax6* double mutants (Toresson et al., 2000). For example, expression of the regulatory genes *Mash1* and *Dlx* is restored in ventral progenitors and the development of the cerebral cortex in general is improved (Toresson et al., 2000).

#### 1.3.2.2 *Pax6* function in area patterning

Similar to dorso-ventral patterning, the first evidence for *Pax6* function in area patterning came from gene marker analysis in the Small eye mouse. These implicated that *Pax6* is important for specifying rostral and lateral area identities associated with motor and somatosensory areas (Bishop et al., 2000; Bishop et al., 2002; Muzio et al., 2002b; Muzio and Mallamaci, 2003). As mentioned above *Pax6* is expressed in a gradient with highest expression in the anterior progenitors that give rise to these areas and opposite to the expression of *Emx2*, which specifies caudal and lateral areas (Bishop et al., 2000; Bishop et al., 2002; Muzio et al., 2002b; Muzio and Mallamaci, 2003). Loss of functional *Emx2* leads to the expansion of *Pax6* expression into caudal regions of the cerebral cortex, resulting in expansion of motor and somatosensory areas into these regions. And vice versa, in *Pax6<sup>Sey</sup>* mice rostral cortical areas at the level of the motor cortex are compressed and primary visual areas are shifted rostral. (Bishop et al., 2002; Muzio et al., 2002a; Muzio et al., 2002b; Muzio and Mallamaci, 2003). Recent work using cortex-specific conditional *Pax6* knockout mice detected a similar rostral shift of area markers as detected in the *Pax6<sup>Sey</sup>* mice (Pinon et al., 2008). However, the distribution of the area specific projections (thalamocortical and corticofugal) were not affected (Pinon et al., 2008). This suggests that cortical area identities and thalamic connections are uncoupled processes and *Pax6* is mainly involved in the former (Pinon et al., 2008). In addition examining *Pax6*-overexpressing mice, it has been

suggested that the relative levels and not the absolute levels of Pax6 expression are important for specifying area identities (Manuel et al., 2007). Or alternatively that the gradient of Pax6 expression is less important, as Pax6-overexpressing mice (transgenic mice carrying several copies of the human PAX6 locus; termed Pax77) did not exhibit significant shifts of cortical domains (Manuel et al., 2007).

### 1.3.2.3 *Pax6 function in the olfactory system*

Pax6 plays different roles in the olfactory system as revealed by analysis of homozygote and heterozygote (which survive into adult stages) Pax6 deficient mice or rats (Nomura et al., 2007). These showed several abnormalities, including dysgenesis of the olfactory epithelium (Matsuo et al., 1993; Davis and Reed, 1996; Anchan et al., 1997) and mislocation of specific neuronal subtypes in the olfactory cortex and olfactory bulb (Lopez-Mascaraque et al., 1998; Jimenez et al., 2000; Hirata et al., 2002; Nomura and Osumi, 2004; Nomura et al., 2006; Nomura et al., 2007).

The olfactory system develops early during development. The first olfactory sensory neurons (which capture the odorant information) of the olfactory placode (later the olfactory – nasal epithelium) send initial axons to the olfactory bulb (OB) primordium (De Carlos et al., 1995). The OB primordium is specified from rostral areas of the dorsal telencephalon and generates the olfactory bulb in form of a protrusion. The olfactory bulb functions as primary processing center of the odorant information (Lopez-Mascaraque et al., 1998; Lopez-Mascaraque and de Castro, 2002) and consists of two types of neurons: (i) projection neurons including mitral and tufted cells and (ii) interneurons produced mainly in the GE, but also from dorsal telencephalic progenitors with many originating especially from the ventral pallium (Toresson and Campbell, 2001; Wichterle et al., 2001; Gorski et al., 2002; Willaime-Morawek et al., 2006; Kohwi et al., 2007; Ventura and Goldman, 2007; Young et al., 2007; Nomura et al., 2007; Cocas et al., 2011). Pax6<sup>Sey</sup> mice do not develop an olfactory bulb at the rostral part. Instead an olfactory-bulb like structure (OBLS) is formed at the lateral part of the telencephalon (Lopez-Mascaraque et al., 1998; Jimenez et al., 2000; Hirata et al., 2002; Lopez-Mascaraque et al., 2005; Nomura et al., 2007). This structure contains accumulated mitral cells and this mislocation seems to be the primary defect in this abnormal development (Lopez-Mascaraque et al., 1998; Jimenez et al., 2000; Hirata et al., 2002; Lopez-Mascaraque et al., 2005; Nomura et al., 2007).

Pax6 function is also important for generation of some interneuron subtypes. Interneurons of the OB can be subdivided into granule cells (GCs) and periglomerular cells (PGCs).

While GCs all express GABA as neurotransmitter, PGCs are more heterogeneous including GABAergic dopaminergic and glutamatergic neurotransmitter types (Nomura et al., 2007). The generation of olfactory-bulb interneurons continues after birth and is in particular investigated as model of adult neurogenesis (Nomura et al., 2007; Kriegstein and Alvarez-Buylla, 2009) from neural stem cells that reside in the telencephalic subependymal zone (SEZ). Pax6 expression is found in these adult stem cells as well as in neuroblasts that migrate along the rostral-migratory stream towards the OB (Hack et al., 2005; Kohwi et al., 2005). Upon arrival in the olfactory bulb, the vast majority of neuroblasts lose Pax6 expression, except the subset destined for dopaminergic neuronal fate (Hack et al., 2005; Brill et al., 2009; Ninkovic et al., 2010). Gain-of Pax6 function by overexpression in-vivo increases the number of dopaminergic tyrosine hydroxylase positive (TH+) PGCs (Hack et al., 2005; Brill et al., 2008). Conversely, the generation of dopaminergic neurons is reduced in the adult olfactory bulb of Pax6 mutant mice (Dellovade et al., 1998; Kohwi et al., 2005; Ninkovic et al., 2010). Thus Pax6 is necessary for specification of dopaminergic periglomerular neurons in the olfactory bulb.

#### *1.3.2.4 Pax6 function in proliferation and neurogenesis*

The role of Pax6 in proliferation appears complex and in a context-dependent manner. In the developing cortex, Pax6 deletion has been described to increase proliferation, in particular at non-apical positions (Gotz et al., 1998; Estivill-Torrus et al., 2002; Haubst et al., 2004; Quinn et al., 2007; Tuoc et al., 2009). This phenotype goes along with several influential changes, one of which as described before the ventralization of dorsal progenitor identity. Moreover, loss of functional Pax6 was reported to result in premature delamination from the apical surface contributing to the non-apical proliferating progenitor increase (Asami et al., 2011). In contrast to the telencephalon, decreased cell proliferation was reported in other regions of Pax6 expression in Pax6 mutants, like the diencephalon (Warren and Price, 1997) and the developing eye (Marquardt et al., 2001). However no change in cell proliferation was detected in the cerebellum of Pax6<sup>Sev</sup> mice (Engelkamp et al., 1999). Thus Pax6 regulates cell proliferation on a rather region- and cell type-specific manner. Notably, on transcriptional level Pax6 has been observed to control both – proliferation promoting and inhibiting factors – even in the same cell type (Holm et al., 2007; Osumi et al., 2008; Sansom et al., 2009).

Neurogenesis is tightly linked to proliferation, as to become a neuron a cell has to leave the cell cycle and differentiate. Several studies with different Pax6 mutants including the Pax6<sup>Sey</sup> (Estivill-Torres et al., 2002), Pax6<sup>-/-</sup>/Pax6<sup>+/+</sup> chimeric mice (Quinn et al., 2007) and conditional deletion of Pax6 in a cortex specific manner (Tuoc et al., 2009) have shown that loss of Pax6 leads to an accelerated withdrawal from the mitotic cycle and results in premature differentiation of the progenitors at early stages (E12/ E13) (Georgala et al., 2011b). Interestingly, overexpression of Pax6 leads to changes of the proliferation rate of late progenitors (E15.5) and also promotes cell-cycle exit at late stages of corticogenesis (Manuel et al., 2007; Georgala et al., 2011b). In any case, the progenitor pool is affected and influences the production of correct neuronal numbers. Indeed, Pax6<sup>Sey</sup> mice are characterized by a thinner cortical plate (Schmahl et al., 1993; Caric et al., 1997; Gotz et al., 1998; Warren et al., 1999; Fukuda et al., 2000; Haubst et al., 2004). But also after conditional deletion and overexpression of Pax6 reduced numbers of neurons have been reported (Tuoc et al., 2009; Georgala et al., 2011b).

As described before, cortical progenitors give rise to different neuronal subtypes with earlier born neurons found in deep-layers and later born neurons found at earlier stages. Studies examining the generation of distinct layers in Pax6<sup>Sey</sup> mice suggested that specifically upper-layer neurons are reduced (Stoykova et al., 1996; Caric et al., 1997; Gotz et al., 1998; Tarabykin et al., 2001; Nieto et al., 2004; Schuurmans et al., 2004). However, a more recent report has examined the layer production after conditional deletion of Pax6, which has had the advantage of analyzing the mutant cortex at juvenile stages (postnatal day 8) (Tuoc et al., 2009). This is the time when all neurons have reached their final location. Conditionally deleting Pax6 from early cortical progenitors resulted in an increase of early born neuronal subsets in the marginal zone and of deep cortical layers (Tuoc et al., 2009). As a consequence the progenitor pool for later-born, upper layer neurons was affected with almost complete loss of upper layer neuronal subtypes (Tuoc et al., 2009). Interestingly, in contrast, the conditional deletion of Pax6 at later stages - when the deep layer neurons were already born - did not affect upper-layer genesis. This suggests that cortical progenitors at different stages must have different requirements for Pax6 or alternatively Pax6 performs different functions at different stages (Tuoc et al., 2009).

As described before, cortical neurons arise from both apical and basal progenitors and Pax6 expression in radial glial cells promotes the generation of basal progenitors. Recent studies have identified several factors important for generation of basal progenitors and

neurogenesis, which are transcriptionally regulated by Pax6. Amongst them, Ngn2 which is expressed in a subset of neuronal committed apical progenitors (Schuurmans et al., 2004; Guillemot, 2005). Pax6 positively regulates Ngn2 via an enhancer (Scardigli et al., 2001), but also synergizes with Ngn2 in the generation of basal progenitors (Scardigli et al., 2001; Miyata et al., 2004; Britz et al., 2006; Guillemot et al., 2006). Both transcription factors promote expression of Tbr2/Eomes, a key factor of basal progenitor identity in the dorsal cortex (Englund et al., 2005; Quinn et al., 2007; Arnold et al., 2008; Sessa et al., 2008; Sansom et al., 2009). Pax6 deficiency results in almost complete loss of Ngn2 and Tbr2 expression leading to abnormally specified basal progenitors (Haubst et al., 2004; Quinn et al., 2007). Indeed the non-apical dividing cells in chimeric mice do not express Tbr2 (Quinn et al., 2007). This is of course part of the influences contributing to the altered production of cortical neurons.

In addition to its function in proliferation, Pax6 is an important neurogenic fate determinant in radial glial cells (Gotz et al., 1998; Hack et al., 2004a). Loss of Pax6 results in a reduced neurogenic potential of radial glial cells (Heins et al., 2002; Haubst et al., 2004). Conversely overexpression of Pax6 in cultured cells enhanced neuron production from radial glial cells (Heins et al., 2002; Haubst et al., 2004). This neurogenic potential of Pax6 is not restricted to time and region, as overexpression of Pax6 in cultures from postnatal astrocytes (Heins et al., 2002) or from adult neurospheres (Hack et al., 2004b) likewise increased neurogenesis.

### **1.3.3 Complexity of Pax6 – structure and isoforms**

The transcription factor Pax6 belongs to the Pax (paired box) family of developmentally regulated transcription factors which commonly share an amino-terminal DNA-binding domain known as the paired domain (PD) (Chalepakis et al., 1992). This domain consists of 128 amino acids and is in itself structured in a bipartite, modular manner divided into its N-terminal PAI-subdomain (3aa-76aa) and its C-terminal RED-subdomain (77aa-131aa) ('PAI-RED') that coincide with an exon boundary (Fig.1-6) (Walther et al., 1991; Czerny et al., 1993; Epstein et al., 1994a; Epstein et al., 1994b; Jun and Desplan, 1996; Xu et al., 1999). Crystallographic analyses using only a PD peptide have shown that both subdomains are comprised of helix-turn helix folds. These can interact with specific DNA-binding sites independently or in a cooperative manner (Epstein et al., 1994a; Yamaguchi et al., 1997). For example, the PAI- subdomain showed direct contacts to its annotated Pax6

consensus site P6CON (Epstein et al., 1994a), while the RED-subdomain contributed to DNA binding by contacting adjacent nucleotides (Epstein et al., 1994b; Xu et al., 1999). In addition, DNA-contact was also established between the N-terminal  $\beta$ -sheets and a linker region between the subdomains (Xu et al., 1999).

The third DNA-binding domain of Pax6, the paired-like homeodomain (HD) is connected to the PD via a glycine-rich linker, followed by a C-terminal transactivation domain (Fig.1-6) (Bouchard, 2003). Similar to other HDs, it harbors a globular domain with three alpha helices (60aa long) and its critical DNA-binding residues are located in helix3. In contrast to sequence specific DNA-binding proteins that use only one DNA-binding domain, Pax6 can use its multiple DNA-binding parts (PAI,  $\beta$ -sheet, linker, RED and HD) or take advantage of a range of their combinations to bind to DNA (Xie and Cvekl, 2011). Earlier studies have defined individual consensus sites for the Pax6 PD (Epstein et al., 1994a) and the HD (Wilson et al., 1993; Czerny and Busslinger, 1995). However, using for example the P6CON consensus sequence to predict and confirm candidate Pax6-binding sites has proven to be difficult (Shimoda et al., 2002; Visel et al., 2007; Wolf et al., 2009). But, recent work has identified several novel variants of Pax6 DNA-binding motifs to which different combinations of the Pax6 binding subdomains bind in-vivo (Xie and Cvekl, 2011) (Fig.1-7).

The PAX6 gene generates multiple transcript variants by alternative splicing or transcription from an alternative promoter. One of the two most commonly expressed Pax6 transcripts that encode a functionally distinct protein is the Pax6(5a) isoform (Fig.1-6). It is generated upon alternative splicing of exon 5a (14 amino acids) which is inserted into the N-terminal PAI subdomain (Walther and Gruss, 1991; Glaser et al., 1992; Puschel et al., 1992). This insertion leads to the abolishment of PAI-subdomain DNA-binding activity, but retains RED-subdomain activity (Epstein et al., 1994b; Kozmik et al., 1997; Anderson et al., 2002). Both splice products, the canonical Pax6 and the Pax6(5a) isoform are found in the brain, developing eye, spinal cord and olfactory epithelium (Walther and Gruss, 1991; Glaser et al., 1992). However the Pax6(5a) transcript is expressed at lower levels and the ratio of both isoforms seems to be critical as reported for eye development (Chauhan et al., 2004).

The second major Pax6 isoform lacks the whole paired domain, restricting its activity to the homeodomain and thus is termed PD-less (Fig.1-6) (Mishra et al., 2002). It is present in brain, eye and pancreas (Mishra et al., 2002) and unlike the Pax6(5a) isoform which is vertebrate specific, variants of the PD-less isoform have also been found in invertebrates. Two studies exist, one reporting that the murine PD-less form of Pax6 is generated by alternative splicing (Mishra et al., 2002), the other reporting that the murine PD-less form is

generated through the usage of an alternative promoter (Kim and Lauderdale, 2006). The quail variant is generated through the use of an alternative start codon for translation in the sequence between the PD and the HD (Carriere et al., 1993) and the PD-less form found in *C.elegans* is transcribed from an internal promoter (Zhang and Emmons, 1995). The PD-less form has been shown to bind to the classical P2 HD Pax6 consensus site, but without activating transcription (Mishra et al., 2002). However, transcriptional activation through the interaction of the PD-less form with the full length Pax6 has been reported in- vitro (Mikkola et al., 2001) and in-vivo (Ninkovic et al., 2010). In the latter study, this interaction has been shown to regulate expression of  $\alpha$ A crystallin, which is important to control survival rates of mature dopaminergic neurons in the adult olfactory bulb.

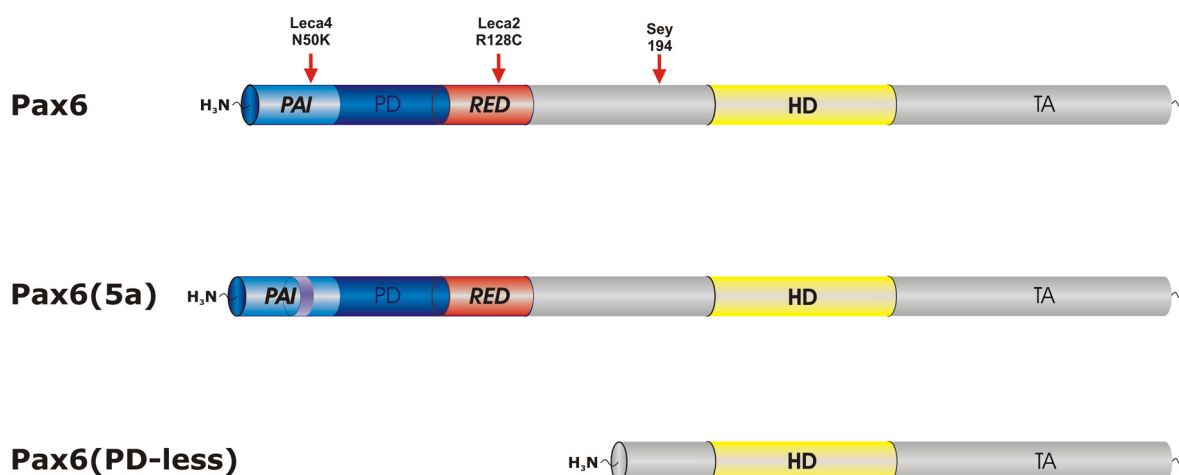


**Figure 1-6 Schematic drawing depicting the domain structure of Pax6 and its two most abundant isoforms**

Canonical Pax6 (422AA) consists of a paired-domain (PD) with bipartite character; subdivided into the N-terminal PAI and the C-terminal RED subdomains (PAI-RED). The PD is linked to the homeodomain (HD) of Pax6 via a glycine rich linker region, followed by a transactivation domain (TA). The 5a-isoform (436AA) is characterized by the insertion of 14 amino acids into the PAI subdomain. The PD-less isoform completely lacks the PD and parts of the linker region of Pax6.

The red arrows indicate the site of mutation occurring in the different Pax6 mutants used in this study. The point mutation in the full mutant Pax6<sup>Sey</sup> creates a truncated protein (Hill et al., 1991), while the point mutation in the Pax6<sup>Leca4</sup> and Pax6<sup>Leca2</sup> mutant affect the DNA-binding of the PAI or RED subdomain, respectively (Thaung et al., 2002).

Motif Names	Motifs
<b>P6CON</b> (Epstein 1994)	
<b>1-1</b> PAI/ $\beta^{GC}$ /L (SELEX)	
<b>1-2</b> PAI/ $\beta^{GC}$ /L (Natural)	
<b>1-3</b> PAI/ $\beta^{GC}$ /L (Natural)	
<b>2-1</b> HD/PAI/ $\beta^{GC}$ /L (SELEX)	
<b>2-2</b> HD/PAI/ $\beta^{GC}$ /L (Natural)	
<b>3-1</b> PAI/ $\beta^{GC}$ /L/RED (SELEX)	
<b>3-2</b> PAI/ $\beta^{GC}$ /L <sup>TT</sup> /RED (Natural)	
<b>3-3</b> PAI/ $\beta^{GC}$ /L <sup>TT</sup> /RED (Natural)	
<b>4-1</b> HD/L/RED (SELEX)	

**Figure 1-7 Pax6 DNA-binding site variants** (taken from Xie *et al.*, 2011)

Summary showing novel variants of Pax6-binding sites recently identified by Selex (Systematic evolution of ligands by exponential enrichment) and subsequently identified natural sites in-vivo. These different motifs are bound by Pax6 using different combinations of its subdomains. The binding affinity of Pax6 has been confirmed by EMSA and Luciferase assay.

### 1.3.4 Molecular mechanisms underlying the multiple functions of Pax6

Recent advances have been made in identifying genes regulated by Pax6 that are important for proliferation, neurogenesis and fate determination (Sansom et al., 2009; Wolf et al., 2009; Coutinho et al., 2011; Xie and Cvekl, 2011). One study using chromatin immunoprecipitation combined with promoter microarray analysis (Chip-on-chip) has reported that Pax6 positively regulates cohorts of genes that promote proliferation, basal progenitor generation and neurogenesis (Sansom et al., 2009). In addition, Pax6 is thought to interplay with other regulators of cortical neurogenesis that impact on one another. In these regards, it has been suggested that Pax6 functions to control the balance between proliferation and differentiation in cortical progenitor cells (Sansom et al., 2009). However, it is still poorly understood how Pax6 instructs its different functions on the molecular level. One option is to utilize its different DNA-binding domains. As described above, the Pax6 protein consists of the paired-domain (PD) carrying a bipartite DNA-binding motif (PAI- and RED-subdomain) which is linked to a paired-like homeodomain (HD). A previous study from our lab used different mutant mouse lines with disruption of the paired-domain (Pax6<sup>Aey18</sup>) or the homeodomain (Pax6<sup>4NEU</sup>) to investigate the impact of the different domains on telencephalic development (Haubst et al., 2004). The Aey18 mutation in Pax6 creates a considerable deletion within the complete PD (Graw et al., 2005) and shows similar defects like the full Pax6 mutant Pax6<sup>Sey</sup> in telencephalic development (Haubst et al., 2004). However, it has then been shown that this mutation affects nuclear localization of the protein (Dames et al., 2010), which explains the similarities to the full Pax6 mutant (Haubst et al., 2004; Graw et al., 2005). The analysis of the 4NEU mutation – which disrupts the DNA-binding property of the homeodomain – has shown that the HD of Pax6 plays a role in the establishment of the pallial-subpallial boundary during forebrain development. Pax6<sup>4NEU</sup> mutants completely lacked the expression of the Wnt-inhibitor and boundary marker SFRP2. However, no other defects were detected in the boundary region and in cell proliferation and neurogenesis (Fig.1-8) (Haubst et al., 2004). Moreover, no defects during cortical development were observed in another homeodomain mutant line – the Pax6<sup>14NEU</sup> (Ninkovic et al., 2010). The homeodomain exerts subtle effects during telencephalic development and one part of the present thesis was to understand the molecular network underlying these effects. However, this implies that the majority of effects Pax6 exerts during telencephalic development should be mediated by the bipartite paired-domain with potentially different contributions of its subdomains. Therefore, the main part of this work concentrated on dissecting the role of the different subdomains of the paired-domain of Pax6 during telencephalic development.

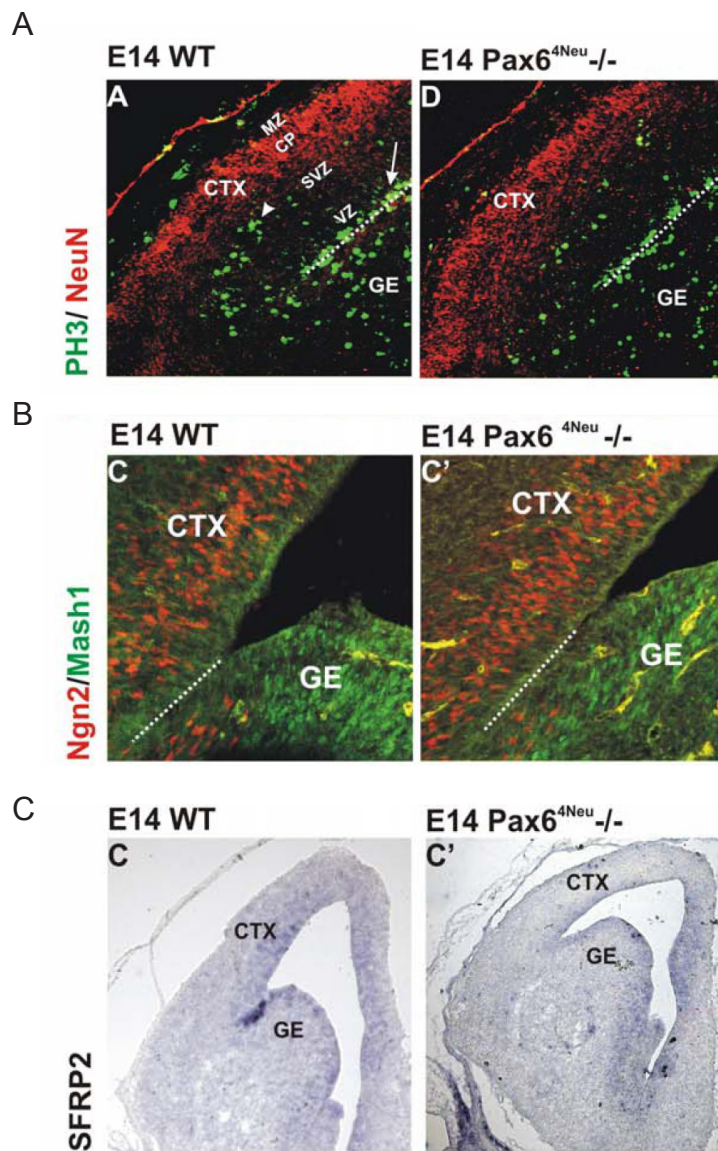


**Figure 1-8 Effect of the Pax6<sup>4NEU</sup> mutation (in the homeodomain) on telencephalic development (adapted from Haubst et al., 2004)**

Short summary of the telencephalic phenotype observed after loss of homeodomain function in the Pax6<sup>4NEU</sup> mutant (characterized by a point-mutation in the DNA-binding helix of the homeodomain). (A) No changes in neurogenesis and proliferation were detected in the Pax6<sup>4NEU</sup> mutant compared to control mice as revealed by NeuN (labeling neurons) and PH3 (labeling mitotic cells) analysis in coronal sections of E14 mutant and WT embryos; micrographs showing examples are depicted. (B) Similar, dorso-ventral patterning was not changed as shown by Ngn2 (dorsal) and Mash1 (mainly ventral) immunostainings. (C) In contrast, expression of SFRP2 (secreted frizzled related protein) 2 at the pallial-subpallial boundary is lost in Pax6<sup>4NEU</sup> mice as depicted by in-situ hybridization. Thus, DNA-binding of the homeodomain of Pax6 is necessary for the correct establishment of the pallial-subpallial boundary.

Abbreviations: CP, cortical plate; CTX, cortex; GE, ganglionic eminence; MZ, marginal zone; SVZ, subventricular zone; VZ, ventricular zone.

## 1.4 A fate determinant from the RNA world: the microRNA

Transcription factors not only regulate the expression of specific mRNAs, but also control expression of microRNAs (miRNAs). However, nothing is known about transcriptional control of microRNAs in the developing cortex. MicroRNAs were first discovered in nematodes in 1993. They are non-coding RNAs that are related to small interfering RNAs (siRNAs), the small RNAs that guide RNA interference (RNAi). The high abundance of miRNAs in the nervous system suggests that miRNAs may represent important post-transcriptional regulators by shaping expression profiles that occur in neural cells (Li and Jin, 2010).

### 1.4.1 The microRNA pathway

To date, hundreds of genomically encoded miRNAs have been described in mice. Two classes of miRNAs can be distinguished dependant on their genomic location: (i) intergenic miRNAs, which are synthesized from their own promoters and (ii) intragenic miRNAs, which are found embedded in intronic or exonic regions and are transcribed as part of their host gene (Ying and Lin, 2005; Kim et al., 2009). The transcription of intergenic miRNA genes can be performed by RNA polymerase II or RNA polymerase III (Lee et al., 2004; Borchert et al., 2006; Kawahra et al., 2012). In contrast, intragenic miRNAs are exclusively transcribed by RNA polymerase II (Lee et al., 2004). Most miRNAs are synthesized by Pol III generating a several kilobases long miRNA precursor termed primary miRNA (pri-miRNA) (Kawahara et al., 2012). These pri-miRNAs are processed in the nucleus by cropping into 60-100nt long intermediates known as pre-miRNAs that form hairpins. This cleavage is performed by the enzymatic complex called microprocessor, which includes the RNase III enzyme Drosha and the dsRNA binding protein DGCR8 (DiGeorge syndrome critical region gene 8) (Gregory et al., 2004). Recently it has been shown that some intronic miRNAs are processed as spliced-out introns and therefore were termed mirtrons (Okamura et al., 2007; Ruby et al., 2007; Ozsolak et al., 2008; Kawahara et al., 2012). Their precursors (pre-mirtrons) have a shorter stem length than that of canonical miRNAs. In the next step, the pre-miRNAs and mirtron hairpins are exported from the nucleus to the cytoplasm by Exportin-5 and Ran-GTP (Yi et al., 2003). Following the export, the pre-miRNA is further processed by the cytoplasmic RNase III enzyme Dicer, which removes the terminal loop thereby generating a 22nt miRNA duplex that bears a 2-nt overhang on its 3' prime end (Bernstein et al., 2001; Grishok et al., 2001; Hutvagner et al., 2001). This short-lived duplex contains the mature miRNA (the guide strand) and the miRNA\* (the passenger strand). The latter may be degraded, while

the mature miRNA is incorporated into the RNA induced silencing complex (RISC). In case that two mature miRNAs originate from the opposite arms of the same pre-miRNA they are distinguished with a -3p or -5p suffix (Schwarz et al., 2003). The RISC complex then guides the mature miRNA to its target mRNA (Hammond et al., 2000; Martinez and Tuschl, 2004). The nucleotides 2-8 within the miRNA's 5' end are known as the "seed" sequence and are crucial for gene silencing (Bartel, 2009). Base-pair matching between this seed sequence of the miRNA with the target mRNA (mostly within the 3' (or 5') untranslated region (UTR) of target RNA) effects gene silencing (Kawahara et al., 2012). This silencing is achieved either by translational repression or target mRNA breakdown (Bartel, 2004; Du and Zamore, 2005; Kawahara et al., 2012). For summary of the microRNA biogenesis pathway see Fig.1-9.

#### **1.4.2 The role of microRNAs in the developing nervous system**

To determine the role of microRNAs in neural differentiation and the developing nervous system, early studies have focused on animal models in which key components of the miRNA pathway have been inactivated globally or in a cell-type specific manner (Lau and Hudson, 2010). For instance, loss of Dicer in Zebrafish lead to defective neural tubes, providing the first evidence that miRNAs are important for brain development (Giraldez et al., 2005; Li and Jin et al., 2004). Similarly, deletion of Argonaute 2 protein in mice prevented neural tube closure (Liu et al., 2004). In contrast, global deletion of Dicer or DGCR8 in mice resulted in more severe phenotypes with early embryonic lethality (Bernstein et al., 2003; Wang et al., 2007). This precluded analysis of neural development, and therefore several studies focused on inactivating Dicer in specific neural cell types, using the Cre-loxP system. For example Dicer was deleted from Purkinje cells (Schaefer et al., 2007), dopaminergic neurons (Hebert and De Strooper, 2007; Kim et al., 2007) or in the retina (Damiani et al., 2008). In all cases, the conditional, cell-type specific loss of Dicer lead to progressive neurodegenerative phenotypes (Hebert and De Strooper, 2007; Schaefer et al., 2007; Damiani et al., 2008). In the developing dorsal telencephalon, Dicer was conditionally deleted using an Emx1-Cre strain (De Pietri Tonelli et al., 2008). This recombination affected corticogenesis early in development as in-situ analysis evidenced the loss of miRNAs by E10.5. Interestingly, this resulted in neuron loss (due to neuronal apoptosis) that occurred before problems were observed in progenitor cells. This led to the reduction of cortical size by E13.5 and defective cortical layering postnatally. Eventually, around midneurogenesis apical and basal progenitors showed proliferation defects and were depleted by apoptosis contributing to this phenotype (De Pietri Tonelli et al., 2008). These results suggest that microRNAs play

an indispensable role in neuronal differentiation. Moreover a recent study has determined the altered proteome after conditional deletion of cortical Dicer and suggested that normal Dicer activity is important for regulating neural stem cell development by maintaining proper signaling pathways related to cell survival and differentiation (Kawase-Koga et al., 2010). However, Dicer knockout studies have two disadvantages: on the one hand it is not clear if the observed defects are caused alone by an impaired miRNA pathway or through other classes of small regulatory RNAs that also require Dicer activity. On the other hand, these studies affect the miRNA repertoire, while it would be of specific interest to identify specific miRNAs required to alter a cellular program.

Recent studies have provided some advances in identifying specific miRNAs and their function in neural differentiation. For example, miRNA-138, miR-338 and miR-219 were found to play a role in oligodendrocyte differentiation and are required for myelination (Lau et al., 2008; Dugas et al., 2010; Zhao et al., 2010). Moreover important transcription factors (Sox6, Foxj3 and Zfp238) in regulating oligodendrocyte proliferation and the mitogen receptor Pdgfra were identified as direct targets of miR-219 in this context. Another example of a well-studied miRNA in neuronal differentiation is miR-9, which is expressed exclusively in the brain. In-utero electroporation of miR-9 in the mouse cortex around midneurogenesis led to a decrease in proliferation of progenitor cells accompanied by premature differentiation (Zhao et al., 2009). Moreover this study showed that miR-9 forms a regulatory feedback loop with the nuclear receptor TLX and thus fine-tunes the balance between progenitor proliferation and differentiation (Zhao et al., 2009). Furthermore, a more recent study added additional factors to the list of miR-9 targets in the developing forebrain. The transcription factors Foxg1, Nr2e1, Gsx2 and Meis2 were identified as direct targets and found dysregulated in miR-9-2/3 double mutant mice. These showed defects in proliferation and differentiation of pallial and subpallial progenitors (Shibata et al., 2011), thus supporting a critical role for this miRNA during neuronal proliferation and differentiation. The authors furthermore suggested that miR-9 may indirectly control Pax6 levels through regulation of Meis2, as Pax6 levels were found reduced in the miR-9-2/3 double mutant telencephali and because Meis2 has been implicated in Pax6 regulation (Agoston and Schulte, 2009; Shibata et al., 2011).

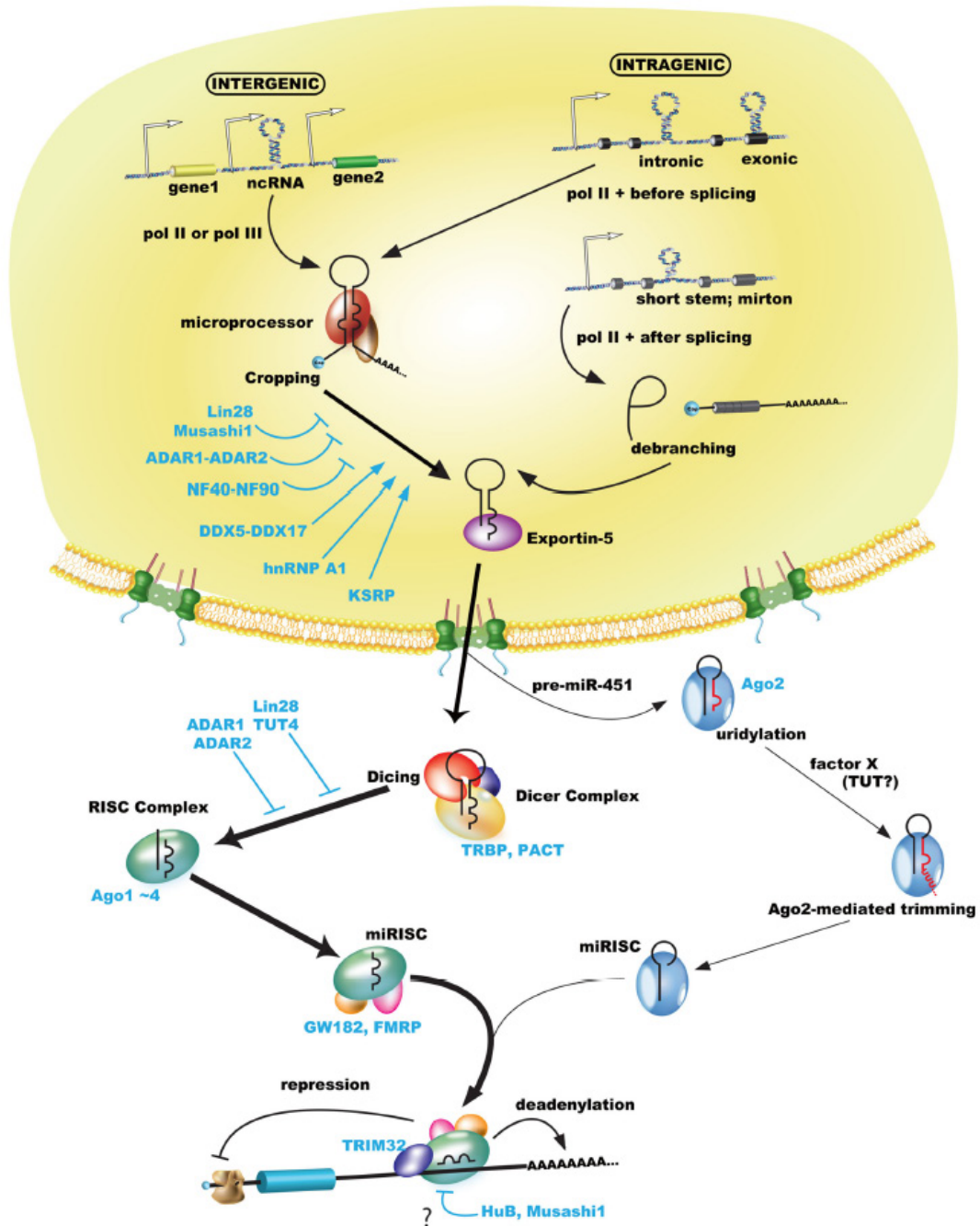


**Figure 1-9 MicroRNA biogenesis pathway** (taken from Kawahara et al., 2012)

Model showing the generation of mature microRNAs including some regulations of RNA-binding proteins at different biogenesis steps (blue text). The process of miRNA generation proceeds from transcription through nuclear processing (cropping), nuclear export, cytoplasmic processing by the Dicer complex (dicing) or Ago2 and finally to incorporation into miRISC (miRNA-loaded RISC). The assembled miRISC can then target mRNAs by base-pairing of the seed sequence. Gene silencing is achieved either by inhibiting translation of the targeted mRNA or by mRNA degradation via deadenylation of poly(A)-tails functions in the miRISC.

### 1.4.3 MicroRNAs in embryonic stem cells

Like the determination of miRNA function in-vivo - in the developing nervous system - the role of the miRNA pathway in embryonic stem cells (ESCs) has been established by loss-of-function studies (Wang et al., 2009b). The conditional inactivation of Dicer in mouse ESCs affects the maturation of miRNAs and impairs the proliferation capacity as well as the cells' differentiation potential (Wang et al., 2009b). However, although Dicer-deficient ESCs are viable, they fail to further differentiate to embryoid bodies (EBs) (Kanellopoulou et al., 2005; Murchison et al., 2005).

The characterization of specific miRNAs in ESCs is also just at its beginning (Wang et al., 2009b). Previously, a cluster of six miRNAs (miR-290 to miR-295) was identified specifically in undifferentiated mouse ESCs and implicated to regulate ESC maintenance and differentiation (Houbaviy et al., 2003; Chen et al., 2007; Benetti et al., 2008; Sinkkonen et al., 2008). In correlation with embryonic neurogenesis in-vivo expression of miR-9 and miR-124 (another brain specific miRNA) are induced during neuronal differentiation from mouse ESCs and affect neural lineage differentiation (Krichevsky et al., 2006).

Taken together, microRNAs represent important regulators during development that add a level of regulation to the genetic programs orchestrated by transcription factors. Therefore understanding miRNA regulation as well as specific miRNA functions during nervous system development is important.

ESC differentiation systems are useful tools for profiling studies, therefore in this thesis the ESC differentiation system according to Bibel et al., 2004 / Bibel et al., 2007 was used to profile miRNA expression. This differentiation protocol allows the generation of a relatively homogeneous population of Pax6 positive radial glial cells from highly proliferative ES cells upon treatment with retinoic acid (RA). When further differentiated, these cells give rise to functional glutamatergic neurons in accordance to neurons derived of Pax6 expressing precursors in the developing mammalian cortex. Therefore this system with radial glia obtained through differentiating ES cells resembled a promising tool to study miRNA expression.

### **1.5 Aim of the thesis**

Given the various functions the transcription factor Pax6 regulates during cerebral cortex development (Osumi et al., 2008; Georgala et al., 2011b), the main aim of my thesis was to investigate the different DNA-binding domains of Pax6 and their individual contributions to Pax6 function during cerebral cortical development. To dissect the importance of these individual DNA-binding domains and in particular of the subdomains of the paired domain of Pax6, I analyzed different mouse-mutant lines each harboring a point-mutation in one DNA-binding domain.

Pax6 acts as a transcriptional regulator of many mRNA coding genes, but may also control expression of miRNA molecules. However, expression and the role of individual miRNAs are still poorly understood. To identify novel miRNA candidates, potentially regulated by Pax6, I performed a miRNA profiling analysis using an ESC-differentiation system (Bibel et al., 2004; Bibel et al., 2007) that comprised Pax6<sup>+</sup> radial glial cells.

## 2 Results

### 2.1 Relevance of the Pax6 homeodomain during cortical development

During development radial glial cells in the developing telencephalon are specified by the transcription factor Pax6, which, as explained before regulates various cellular functions. On the molecular level, Pax6 has several options to mediate its functions utilizing its different DNA-binding domains. Immunohistochemical analysis of the homeodomain mutant mouse line Pax6<sup>4Neu</sup> has attributed to the HD of Pax6 a role in the establishment of the pallial-subpallial boundary during forebrain development (Favor et al., 2001; Haubst et al., 2004). However, other Pax6 regulated functions were unaffected (Favor et al., 2001; Haubst et al., 2004). This mouse line was generated in a mutagenesis screen for dominant mutations affecting eye morphology and carries a point mutation in the third helix of the homeodomain (Ser273Pro), critical for DNA-binding (Favor et al., 2001). In order to gain more insights into the molecular network underlying homeodomain function in the developing telencephalon, this homeodomain mutant line was used to perform a transcriptome analysis.

#### 2.1.1 Gene expression analysis of the homeodomain mutant Pax6<sup>4NEU</sup> during forebrain development

To investigate homeodomain mediated effects of Pax6 on transcriptional level a genome wide expression analysis was performed on E12 cortical tissue from homozygous Pax6<sup>4Neu</sup> and compared to corresponding wild type littermates. The time point E12 was chosen to minimize potential secondary effects and to compare the results to existing microarray data obtained from Pax6<sup>Sey</sup> mice at E12 (Holm et al., 2007). mRNA of three biological replicates for each genotype derived from three different litters were hybridised to whole-genome Affymetrix MOE430 2.0 arrays. Gene expression differences between WT and mutants were assessed by a filter consisting of statistical significance (FDR<10%) in at least two of the three statistical tests performed (see Material and Methods). Divisive clustering (Fig.2-1A) and agglomerative clustering (data not shown) of the samples showed that the samples did not cluster according to their genotype, likely due to the low expression changes observed. Furthermore, one of the WT samples clustered poorly with its corresponding Pax6<sup>4Neu</sup> homozygous littermate and showed an up-regulation of Pax6 mRNA levels similar to the homozygous samples. As the mRNA level of Pax6 is known to be up-regulated in Pax6 mutants due to Pax6's negative auto regulatory function (Manuel et al., 2007), this was a

strong criterion to exclude this WT sample for further analysis. Finally, after exclusion of WT sample 3, the analysis revealed very few and very mild significant changes in gene expression between wild-type and Pax6<sup>4Neu</sup> cortices. In total the expression of 36 genes was altered of which six genes were up-regulated and 30 genes were down-regulated (Fig.2-1B). Amongst these two genes known to be regulated by Pax6, namely Pax6 itself and Cadherin4 were identified (Andrews and Mastick, 2003; Manuel et al., 2007), as well as three additional genes (Ngn1, Ctnnd2, Fhl1) that were found similarly down-regulated in the functional Pax6 null mice (Holm et al., 2007). However, no alterations in expression levels of pallial-subpallial boundary genes were detected. From the 36 genes, 14 genes were selected for q-PCR confirmation analysis. All but one gene showed the same expression trend, however using one-way Anova statistical analysis only one of these genes (Prr15) could be confirmed as significantly regulated (Fig.2-1C,C'). In conclusion, the very few and low expression changes observed in the Pax6<sup>4Neu</sup> mutant with microarray analysis could not be validated applying q-PCR analysis as a second method. Thus transcriptional regulation by the homeodomain of Pax6 seems to play no impact on forebrain development, which is in strong contrast to e.g. the role of the homeodomain of Pax6 during eye development (Kozmik, 2005).

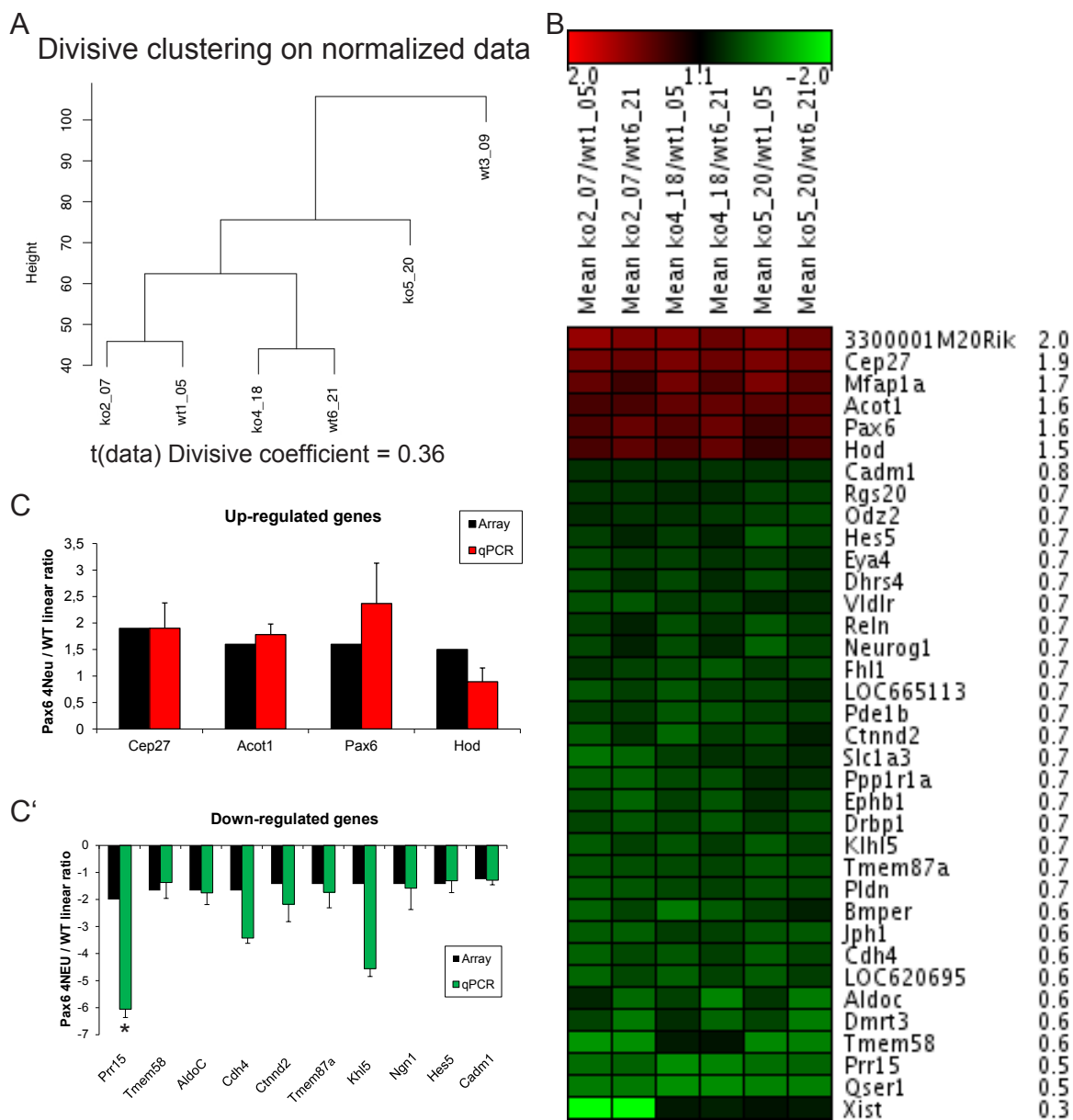


**Figure 2-1 Transcriptome analysis of Pax6<sup>4NEU</sup> cortices**

(A) Divisive clustering analysis of E12 Pax6<sup>4NEU</sup> and wild-type control cortical tissue (the label ko stands for homozygous Pax6<sup>4NEU</sup>). (B) Heatmap representations of linear ratios of genes deregulated between Pax6<sup>4NEU</sup> and wild-type cortices. Colors indicate higher (red) or lower (green) expression values. (C and C') Histograms depicting the linear ratio of gene expression levels between Pax6<sup>4NEU</sup> and the corresponding WT littermates measured by Affymetrix array analysis or quantitative RT-PCR; Data are shown as mean  $\pm$  SEM;

## 2.2 Functional dissection of the paired-domain of Pax6 during cortical development

The above and previously described observation, that the homeodomain plays hardly any role during telencephalic development (Haubst et al., 2004; Ninkovic et al., 2010), suggested that the multiple functions of Pax6 during forebrain development are mediated via its paired domain. To examine to which extent the two subdomains of the paired domain ascertain specific Pax6 functions, two mouse mutants each carrying a point-mutation in one subdomain of the bipartite paired DNA-binding motif (PAI or RED domain respectively) were analysed. Both mouse lines ( $Pax6^{Leca4}$  and  $Pax6^{Leca2}$ ) were recently identified in an ENU-induced screen for eye mutations (Thaung et al., 2002) and named lens-corneal adhesion (Leca) after the occasional occurrence of adhesion between the lens and the cornea in some of the four newly reported lines (Leca1-Leca4) (Thaung et al., 2002). The  $Pax6^{Leca4}$  mutation results in a single base pair substitution of lysine for asparagine (N50K) in the PAI-subdomain and is predicted to disrupt DNA-binding ((Thaung et al., 2002) and in-silico analysis by our collaborator Dierk Niessing). The  $Pax6^{Leca2}$  mutation is the consequence of the substitution of cysteine for arginine (R128C) in the RED- subdomain, a mutation that has also been observed in patients (Azuma et al., 1996; Thaung et al., 2002). Previous studies and in-silico predictions have reported and proposed decreased or absent DNA-binding ability for this mutation (Yamaguchi et al., 1997; Thaung et al., 2002; Chauhan et al., 2004; Shukla and Mishra, 2012). In order to investigate the individual roles of the PAI and RED subdomains of Pax6 during forebrain development, the phenotypes of these subdomain mutant mice were examined. Finally, the results obtained from the PAI- ( $Pax6^{Leca4}$ ) and RED-subdomain ( $Pax6^{Leca2}$ ) mutants were compared to the phenotype of the functional Pax6 null mice  $Pax6^{Sey}$  (Hill et al., 1991).

### 2.2.1 Gross phenotypical differences of $Pax6^{Leca4}$ (PAI-domain) and $Pax6^{Leca2}$ (RED-domain) mutant mice

Morphological analysis of E14 old homozygote  $Pax6^{Leca4}$  and  $Pax6^{Leca2}$  mutant embryos revealed the presence of craniofacial defects with an abnormal development of frontonasal regions in both mutants (see arrows in Fig. 2-2B' and C'). Moreover, both mutants displayed eye abnormalities (Fig. 2-2B',C'), which have already been studied in more detail in the  $Pax6^{Leca4}$  mutant (Ramaesh et al., 2009). These two morphological phenotypes are similar to the phenotype found in the functional null allele (Fig.2-2A') (Hill et al., 1991; Tzoulaki et al., 2005). Furthermore, morphological analysis of mutant telencephali at midneurogenesis

from E14 embryos of both mutants displayed clear defects in olfactory bulb (OB) development.  $Pax6^{Leca4}$  and  $Pax6^{Leca2}$  mutant brains only possessed remnants of olfactory bulbs (Fig.2-2B''',C'''). However, this phenotype was incompletely penetrant in the  $Pax6^{Leca2}$  mutant with variable sizes of remnant olfactory bulbs ranging from small residual structures to clear olfactory bulbs, though always still smaller compared to wild-type controls (Fig.2-2C''-C'''). Nevertheless, this variability is similar to the reported incomplete penetrance of eye malformations in the  $Pax6^{Leca2}$  mutant (Thaung et al., 2002).

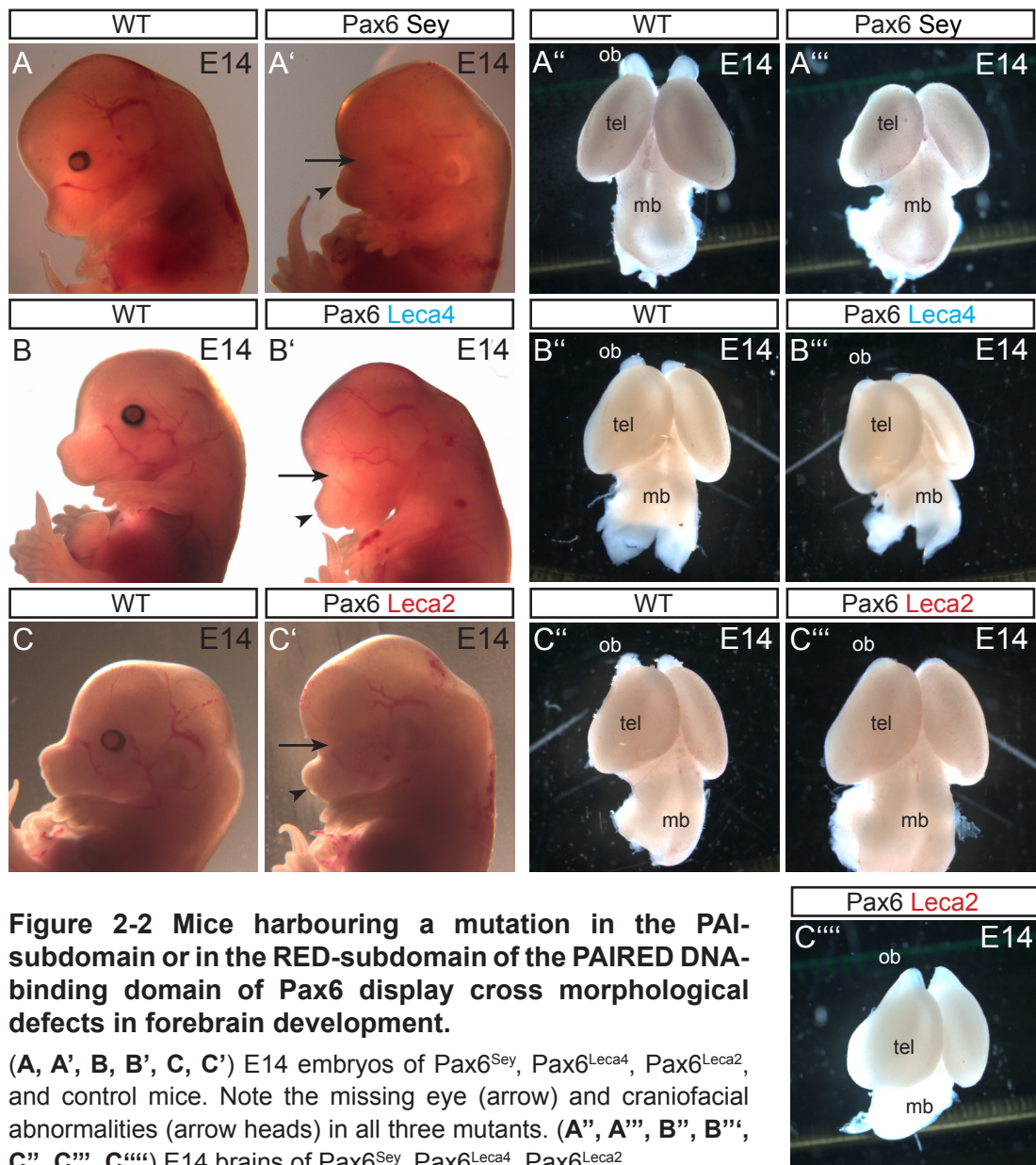


**Figure 2-2 Mice harbouring a mutation in the PAI-subdomain or in the RED-subdomain of the PAIRED DNA-binding domain of Pax6 display cross morphological defects in forebrain development.**

(A, A', B, B', C, C') E14 embryos of  $Pax6^{Sey}$ ,  $Pax6^{Leca4}$ ,  $Pax6^{Leca2}$ , and control mice. Note the missing eye (arrow) and craniofacial abnormalities (arrow heads) in all three mutants. (A'', A''', B'', B''', C'', C''', C''') E14 brains of  $Pax6^{Sey}$ ,  $Pax6^{Leca4}$ ,  $Pax6^{Leca2}$  and control mice. Note the reduction in olfactory bulb size in both *Leca* mutant mice and the complete absence in the  $Pax6^{Sey}$  mutant. Also note the different penetrance of this phenotype in the  $Pax6^{Leca2}$  mutant.

Abbreviations: Ob, olfactory bulb; tel, telencephalon; mb, midbrain.

### 2.2.1.1 *Pax6<sup>Leca2</sup>, but not Pax6<sup>Leca4</sup> mice survive into adulthood*

Most homozygous Pax6 mutants are lethal at birth, which is also the case for the Pax6<sup>Leca4</sup> mutant (Ramaesh et al., 2009). In contrast, homozygous Pax6<sup>Leca2</sup> mutants developed to adulthood. However Mendelian distribution of the homozygous progeny analysed in 311 pups was slightly abnormal at birth. Approximately 21% of the homozygous mice survived into adulthood compared to normal 25% (n=64/311) (Fig.2-3B). All adult Pax6<sup>Leca2</sup> mutants showed growth retardations with reduced body size compared to controls (Fig.2-3A,A'). However, besides the incompletely penetrant OB-phenotype, brain size of Pax6<sup>Leca2</sup> mutants compared to wild-type controls appeared normal (Fig.2-3C-C'').

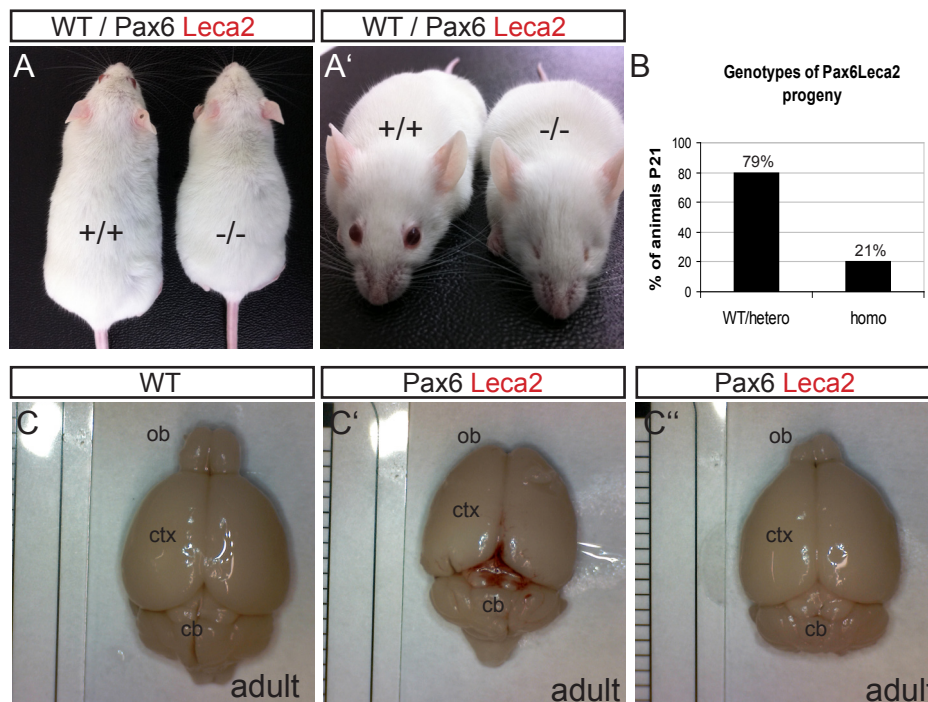


**Figure 2-3 Pax6<sup>Leca2</sup> mice survive into adulthood**

(A,A') Eight week old adult Pax6<sup>Leca2</sup> and control littermate. (B) Histogram depicting the Mendelian distribution of Pax6<sup>Leca2</sup> mice. (C-C'') Brains of eight week old adult Pax6<sup>Leca2</sup> and control mice. Note the variable penetrance of ob size in the Pax6<sup>Leca2</sup> mutant.

Abbreviations: cb, cerebellum; ctx, cortex; ob, olfactory-bulb.

### 2.2.1.2 *Pax6<sup>Leca4</sup> and Pax6<sup>Leca2</sup> mice exhibit no 'olfactory bulb-like structure (OBLS)'*

The full Pax6 mutant, Pax6<sup>Sey</sup>, completely lacks olfactory bulbs (Fig.2-2A''')(Hogan et al., 1986) and instead develops an 'olfactory bulb-like structure' (OBLS,(Jimenez et al., 2000)) within the ventral telencephalon due to the aberrant assembly of mitral cells, the first differentiating neurons in the OB. In order to investigate whether such an OBLS is also present in Pax6<sup>Leca4</sup> or Pax6<sup>Leca2</sup> mutant brains next to the remnant OBs, mitral cell localization in the ventral telencephalon was investigated using immunohistochemistry for reelin (Ogawa et al., 1995), an extracellular glycoprotein expressed by mitral cells (Perez-Garcia et al., 2004). No miss-localisation of reelin positive mitral cells in the ventral telencephalon was observed in Pax6<sup>Leca4</sup> or Pax6<sup>Leca2</sup> mutant brains (Fig.2-4A-B') while the OBLS was readily detected in Pax6<sup>Sey</sup> mice (Fig.2-4C,C'). Thus no OBLS is present in both mutants initially forming an adequate olfactory bulb anlage, which then fails to normally extend in these mice.

### 2.2.1.3 *Pax6<sup>Leca2</sup> mutants lack TH+ interneurons in the adult olfactory bulb*

Neuronal sub-populations in the olfactory bulb are in part derived from Pax6 positive progenitors during development (Dellovade et al., 1998; Kohwi et al., 2005; Cocas et al., 2011). Moreover Pax6 is expressed in the adult OB in a subpopulation of periglomerular interneurons (PGN) where it acts as a fate determinant of the dopaminergic PGN subtype (Hack et al., 2005; Brill et al., 2009). Given that OB structures, although reduced in size, do develop in Pax6<sup>Leca2</sup> mutant mice, the presence of neuronal subpopulations were investigated in adult Pax6<sup>Leca2</sup> mutants by immunohistochemistry. Dopaminergic PGNs were visualized by immunohistochemistry against tyrosine hydroxylase (TH, a rate limiting enzyme in the biosynthesis of dopamine) on sections from adult Pax6<sup>Leca2</sup> mice that had a mild olfactory bulb reduction. Interestingly, homozygous Pax6<sup>Leca2</sup> mutants completely lacked TH immunoreactivity (Fig.2-5A-B'), whereas expression of calretinin, Tbr1 and Tbr2 (markers for other subtypes of PGN (Kosaka et al., 1995; Toida et al., 2000; Panzanelli et al., 2007; Parrish-Aungst et al., 2007) were still present (Fig.2-5). Besides a potential increase in the number of reelin expressing mitral cells (Fig.2-5D,D'), the overall structural organization of the olfactory bulb layers appeared normal in Pax6<sup>Leca2</sup> mice with mild olfactory bulb reduction (all examples in Fig.2-5). However in severely reduced olfactory bulbs, the structural organization of the bulb was lost (Fig.2-6). These data suggest an important role of the RED-subdomain in Pax6 mediated fate specification of dopaminergic periglomerular interneurons. However, it is important to mention that the role of the PAI-subdomain in this context remains unexp-

lained, as this was not analysed due to the neonatal death of Pax6<sup>Leca4</sup> mice.

Taken together, the above described observations suggest that both the PAI and the RED subdomain are required for eye, craniofacial and olfactory bulb development.

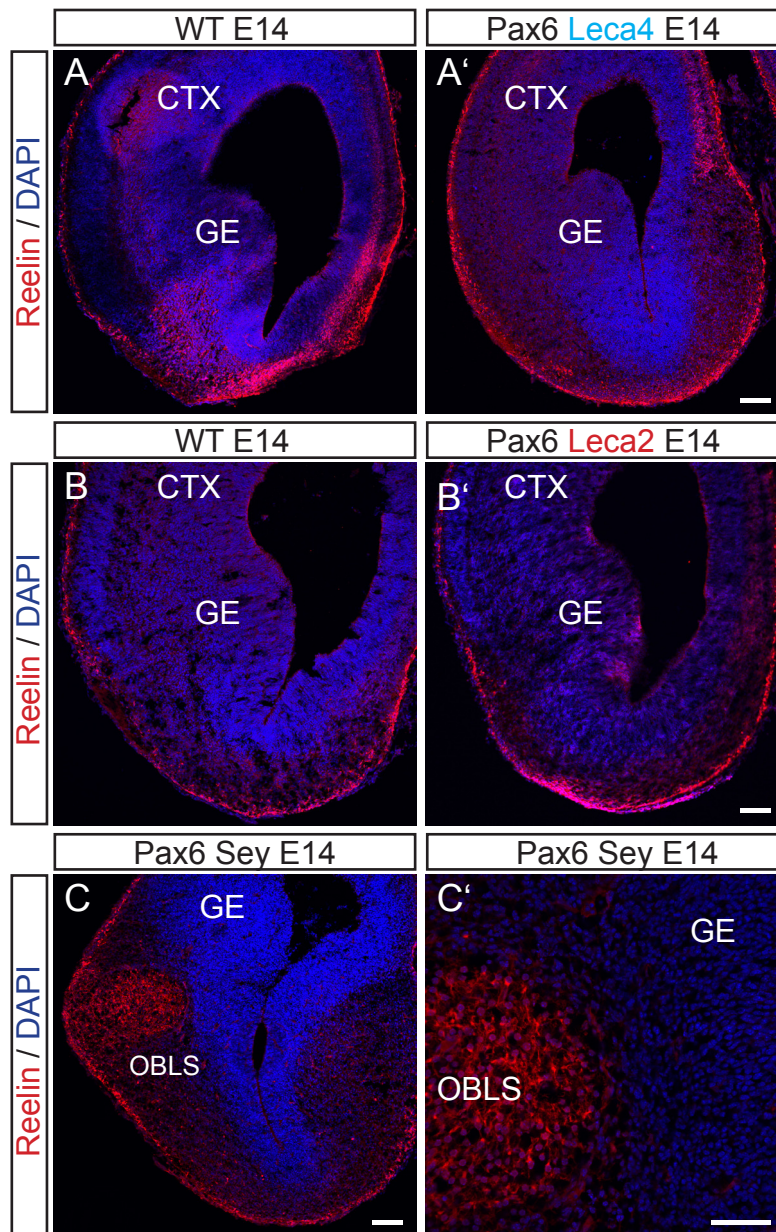


**Figure 2-4 Mice harbouring a mutation in the PAI-subdomain or in the RED-subdomain of the Paired DNA-binding domain of Pax6 do not develop an OBLS.**

(A-C') Immunofluorescence for reelin (red) combined with DAPI staining (blue) on coronal sections of E14 dorsal telencephalon of Pax6<sup>Leca4</sup>, Pax6<sup>Leca2</sup>, Pax6<sup>Sey</sup> and control mice. Note that no aberrant accumulation of reelin positive cells, the OBLS, is found in the ventral-lateral telencephalon of both Leca mutant mice in contrast to Pax6<sup>Sey</sup> mice.

Abbreviations: CTX, cortex; GE, ganglionic eminence; OBLS, olfactory-bulb like structure. Scale bars in A-C: 100  $\mu$ m, in C': 100 $\mu$ m.

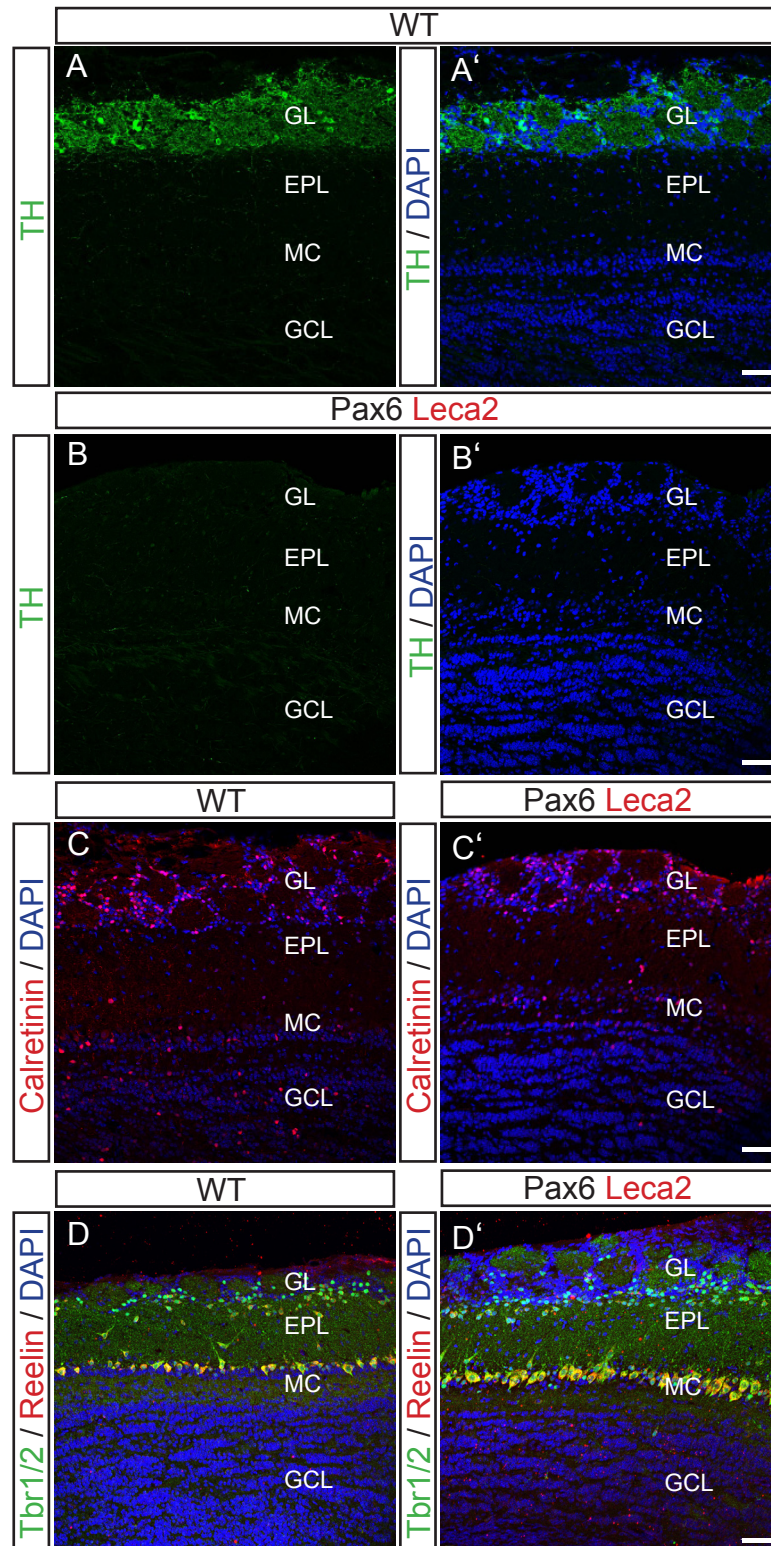


**Figure 2-5 Expression of neuronal subtypes in the adult Pax6<sup>Leca2</sup> mutant olfactory bulb**

(A-B') Micrographs depicting immunoreactivity for Thyroxin-Hydroxylase (TH) in sagittal sections of the olfactory bulb of adult brains of Pax6<sup>Leca2</sup> and corresponding wild-type (WT) control littermate. Note the absence of TH<sup>+</sup> cells in Pax6<sup>Leca2</sup> mutant OB. (C-D') Micrographs of adult sagittal sections immunoreactive for calretinin (C,C') or reelin and Tbr1/2 (D,D') in Pax6<sup>Leca2</sup> and their WT control littermate. Scale bars: 50µm.

Abbreviations: GL, glomerular layer; EPL, external plexiform layer; MC, mitral cells; GCL, granule cell layer.

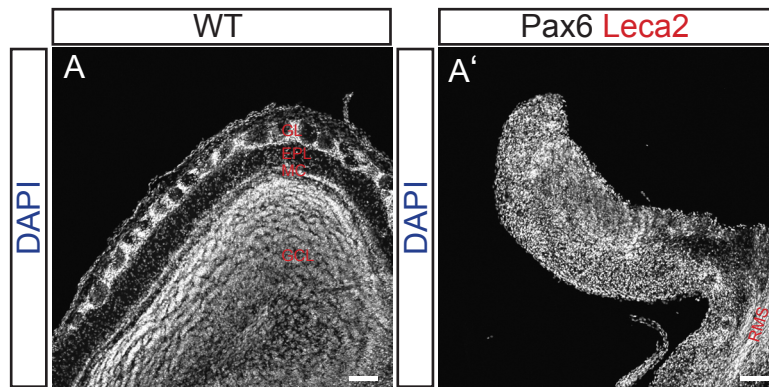


**Figure 2-6 Example of a disturbed olfactory bulb structure of an adult Pax6<sup>Leca2</sup> mutant mouse**

(A,A') Micrographs of a representative sagittal section of a disturbed olfactory bulb of adult Pax6<sup>Leca2</sup> and corresponding control WT littermate. Some Pax6<sup>Leca2</sup> olfactory bulbs have lost their structural organization completely as shown in the presented example. Scale bars: 100µm.

Abbreviations: GL, glomerular layer; EPL, external plexiform layer; MC, mitral cells; GCL, granule cell layer; RMS, rostral migratory stream.

### 2.2.2 Telencephalic development in Pax6<sup>Leca4</sup> (PAI-domain) and Pax6<sup>Leca2</sup> (RED-domain) mutant mice

In order to investigate defects in telencephalic development, gross analysis of the cerebral cortex of Pax6<sup>Leca4</sup> and Pax6<sup>Leca2</sup> mutant mice were performed. Anatomically matched, DAPI stained coronal sections from rostral to caudal regions of E14 mutant and control telencephali were compared. Pax6<sup>Leca4</sup> mutants showed a clear reduction in cortical thickness compared to controls, while no reduction was observed in Pax6<sup>Leca2</sup> mutant mice (Fig.2-7). Because a proliferation phenotype observed in the Pax6<sup>Leca2</sup> mutant (see below) was only detected in rostral regions and in order to compare both mutants, all analysis of both mutants were performed on rostral regions only. Therefore also the quantification of the radial thickness in the Pax6<sup>Leca4</sup> mutant cortex was performed at rostral levels. The entire cortex at lateral and central positions of the dorsal telencephalon was measured at E14, revealing a mild but significant reduction in radial length at lateral position and reduction of about one third at midcortex position in Pax6<sup>Leca4</sup> mutant cortices (Fig.2-8A-A''). A similar reduction of radial thickness has also been observed in the functional Pax6 null allele (Asami et al., 2011). In contrast, no reduction in radial thickness was found in the Pax6<sup>Leca2</sup> mutant (Fig.2-8B-B''). Taken together, this result suggests, that the thickness of the cerebral cortex mainly depends on a functional PAI subdomain.

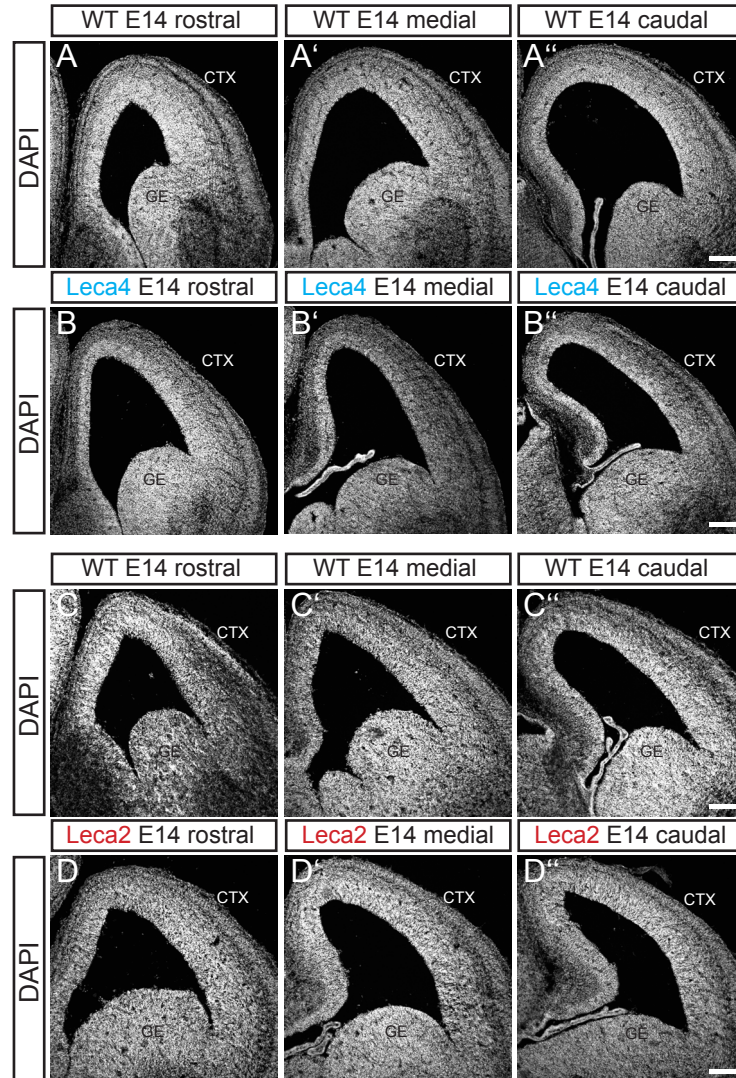


**Figure 2-7 Overview telencephalic development in the PAI and in the RED-subdomain mutants**

(A-D'') Micrographs of representative coronal sections from rostral to caudal of the E14 telencephalon of Pax6<sup>Leca4</sup> (B-B''), Pax6<sup>Leca2</sup> (D-D'') and their WT littermates (A-A'', B-B'').

Scale bars: 100  $\mu$ m.

Abbreviations: CTX, cortex; GE, ganglionic eminence.

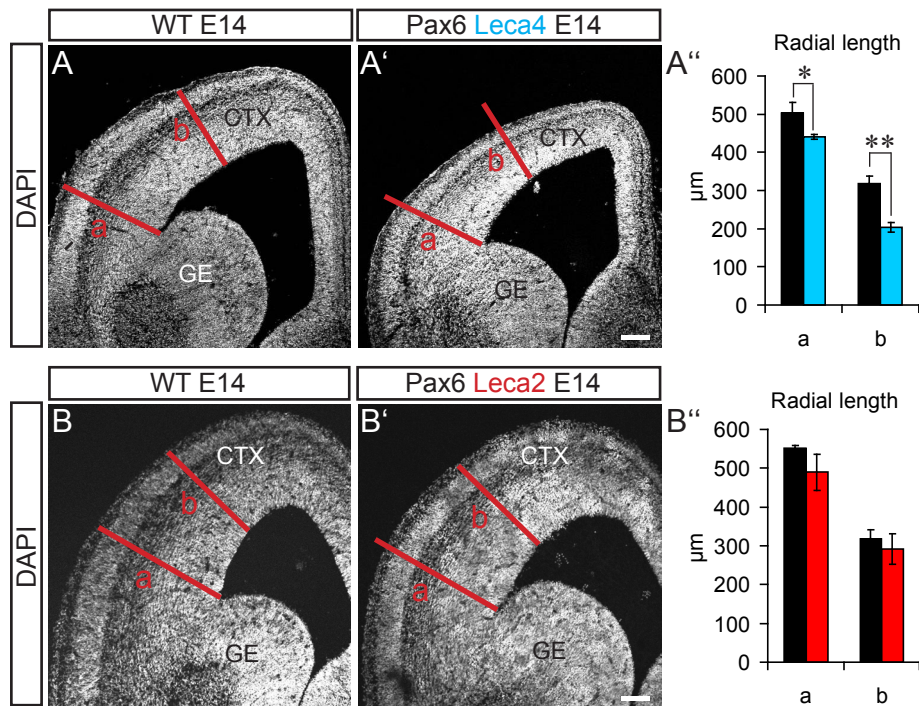


**Figure 2-8. Telencephalic development in the PAI and in the RED-subdomain mutants at midneurogenesis**

(A,A',B,B') Micrographs of representative coronal sections of the rostral E14 telencephalon of Pax6<sup>Leca4</sup> (A'), Pax6<sup>Leca2</sup> (B') and their WT littermates (A, B).

(A'',B'') Histograms depicting radial length of the cerebral cortex at the two positions (a, b) indicated by red lines in A-B'. Note the reduction in radial cortical length in the Pax6<sup>Leca4</sup> but not Pax6<sup>Leca2</sup> mutant mice. Data are shown as mean  $\pm$  SEM, n (embryos analysed)  $\geq$  3 ; \*p<0.05, \*\*p<0.01. Scale bars: 100  $\mu$ m.

Abbreviations: Ob, olfactory bulb; tel, telencephalon; mb, midbrain. CTX, cortex; GE, ganglionic eminence.

### 2.2.3 Progenitor proliferation is differently affected in the cerebral cortex of Pax6<sup>Leca4</sup> (PAI domain) and Pax6<sup>Leca2</sup> (RED domain) mutant mice

As Pax6 controls progenitor proliferation in the developing cortex, alterations in proliferation may account for the observed reduction of radial thickness in the Pax6<sup>Leca4</sup> mutant. In order to examine proliferation of apical and basal progenitors, immuno-histochemistry against phospho-Histone 3 (PH3) was performed in both mutants. PH3 marks cells in G2/M-phase of the cell cycle (Hendzel et al., 1997) and as the two progenitor populations divide at different positions thus allows the discrimination between apical and basally dividing cells (Haubensak et al., 2004; Miyata et al., 2004; Noctor et al., 2004). Dividing precursors were quantified per hemisphere in several sections at rostral positions at two developmental stages – E12, when the first SVZ cells begin to show and at E14, representing midneurogenesis. Quantifications at E12 were performed across the entire dorsal wall length from lateral to medial position. At E14, a 150- $\mu$ m wide radial stripe was examined (see also Material and Methods). In the Pax6<sup>Leca4</sup> mutant proliferation was significantly decreased compared to their wild-type siblings at both precursor positions and at both developmental stages analysed (Fig.2-9). Interestingly, clustering of apical PH3 positive cells was observed in the Pax6<sup>Leca4</sup> mutants at E12. Conversely, apical and basal mitosis were significantly increased in the cerebral cortex of Pax6<sup>Leca2</sup> mutants compared to controls with almost double the number of proliferating cells at the apical surface and double the number at basal position at embryonic day E14 (Fig.2-10D-F). However, this increase in proliferating progenitors was not yet significant at E12 (Fig.2-10A-C). Intriguingly, these proliferation phenotypes in both the Pax6<sup>Leca4</sup> and the Pax6<sup>Leca2</sup> mutant cerebral cortex deviate from the proliferation phenotype observed in full Pax6 mutants such as Pax6<sup>Sey</sup> or after conditional Pax6 deletion, which show a normal number of apical, but increased number of basal progenitors (Gotz et al., 1998; Haubst et al., 2004; Tuoc et al., 2009).

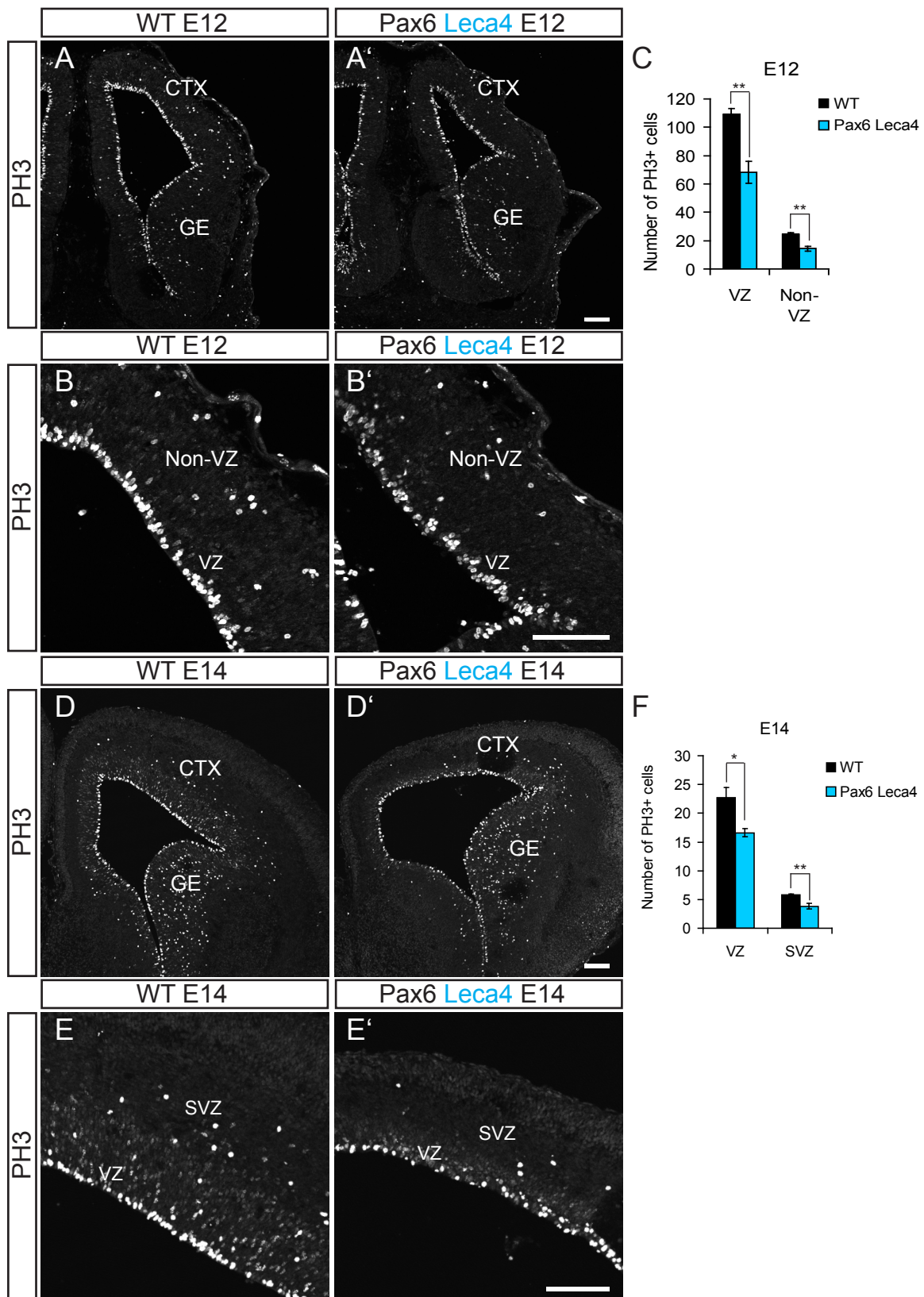


**Figure 2-9. Progenitor proliferation in the PAI subdomain mutant Pax6<sup>Leca4</sup>**

(A-B',D-E') Micrographs of E12 and E14 coronal telencephalic sections depicting cells immunoreactive for phosphohistone H3 (PH3, white) in the Pax6<sup>Leca4</sup> mutant and its WT littermate. (C, F) Histograms showing the number of PH3-positive progenitors in Pax6<sup>Leca4</sup> and their WT littermates at E12 (C; per entire ctx) and E14 (F; per 150 $\mu$ m thick radial stripe). Data are shown as mean  $\pm$  SEM, n (embryos analysed)  $\geq$  3; \* $p$ <0.05, \*\* $p$ <0.01. Note the significant decrease in VZ and SVZ progenitors in the Pax6<sup>Leca4</sup> mutant. Scale bars: 100  $\mu$ m. Abbreviations: CTX, cortex; GE, ganglionic eminence; SVZ, subventricular zone; VZ, ventricular zone

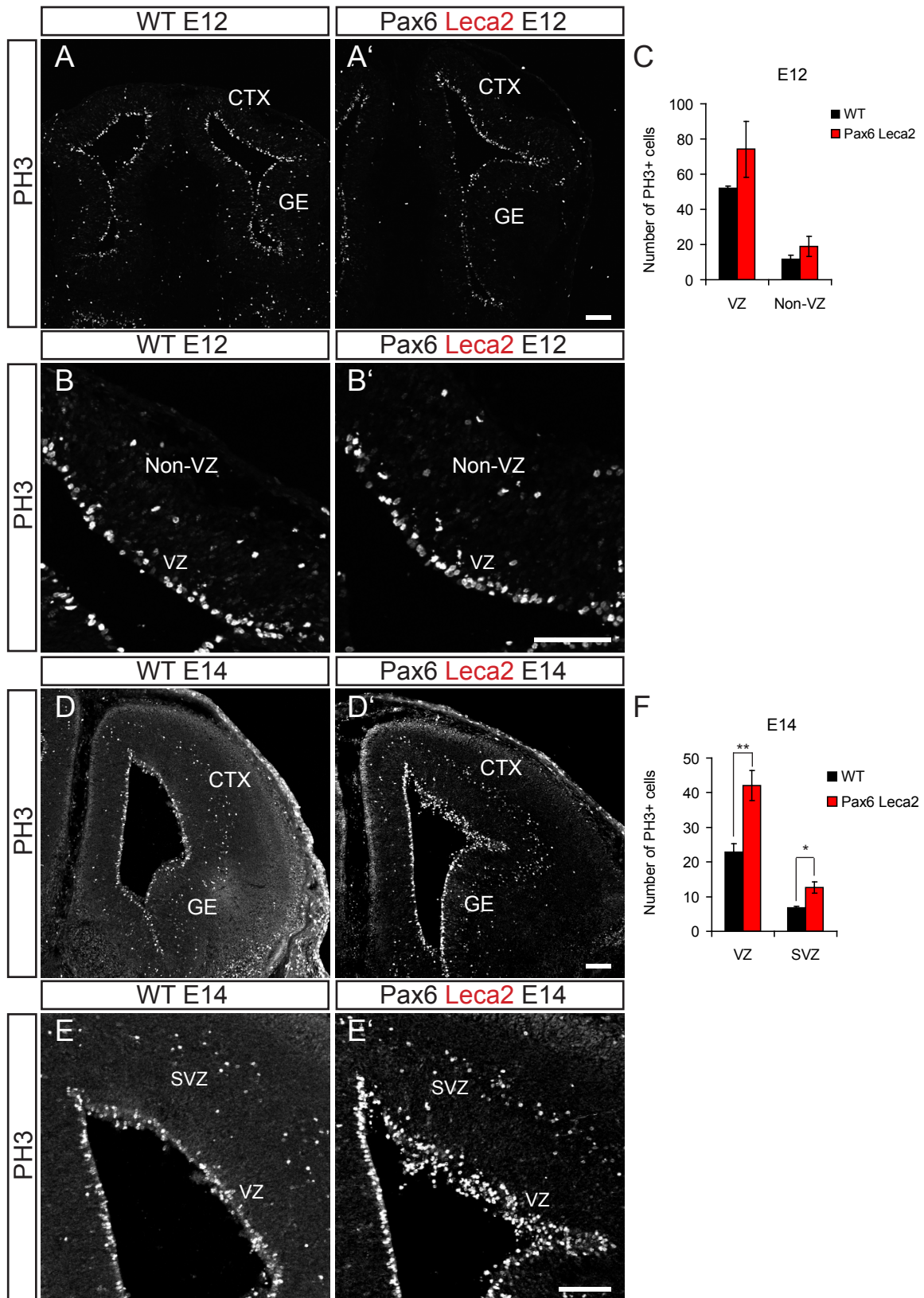


**Figure 2-10 Progenitor proliferation in the RED subdomain mutant Pax6<sup>Leca2</sup>**

(A-B',D-E') Micrographs of E12 and E14 coronal telencephalic sections depicting cells immunoreactive for phosphohistone H3 (PH3) in the Pax6<sup>Leca2</sup> mutant and its WT littermate. (C, F) Histograms showing the number of PH3-positive progenitors in Pax6<sup>Leca2</sup> and their WT littermates at E12 (C; per entire CTX) and E14 (F; per 150µm thick radial stripe). Data are shown as mean ± SEM, n (embryos analysed) ≥ 3; \*p<0.05, \*\*p<0.01. Note the increase in VZ and SVZ progenitors in the Pax6<sup>Leca2</sup> mutant. Scale bars: 100 µm. Abbreviations: CTX, cortex; GE, ganglionic eminence; SVZ, subventricular zone; VZ, ventricular zone

### 2.2.3.1 Progenitor identity in *Pax6<sup>Leca4</sup>* and *Pax6<sup>Leca2</sup>* mutant mice

In order to examine whether the changes in progenitor proliferation observed in the *Pax6<sup>Leca4</sup>* and *Pax6<sup>Leca2</sup>* mutant cortices are accompanied by changes in progenitor identity, their molecular fate and morphology were examined next. As described before, the apically and basally proliferating cells present two distinct types of progenitors. The first type is radial glial cells which are specified by Pax6 and undergo mitosis at the apical surface (Malatesta et al., 2000; Miyata et al., 2001; Noctor et al., 2001b; Heins et al., 2002; Miyata et al., 2004). The second population, basally dividing SVZ progenitors arise from the radial glia cells and were previously characterized as neuronal progenitors (Haubensak et al., 2004; Miyata et al., 2004; Noctor et al., 2004). On molecular level it has been shown that the transition from radial glial cells to basal progenitors is associated with the up-regulation of the T-domain transcription factor Tbr2 (Bulfone et al., 1999) directly controlled by Pax6 and sub-sequentially associated with the down-regulation of Pax6 protein levels (Englund et al., 2005). Thus immunohistochemistry against Pax6 and Tbr2 allowed examining the molecular fate of VZ progenitors that divide apically and SVZ progenitors that divide basally, respectively. Remarkably, expression of Tbr2 was maintained in the cortices of both subdomain mutants (Fig.2-11), which is in contrast to the loss of Tbr2 expression in *Pax6<sup>Sev</sup>* mice (Stoykova et al., 2000; Toresson et al., 2000; Sansom et al., 2009). Moreover, Pax6<sup>+</sup> and Tbr2<sup>+</sup> progenitors were detected at their proper localization (Fig.2-11). However in line with the observed changes in proliferation of the cortex, the number of Pax6<sup>+</sup> cells in the VZ and Tbr2<sup>+</sup> cells in the SVZ appeared decreased in the *Pax6<sup>Leca4</sup>* mutant (Fig.2-11A,A') and increased in the *Pax6<sup>Leca2</sup>* mutant cortex (Fig.2-11B,B').

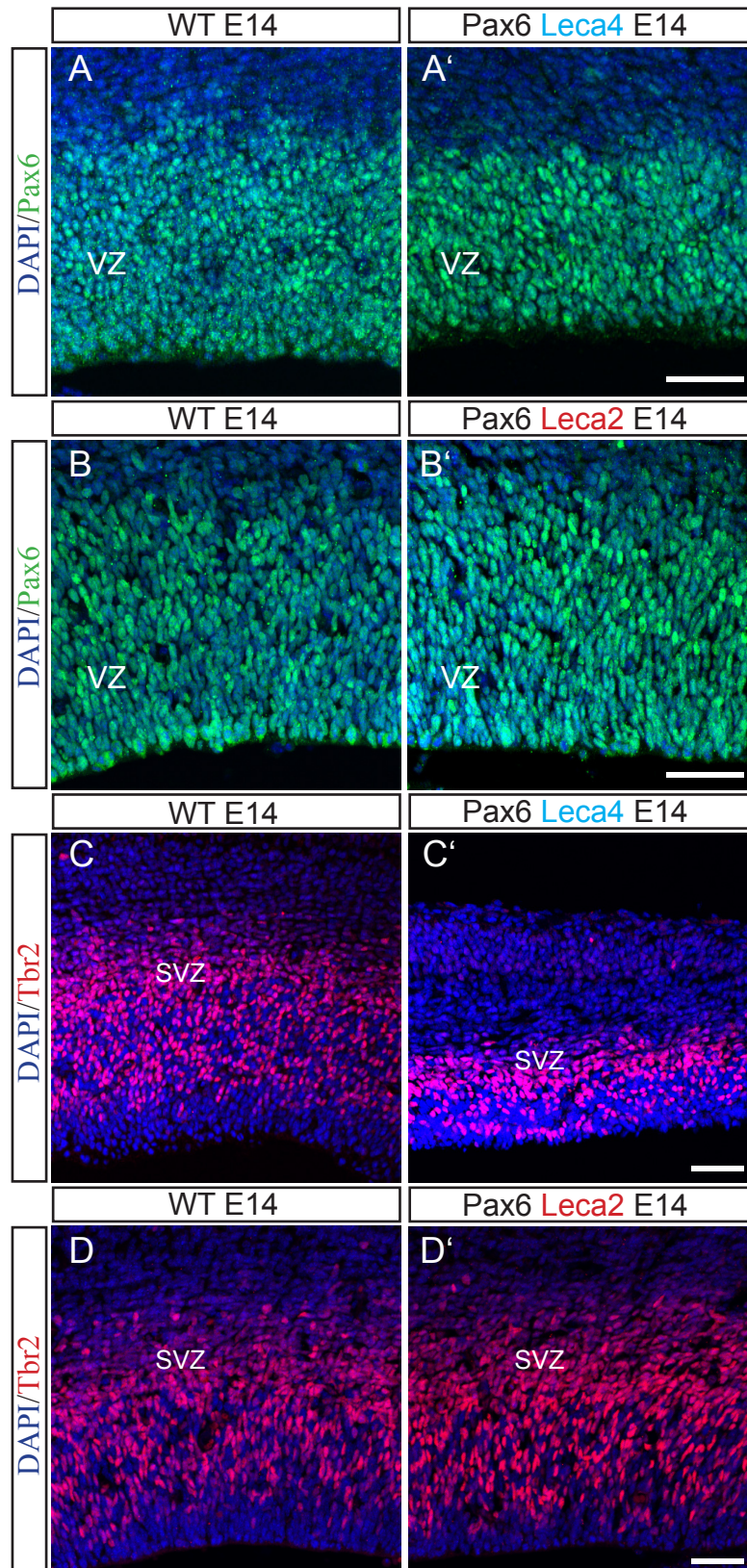


**Figure 2-11 Progenitor identity in Pax6<sup>Leca4</sup> and Pax6<sup>Leca2</sup> mutant mice**

(A-D') Micrographs depicting immunoreactivity for Pax6 (A-B') and for Tbr2 (C-D') on coronal sections of E14 dorsal telencephalon of Pax6<sup>Leca4</sup>, Pax6<sup>Leca2</sup> and their WT littermates.

Scale bars: 50  $\mu$ m. Abbreviations: VZ, ventricular zone; SVZ, subventricular zone.

In addition to the molecular fate and localization of Pax6+ radial glial cells, their morphology was examined next by immunohistochemistry against RC2. RC2 recognizes posttranslational modifications of nestin in Pax6+ radial glial cells (Park et al., 2009) and hence labels their radial processes. For the Pax6<sup>Leca4</sup> as well as the Pax6<sup>Leca2</sup> mutant grossly normal radial glia morphology in the cerebral cortex was detected (Fig.2-12). Taken together, progenitor number, but not identity, is distinctly affected in the Pax6<sup>Leca4</sup> and Pax6<sup>Leca2</sup> mutants, suggesting that the PAI domain may promote and the RED domain may inhibit proliferation.

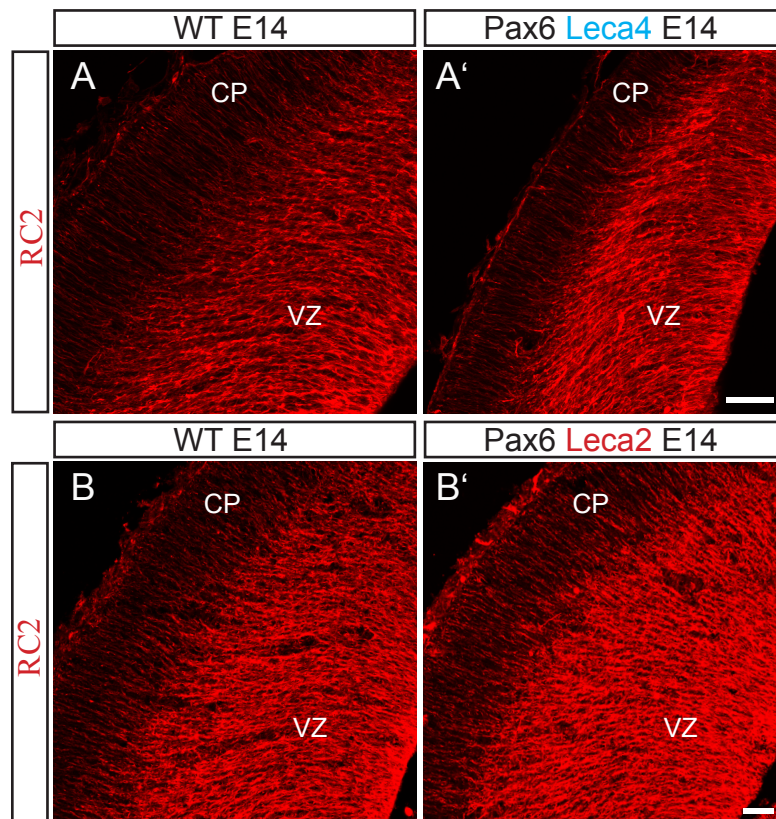


**Figure 2-12 Radial glial morphology in Pax6<sup>Leca4</sup> and Pax6<sup>Leca2</sup> mutant mice**

(A-B') Micrographs depicting immunoreactivity for RC2 on coronal sections of E14 dorsal telencephalon of Pax6<sup>Leca4</sup>, Pax6<sup>Leca2</sup> and their WT littermates.

Scale bars: 50  $\mu$ m. Abbreviations: CP, cortical plate; VZ, ventricular zone.

#### 2.2.4 The role of the PAI and the RED subdomain in dorso-ventral patterning of the telencephalon

One possible explanation for the strikingly different proliferation phenotypes between the Leca mutants and the functional Pax6 null mice are differences in dorso-ventral patterning. As mentioned in the introduction, Pax6 functions also as regulator of dorso-ventral patterning and loss of functional Pax6 leads to the up-regulation of transcription factors in the

dorsal telencephalon which are normally restricted to the ventral telencephalon (Stoykova and Gruss, 1994; Stoykova et al., 1996; Stoykova et al., 1997; Toresson et al., 2000; Yun et al., 2001; Heins et al., 2002). Indeed the proliferation behaviour observed after complete loss of Pax6, with an increase in basal but not apical progenitors resembles one characteristic of the endogenous proliferation properties in the ventral telencephalon, namely a particularly high number of proliferating basal progenitors (Bhide, 1996). In order to assess if the observed proliferation differences between the Leca mutants and the functional Pax6 null mice correlate with patterning defects, the expression of the ventral transcription factors Gsx2, Olig2 and Mash1 were analysed by immunohistochemistry at E14. Localization of TF-positive cells was characterized according to their expression in the different regions of the dorsal telencephalon (pallium) as depicted in Fig.2-13. In contrast to the Pax6<sup>Sey</sup> cerebral cortex, no Gsx2 positive cells were detected in the medial (not shown) and dorsal pallium of the Pax6<sup>Leca2</sup> and Pax6<sup>Leca4</sup> mutants (Fig.2-14). However, in the region of the ventral and lateral most pallium scattered Gsx2 positive cells were found in the Pax6<sup>Leca4</sup>, but not Pax6<sup>Leca2</sup> mutant (Fig.2-14A-B'). The same expression pattern was observed for Olig2, with no expression change in the Pax6<sup>Leca2</sup> mutant compared to controls and similar spread of Olig2-immunoreactive cells at the ventral and lateral pallium in the Pax6<sup>Leca4</sup> mutant (Fig.2-15). The few scattered Olig2-immunoreactive cells detected in all cortices at dorsal pallium position (indicated by red arrowheads in Fig.2-15A,B,C) are Olig2+ oligodendrocyte progenitors that normally migrate into the dorsal telencephalon at subventricular zone positions. Thus in the Pax6<sup>Leca4</sup> mutant the ventral transcription factors Gsx2 and Olig2 do not respect the pallial-subpallial boundary (PSB) leading to ventralisation of the ventral and lateral most pallium epithelium, which is reminiscent to the phenotype observed in the Pax6<sup>Sey</sup> mutant. However expression of these transcription factors in the largest pallial regions – the dorsal and medial pallium - was absent in the Pax6<sup>Leca4</sup> mutant. In contrast, dorso-ventral patterning in all pallial regions was entirely preserved in the Pax6<sup>Leca2</sup> mutant telencephalon.

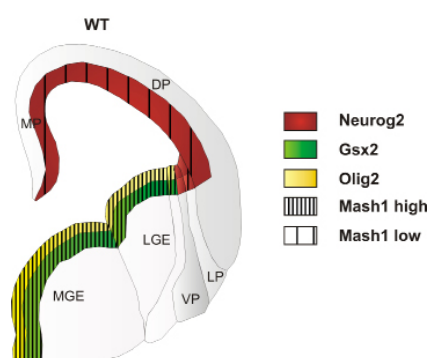


**Figure 2-13 Expression patterns of dorso-ventral patterning factors**

Model summarizing the expression patterns of the transcription factors Neurog2, Gsx2, Olig2 and Mash1 in a WT telencephalon, including depiction of the different regions of the dorsal telencephalon (pallium) and ganglionic eminence (subpallium).

Abbreviations: CTX, cortex; LGE, MGE, GE, lateral-, medial-, ganglionic eminence respectively; MP, DP, VP, LP, medial-, dorsal-, ventral-, lateral-pallium respectively.

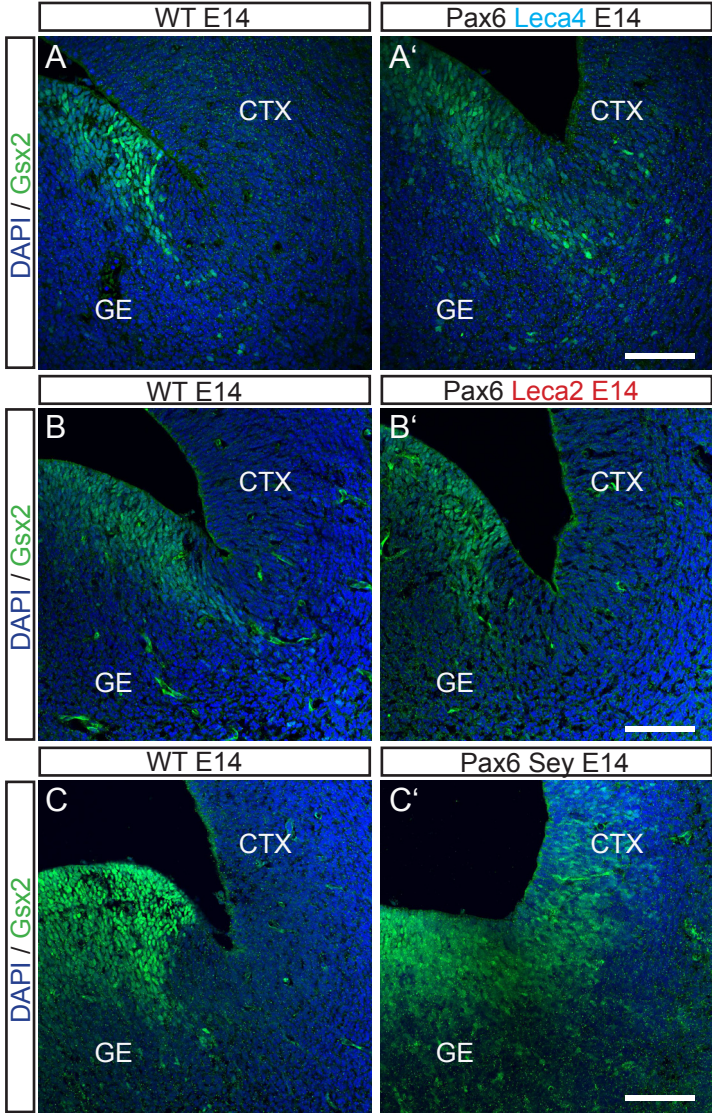


**Figure 2-14 Gsx2 expression in Pax6<sup>Leca4</sup> and Pax6<sup>Leca2</sup> mutant mice**

(A-C') Micrographs depicting immunoreactivity for Gsx2 on coronal sections of E14 dorsal telencephalon of Pax6<sup>Leca4</sup>, Pax6<sup>Leca2</sup>, Pax6<sup>Sey</sup> and their WT littermates. Note the broad spread of Gsx2 into the cortex in Pax6<sup>Sey</sup> mutants.

Scale bars: 100 µm. Abbreviations: CTX, cortex; GE, ganglionic eminence;

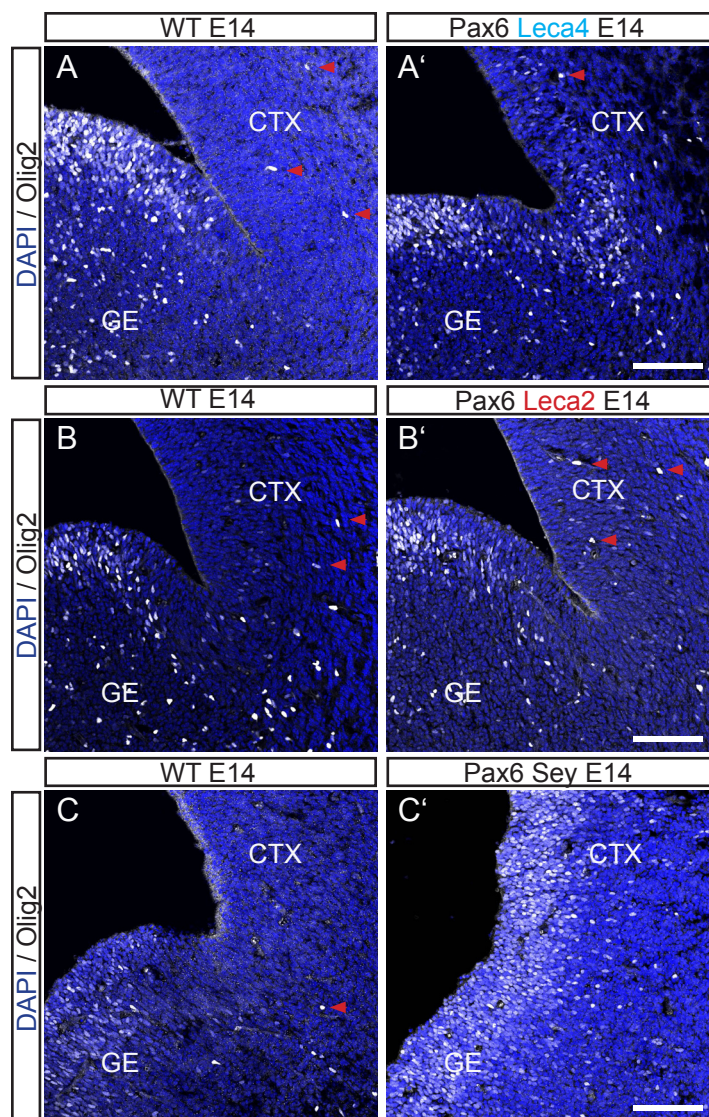


**Figure 2-15 Olig2 expression in Pax6<sup>Leca4</sup> and Pax6<sup>Leca2</sup> mutant mice**

(A-C') Micrographs depicting immunoreactivity for Olig2 on coronal sections of E14 dorsal telencephalon of Pax6<sup>Leca4</sup>, Pax6<sup>Leca2</sup>, Pax6<sup>Sey</sup> and their WT littermates. Red arrowheads indicate naturally migrating Olig2+ oligodendrocyte precursors.

Scale bars: 100  $\mu$ m. Abbreviations: CTX, cortex; GE, ganglionic eminence.

In contrast to *Gsx2* and *Olig2*, expression of *Mash1* is normally detected in dorsal and ventral progenitors although its highest expression is in the ventral telencephalon. Remarkably, immunostaining against *Mash1* revealed an up-regulation in a rather wide-spread manner in both *Pax6<sup>Leca2</sup>* and *Pax6<sup>Leca4</sup>* mutant cerebral cortices (Fig.2-16A-B'). However compared to the *Pax6<sup>Sey</sup>* cerebral cortex *Mash1* was up-regulated in fewer cells (Fig.2-16).

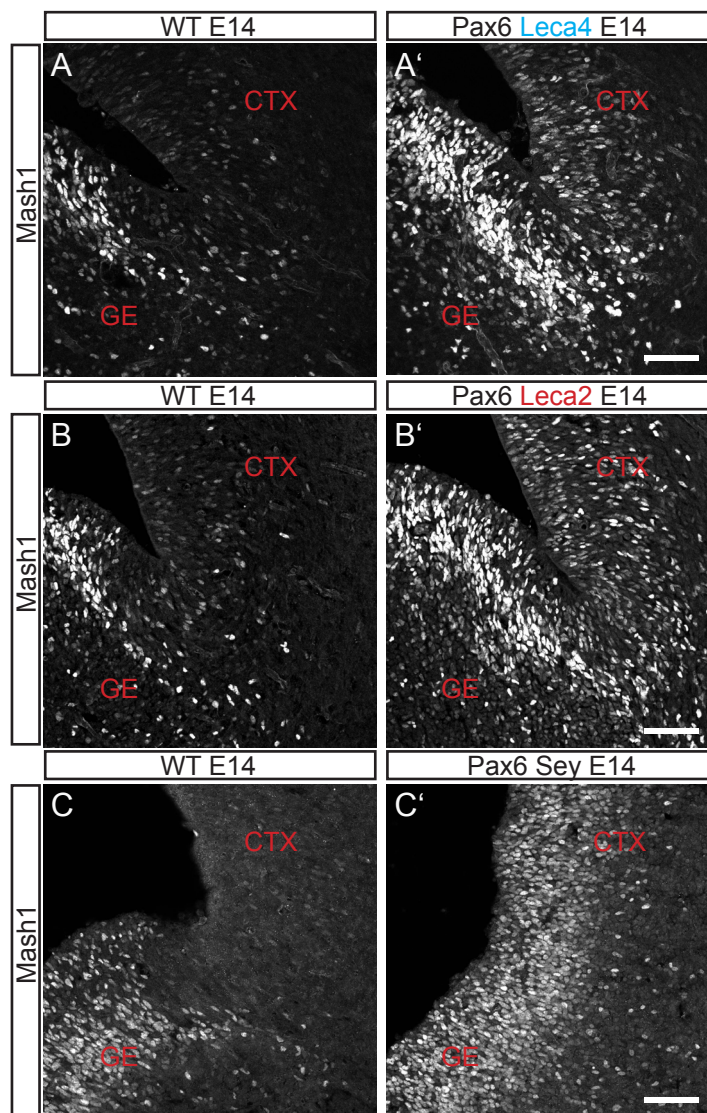


**Figure 2-16 Mash1 expression in *Pax6<sup>Leca4</sup>* and *Pax6<sup>Leca2</sup>* mutant mice**

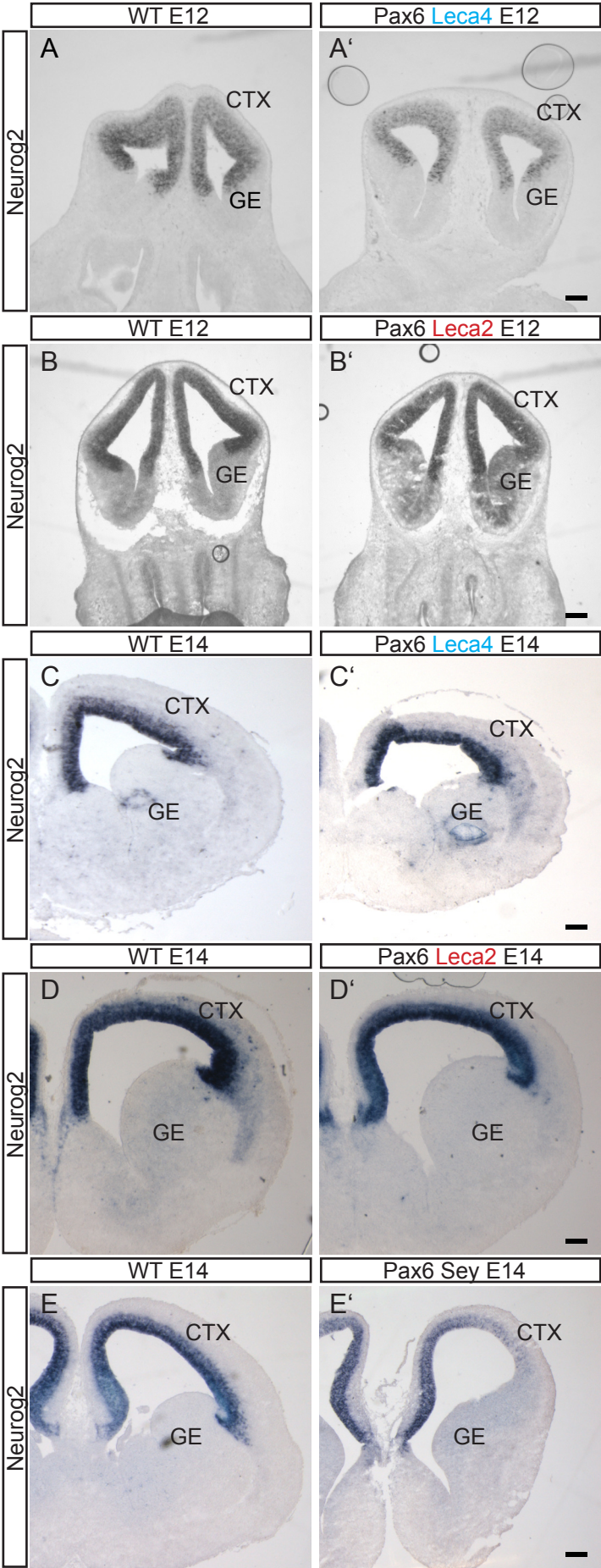
(A-C') Micrographs depicting immunoreactivity for *Mash1* on coronal sections of E14 dorsal telencephalon of *Pax6<sup>Leca4</sup>*, *Pax6<sup>Leca2</sup>*, *Pax6<sup>Sey</sup>* and their WT littermates.

Scale bars: 100  $\mu$ m. Abbreviations: CTX, cortex; GE, ganglionic eminence.

---

Given that in the dorsal progenitors Mash1 and the bHLH transcription factors Neurog1/2 (Fode et al., 2000; Britz et al., 2006) counter regulate each other and that Neurog1/2 expression were not only down-regulated in the Pax6<sup>Sey</sup> cerebral cortex (Haubst et al., 2004) but also Neurog2 had been shown to be a direct target of the paired domain of Pax6 (Scardigli et al., 2003), prompted the analysis of Neurog2 expression as possible cause for the increase in Mash1 expression. In situ hybridisation with a Neurog2 specific probe was performed at E12 and E14 in both Pax6<sup>Leca2</sup> and Pax6<sup>Leca4</sup> mutant cortices and on Pax6<sup>Sey</sup> E14 cortex as control. Strikingly, at both embryonic stages strong Neurog2 mRNA signal was present throughout the cerebral cortex of both Pax6<sup>Leca4</sup> and Pax6<sup>Leca2</sup> mutants (Fig.2-17A-D') in pronounced contrast to the Pax6<sup>Sey</sup> cerebral cortex (Fig. 2-17E,E').

Taken together, these data suggest that both the PAI and RED subdomains may be required to restrain Mash1 expression from the cerebral cortex, while either of them appears sufficient to allow relatively normal Neurog2, Gsx2 and Olig2 expression in the medial and lateral pallium. However, the PAI, but not RED subdomain plays a pivotal role for the proper specification of the ventral and lateral most pallial regions.



#### 2.2.4.1 Molecular specification in Pax6<sup>Sev</sup>/Gsx2 double mutants

The severe ventralization in the cortex of Pax6<sup>Sev</sup> mutants likely contributes to some defects seen in this mutant. Indeed, analysis of double mutants for Pax6 and Gsx2 had shown that Gsx2 is required to repress Pax6 and that cortical and striatal development is much improved in these mice compared to their respective single mutants (Toresson et al., 2000). However, although LGE specification (distorted in the Gsx2 single mutant) was restored in the double mutants, remaining ectopic expression of Mash1 and Dlx factors in cortical progenitors and reduced levels of Neurog2 were reported (Toresson et al., 2000). In order to evaluate the restoration of molecular specification of the loss of Tbr2 in the telencephalon of Pax6<sup>Sev</sup> mice and ectopic Olig2 expression, their expression was assessed in the double mutants at E14 and their respective single mutants as control. Interestingly, Olig2 expression was not affected in the Gsx2 single mutant, however high ectopic expression of Olig2 throughout the cortex was detected in the double mutant (Fig.2-18). Furthermore, the almost complete loss of Tbr2 expression observed in the Pax6<sup>Sev</sup> mutant was also present in the double mutant (Fig.2-18). Interestingly, similar to the reported ectopic expression of Neurog1&2 in mutant LGE cells in the Gsx2 single mutant (Toresson et al., 2000), also Tbr2 expression was detected ectopically in the Gsx2 single mutant (Fig.2-18C). Taken together, although the deletion of the ventral transcription factor Gsx2 can rescue some defects observed in the Pax6<sup>Sev</sup> mutant (Toresson et al., 2000), it did not restore ventralization of the dorsal telencephalon. Thus, loss of functional Pax6 is predominant in the double mutant and comparison to the Leca mutations reveals that a single subdomain (PAI or RED) is sufficient to maintain dorsal telencephalon identity.

#### Figure 2-17 Neurog2 expression in Pax6<sup>Leca4</sup> and Pax6<sup>Leca2</sup> mutant mice

(A-E') Micrographs showing the representative Neurog2 (marking dorsal telencephalon) mRNA in situ hybridization on coronal sections of E12 and E14 dorsal telencephalon of Pax6<sup>Leca4</sup>, Pax6<sup>Leca2</sup>, E14 Pax6<sup>Sev</sup> and their WT littermates. Note that Neurog2 mRNA expression is maintained in the Pax6<sup>Leca4</sup> and Pax6<sup>Leca2</sup> mice.

Scale bars: 100 µm. Abbreviations: CTX, cortex; GE, ganglionic eminence.

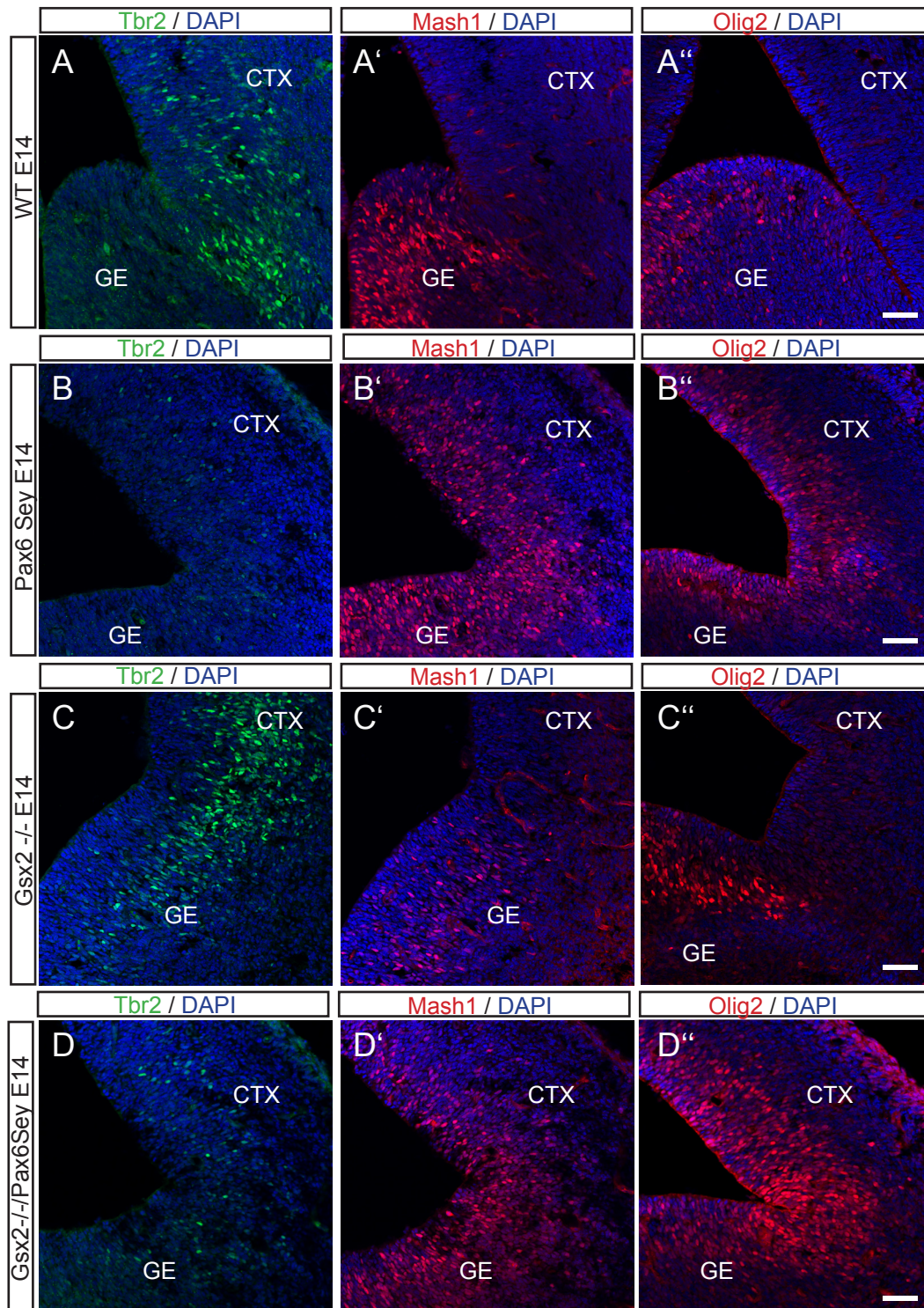


**Figure 2-18 Patterning of the telencephalon in Pax6<sup>Sey</sup>/Gsx2 double mutants**

(A-D) Micrographs of E14 coronal telencephalic sections depicting cells immunoreactive for Tbr2 (green), Mash1 (red) and Olig2 (red) in WT, Pax6<sup>Sey</sup>, Gsx2-knockout mice and Pax6<sup>Sey</sup>/Gsx2 double knockout mice.

Scale bars: 50  $\mu$ m. Abbreviations: CTX, cortex; GE, ganglionic eminence.

### 2.2.5 The role of the PAI and the RED subdomain in the regulation of neurogenesis

The presence of the two neurogenic genes *Neurog2* and *Tbr2* and the reduction in progenitor numbers in the *Pax6<sup>Leca4</sup>* cerebral cortex raised the question to which extent neurogenesis is affected in both *Pax6* subdomain mutants. Neurogenesis was first examined by immunostaining against the neuronal marker protein *Map2* labelling all differentiating neurons in the cortical plate (CP) and against the T-box protein *Tbr1*, which is found enriched in layer 6 neurons. While in the *Pax6<sup>Leca4</sup>* cerebral cortex both stainings showed that the thickness of the cortical plate was notably thinner compared to wild-type littermates (Fig.2-19), the mutation in the RED subdomain in the *Pax6<sup>Leca2</sup>* mutant had no effect on cortical plate thickness (Fig.2-19). The latter was further confirmed by *NeuN* staining in the adult *Pax6<sup>Leca2</sup>* mutant cortex (Fig.2-19C,C'). As described before, during neurogenesis different neuronal subtypes are generated at distinct developmental stages, migrate from the proliferative zones towards the pial surface and settle there in an in-side out manner forming the cortical plate. Given the decrease in CP thickness in the *Pax6<sup>Leca4</sup>* cerebral cortex, the generation of different neuronal layer subtypes was examined next. Immunohistochemical analysis of the *Foxp2* protein present in layer 6 neurons, the layer 5b neuron marker *Ctip2* and the layer 2-4 neuronal marker *Cux1* revealed a reduction of neurons in each layer at E17 in the *Pax6<sup>Leca4</sup>* cerebral cortex (Fig.2-20). Consistent with the normal thickness of the CP, all layers were of normal size in E17 *Pax6<sup>Leca2</sup>* mutants (Fig.2-20). Taken together, neurons are reduced in number in the cortical plate of *Pax6<sup>Leca4</sup>* mutants, but not affected in the *Pax6<sup>Leca2</sup>* mutant. This suggests that the PAI subdomain and not the RED subdomain of *Pax6* plays a key role in the regulation of neurogenesis in the cerebral cortex.

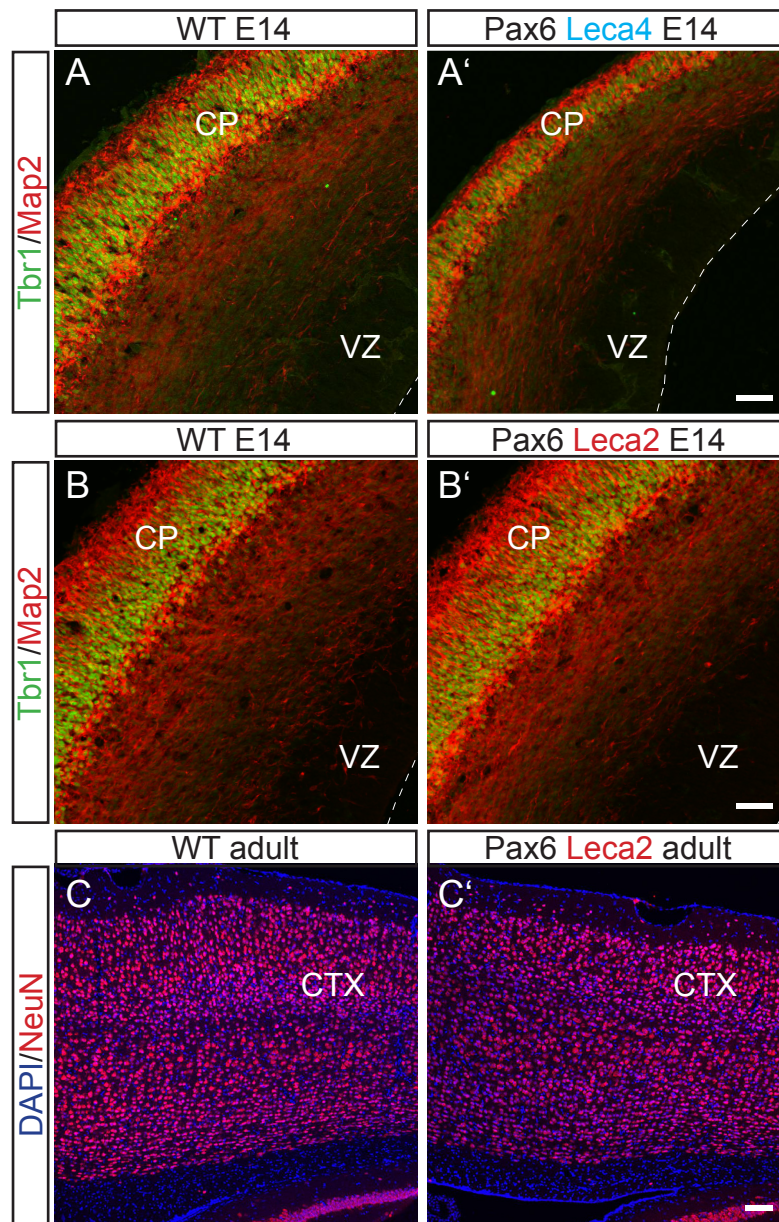


**Figure 2-19 Cortical plate reduction in the PAI-subdomain deficient ( $Pax6^{Leca4}$ ) but not in the RED-subdomain deficient ( $Pax6^{Leca2}$ ) mutant mice**

(A-B') Representative micrographs of cells immunoreactive for Tbr1 marking layer 6 neurons (green) and Map2 marking the cortical plate (red) in the coronal sections of E14 dorsal telencephalon of  $Pax6^{Leca4}$ ,  $Pax6^{Leca2}$ , and their littermates. Note the cortical plate reduction in the  $Pax6^{Leca4}$  mice. Dashed lines indicate the ventricular surface. (C,C') Immunofluorescence for NeuN (red) combined with DAPI staining (blue) on sagittal sections of the cortex of eight week old  $Pax6^{Leca2}$  and control mice. Scale bars: 100  $\mu$ m.

Abbreviations: CTX, cortex; CP, cortical plate; VZ, ventricular zone.

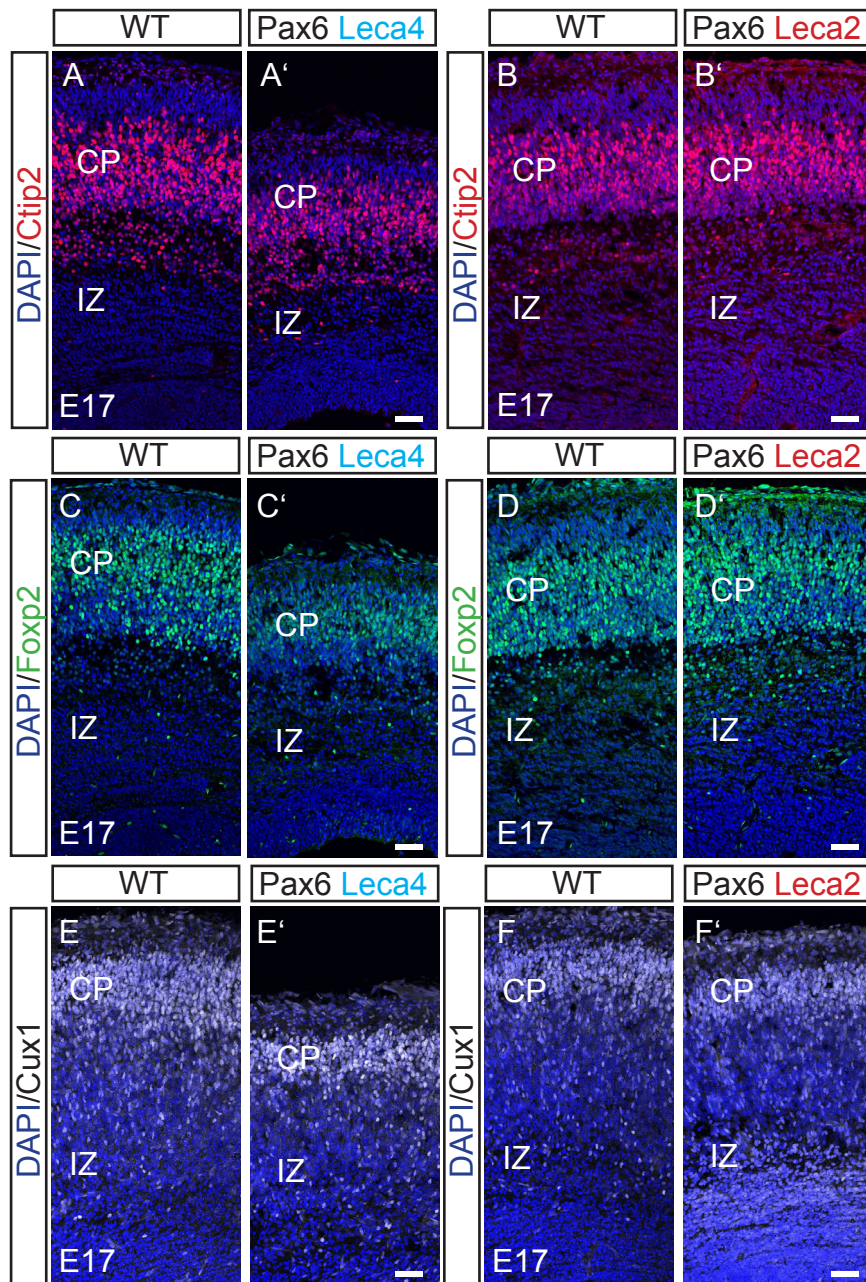


**Figure 2-20 Neurogenesis is impaired in the PAI-subdomain deficient ( $Pax6^{Leca4}$ ) mice but not in the RED-subdomain deficient ( $Pax6^{Leca2}$ ) mice**

(A-F') Immunofluorescence for Ctip2 (red) or Foxp2 (green) or Cux1 (white) combined with DAPI staining (blue) on coronal sections of E17 dorsal telencephalon of  $Pax6^{Leca4}$ ,  $Pax6^{Leca2}$  and control mice. Note the reduced expression of all three layer markers in the cortical plate of  $Pax6^{Leca4}$  but not  $Pax6^{Leca2}$  mice. Scale bars: 100  $\mu$ m.

Abbreviations: CP, cortical plate; IZ, intermediate zone.

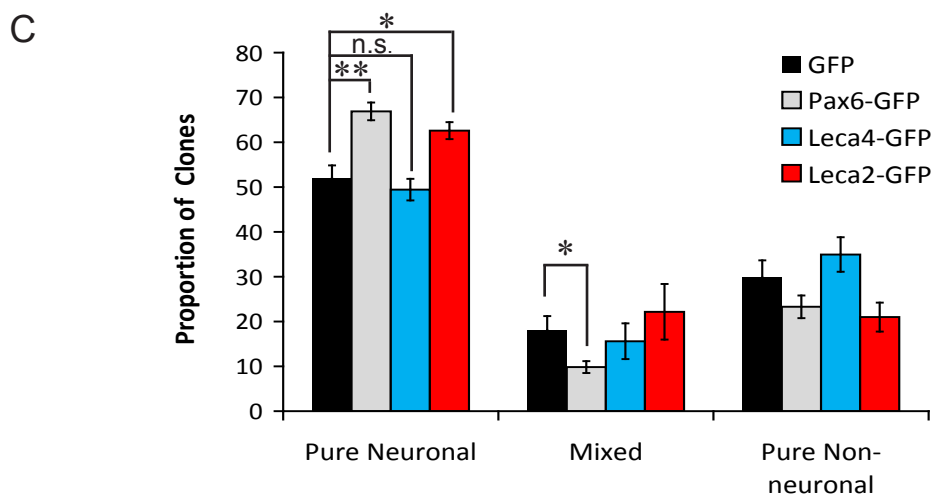
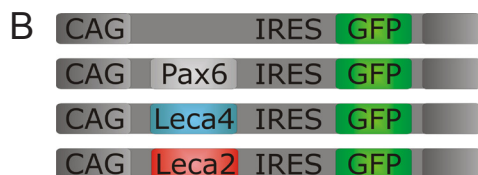
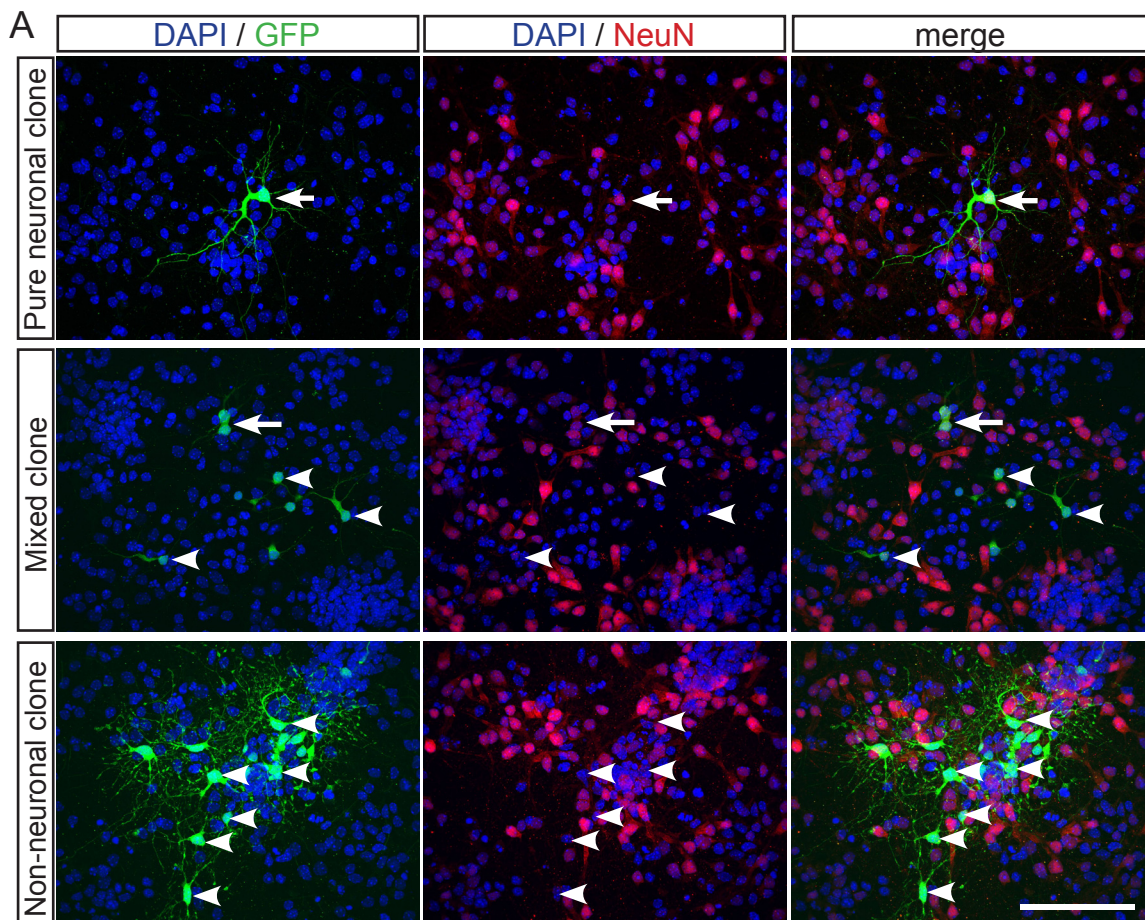
### 2.2.5.1 *Effect of Pax6Leca4 and Pax6Leca2 mutation on neurogenesis in-vitro*

In order to understand whether the impaired neurogenesis in the Pax6<sup>Leca4</sup> mutant cerebral cortex is linked to the reduced proliferation of progenitors or is caused by additional defects of neurogenesis as previously described for the full Pax6 mutant Pax6<sup>Sey</sup> (Heins et al., 2002; Haubst et al., 2004), the direct neurogenic capacity of the Pax6 Leca mutant forms was analysed in gain-of-function experiments. Dissociated primary cultures of WT E14 cerebral cortex cells were infected with replication incompetent MLV-based retroviruses expressing either only an eGFP reporter, or eGFP together with the Leca4 or Leca2 mutant form of Pax6 or the wild-type form of Pax6 used as positive control. The retrovirus reverse transcribed DNA integrates only in the genome of dividing cells and then is inherited to the daughter cells. Hence with an infection at clonal density (less than 50 clones per coverslip) the progeny of a single infected cell represents a clone. To assess the direct neurogenic capacity, the fate of the progeny of single progenitor cells seven days after infection was determined using immunocytochemistry for the neuronal marker NeuN. Depending on the composition, the clones were classified as pure neuronal clone, when only neurons were present in the clone, as mixed clone when it contained both NeuN+ and NeuN-negative cells and as pure non-neuronal clone when exclusively NeuN-negative cells were detected (examples are shown in Fig.2-21A and Fig.2.22A). Consistent with previous data (Heins et al., 2002; Haubst et al., 2004), overexpression of wild-type Pax6 significantly increased the fraction of pure neuronal clones (Fig. 2-21). Similarly, after forced expression of the Leca2 mutant form of Pax6 a comparable, significant increase in the percentage of pure neuronal clones was determined (Fig. 2-21). In contrast, the PAI deficient Leca4 mutant form of Pax6 did not influence clone composition compared to the GFP-only vector control (Fig. 2-21). Thus the mutation in the PAI but not the mutation in the RED subdomain affects the neurogenic capacity of Pax6, suggesting a selective role for the PAI subdomain in neurogenic fate instruction in these cells.

---

#### **Figure 2-21 The PAI-subdomain has a selective role in neurogenic fate instruction**

(A) Representative images of neuronal, mixed and non-neuronal clones derived from the progenitors isolated from the E14 cerebral cortex and infected with the CAG control retrovirus. Arrows indicate double labelled cells and arrowheads only GFP positive cells. Scale bar: 50  $\mu$ m. (B) Schematic drawings of the retroviral constructs used for the overexpression experiments.



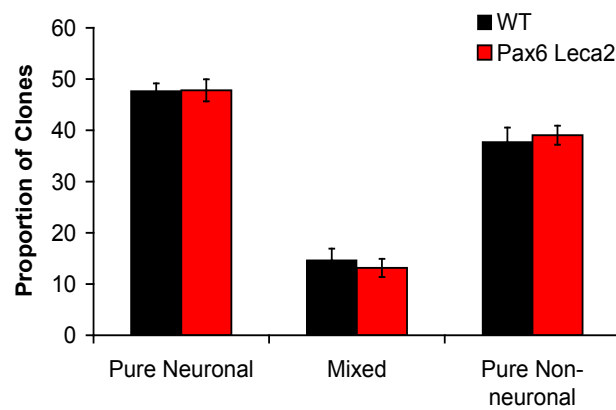
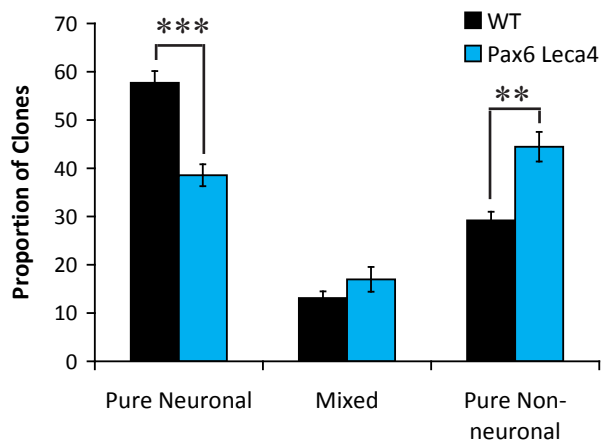
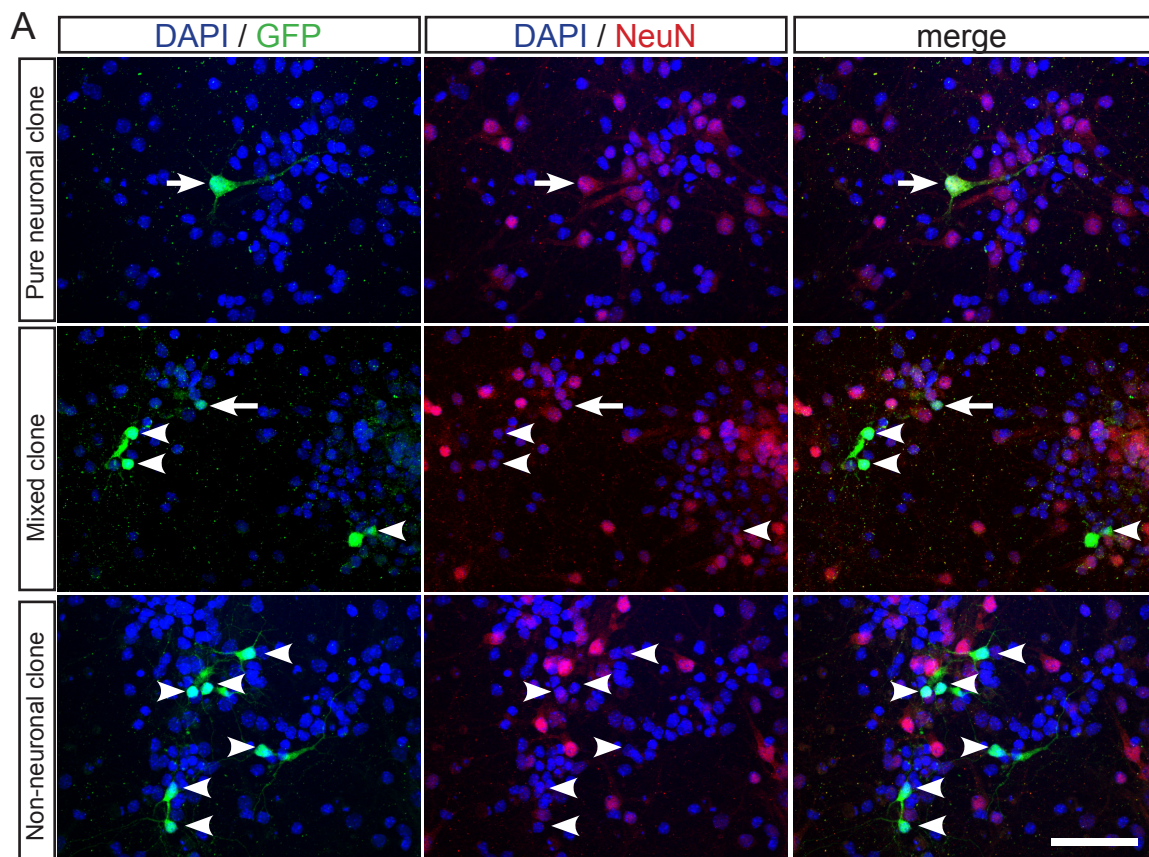
To further investigate this conclusion, the same clonal analysis was performed in cultures isolated from E14 Pax6<sup>Leca4</sup> and Pax6<sup>Leca2</sup> mutant cerebral cortices infected with a GFP control virus as reporter. In line with the previous results, a reduction of pure neuronal clones compared to those from their wild-type littermates was found in cultures from the Pax6<sup>Leca4</sup> mutant cortex (Fig. 2-22B). Furthermore, no change in clone composition was detected from the cells of the Pax6<sup>Leca2</sup> mutant cortex (Fig. 2-22C). These results therefore further support a role of the PAI subdomain of Pax6, but not the RED subdomain for neuronal fate specification in progenitors of the cerebral cortex.

Pure neuronal clones normally consist of one or two neurons only compared to mixed or pure non-neuronal clones that on average possess a larger clone size (examples see Fig.2-21A, Fig.2-22A). Hence, consistent with the generation of fewer pure neuronal clones from Pax6<sup>Leca4</sup> cultures, a significant increase in the overall clone size was determined ( $p < 0.05$ ; Appendix Table 5-1). Furthermore, no reduction in clone size was detected in cultures from the Pax6<sup>Leca2</sup> mutant (Appendix Table 5-1). The size of the clones after forced expression of the Leca mutant forms of Pax6 showed a trend in line with the in-vivo proliferation data. Overexpression of Pax6<sup>Leca4</sup> decreased the size of clones generated from infected progenitors, while forced expression of the RED subdomain mutant Leca2 was no longer able to reduce clone size (Appendix Table 5-1). Thus, these data further support the selective effects of the RED and the PAI domain on proliferation with an increased proliferation after loss of function of the anti-proliferative RED domain and decreased proliferation seen after loss of function of the pro-proliferative PAI domain, respectively.

---

### **Figure 2-22 Pax6<sup>Leca4</sup> but not Pax6<sup>Leca2</sup> progenitors show deficiency in neuronal fate commitment**

(A) Representative images of neuronal, mixed and non-neuronal clones derived from the progenitors isolated from the E14 cerebral cortex and infected with the Pmxig control retrovirus. Arrows indicate double labelled cells and arrowheads only GFP positive cells. Scale bar: 50  $\mu$ m. (B,C) Histograms depicting the clone types generated from the E14 cortical progenitors isolated from the Pax6<sup>Leca4</sup> mutant (B), Pax6<sup>Leca2</sup> mutant (C) or their WT littermates. Note the significant decrease of pure neuronal clones and increase of non-neuronal clones (blue bars) in the cultures isolated from the Pax6<sup>Leca4</sup> mutant cortex compared to the corresponding WT control. Data are shown as mean  $\pm$  SEM; n (coverslip analysed)  $\geq$  6; \*\* $p < 0.01$ , \*\*\* $p < 0.001$ ; one-way Anova test.

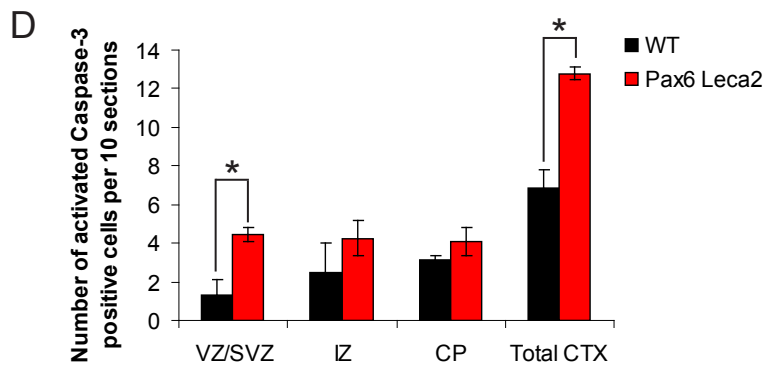
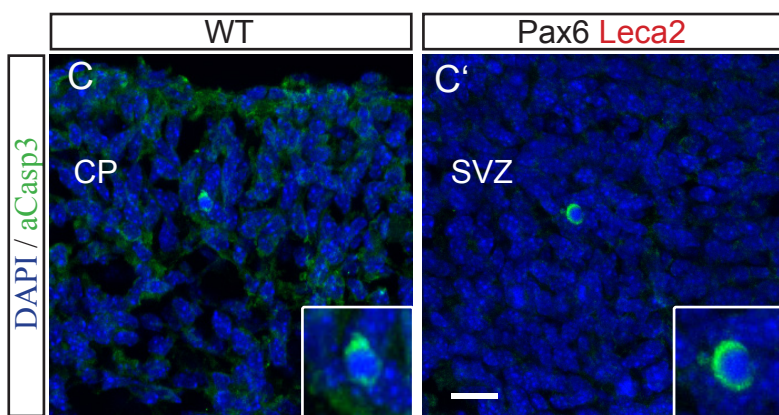
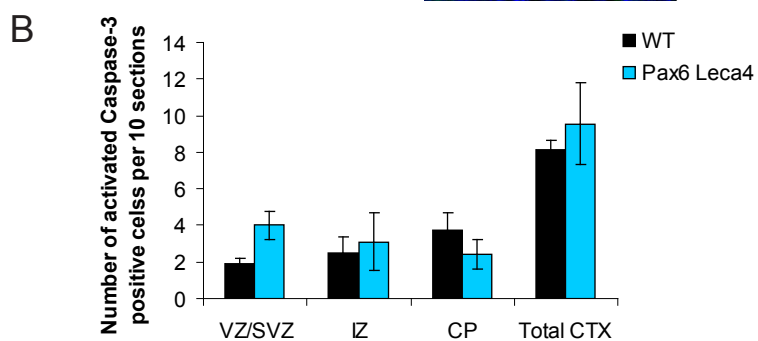
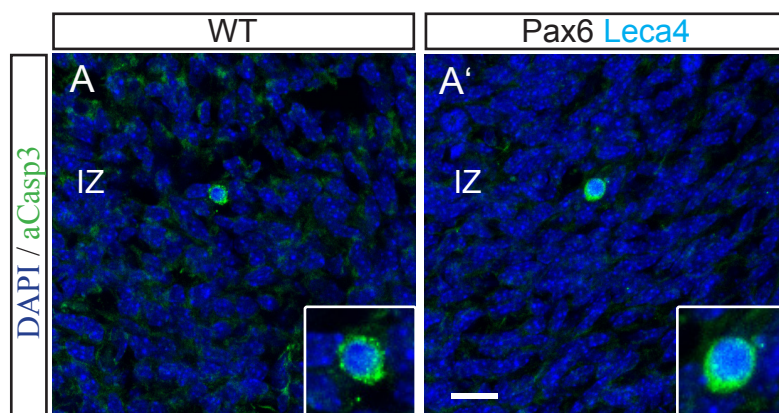


### 2.2.6 Cell death analysis in the Pax6<sup>Leca2</sup> and Pax6<sup>Leca4</sup> mutant cortex at midneurogenesis

One possible explanation for the increase in mitotic progenitors in the Pax6<sup>Leca2</sup> mutant cortex but apparently normal neuronal output might be changes in cell survival as Pax6 has also been implicated to play a role in this context (Nikoletopoulou et al., 2007; Ninkovic et al., 2010). Therefore programmed cell death was examined in WT and both Pax6 Leca mutant cortices using activated-Caspase3 staining. Although Nikoletopoulou et al. reported increased cell death in Pax6<sup>Sey</sup> mice only at E12, programmed cell death was analysed at E14 in the Leca mutants. This is because the significant increase in mitotic progenitors in the Pax6<sup>Leca2</sup> mutant was observed at E14 and not at E12. Indeed, in the Pax6<sup>Leca2</sup> mutant cortex the number of apoptotic cells was significantly increased by almost two-fold compared to the corresponding wild-type littermate (Fig.2-23C-D). Interestingly, when subdividing the cortex into the progenitor zones (VZ/SVZ), the intermediate zone (IZ) and cortical plate (CP), the significant increase in activated-Caspase3 positive cells was specifically located in the VZ/SVZ of the Pax6<sup>Leca2</sup> mutant cortex (Fig.2-23D), the regions of increased PH3+ cells (Fig.2-10). In contrast, the number of apoptotic cells was unchanged in the cerebral cortex of Pax6<sup>Leca4</sup> mutants compared to its respective wild-type littermate at embryonic day E14 (Fig.2-23A-B). Thus, the increased proliferation observed in the Pax6<sup>Leca2</sup> mutant cortex goes along with an increase in cell death of progenitors, possibly accounting for the observed normal cortical size.

#### Figure 2-23 Increased cell death in the Pax6<sup>Leca2</sup> mice (RED-subdomain) but not in the Pax6<sup>Leca4</sup> mice (PAI-subdomain)

(A,A',C,C') Micrographs of E14 coronal telencephalic sections depicting cells immunoreactive for activated Caspase-3 (green) in Pax6<sup>Leca4</sup>, Pax6<sup>Leca2</sup> and their WT littermates. (B,D) Histograms showing the number of activated Caspase-3 -positive cells in the VZ/SVZ, IZ, CP and per total CTX in Pax6<sup>Leca4</sup>, Pax6<sup>Leca2</sup> and their WT littermates at E14. Data are shown as total numbers per 10 sections  $\pm$  SEM, n (embryos analysed)  $\geq$  3; (av. 15 sections per embryo) \*p<0.05. Note the increase in apoptotic cells in the VZ/SVZ in Pax6<sup>Leca2</sup> but not Pax6<sup>Leca4</sup> mutants. SVZ, subventricular zone; IZ, intermediate zone; CP, cortical plate; CTX, cortex. Scale bars: 10  $\mu$ m.



### 2.2.7 Genome-wide expression analysis in the Pax6<sup>Leca4</sup> (PAI domain) and Pax6<sup>Leca2</sup> (RED domain) mutant cerebral cortex

The distinct effects of the PAI and RED subdomain mutations on neurogenesis and progenitor proliferation observed in both Leca mutants prompted the analyses of genome-wide expression changes in the developing cerebral cortices of these mutants. To get further insight into the specific molecular changes and to which extent they reflect the phenotypes observed, microarray analysis in rostral regions of E14 wild-type and mutant cerebral cortices were performed. The time point E14 was chosen as the phenotype in Pax6<sup>Leca2</sup> mutants was not yet fully apparent at E12 and analysis of the rostral cortex was selected to avoid indirect influences by potential changes in arealisation. RNA was hybridised to whole-genome Affymetrix MOE430 2.0 arrays and gene expression differences between WT and mutants were determined applying the following three criteria: first, genes considered significantly changed in their expression, were tested significant (FDR<10%) in several statistical tests performed (see Material and Methods); second, genes were selected based on a 1.4 fold change difference between wild-type and mutant cortices and thirdly, by an average absolute expression level of >50. This analysis revealed in the PAI domain mutant Pax6<sup>Leca4</sup> 416 probe sets with significantly altered expression, of which 179 (43%, Appendix Table 5-2) showed a reduced expression level (Fig.2-24A). In comparison, in the RED-subdomain mutant Pax6<sup>Leca2</sup> 94 differentially expressed probe sets were detected, of which 59 (63%, Appendix Table 5-3) were down-regulated (Fig.2-24B). From the Pax6<sup>Leca4</sup> and Pax6<sup>Leca2</sup> transcriptome, several genes were selected for q-PCR confirmation analysis. All of the selected genes were significantly validated by q-PCR, showing the same up- or down-regulation as detected in the array (Fig.2-24C-D'). The linear ratios measured by q-PCR, were in most cases higher than the ratios detected in the array.

#### Figure 2-23 Increased cell death in the Pax6<sup>Leca2</sup> mice (RED-subdomain) but not in the Pax6<sup>Leca4</sup> mice (PAI-subdomain)

(A,A',C,C') Micrographs of E14 coronal telencephalic sections depicting cells immunoreactive for activated Caspase-3 (green) in Pax6<sup>Leca4</sup>, Pax6<sup>Leca2</sup> and their WT littermates. (B,D) Histograms showing the number of activated Caspase-3 -positive cells in the VZ/SVZ, IZ, CP and per total CTX in Pax6<sup>Leca4</sup>, Pax6<sup>Leca2</sup> and their WT littermates at E14. Data are shown as total numbers per 10 sections  $\pm$  SEM, n (embryos analysed)  $\geq$  3; (av. 15 sections per embryo) \*p<0.05. Note the increase in apoptotic cells in the VZ/SVZ in Pax6<sup>Leca2</sup> but not Pax6<sup>Leca4</sup> mutants. SVZ, subventricular zone; IZ, intermediate zone; CP, cortical plate; CTX, cortex. Scale bars: 10  $\mu$ m.

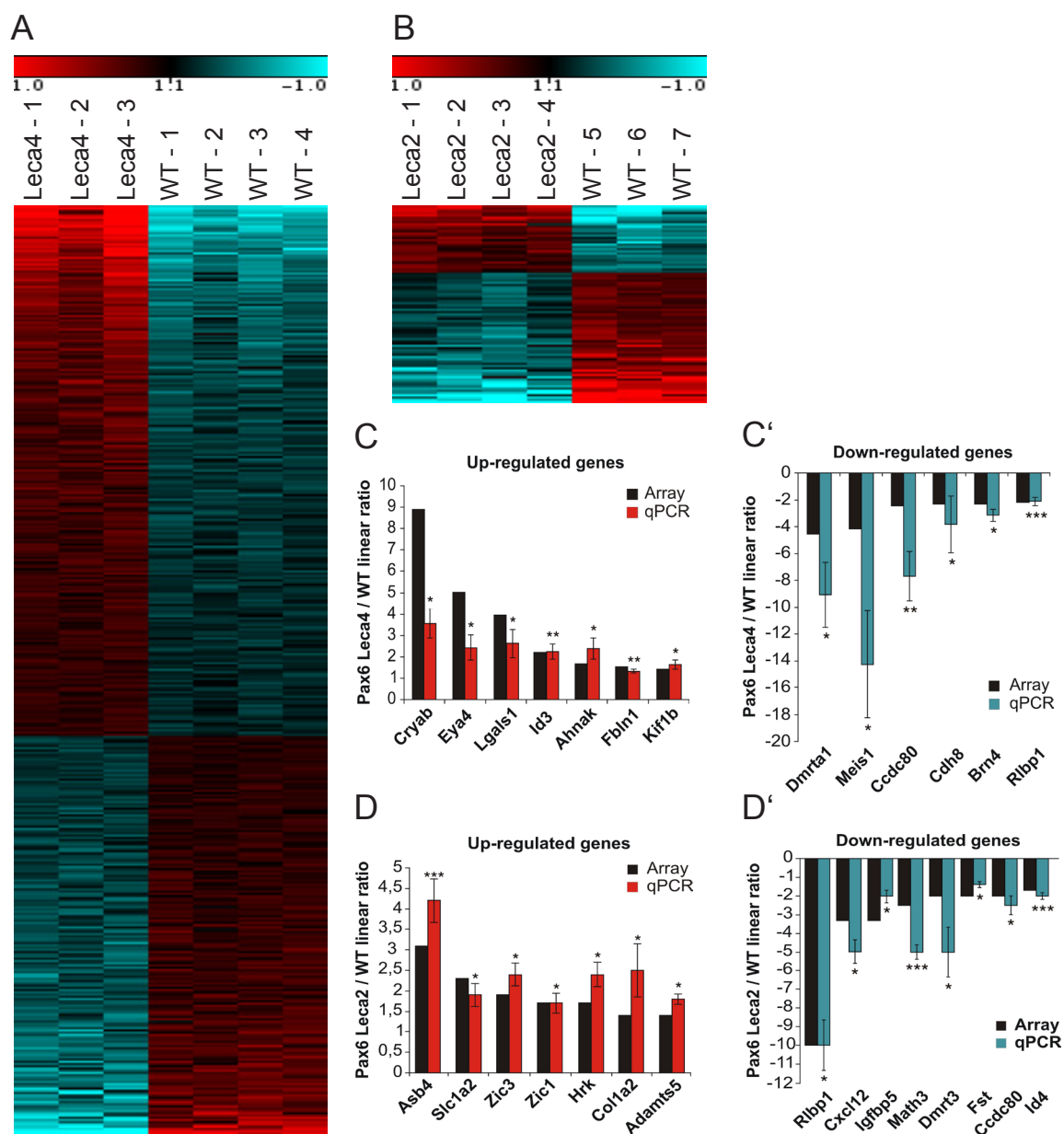


**Figure 2-24 Transcriptome analysis of Pax6<sup>Leca4</sup> mice (PAI-subdomain) and Pax6<sup>Leca2</sup> mice (RED-subdomain)**

(A,B) Heatmap representations of expression values of genes deregulated in the (A) Pax6<sup>Leca4</sup> or (B) Pax6<sup>Leca2</sup> E14 rostral cortex compared to the corresponding WT littermates. Red/blue indicate higher/lower expression values. (C,C' and D,D') Histograms depicting the linear fold change of gene expression levels between Pax6<sup>Leca4</sup> or Pax6<sup>Leca2</sup> and the corresponding WT littermates measured by Affymetrix array analysis or quantitative RT-PCR; Data are shown as mean  $\pm$  SEM; \* $p < 0.05$ , \*\* $p < 0.01$ , \*\*\* $p < 0.001$ ; one-way Anova test.

### 2.2.7.1 *Differentially expressed genes in the Pax6<sup>Leca4</sup> mutant cortex*

Consistent with the neurogenesis defect in the Pax6<sup>Leca4</sup> mutant, the transcriptome analysis of this mutant revealed several deregulated genes known to play a role in regulation of neurogenesis. Amongst them, multiple components of the retinoic acid (RA) signalling pathway, such as the recently identified direct Pax6 target Rlbp1 (Boppana et al., 2012) as well as the cellular retinol binding protein 1 (Rbp1) and the carrier of the retinol metabolite RA (Crabb2). Furthermore, molecules of the Wnt-signalling pathway, which play essential roles in coordinating cortical neurogenesis showed altered expression levels. Amongst these, the Wnt7a ligand, which has been implicated to promote neurogenesis, was found down-regulated (Hirabayashi et al., 2004). Whereas the inhibitor of differentiation 3 (Id3) known to inhibit precocious differentiation of cortical progenitors and the Wnt5a ligand, a representative of non-canonical Wnt ligands implicated in regulating neurogenesis through maintenance of progenitors were both found up-regulated (Lyden et al., 1999; Endo et al., 2012). Besides signalling pathways, many mRNAs encoding for transcription factors involved in neurogenesis were found to be down-regulated in the Pax6<sup>Leca4</sup> mutant cortex compared to the control. Amongst these, for example, the Pou3f4 (Brn4) transcription factor required for neuronal differentiation and maturation of newborn neurons (Shimazaki et al., 1999), the Cux2 transcription factor important for controlling proliferation rates of intermediate progenitors and the number of upper layer neurons (Cubelos et al., 2008) or the Tcfap2c (AP-2gamma) transcription factor involved in regulating basal progenitor and laminar fates (Pinto et al., 2009). Others comprise the transcription factors Dmrt1a, Meis1, Sall3 or Pbx3 (Knoepfler and Kamps, 1997; Huang et al., 2005; Harrison et al., 2008; Heine et al., 2008; Heng et al., 2012). Taken together, signalling pathways and transcription factors all known to be involved in regulation of neurogenesis were deregulated in the Pax6<sup>Leca4</sup> cortex reflecting changes of the PAI-mediated neurogenic program, which were in line with the observed neurogenic defect.

Further consistent with the distinct functions of the Leca4 mutation, genes promoting cell cycle exit such as Gadd45 were up-regulated in the Pax6<sup>Leca4</sup> mutant cerebral cortex. On the other hand pro-proliferative factors like Id2 (Uribe and Gross, 2010) or tenascin C (von Holst et al., 2007) were decreased in expression. Moreover, the mRNA of the bcl-2 gene, which in its phosphorylated status constitutes an M-phase marker (Ling et al., 1998), was decreased.

Taken together, in line with the observed decrease of proliferating cells in the Pax6<sup>Leca4</sup> mutant cortex, the transcriptome analysis of this mutant furthermore revealed expression

changes of several molecules involved in positive or negative regulation of proliferation, which were down or up regulated respectively. This supports the PAI mediated pro-proliferative function of Pax6 in cortical progenitors.

#### 2.2.7.2 *Differentially expressed genes in the Pax6<sup>Leca2</sup> mutant cortex*

Consistent with the less severe phenotype observed in the Pax6<sup>Leca2</sup> mutants, the transcriptome analysis of the Pax6<sup>Leca2</sup> mutant revealed fewer gene expression changes compared to the Pax6<sup>Leca4</sup> mutant cortex (94 vs. 416). In correlation with the increase of mitotic cells observed in the Pax6<sup>Leca2</sup> mutant cortex, transcription factors known to promote proliferation, such as Zic1 (Pourebahim et al., 2007; Brill et al., 2010; Watabe et al., 2011) and Zic3 (Inoue et al., 2007) were found to be up-regulated. Noteworthy, the up-regulated genes in the Pax6<sup>Leca2</sup> mutant cortex furthermore revealed two mRNAs encoding for pro-apoptotic genes. Both genes, the Harakiri (Hrk) and the Bcl2-like-11 (Bcl2l11; also known as Bim) belong to the BH3-domain only containing subgroup of pro-apoptotic Bcl2-family members and facilitate apoptosis (Putchu et al., 2001; Ghosh et al., 2011). Interestingly, it has been shown that changes in the phosphorylation status of Bcl2l11 during mitosis are implicated to correlate with prolonged mitotic arrest which precedes cell death (Mac Fhearraigh and Mc Gee, 2011).

Consistent with the in vivo and in vitro results described above, the transcriptome analysis of the Pax6<sup>Leca2</sup> mutant did not reveal major changes of neurogenic molecules, further supporting the role of the PAI but not the RED subdomain in regulation of neurogenesis during forebrain development.

Taken together, the transcriptome analysis of the Pax6<sup>Leca2</sup> mutant correlates with the observed phenotype in this mutant, including support for an anti-proliferative role of the RED subdomain of Pax6.

#### 2.2.7.3 *Comparison of differentially expressed genes between the Pax6<sup>Leca4</sup> and Pax6<sup>Leca2</sup> mutant cortex*

As depicted in the Venn-diagram (Fig.2-25A), the comparison of both mutant transcriptomes revealed only 17 probe sets commonly regulated in both mutants (Appendix Table 5-4). Thereof, 15 probe sets were regulated in the same manner in both mutants and the majority of which were down-regulated. Noteworthy, amongst these one recently identified direct Pax6 target, the Rlbp1 gene (Boppana et al., 2012) was found. Furthermore, only two

probes, of Neurogenin1 and Dnajc1 (Appendix Table 5-4) showed opposite regulation being down- or up-regulated in the cerebral cortex of Pax6<sup>Leca2</sup> or Pax6<sup>Leca4</sup> embryos, respectively. Thus, the comparison of both transcriptomes revealed little overlap supporting that the PAI and the RED domain of Pax6 regulate distinct genes independently.

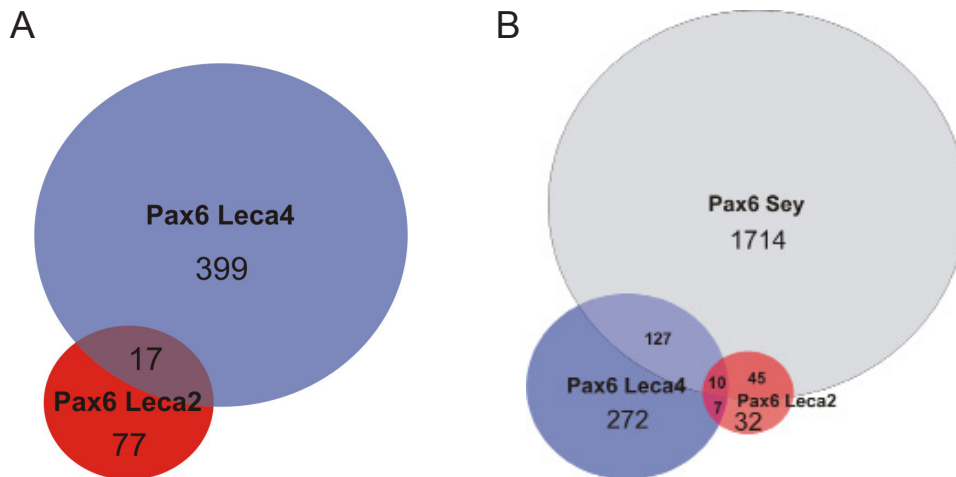


**Figure 2-25 Comparison of transcriptome data from Pax6<sup>Leca4</sup>, Pax6<sup>Leca2</sup> and Pax6<sup>Sey</sup> mice**

(A,B) Venn diagrams depicting the overlap between the deregulated probe sets observed in the Pax6<sup>Leca4</sup> and Pax6<sup>Leca2</sup> cortices (A) and Pax6<sup>Sey</sup> cortices (B). Note the small proportion of commonly regulated genes in Pax6<sup>Leca2</sup> and Pax6<sup>Leca4</sup> cortices.

#### 2.2.7.4 Comparison of differentially expressed genes between the Pax6 Leca mutant cortices and the functional Pax6 null mutant Pax6<sup>Sey</sup>

In order to further understand the individual expression differences the same microarray was performed for the functional null mutant Pax6<sup>Sey</sup>. Consistent with the more severe phenotype in Pax6<sup>Sey</sup> mutants, a much larger number of genes was significantly altered in expression (1898; data set not shown) as compared to the transcriptomes of the Leca mutants (Fig.2-25B) and the total overlap between all three mutants was very low (10 probe sets; see within Appendix Tables 5-5 and 5-6). In fact, in line with the severe ventralization of the dorsal telencephalon present solely in the Pax6<sup>Sey</sup> mutant and absent in the Leca mutant cortices, the set of genes deregulated in the Pax6<sup>Sey</sup> mutant cortex comprised many ventral factors. Notably, amongst them the highly up-regulated transcription factors Olig2, Gsx1/2, Mash1 and the Dlx transcription factor family, while both in line with the protein data (Fig.2-14,15,16), only Ascl1/Mash1 was increased in both Leca mutant cerebral cortices. Although

Olig2 mRNA was found elevated also in the Leca2 mutant cortex, this was not detected on protein levels (Fig.2-15). Moreover, many genes encoding for centrosome associated proteins and normally strongly expressed in the ventral telencephalon, were up-regulated in the Pax6<sup>Sev</sup> mutant but were not affected in either of the Leca mutants. For example, the expression of the direct Pax6 target Spag5 which regulates the orientation of cell division (Asami et al., 2011) or Aspm, a protein known to control spindle orientation (Fish et al., 2006) was not changed in both Leca mutant cortices. However, further consistent with the phenotypes, the genes involved in regulation of neurogenesis affected in the Pax6<sup>Leca4</sup> mutant (see above) were similarly affected in the Pax6<sup>Sev</sup>, but not in the Pax6<sup>Leca2</sup> mutant cortex. Taken together, this comparison further supports that the distinct sets of regulated genes found in these mutant cortices in fact correspond to the distinct roles of Pax6 reflected by the individual phenotypes.

#### *2.2.7.5 Comparison of the differentially expressed genes in the Pax6 Leca mutant cortices and Pax6-Chip data*

In order to evaluate the potential abundance of direct and indirect targets of Pax6 amongst the genes found altered in the PAI and RED domain mutant cerebral cortices, the transcriptomes were compared with Pax6 chromatin-immunoprecipitation (ChIP) data provided from our collaborator Ales Cvekl. He obtained Pax6 ChIP data from E15 WT cerebral cortex, lens and pancreas cells (Xie et al. 2012, submitted). Interestingly, the comparison showed an overlap of about 20% for the deregulated genes found in the Pax6<sup>Leca4</sup> (82/416) but also for the deregulated genes found in the Pax6<sup>Leca2</sup> mutant (20/94). Amongst these, few previously described direct targets were found, like Cspg2, Rlbp1 or Pax6 itself (Appendix Table 5-2 and 5-3). Interestingly only three genes with positive Pax6-ChIP signal were determined in both Leca mutant transcriptomes (Rlbp1, Neurogenin1, Ccdc80). Whereas most were detected either in the pool of genes only regulated in the Pax6<sup>Leca4</sup> mutant (e.g. Cdh8, Crabp1 and Tnc) or in the Pax6<sup>Leca2</sup> mutant (e.g. Bcl2l11, Neurod4, Id4, Zic1 and Zic3). Thus, this once more supports the individual regulations exerted by the PAI and the RED subdomain of Pax6 and reveals Pax6 direct target genes dependant on PAI or RED domain mediated function.

### **2.2.8 Superactivation by the RED domain mutation of Pax6**

Given that the PAI and RED domain mutants display distinct phenotypes including the above described different gene expression changes, implies that the two subdomains may distinctly regulate gene expression. However cooperative effects have also been observed between the PAI and RED, but also with the other domains of Pax6 (Jun and Desplan, 1996; Singh et al., 2000; Mikkola et al., 2001; Mishra et al., 2002; Xie and Cvekl, 2011). In order to investigate the transactivation properties of the Leca mutant proteins, luciferase assays were performed on different published Pax6 consensus sites (Epstein et al., 1994a). When examining the transactivation potential of the Leca2 mutant form of Pax6 on two Pax6 consensus sites, gain of transcriptional activation was measured (Fig.2-26). Luciferase reporter assays on constructs containing the paired domain consensus site P6CON together with the homedomain consensus site P3 as well as on a reporter construct containing only the P3 binding site, resulted in a significant superactivation by the Leca2 mutant form of Pax6. Moreover, this result was independent from the level of endogenous WT Pax6 protein, as superactivation was detected in both P19 cells (which contain endogenous Pax6 protein) and HEK cells (which are devoid of endogenous Pax6 protein) (Fig.2-26). Conversely, the Leca4 mutant form of Pax6 showed no enhanced transactivation on the P6CON-P3 and P3 constructs compared to WT Pax6. Thus, gain of function exerted by the Leca2 mutation may result in superactivation, potentially dependent on the cellular environment.

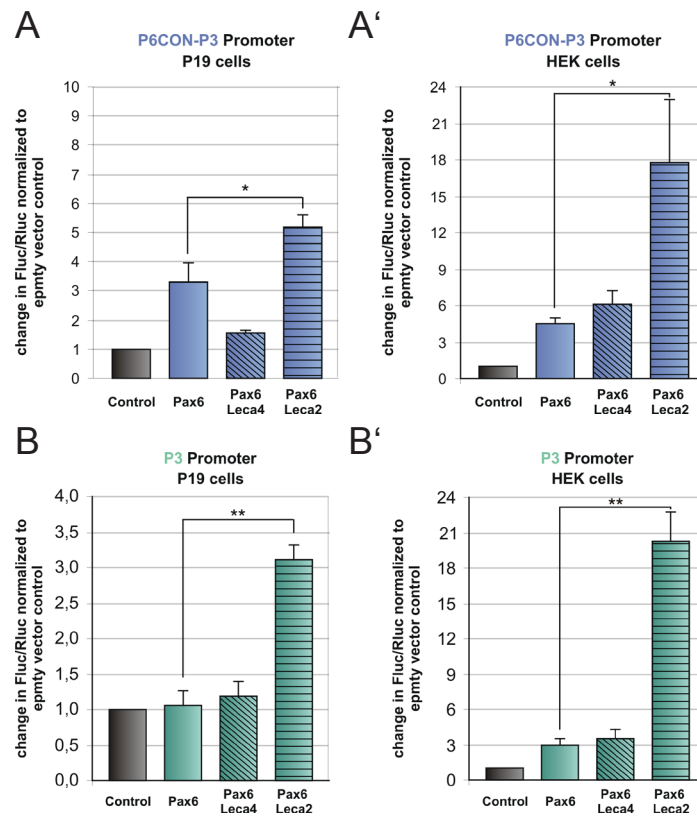


**Figure 2-26 Transactivation analysis on the Pax6-consensus sites P3-P6CON and P3**  
**(A-B')** Histograms depicting the transactivation properties on the published Pax6 consensus sites P3-P6CON (A,A') and P3 (B,B') by WT Pax6, Pax6Leca2 and Pax6Leca4 measured as reporter gene activation in luciferase assay in P19 and HEK cells. Data are shown as the mean  $\pm$  SEM. \* $p < 0.05$ , \*\* $p < 0.01$ .

## **2.3 Fate determinants at post-transcriptional level: microRNA expression during neuronal differentiation**

The transcription factor Pax6 may not only regulate mRNA coding genes, but also control the expression of microRNA molecules. These have been shown to play a role in CNS development and have been implicated in controlling various cellular processes including self-renewal and fate specification (Fineberg et al., 2009; Shi et al., 2010). However the expression and role of single microRNAs is still poorly understood. To identify new miRNAs involved in radial glia specification and differentiation, potentially controlled by the transcription factor Pax6, a miRNA and mRNA profiling was performed at different stages during neuronal differentiation with a differentiation system generating Pax6+ progenitors.

### **2.3.1 The screening system: in-vitro differentiation from ESC to glutamatergic neurons**

In order to identify microRNAs that are differentially expressed during neuronal differentiation an in-vitro differentiation culture was used. It has been previously shown that homogeneous populations of Pax6+ cells with radial glia properties can be derived from embryonic stem cells (ESC) that can be further differentiated into neurons (Bibel et al., 2004; Conti et al., 2005; Pollard et al., 2006; Bibel et al., 2007; Gaspard et al., 2008). Using the culture system according to Bibel et al. 2007, highly proliferative embryonic stem cells were exposed to retinoic acid (RA) at the cellular aggregate (CA) stage, inducing their differentiation into a relatively homogeneous population of Pax6 positive radial glia cells. When further differentiated, these cells gave rise to functional glutamatergic neurons very much similar to neurons derived of Pax6 expressing precursors in the developing mammalian cortex. To analyse microRNA expression, five different time points covering the course of differentiation were selected (Fig.2-27). After depletion of feeder cells, the embryonic stem cells were cultured in a medium that induced formation of cellular aggregates (CA). The first sample was collected four days after beginning of aggregate formation, just before the first addition of RA. Thus the cells at this stage reside in an undifferentiated ESC like state (sample 1: CAd4). The cellular aggregates were cultured over eight days and treated twice with the inductive stimulus retinoic acid at day four and six. The next samples were collected at day six (before the 2nd addition of RA; sample 2: CAd6) and day eight (sample 3: CAd8). At CAd8, the cells resembled neural precursors with some radial glia properties, such as the expression of Pax6. After dissociation of the aggregates and plating on Poly-dL-Ornithine (PORN) and

laminin coated dishes, the neural precursors adopted the distinct, spindle-shaped morphology of radial glial cells. The fourth sample was taken at this stage, 14 hours after plating (sample 4: P14h). Finally as differentiation was continued with different culture media, these progenitors differentiated into a homogenous population of glutamatergic neurons and the last sample was collected seven days after plating of the aggregates (sample 5: N7).

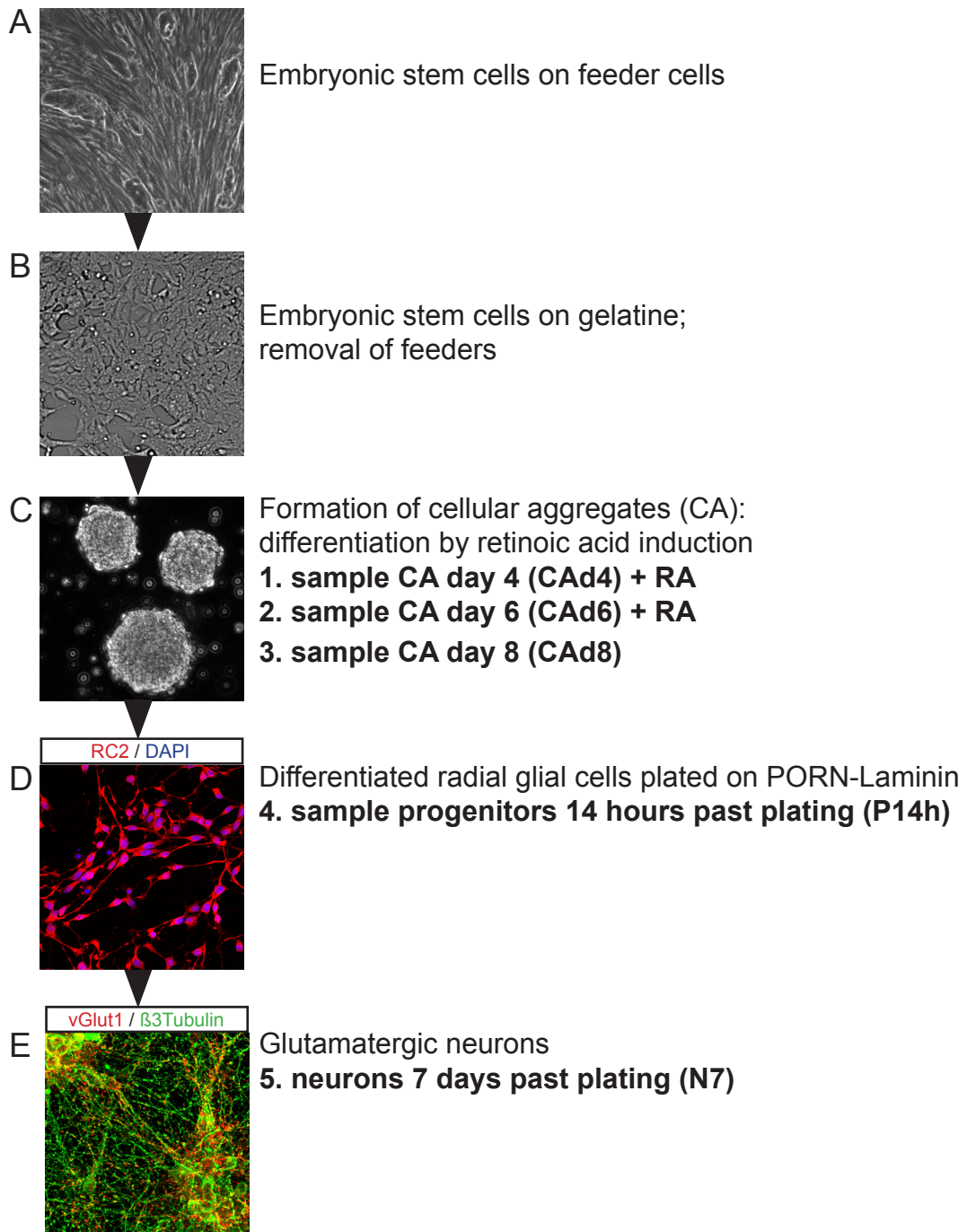


**Figure 2-27 Scheme depicting the embryonic stem cell differentiation protocol according to Bibel et al., 2007 for miRNA profiling**

(A-D) Micrographs depicting the different stages of differentiation from mouse ESC (A) to glutamatergic neurons (E). (A,B) Brightfield images of ESC (potato shaped colonies) on a dense feeder layer (A) and of ESC cultured on gelatine, depleted of feeder cells (B). (C) Brightfield image of cellular aggregates eight days after aggregate formation induced by addition of retinoic acid (RA). (D) Differentiated radial glial like cells 14 hours after plating on PORN-Laminin coated dishes, stained for the radial glial marker RC2 (red). (E) Glutamatergic neurons seven days after plating stained for beta3Tubulin (green) and vGlut1(red). Note the five different time points selected for miRNA profiling are described under C-E.

---

**2.3.2 Differentially expressed microRNAs during differentiation**

For microRNA profiling, total RNA (including all mRNA and microRNA species) was extracted from three replicates of each of the five different time points and microRNA array analysis was performed using the miRCURY LNATM platform (Exiqon, Denmark). Briefly, miRNAs were hybridized to miRCURY™ LNA Arrays (v.11.0) that contained capture probes for all microRNAs in human, mouse, rat and their related viruses as annotated in miRBase Release v.11.0. Quantified signals were normalized using the global Lowess (LOcally WEighted Scatterplot Smoothing) regression algorithm and expression differences between the different sample groups were determined. For mRNA profiling, total RNA from the same samples were DNase I digested and hybridized to whole-genome Affymetrix MOE430 2.0 arrays and gene expression was determined as described before.

The miRNA analysis revealed 89 microRNAs that are differentially expressed over the time course of differentiation (Fig.2-28). A clear change of miRNA expression was most noted between the more undifferentiated stages (CA<sub>d4</sub>, CA<sub>d6</sub>) and the first neural progenitor stage CA<sub>d8</sub> (Fig.2-28). Moreover, several patterns of expression were identified. These include ESC specific microRNAs that are down-regulated during differentiation and neuron specific microRNAs that are up-regulated during differentiation. While these two expression patterns comprised most differentially regulated miRNAs, some miRNAs showed a peak expression at the progenitor stage or had a minimal expression at the progenitor stage.

Amongst the ES-cell specific miRNAs, members belonging to the miR-290-295 cluster coding for a family of microRNAs were identified. This cluster has been linked to a number of functions in mouse embryonic stem cells, such as maintenance of pluripotency or proliferation (Benetti et al., 2008; Wang et al., 2008c). In line with previous results its expression decreased during differentiation. Furthermore, miR-9 was found amongst the miRNAs that started to be expressed at the progenitor stage. MiR-9 is an important regulator of neural progenitor cell differentiation (Shibata et al., 2011). Moreover, consistent with its in-vivo ex-

pression the brain specific microRNA-124 was found up-regulated at highest levels in the neuronal fraction. However, the most interesting candidates are miRNAs that showed an alternating expression pattern as this most likely plays a specific role in regulation of neural stem cell proliferation and differentiation. The miRNAs up-regulated and with peak expression in radial glia like progenitors comprised four molecules: miR-193; miR-126-3p; miR-92b and miR-219. These were strongly down-regulated at the neuronal stage. Amongst them only miR-92b has been reported to be expressed in neural precursors in the developing zebrafish brain (Kapsimali et al., 2007), however its function in these cells remains elusive. Recent studies have identified miR-219 as an important regulator of oligodendrocyte differentiation in the brain (Dugas et al., 2010; de Faria et al., 2012), while miR-193 has not been described in any neural tissue yet. The most studied and the only non-intergenic miRNA of these four (located within an intron of the EGFL7 (EGF-like domain-containing protein 7) gene) is miR-126-3p. MiR-126-3p has been implicated in regulation of angiogenesis and vascular integrity amongst other roles (Wang et al., 2008a). The expression of these microRNAs correlated with the expression pattern of Pax6, however it remains to be identified whether these microRNAs are under the control of Pax6.

For several miRNAs from the screen - comprising different expression patterns - LNA-based in-situ hybridization was performed in order to test their expression in the developing forebrain. The distinct expression patterns of miR-9, miR-124, miR-92b and miR-126-3p observed in the screen were investigated on E14 forebrain tissue sections (Fig.2-28B). The expression observed of all of them correlated with their expression determined in the array (Fig.2-28).

Taken together, the miRNA profiling at different stages of neuronal differentiation has revealed interesting expression patterns and novel candidate miRNAs, especially those only expressed in progenitor cells. Moreover, including the mRNA profile of the same sample groups provides a good starting point for future microRNA - gene regulation analysis. Further studies will elucidate the function of these miRNAs during brain development and it will be necessary to show their importance.

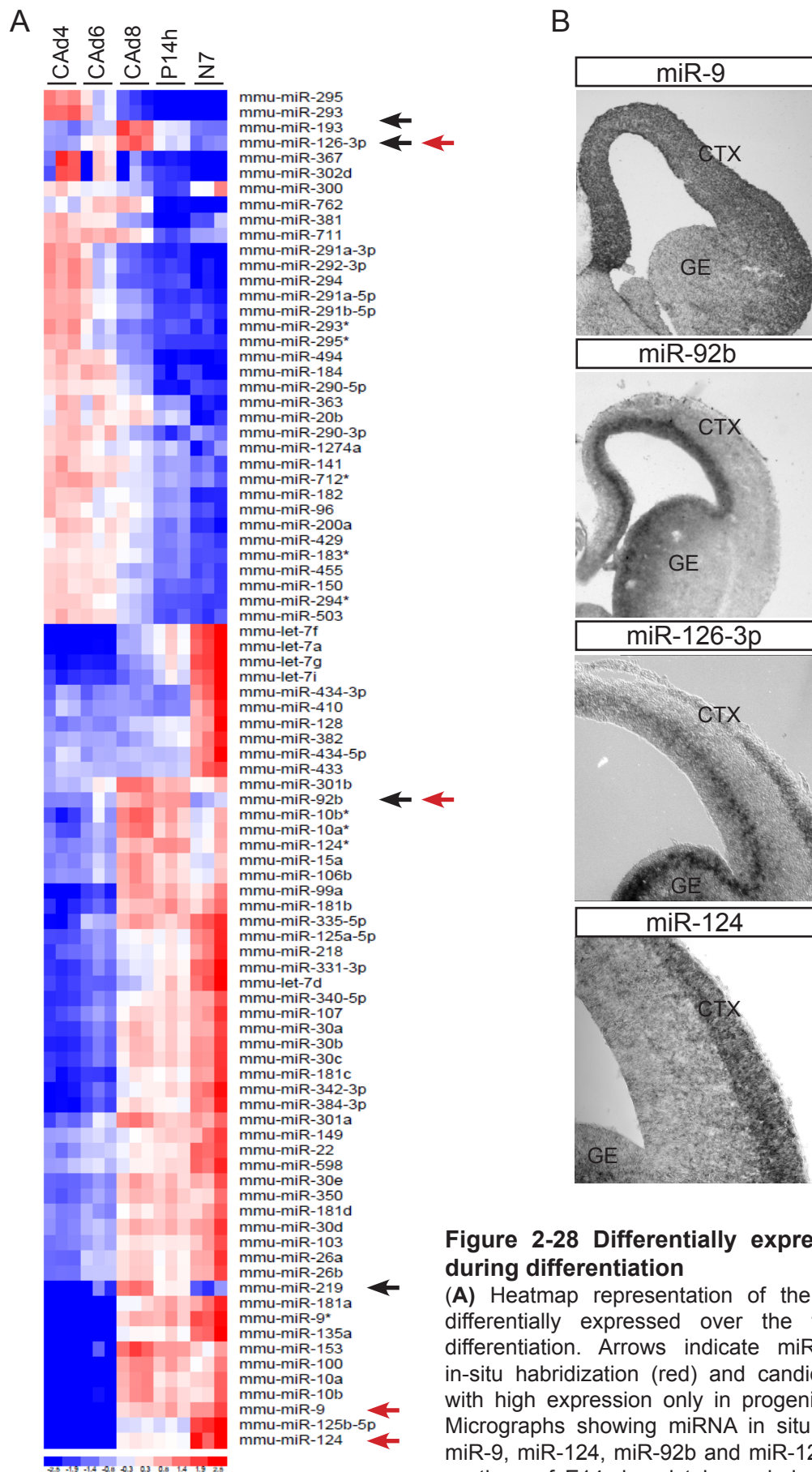


**Figure 2-28 Differentially expressed miRNAs during differentiation**

(A) Heatmap representation of the miRNAs found differentially expressed over the time course of differentiation. Arrows indicate miRNAs performed in-situ hybridization (red) and candidate microRNAs with high expression only in progenitors (black). (B) Micrographs showing miRNA in situ hybridisation of miR-9, miR-124, miR-92b and miR-126-3p on coronal sections of E14 dorsal telencephalon. Abbreviations: CTX, cortex; GE, ganglionic eminence.

## 3 Discussion

### 3.1 Summary

The main aim of this work was to dissect the distinct roles of the DNA-binding domains of the transcription factor Pax6 in the developing cerebral cortex. Towards this end the individual functional impacts of the DNA-binding domains were assessed by the analysis of domain-specific mouse mutants. As a first result I could confirm that Pax6 utilizes its paired domain (PD) to exert its distinct functions during cortical development, while the homeodomain plays no important role. I demonstrated that the PAI subdomain of the PD is crucial for the regulation of neurogenesis by Pax6 which is not dependent on RED-subdomain function. In contrast, both subdomains are necessary and sufficient to control progenitor proliferation in opposing manners with the PAI-subdomain promoting proliferation and the RED-subdomain inhibiting proliferation. Genome-wide expression analysis of both PD subdomain mutants furthermore revealed distinct molecular changes in agreement with the individual phenotypes observed. Consistent with the neurogenic defect in the PAI subdomain mutant, key neurogenic regulators such as the transcription factors Meis1, Tcf2c, Dmrt1a or Cux2 were altered in their expression, thus unraveling these factors as candidate Pax6 PAI-mediated targets. Moreover I show that the function of Pax6 in regard to patterning during telencephalic development is achieved by both subdomains in a largely redundant manner. Taken together, my work demonstrated a modular function of Pax6 with even the subdomains exerting distinct roles, thus further leading to the identification of novel targets likely mediating the distinct functions of Pax6.

Towards identifying novel targets of Pax6, I also performed a screen for microRNAs in Pax6<sup>+</sup> radial glia. This screen was conducted at different stages of neural differentiation of embryonic stem cells that recapitulates Pax6<sup>+</sup> neurogenesis similar to neurogenesis seen in the developing telencephalon. This analysis revealed a number of microRNAs induced during differentiation from neural progenitors to neurons. In conjunction with Pax6 up-regulation, I successfully identified four microRNA candidates that were exclusively expressed at the neural progenitor stage when Pax6 levels are highest.

### **3.2 The paired subdomains - PAI and RED - of Pax6 are crucial for Pax6 function and show selective roles during cortical development**

#### **3.2.1 The PAI and the RED subdomain of Pax6 regulate dorso-ventral patterning in a redundant manner**

The loss of full Pax6 function leads to severe changes in patterning of the dorsal telencephalon (Stoykova et al., 2000; Toresson et al., 2000; Yun et al., 2001; Haubst et al., 2004). Dorsal progenitor cells ectopically miss-express ventral genes in the Pax6 deficient condition such as the transcription factors Gsx2, Olig2, Mash1 or the Dlx family of TFs, thereby reducing the expression of dorsal factors like Ngn2 and Tbr2. As a consequence the neuronal fate changes from glutamatergic to GABAergic neurogenesis in the absence of Pax6 (Stoykova et al., 2000; Toresson et al., 2000; Heins et al., 2002; Muzio et al., 2002a; Scardigli et al., 2003; Kroll and O'Leary, 2005; Quinn et al., 2007; Tuoc et al., 2009). This has been observed not only in the Pax6 mutant Pax6<sup>Sev</sup> (lacking the transactivation domain of this TF), but also after cortex-specific deletion of Pax6 (Emx1-Cre Pax6flx/flx) (Tuoc et al., 2009), in Pax6<sup>Sev</sup> deficient cells in mouse chimeras (Quinn et al., 2007) or even upon acute deletion of Pax6 by Cre electroporation in the Pax6flx/flx mouse line (Asami et al., 2011). In pronounced contrast, the present work revealed that this phenotype was not visible in both Pax6 Leca mutant mice. As observed in immunohistochemical and the transcriptome analysis, none of the ventral transcription factors Gsx2, Olig2 or Dlx1/2/5/6 were miss-expressed in a wide-spread manner in the Leca mutant dorsal cerebral cortex. However one exception was the transcription factor Mash1, which was ectopically up-regulated in both mutants. This observation was rather surprising as the expression of Ngn2, which represses Mash1 expression in the dorsal telencephalon was maintained in both Leca mutants (Fode et al., 2000; Parras et al., 2002; Schuurmans et al., 2004). In addition, the expression of the dorsal transcription factor Tbr2 was also normal in the cerebral cortex of the Leca mutant mice. As these transcription factors are involved in specifying the glutamatergic phenotype (Schuurmans et al., 2004; Sessa et al., 2008) and no increase in GABAergic neurons or accumulation in white matter ectopias was seen (data not shown), this explains why glutamatergic neurogenesis could be maintained in both Leca mutants. These data reveal that relatively normal gene regulation in dorso-ventral patterning is sufficiently achieved by either the PAI or the RED subdomain of Pax6.

However, PAI mediated gene regulation seems to have a more dominant function in subdomains of the dorsal telencephalon. This is because ectopic expression of the transcription

factors *Gsx2* and *Olig2* were detected in the small compartments closest to the ventral telencephalon - the lateral and ventral pallium in the PAI deficient mutant *Pax6<sup>Leca4</sup>*, but not in the RED domain mutant *Pax6<sup>Leca2</sup>* (for summary see Fig.3-1). Between the ventral pallium and the dorsal most part of the subpallium lies the genetically and morphologically defined pallial-subpallial boundary (Shimamura et al., 1997; Shimamura and Rubenstein, 1997). In addition to the spread of *Gsx2* and *Olig2* positive cells across this boundary, the microarray analysis revealed a profound up-regulation of the transcription factor *Dbx1*, which is expressed in this region (Teissier et al., 2010). Likewise *Dbx1* expression was also highly up-regulated in the *Pax6<sup>Sey</sup>* mutant cortex, but its expression was unaffected in the *Pax6<sup>Leca2</sup>* mutant cortex, further supporting a PAI-mediated control by *Pax6* in this region. However, no change of the Wnt-inhibitor *SFRP2*, which is absent after full *Pax6* deletion or after disruption of the homeodomain of *Pax6* was detected (Haubst et al., 2004). Moreover glial fascicles at the PSB are formed normally in the *Leca* mutants, which is in contrast to the failure of fascicle formation observed in the functional *Pax6* null mice (Haubst et al., 2004). Taken together, these data suggest that the correct formation and specification of the PSB and the ventral pallium involves distinct regulatory mechanisms exerted specifically by the PAI-subdomain and the homeodomain of *Pax6*.

It is important to note, that this relatively normal patterning observed in both mutants has a considerable benefit for the mutation analysis. It simplifies the analysis of individual sub-domain specific contributions to the observed phenotypes and thus allows more precise identification of PAI or RED domain mediated functions of *Pax6*. It also improves the discrimination of direct effects from indirect effects that would occur due to changes in patterning.

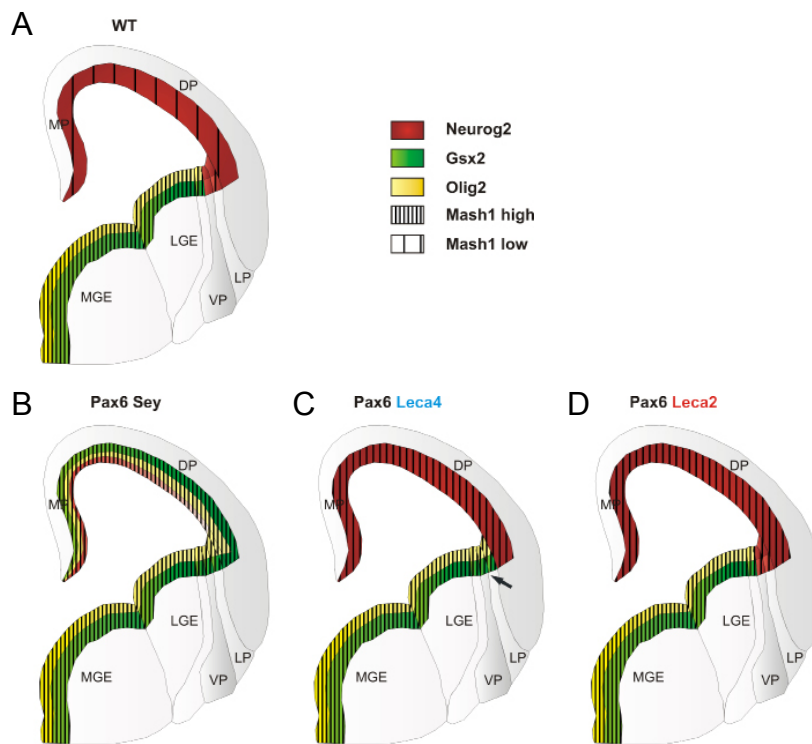


**Figure 3-1 PAI- and RED-subdomains are largely redundant in controlling dorso-ventral telencephalic patterning**

(A-D) Models summarizing the expression results of the transcription factors Neurog2, Gsx2, Olig2 and Mash1 in all mutants compared to their expression in WT telencephalon. Note the ectopic expression in the ventral and lateral pallium in the Pax6<sup>Leca4</sup> mutant (indicated with an arrow).

Abbreviations: CTX, cortex; LGE, MGE, GE, lateral-, medial-, ganglionic eminence respectively; MP, DP, VP, LP, medial-, dorsal-, ventral-, lateral-pallium respectively.

### 3.2.2 The PAI and the RED subdomains of Pax6 exert distinct and opposing functions on progenitor proliferation

Cortical development is characterized by the presence of two distinct types of progenitor cells. Surprisingly, proliferation of both of these progenitor pools is affected in an opposite manner in the PAI subdomain mutant Pax6<sup>Leca4</sup> versus the RED subdomain mutant Pax6<sup>Leca2</sup>. These two progenitor types present in the developing cortex can be distinguished by their location during mitosis. While apical ventricular zone progenitors that originate from the neuroepithelium exclusively undergo mitosis at the apical surface, basal progenitors that arise from apical progenitors divide only in the subventricular zone. The quantification of dividing cells in the PAI mutant Pax6<sup>Leca4</sup> revealed a decrease in the number of apically and basally dividing cells already from E12 on, while the RED mutation in the Pax6<sup>Leca2</sup> mu-

tant increased the number of proliferating cells of both progenitor fractions during midneurogenesis (E14). Interestingly, these phenotypes diverge from the proliferation phenotype observed after loss of full Pax6 function, which affects only the basal progenitor pool. The selective increase in basally dividing cells after loss of Pax6 function (Gotz et al., 1998; Haubst et al., 2004; Tuoc et al., 2009) most likely is the consequence of several alterations. Amongst them the most influential is the ventralization of the dorsal cortex in these Pax6 deficient mice. Supporting this fact is the evidence that ventral telencephalic progenitors possess a faster cell cycle (Bhide, 1996) and are present in a much higher number in the subventricular zone of the ventral forebrain (Bhide, 1996). The ventralization moreover includes the loss of Tbr2 expression in the basal progenitors and thus this population is likely not correctly specified in Pax6 deficient cells (Haubst et al., 2004; Quinn et al., 2007). In addition, a recent analysis from our lab has shown that apical progenitors increasingly delaminate from the apical surface in Pax6<sup>Sey</sup> mice and show alteration in the mode of cell division but no defects in cell cycle length (Asami et al., 2011). In contrast to these findings in full Pax6 mutants, the proliferation phenotypes observed in the Leca mutants show no patterning defects and allow normal Tbr2 expression. This suggests that Pax6 may regulate basal progenitors by a different, indirect mechanism as Pax6 is not expressed in basal progenitors and as no ectopic expression was observed in the Leca mutants. The observed opposing effects on apical progenitors in the Leca mutants together with the lack of any effect on this progenitor subtype in full Pax6 mutants suggests, that the effects of both subdomains largely outcompete each other in these progenitors. Taken together the present analysis of the specific paired subdomains unravels how Pax6 can exert apparently opposing functions in the same cortical progenitor population with the intact RED subdomain inhibiting and the intact PAI subdomain promoting proliferation. Interestingly, available transcriptome data after loss or gain of Pax6 function and chromatin-immunoprecipitation data have provided evidence that Pax6 regulates pro- and anti-proliferative factors even within the same cell type (Holm et al., 2007; Osumi et al., 2008; Sansom et al., 2009). Further consistent with the above, the genome-wide transcriptome analysis of the Pax6<sup>Leca4</sup> mutant cortex indeed revealed expression changes of some genes that have been linked to regulating proliferation, such as Gadd45, Lmo4, Id2 or tenascin C. In this context, the Gadd45 mRNA, which is considered to play an important role in negative growth arrest control is up-regulated in the Pax6<sup>Leca4</sup> cortex (Yang et al., 2009). Conversely, the inhibitor of differentiation (Id2), which exhibits a potent self-renewal and proliferation potential in cortical neural progenitors (Jung et al., 2010), is down-regulated. It has been shown that

overexpression of Id proteins in cortical progenitors leads to inhibition of expression of neuron-specific genes (Cai et al., 2000). Moreover, expression of Tenascin C, another pro-proliferative factor, whose expression has been known to be controlled by Pax6 (Stoykova et al., 1997; von Holst et al., 2007) was decreased in the Pax6<sup>Leca4</sup> mutant cortex. All these factors may explain the observed decrease in proliferation in the Pax6<sup>Leca4</sup> mutant. Interestingly, none of these factors were regulated in an opposite direction in the Pax6<sup>Leca2</sup> mutant cortex, suggesting that the PAI and the RED subdomain exert their opposing roles through distinct molecular control and their targets do not overlap. Accordingly, distinct transcription factors promoting proliferation were found increased in the Pax6<sup>Leca2</sup> mutant cortex, such as Zic1 and Zic3 (Inoue et al., 2007; Pourebrahim et al., 2007; Brill et al., 2010; Watabe et al., 2011). Zic3 overexpression in cortical radial glial cells inhibits neuronal differentiation (Inoue et al., 2007). Altogether, mutation of the RED subdomain affects different genes involved in cellular proliferation as compared to the mutation of the PAI subdomain.

While in both Pax6 subdomain mutants changes in genes involved in proliferation were observed, changes in genes encoding for centrosome associated proteins were not observed. This is interesting as these are distinctively regulated in both the Pax6<sup>Sey</sup> cerebral cortex and after acute deletion of Pax6 (Holm et al., 2007; Asami et al., 2011). Moreover, one such protein - Spag5 (or mAstrin; (Cheng et al., 2007; Thein et al., 2007)) has previously been identified as direct Pax6 target, regulating differences in orientation and mode of cell division (Asami et al., 2011). However, this and other genes were not affected in either of the Leca mutants. Similarly, the RED subdomain mediated effect on proliferation seems to be uncoupled from the role of Pax6 in fate decisions. Although proliferation of apical and basal progenitors is profoundly increased in the Pax6<sup>Leca2</sup> mutant cortex, neither a change in progenitor identity, nor in the later neuronal output were observed (see below). However, although there was no evidence from the microarray analysis, it can't be ruled out that the increase or decrease in mitotic cells observed in the Leca mutants may also result from M-phase problems such as defects in M-phase progression. In order to discriminate this possibility, analysis needed would be time-laps microscopy of mutant progenitors.

In summary, using mutants with specific disruption of either the PAI or the RED subdomain respectively, allowed to unravel opposing roles of the transcription factor Pax6 on proliferation of neural stem cells during cortical development. This finding provides for the first time a molecular explanation on how Pax6 can balance proliferation versus differentiation, a previously proposed Pax6 function (Sansom et al., 2009).

These findings are particularly remarkable, as Pax6 is implicated in distinct regulation of

proliferation in specific cell types and regions of the nervous system (Haubst et al., 2004) (Marquardt et al., 2001; Sakurai and Osumi, 2008; Sansom et al., 2009). In this context, one previous study showed that the absence of Pax6 leads to aberrant proliferation of postnatal glial progenitor cells (Sakurai and Osumi, 2008). Moreover, loss of Pax6 in the developing retina (Marquardt et al., 2001) or diencephalon (Warren and Price, 1997) results in decreased proliferation, while basal proliferation is increased in the thalamus (Wang et al., 2011a) and the telencephalon (as described above). These cell-type and region specific proliferation effects of Pax6 may reflect the distinct molecular control utilized by different domains of Pax6 as shown in the present work for the PAI and RED domain in the developing cortex, however this remains to be examined for the different regions.

### **3.2.3 The PAI subdomain of Pax6 is responsible for its neurogenic function**

Neurogenesis is tightly linked to proliferation and likewise depends on Pax6 function. Loss of Pax6 protein during cortical development results in reduced number of cortical neurons (Schmahl et al., 1993; Heins et al., 2002; Haubst et al., 2004; Tuoc et al., 2009). Here I addressed the question if one or if both PD-subdomains of Pax6 would be involved in regulation of cortical neurogenesis. The gross morphological analysis of the PAI-mutant Pax6<sup>Leca4</sup> showed that the overall cerebral cortex of this mutant was smaller and shorter, including the presence of a thinner cortical plate with reduced number of neurons. Interestingly, this overall morphology is reminiscent of the phenotype observed after loss of full Pax6 function (Schmahl et al., 1993; Heins et al., 2002; Asami et al., 2011), even despite the absence of mispatterning in the Pax6<sup>Leca4</sup> mutant. In contrast, analysis of the cerebral cortex of the Pax6<sup>Leca2</sup> mutant mice did not reveal an aberrant phenotype in cortical neurogenesis. Even at adult stages, cortical neuron numbers appeared normal in the RED-subdomain mutant. These distinct neurogenic effects were furthermore confirmed by clonal analysis of isolated mutant progenitor cells in vitro, which showed a reduced production of neuronal progeny from Pax6<sup>Leca4</sup> cells but not Pax6<sup>Leca2</sup> mutant cells. This suggests that the PAI-subdomain, but not the RED-subdomain plays an important role in regulating neurogenesis. Moreover, neurogenesis elicited by forced expression of Pax6 (Heins et al., 2002; Hack et al., 2004a; Haubst et al., 2004) in vitro could still be increased by Pax6 carrying the Leca2 mutation in the RED domain, but not by Pax6 carrying the Leca4 mutation in the PAI domain. Thus, the PAI domain is essential for neuronal fate instruction, while the RED domain does not participate in this function of Pax6 in embryonic progenitors.

The absence of a neurogenic phenotype in the RED-subdomain mutant is not entirely un-

expected, as a previous analysis of the Pax6(5a)<sup>-/-</sup> mouse mutant (which is characterized by deficiency of producing the 5a-isoform of Pax6 which exerts its paired domain mediated function solely through the RED-subdomain) revealed no cerebral cortex phenotype in this line (Haubst et al., 2004). Moreover, even forced expression of the 5a-isoform of Pax6 in vitro failed to show a neurogenic effect (Haubst et al., 2004). However, of course it would not have excluded a neurogenic function of the RED-subdomain mediated by the canonical isoform of Pax6, which the present analysis of the Leca2 mutant now also addressed.

Consistent with the PAI-mediated function in regulation of cortical neurogenesis, the microarray analysis revealed deregulation of some mRNAs encoding neurogenic factors only in the Pax6<sup>Leca4</sup> mutant but not the Pax6<sup>Leca2</sup> mutant cortex, including members of the Wnt-signalling and the RA-signalling pathway as well as the transcription factors Meis1, Brn4 or Dmrt1. For example, the RA-signaling pathway is important during cortical neurogenesis and altered RA signalling affects the size of the telencephalon and influences expression of neurogenic markers (Giardino et al., 2000; Smith et al., 2001; Haskell and LaMantia, 2005). Notably three members of this pathway were down-regulated in the Pax6<sup>Leca4</sup> cortex – Rlbp1, Rbp1 and Crabp2. While Rlbp1 has been recently identified as a direct Pax6 target gene (Boppana et al., 2012), Rbp1 and Crabp2 interestingly were identified as candidate target genes in the Pax6 ChIP performed by our collaborator Ales Cvekl. This concerted regulation of several molecules of the RA-signalling pathway, may be an important new pathway controlled by Pax6. Notably, while Rbp1 and Crabp2 are possibly dependent only on PAI-subdomain mediated regulation, Rlbp1 was similarly down-regulated also in the Pax6<sup>Leca2</sup> mutant. However, the other still expressed RA-pathway proteins may compensate for loss of Rlbp1 function in the Pax6<sup>Leca2</sup> mutant as similar to the Pax6<sup>Leca2</sup> mutant no defects in neurogenesis were observed in Rlbp1 single mutants (Boppana et al., 2012).

Neurons within the cortical plate are generated at different time-points during differentiation from apical and basal progenitors. This way distinct subtypes of neurons arise that can be distinguished by their laminar position and marker expression. These subtypes of neurons can be placed into two broad classes – deep layer neurons born earlier during neurogenesis and upper layer neurons generated later (Molyneaux et al., 2007). As mentioned before, loss of Pax6 function in the Pax6<sup>Sey</sup> mutant leads to a reduction in neuron numbers. Interestingly this affects specifically upper layer neurons (Stoykova et al., 1996; Schuurmans et al., 2004). A similar phenotype was observed after conditional deletion of Pax6 with an early expressing Cre-line, with almost complete absence of late born neurons and an increased number of early born neurons (Tuoc et al., 2009). Remarkably, layer marker analysis

in the Pax6<sup>Leca4</sup> mutant revealed that different neuronal sub-lineages seem to be reduced equally in their abundance. There are several reasons that may explain this phenotype and its discrepancy to the phenotype after loss of full Pax6 function. The most likely explanation is the existence of a relatively normal specification of basal progenitors in the Pax6<sup>Leca4</sup> mutant, which give rise to the majority of upper layer neurons. In the Pax6 deficient cortex, the identity of basal progenitors is altered as they fail to express several factors – Tbr2, Cux2, Satb2 and Svet1 (Tarabykin et al., 2001; Nieto et al., 2004; Zimmer et al., 2004; Englund et al., 2005; Cubelos et al., 2008; Cubelos et al., 2010). These factors are involved in specification and differentiation of upper layer neurons from basal progenitors and except for Cux2 are not affected in their expression in the Pax6<sup>Leca4</sup> mutant. The transcription factor Cux2 regulates the cell-cycle exit rate of basal progenitors and thereby controls in particular the number of upper cortical neurons generated (Cubelos et al., 2008). Moreover, expression of the deep layer subtype marker Foxp2 is decreased in the Pax6<sup>Leca4</sup> mutant. In contrast it is increased in the Pax6<sup>Sey</sup> mutant cortex, which is consistent with the observed increase of deep layers after conditional deletion of Pax6 (Tuoc et al., 2009). In this line it was suggested that the increase in basal proliferation and an increase in the cell-cycle exit rate especially seen in the SVZ region leads to the depletion of the progenitor pool contributing to the loss of upper layer neurons after loss of Pax6 function (Tuoc et al., 2009). Consistent with this, when Pax6 was deleted at a later time-point during cortical neurogenesis (when early born neurons were already specified), the subsequent formation of upper-layer neurons was not affected (Tuoc et al., 2009). Although cell-cycle exit rate was not analyzed in the Pax6<sup>Leca4</sup> mutant, Leca4 mutant progenitors possess a different proliferation phenotype – a decrease in apical and basal proliferation – which likely accounts for the decrease in neuron numbers of all layers. In this context the presence of misspatterning also adds on the phenotype in the Pax6 deficient cortex.

Taken together, the PAI subdomain is important for Pax6 function in specifying both deep- and upper layer identities, like for example the Cux2 or Foxp2 lineage and its disruption affects these subtypes. However, analysis of the cell-cycle exit rate of progenitors and quantitative data of neuronal birth dates would help clarifying the role exerted by the PAI domain in laminar specification.

One remaining question is how the profound increase in progenitor proliferation in the Pax6<sup>Leca2</sup> mutant cortex can be explained without a subsequent increase in neuron numbers? One possibility could be that the increase of progenitors is counter regulated via apoptosis.

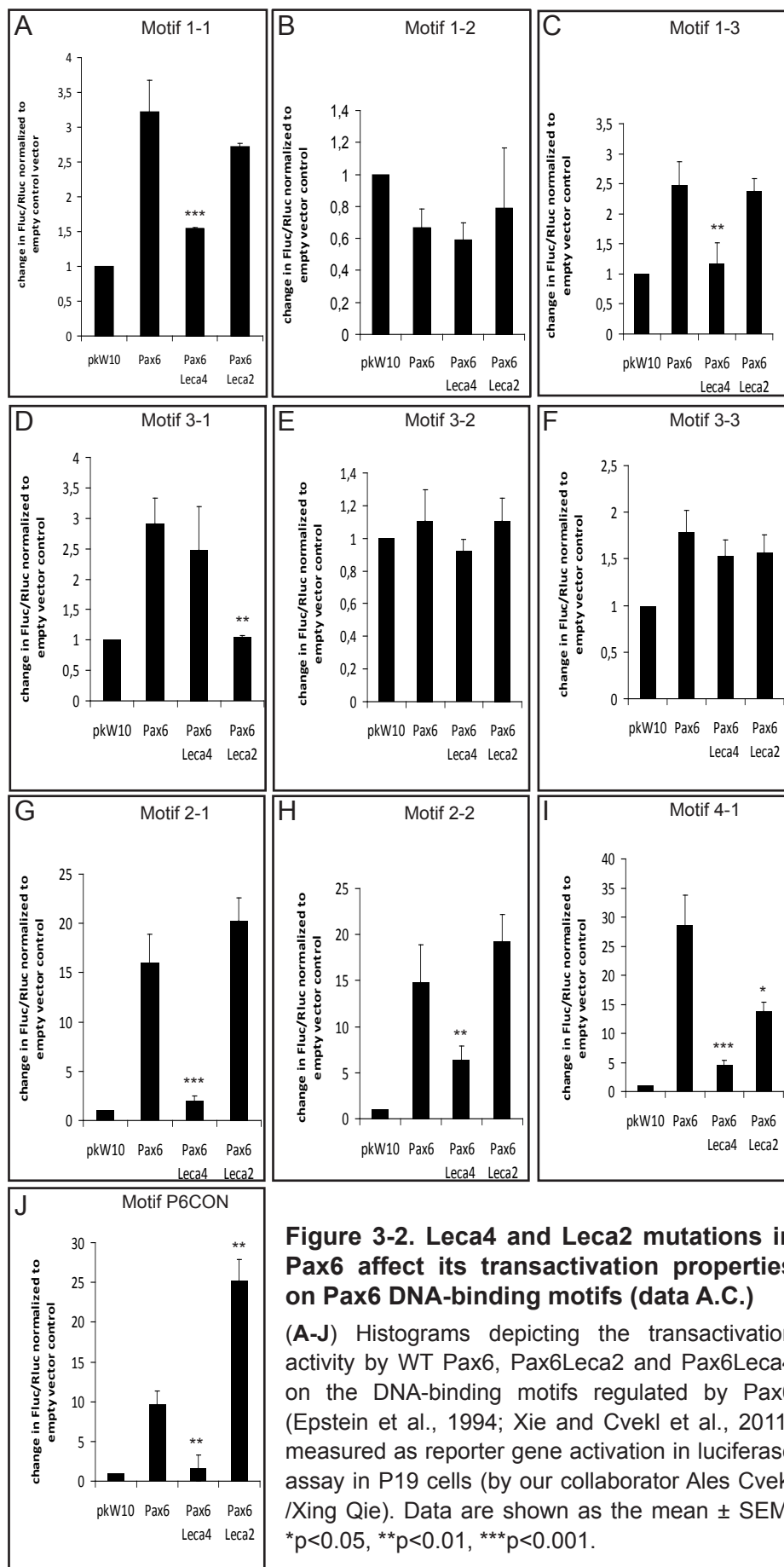
Indeed, it has been shown that neuronal progenitor cells possess a caspase-dependant apoptotic pathway, which may regulate progenitor numbers (D'Sa-Eipper and Roth, 2000). Moreover, Pax6 has been implicated to play a role in cell survival and decreased as well as increased Pax6 levels lead to profound apoptosis (Nikoletopoulou et al., 2007; Ninkovic et al., 2010). In order to test for this possibility we used a specific antibody against the activated caspase-3 – a procaspase of the apoptotic pathway. This analysis showed that apoptosis is increased in the Pax6<sup>Leca2</sup> mutant cortex. Moreover the increase is detected mainly in the progenitor zones. In agreement with this finding, expression of two pro-apoptotic genes – Bcl2l11 and Hrk - was found up-regulated in the transcriptome of the Pax6<sup>Leca2</sup> mutant cortex. In addition, these two pro-apoptotic genes were detected in the Pax6-Chip analysis from Ales Cvekl. This may suggest that Pax6 is able to suppress the activation of the apoptotic machinery. Indeed, it has been shown that Pax6 is able to do so in adult olfactory-bulb interneurons (Ninkovic et al., 2010). However, in this context suppression was achieved not via direct regulation of genes of the apoptotic pathway, but indirect through controlling the expression of the crystalline alphaA gene, which in turn is able to block apoptosis by inhibition of procaspase-3. If Pax6 may not directly control apoptotic genes, it is also conceivable that the increase in apoptosis is caused by the misspecification of the progenitors, as reported for an earlier stage in Pax6<sup>Sey</sup> mice (Nikoletopoulou et al., 2007).

As the reduction in cortical size of the Pax6<sup>Leca4</sup> mutant might also be the consequence of concomitant cell death, apoptosis was also examined in this mutant. However, I did not observe a significant increase in apoptosis in the PAI-subdomain mutant, suggesting that the reduced proliferation accounts for the phenotype.

### **3.2.4 The Leca mutations in the PAI and the RED subdomain of Pax6 affect its function through distinct binding sites**

In general mutations leading to amino acid changes (which don't lead to nonsense-mediated decay mutations) can have variable effects on the function of a protein depending on the changes occurring with its secondary structure. The fact that the PAI/ Leca4 mutation and the RED/ Leca2 mutation lead to distinct phenotypes, implicate that these mutations do not have a deleterious effect on Pax6 protein function. If this would be the case, these mutations would have resulted in phenocopies of the complete null mutant. Predictions of structural changes regarding the DNA-binding properties of the PAI and RED subdomains propose selective disruptions of the DNA-binding activities, which is in agreement with the distinct expression changes observed in the Leca mutants. The amino acid mutated in the

Pax6<sup>Leca4</sup> mutant (N50) is the first amino acid residue in the DNA-contacting helix of the PAI-subdomain. Moreover, crystallographic analysis of the paired domain has shown that this amino acid makes a direct contact with an invariant T –residue that has been found in many Pax6-binding site motifs (Xu et al., 1999; Xie and Cvekl, 2011). Also, the N50 amino acid is present in a cluster of seven amino acid residues which make up Pax6' unique DNA-binding specificity of this domain compared to other Pax proteins (Czerny and Busslinger, 1995). Along this line, our collaborator Dierk Niessing predicted the N50K mutation to disrupt the interaction of the PAI-subdomain and DNA. For the R128 amino acid mutated in the Pax6<sup>Leca2</sup> mutant, bioinformatic calculations (by Dierk Niessing) suggested a perfect DNA-binding distance of 2.1Å of this amino acid to DNA and hence the mutation is predicted to disrupt the DNA-binding capacity of the RED-subdomain. In line with these predictions EMSA studies revealed decreased or absent DNA-binding of the RED-subdomain after R128C mutation (Yamaguchi et al., 1997; Chauhan et al., 2004). These studies also showed that the RED-subdomain mutation has no impact on the PAI-subdomain DNA-binding properties as the mutated protein was still able to bind to P6CON consensus site (PAI-domain specific consensus sequence). The selective effect of the mutations on each subdomain without affecting the other domain was further confirmed by gene expression reporter assays performed by our collaborator Ales Cvekl. Using his previously identified novel Pax6-binding site motifs which harbour different combinations of PAI and RED (and some with HD) binding sites (see Introduction Fig. 1.7), he could show that the Leca4 mutation within the PAI-subdomain affected mainly transcriptional activation of PAI-site motifs, but not of RED-site motifs (Fig.3-2). Likewise, the Leca2 RED-subdomain mutation disrupted transcriptional activation mediated via the RED domain. However, one of the novel motifs was affected by both mutations with decreased activation (Fig.3-21). Indeed, cooperation of the PAI and the RED domain has previously been observed (Yamaguchi et al., 1997; Chauhan et al., 2004). Nevertheless, still bearing indirect effects in mind, the luciferase experiments described above and the genome-wide expression analysis performed in the present study corroborate a rather discrete modular function of the individual subdomains. Furthermore, the comparison of the Pax6 ChIP data (Xie et al., unpublished) with all transcriptomes – of the Leca mutants and of the Pax6<sup>Sev</sup> mutant – revealed an overlap of 23% of the genes (Appendix Table 5-7). As almost all of them were regulated in the same direction in the mutants, this suggests that they are direct targets of Pax6, rather than indirectly affected by mispatterning of the Pax6<sup>Sev</sup> cerebral cortex.



### 3.2.5 The Leca mutation in the RED subdomain of Pax6 leads to enhanced transcriptional activation in vitro

In contrast to the reporter assays performed on the novel Pax6 DNA-binding motifs (Ales Cvekl; (Xie and Cvekl, 2011)), reporter assays on classical Pax6 consensus sites in vitro showed superactivation by Pax6 with the RED domain mutation, but not with the PAI domain mutation. Most notably here, besides enhanced activation of the paired domain target sequence P6CON (performed by Ales Cvekl; Fig. 3-2J) and the combined PD and homeodomain target sequence (P6CON-P3), even the construct containing only the HD target sequence P3 showed increased transcriptional activation. One possible explanation for these results may be changes of the secondary structure affecting the homeodomain of the Pax6 Leca2 mutant protein. Indeed, a recent publication using bioinformatic tools to predict changes of the secondary structure through the Leca2 mutation suggested that the R128C mutation not only affects the RED-subdomain, but changes the structure of the homeodomain and the transactivation domain: creating an altered homeodomain with an additional helix as well as two short additional helices in the transactivation domain (Shukla and Mishra, 2012). In regard to the homeodomain, although it has been shown by loss of HD function that the HD of Pax6 plays no important role in the developing cerebral cortex (Haubst et al., 2004; Ninkovic et al., 2010), it cannot be ruled out that enhanced independent binding of the HD of Pax6 may well have an effect. And consequently may be involved in the observed Leca2 cerebral cortex phenotype. Taken together, structural changes of the Pax6 protein might influence the transcriptional activation potential of the distinct DNA-binding domains. However, experimental proof for structural changes affecting the DNA-binding domain has yet to be done.

A second possibility for the superactivation by the RED-subdomain mutation on the PD and HD consensus sequences is that protein-protein interactions are affected. In pancreas development, it has been shown that Pax6 interacts for example with the Maf transcription factor leading to synergistic activation of the glucagon promoter (Planque et al., 2001). Likewise, Pax6 cooperates with other transcription factors during lens development, such as Sox2 (Kamachi et al., 2001). Moreover, Pax6 has also been proposed to recruit chromatin remodelling complexes to gene loci (He et al., 2010).

However a different type of protein-protein interaction – between Pax6 and its nuclear import protein is for example likely not affected by the Leca2 RED subdomain mutation. It has previously been shown that the paired-domain harbours a non-classical nuclear localization sequence (Dames et al., 2010). Deletion of this sequence resulted in cytoplasmic localiza-

tion of Pax6. However, some Pax6 staining was still visible in the nucleus, suggesting that Pax6 harbours an additional NLS. In any case, the Leca mutations do not affect localization of the mutant Pax6 protein as immunostaining for Pax6 revealed exclusive nuclear localization in Pax6 Leca mutant cortices as observed for the wild-type Pax6 protein. This shows that the secondary structure of the Leca mutant proteins is preserved for interaction with certain proteins such as its nuclear-import proteins.

Another possibility is that the interaction of Pax6 with a repressor-complex is disturbed, leading to abnormal transcriptional levels of certain genes. Possibly also interactions of Pax6 important to exert a repressive role might be affected. For example Pax6 has been shown to negatively affect the androgen receptor (AR) activity, competing with a transcriptional activator for AR-interaction on AR target genes (Elvenes et al., 2011).

In conclusion, several possibilities, affecting domain binding or protein interactions might be the cause for the superactivation observed by the Leca2 mutation on Pax6 consensus sites in vitro. In any case, different activation levels were detected using different cell lines in this and previous reported studies (Chauhan et al., 2004; Shukla and Mishra, 2012) suggesting that effects might vary depending on the cell type and context.

Taken together, superactivation of Pax6 targets through the Leca2 mutation were observed on the classical Pax6 consensus sites in vitro but not on any of the recently identified novel Pax6 motifs. Nevertheless, it cannot be ruled out that gain-of transcriptional activity contributes to the observed phenotype in the Pax6<sup>Leca2</sup> mutant.

### **3.3 The role of the homeodomain and region-specific differences of the function of the different DNA-binding domains of Pax6**

A previous study in our lab using a Pax6 homeodomain mutant mouse line (Pax6<sup>4NEU</sup> carrying a point-mutation in the HD), revealed that this domain of Pax6 plays only a minor role during cortical development with subtle effects on the specification of the PSB (Haubst et al., 2004). These findings suggest a dominating regulatory function of the paired domain of Pax6 during cortical development. Indeed, the attempt to identify possible candidates for HD-mediated function in the present study by microarray analysis of the Pax6<sup>4NEU</sup> line did not reveal gene expression changes. This further corroborates a PD-specific regulatory function in the developing forebrain. In contrast, the homeodomain of Pax6 does play an important regulatory role in other regions of Pax6 expression, e.g. during eye development, homeodomain and paired domain function are both essential. In agreement, all Pax6 mutant mice independent of the localization of the mutation show defects in eye development,

including both Leca mutants (Favor et al., 2001; Thaug et al., 2002; Favor et al., 2008; Ramaesh et al., 2009). However, the distinct domain disruptions result in different phenotypes. Besides Pax6 activity levels, which play an important role in the manifestation of the distinct eye defects (Favor et al., 2008) the different phenotypes are also attributable to loss of the individual DNA-binding domain function. Moreover, even distinct regulatory elements controlled by the homeodomain or the paired domain of Pax6 have been identified in genes expressed in the eye. While the homeodomain exclusively recognizes regulatory elements of the rhodopsin genes (Sheng et al., 1997), paired domain binding sites have been mapped to cis regulatory elements of the crystalline gene family (Piatigorsky, 1998; Niimi et al., 1999). Moreover, the homeodomain and the paired domain of Pax6 have been shown to be able to act both independently or cooperatively to control the expression of different genes (Sheng et al., 1997). While during eye development, the homeodomain controls gene expression, it possesses a modulating role of Pax6 function during alpha-cell development in the pancreas (Dames et al., 2010). These findings suggest that a selective usage of different DNA-binding domains of Pax6 may reflect one mechanism, which contributes to the region-specific differences of Pax6 function. It has been recently shown by Fong et al., 2012, that there are three different levels of gene regulation: 1. DNA-binding site recognition; 2. Epigenetic/ chromatin accessibility; 3. Co-factor availability in different cell-types/ tissues. This maybe one explanation why the Pax6 domains have altered roles in different tissues. This study further corroborates that the paired domain itself is subdivided into two domains that target independent genes, thereby giving another level of combinatorial possibilities. In summary, Pax6 can control gene expression by the PAI, the RED and the HD in different combinatorial and modulatory ways. The identification of PAI and RED domain target candidates reveal a clear level of regulation through Pax6. The selective function of those domains may depend on the above mentioned prerequisite for gene expression regulation (chromatin accessibility and co-factor availability; (Fong et al., 2012)).

In this study, I dissected domain specific functions of the transcription factor Pax6 during cerebral cortex development. Human cases of Pax6 mutations are known to suffer from brain and/or eye defects or develop diabetes later in life. Therefore understanding the complex molecular function exerted by Pax6 is especially relevant in regard to such human diseases.

### **3.4 Identification of new microRNA candidates during neuronal differentiation**

The process of neuronal differentiation not only involves the regulation of distinct protein-coding genes by transcription factors like Pax6, but also depends on the control and expression of distinct microRNAs. In this study, a microRNA profile was carried out to identify novel microRNA candidates associated with neuronal differentiation. I utilized an ESC-differentiation system (Bibel et al., 2004; Bibel et al., 2007), which allowed to analyze relatively homogenous key stages during neuronal differentiation. These included an ESC-like stage, two neural progenitor stages characterized by Pax6 positive radial glia like progenitors and lastly a stage containing differentiated glutamatergic neuronal progeny. I found different expression patterns of microRNAs expressed over the time course of differentiation. ESC specific microRNAs, such as the known miR-250 cluster important for maintenance of pluripotency and proliferation (Benetti et al., 2008; Wang et al., 2008b) were down-regulated at the progenitor stage, while most of the microRNAs which started to be expressed at the progenitor stage, such as the well-studied miR-9/9\* showed an enrichment of expression at the neuronal stage. These patterns were expected as shown for previous expression profiles of other neuronal differentiation systems (Sempere et al., 2004; Huang et al., 2009). However, remarkably few microRNA candidates with exclusive expression at the neuronal progenitor stage were identified in the present screen. Amongst them one microRNA (miR-92b), which has previously been shown to be expressed in the proliferative zones of the adult and larval zebrafish brain (Kapsimali et al., 2007). In line with the screen and the zebrafish expression pattern, I detected exclusive localization of miR-92b also in the proliferative zone of the developing mouse forebrain. Furthermore, miR-126-3p, miR-193 and miR-219 were identified as novel candidates expressed exclusively in neuronal progenitors. The role of miR-126-3p is most studied in endothelial cell development. Together with its host gene *Egfl7*, miR-126-3p is expressed in endothelial cells and both play important roles in vascular development (Fish et al., 2008; Wang et al., 2008a). Moreover, miR-126-3p has been shown to inhibit proliferation of breast cancer cells or human embryonic kidney cells (Iorio et al., 2005). In contrast, the miR-193 has been reported to exert a pro-proliferative effect in mesenchymal stem cells after laser irradiation, indirectly regulating the cyclin-dependant kinase 2 (CDK2) (Wang et al., 2012). Several studies of the microRNA miR-219 have identified its role in regulation of oligodendrocytes differentiation in the brain (Dugas et al., 2010; de Faria et al., 2012). Further studies will be necessary and it will be interesting to investigate the role of the novel miRNA candidates in neuronal progenitors identified within the present screen.

Loss and gain-of function experiments could be useful to understand their role in neuronal progenitor cells.

Compared to the number of microRNAs which are down-regulated at the progenitor stage or which start to be expressed from this stage on, the progenitor only expressed microRNAs are surprisingly very few. This may suggest an important function of these specific candidates in targeting genes expressed at this stage, which either need to be cleared to allow the cell to further differentiate or to facilitate robustness to progenitor specific gene expression programs. Indeed, it has been shown that microRNAs can act as switch or fine-tuners of gene expression (Mukherji et al., 2011). Moreover, the combination of the microRNA and mRNA profile generated in this study together with computational methods will help identify targeted genes. The expression of miRNAs and their targeted mRNAs are often largely non-overlapping with temporal or spatial separation (Farh et al., 2005; Stark et al., 2005). In such mutual exclusive expression, the microRNA is thought to function to maintain low levels of target gene expression. Indeed, many examples have been reported that show mutual exclusive expression of the miRNA and its targeted mRNA in temporal or spatial domains (Stark et al., 2005).

Lastly, given the importance of Pax6 in neuronal progenitors, it would be interesting to unravel whether Pax6 may be involved in the control of distinct microRNA genes. As key ES cell transcription factors have been shown to bind to promoters of microRNAs, which are dominantly expressed in ES cells (Marson et al., 2008), it is likely that Pax6 as a key determinant during neuronal differentiation also controls the expression of distinct microRNAs important for proliferation of progenitors and or their differentiation.

## 4 Material and Methods

### 4.1 Materials

#### 4.1.1 Chemicals

<i>Chemical</i>	<i>Company</i>
Ampicillin	Roth
Aqua Poly/Mount	Polyscience Inc.
Boric acid	Roth
Bovine Serum albumin (BSA)	Sigma
DAPI (4,6-dasmindino-2-phenylindol)	AppliChem
Diethyl ether	Merck
Difco LB-Agar	Hartenstein Laborversand
DMSO	Sigma
DNA Ladder (Generuler 1kb)	Fermentas
EDTA	Merck
Ethanol	Merck
Ethidium bromide	Roth
Gelatine	Sigma
Glycerol	Sigma
Glycine	AppliChem
HEPES	Roth
Isopropanol	Merck
Mercaptoethanol	Sigma
Normal goat serum (NGS)	Vector Laboratories
Orange G	Sigma
Paraformaldehyde (PFA)	Merck
PCR buffer (10x Taq Buffer with (NH <sub>4</sub> ) <sub>2</sub> SO <sub>4</sub> )	Fermentas
PCR dNTP Mix (25mM each)	Fermentas
PCR reagent: MgCl <sub>2</sub> (25mM)	Fermentas
Potassium chloride	Merck
Potassium dihydrogen phosphate (KH <sub>2</sub> PO <sub>4</sub> )	Merck
Ringer infusion solution	Braun

<b>Sodium azide</b>	Merck
<b>Sodium chloride</b>	Fisher Bioreagents
<b>Sodium citrate</b>	Merck
<b>Sodium hydroxide</b>	Roth
<b>Sodium phosphate (Na<sub>2</sub>HPO<sub>4</sub>-7H<sub>2</sub>O)</b>	Roth
<b>Taq DNA Polymerase</b>	Fermentas
<b>Tissue Tek</b>	Hartenstein Laborversand
<b>Tris-HCL</b>	Roth
<b>Triton-X-100</b>	Roth
<b>Tween-20</b>	Sigma

#### 4.1.2 Kits

<b><i>Kit</i></b>	<b><i>Company</i></b>
<b>Dual-Luciferase Reporter Assay System</b>	Promega
<b>Genra Puregene Tail-DNA extraction kit</b>	Qiagen
<b>Qiaprep MaxiPrep</b>	Qiagen
<b>Qiaquick gel extraction kit</b>	Qiagen
<b>Qiaquick PCR Purification kit</b>	Qiagen
<b>RNA extraction Kit mini</b>	Qiagen
<b>RNA extraction Kit micro</b>	Qiagen
<b>RNA extraction Kit miRNAs</b>	Qiagen
<b>StrataClone PCR kit</b>	Stratagene

#### 4.1.3 Culture reagents and media

##### 4.1.3.1 General tissue culture reagents

<b><i>Reagent</i></b>	<b><i>Company</i></b>
<b>B-27 Serum-Free Supplement</b>	Gibco (Invitrogen)
<b>Bovine serum albumin (BSA)</b>	Sigma
<b>DMEM (Dulbecco's Modified Eagle Medium) + 4.5g/ml glucose</b>	Gibco (Invitrogen)

<b>DMEM (Dulbecco's Modified Egel Medium) + 4.5g/ml glucose and GlutaMAX</b>	Gibco (Invitrogen)
<b>DMSO</b>	Sigma
<b>EBSS (Earle's Balanced Salt Solution)</b>	Gibco (Invitrogen)
<b>FCS (Fetal Calf Serum)</b>	Pan
<b>HBSS (Hank's balanced salt solution)</b>	Gibco (Invitrogen)
<b>HEPES (1M)</b>	Gibco (Invitrogen)
<b>L-Glutamine (200mM)</b>	Gibco (Invitrogen)
<b>Lipofectamine 2000</b>	Invitrogen
<b>Opti-MEM + GlutaMAX</b>	Gibco (Invitrogen)
<b>Penicillin/Streptomycin (Pen/Strep)</b>	Gibco (Invitrogen)
<b>Poly-D-Lysine (PDL)</b>	Sigma
<b>Tris-HCl (1M)</b>	Rockland
<b>Trypan Blue</b>	Gibco (Invitrogen)
<b>Trypsin (EDTA), 0.05%</b>	Gibco (Invitrogen)

#### 4.1.3.2 Embryonic stem cell culture reagents

<b>Reagent</b>	<b>Company</b>
<b><u>EB Medium:</u></b>	
<b>DMEM + NaPyruvat w/o L-Glutamine</b>	Gibco (Invitrogen)
<b>FCS (Fetal Calf Serum)</b>	Pan
<b>L-Glutamine</b>	Gibco (Invitrogen)
<b>Mercaptoethanol</b>	Sigma
<b>Non-essential amino acids</b>	Gibco (Invitrogen)
<b>Penicillin/Streptomycin (Pen/Strep)</b>	Gibco (Invitrogen)
<b><u>ES Medium:</u></b>	
<b>All ingredients of EB Medium plus</b>	
<b>LIF (Leukemia Inhibitory Factor)</b>	Chemicon
<b><u>N2 Medium:</u></b>	
<b>BSA (Bovine Serum Albumin)</b>	Gibco (Invitrogen)
<b>DMEM w/o L-Glutamine</b>	Gibco (Invitrogen)

<b>F-12 (HAM) Nutrient Mixture + L-Glutamine</b>	Gibco (Invitrogen)
<b>Human Transferrin</b>	Sigma
<b>L-Glutamine</b>	Gibco (Invitrogen)
<b>Insulin</b>	Sigma
<b>Penicillin/Streptomycin (Pen/Strep)</b>	Gibco (Invitrogen)
<b>Progesterone</b>	Sigma
<b>Putrescine</b>	Sigma
<b>Sodium Selenite</b>	Sigma
<b><u>Complete Medium:</u></b>	
<b>All trans Retinol</b>	Sigma
<b>Biotin</b>	Sigma
<b>BSA (Bovine Serum Albumin)</b>	Gibco (Invitrogen)
<b>Catalase</b>	Sigma
<b>DMEM w/o L-Glutamine</b>	Gibco (Invitrogen)
<b>D+-Galactose</b>	Sigma
<b>Ethanolamine</b>	Sigma
<b>Glutathione</b>	Sigma
<b>Human Transferrin</b>	Sigma
<b>Insulin</b>	Sigma
<b>L-Alanine</b>	Sigma
<b>L-Carnitine</b>	Sigma
<b>L-Proline</b>	Sigma
<b>Linoleic acid</b>	Sigma
<b>Linolenic acid</b>	Sigma
<b>Na-Pyruvate</b>	Sigma
<b>Na-Selenite</b>	Sigma
<b>Progesterone</b>	Sigma
<b>Putrescine</b>	Sigma
<b>Retinylacetat</b>	Sigma
<b>SOD (Super Oxid Dismutase)</b>	Sigma
<b>Tocopherol</b>	Sigma
<b>Tocopherolacetat</b>	Sigma
<b>Vitamine B12</b>	Sigma
<b>Zinc sulfate</b>	Sigma
<b><u>Others:</u></b>	
<b>Retinoic acid (RA)</b>	Sigma

## 4.1.4 Cell lines

<i>Cell line</i>	<i>Company / Origin</i>
<b><u>Bacterial strains:</u></b>	
<i>E.coli</i> XL1-Blue	Stratagene
<i>E.coli</i> DH5 $\alpha$	Invitrogen
<i>E.coli</i> TOP10	Invitrogen
<b><u>Eucaryotic cell lines:</u></b>	
Embryonic stem cells (mouse; J1)	Kind gift of Yves-Allain Barde
Human embryonic kidney (HEK) cells	
P19 carcinoma cells (mouse)	Kind gift of Francois Guillemont

## 4.1.5 Cloning and expression plasmids

<i>Plasmid</i>	<i>Origin</i>
pCAG-GFP-DEST	Kind gift of Paolo Malatesta
pCAG-Leca2-GFP	Tessa Walcher
pCAG-Leca4-GFP	Tessa Walcher
pCAG-Pax6-GFP	Kind gift of Robert Blum
pENTR1A	Invitrogen (Gateway)
pGL3-P3	Kind gift of Anastasia Stoykova
pGL3-P6CON-P3	Kind gift of Anastasia Stoykova
pMXIG-IRES-GFP	Nosaka et al. 1999
pRenilla-TK	Promega
pSC-A (StrataClone PCR Cloning Vector)	Stratagene

## 4.1.6 Primary antibodies

<i>Antigen</i>	<i>Species</i>	<i>Company</i>	<i>Dilution</i>	<i>Treatment</i>
<b>Activated Caspase 3</b>	Rabbit	Millipore	1:100	Biotin-streptavidin signal amplification
<b>Ascl1 (Mash1)</b>	mouse IgG1	kindly provided by O.Raineteau	1:150	
<b>Calbindin</b>	rabbit	Swant	1:200	
<b>Calretinin</b>	rabbit	Swant	1:200	
<b>Ctip2</b>	rat	Abcam	1:200	
<b>Cux1</b>	rabbit	Santa Cruz	1:200	
<b>Foxp2</b>	rabbit	Abcam	1:200	
<b>GFP</b>	chick	Aves Labs	1:1000	
<b>Gsx2 (Gsh2)</b>	rabbit	kindly provided by K.Campbell	1:1000	
<b>Map2</b>	mouse IgG1	Sigma	1:200	
<b>NeuN</b>	mouse IgG1	Millipore	1:100	
<b>Olig2</b>	rabbit	Millipore	1:200	
<b>Pax6</b>	rabbit	Millipore	1:500	
<b>Pax6</b>	mouse IgG1	Dev. Hybridoma Bank	1:50	Citrate-buffer pre-treatment
<b>phospho histone H3 (PH3)</b>	rabbit	Millipore	1:500	
<b>RC2 monoclonal antibody 'radial cell 2'</b>	mouse IgGM	kindly provided by P. Leprince	1:200	
<b>Reelin (E4)</b>	mouse IgGM	kindly provided by A. Goffinet	1:200	
<b>Tbr1</b>	rabbit	Abcam	1:200	
<b>Tbr2</b>	rabbit	Abcam	1:500	
<b>Tyrosine hydroxylase</b>	rabbit	Millipore	1:200	

## 4.1.7 Primers used for q-PCR analysis

<b>Primer Name</b>	<b>Primer sequence forward</b>	<b>Primer sequence reverse</b>
<b>Acot1</b>	TTTGCAAAGCCCTCTGGTAG	GAAGTAAGGGGGCTCGATGTAATG
<b>Adamts5</b>	AGTCATTGGGTCAAGCCCTGGC	AGCTGCAGTCATAGTGCACACCC
<b>Ahnak</b>	GCTCTGAAGTGGTTCTGAGCGGG	CACTGTGATGGTGC GGCTCTGG
<b>AldoC</b>	GCCATCAACCGCTGCCCACTT	GCTGCCGCTCCGCCATCTC
<b>Asb4</b>	CTGAGATCTGCTACCAGCT	CCATCGAATGTGTTTCATAGGC
<b>Brn4 (Pou3f4)</b>	GCAGGGAGTTC CAGCAATGGG	GCCCAGTTGCAGATCTTCGCGT
<b>Cadm1</b>	AACCCCAACAGGCAGACCATTTAC	CTCCCCTTCAACTGCCGTGTCTTT
<b>Ccdc80</b>	AAGACTCCTCCTGATCACCCTCCC	CCACAGAGATCCTCCTGGTGGC
<b>Cdh4</b>	ATTGGCCCTATGTCTTTGAGTTG	ATGGGCACACCTTGACCTTTATGA
<b>Cdh8</b>	TCGCTACGACGACGAAGGAGGAG	TGGCAATCCCCACCGGGGTAAAA
<b>Cep27</b>	GTGGCGAGA ACTACAAACAGAA	AAAAAAGGTAAAGGAGGCACTATG
<b>Col1a2</b>	GCTGCCACCATTGATAGTCT	CCAGAGTGGAACAGCGATT
<b>Cryab</b>	GGCACCCAGCTGGATTGACACC	TGAAGCCATGTTTCGCTCTGGCG
<b>Ctnnd2</b>	GGTGCGCCCGCTGAAGACAT	AAGGACGGGCTGCAGAGTAGAAGT
<b>Cxcl12</b>	TGTGCCCTTCAGATTGTTGCACGGC	ACTGCCCTTG CATCTCCCACGG
<b>Dmrt3</b>	AGACTAGAGCGGACTGAGCAGGC	GTGTTTCGCTTCGCGATACGCC
<b>Dmrta1</b>	ACTAGCTTTTCAGCCCACTGCGC	TGCTTGCTAGGGAGGTGGGACG
<b>Eya4</b>	CCTACAGCCTGCCTGCCTACGA	GGTGCAAAGCTGGAACCTGGCA
<b>Fbln1</b>	GACGGCATGACTGTGGGTGTCTG	CGTTCGGGTGGGAAACTACGCC
<b>Fst</b>	TTCCAAGTTGGCAGAGGTCGC	AGCAGGCAGCTTCCTTCATGGC
<b>Gapdh</b>	TGGATGCAGGGATGATGTTTC	ATTCAACGGCACAGTCAAGG
<b>GLT-1 (Slc1a2)</b>	ATGCTCATCCTCCCTCTTATCATC	CTTTCTTTGTCACTGTCTGAATCTG
<b>Hrk</b>	CCTTATTTGGGGGACACTTGAGGGC	GGGGTAGACAGACTTCCCAGAGCC
<b>Id3</b>	TCCGCATCTCCC GATCCAGACAG	TCCCAGAGTCCCAGGGTCCCAA
<b>Id4</b>	GTTACGAGCATTACCGTA	AAGGTTGGATTACGATTGC
<b>Igfbp5</b>	AAGAAGCTGACCCAGTCCAA	GAATCCTTTGCGGTACAGT
<b>Khl5</b>	TGACATGAACATCCCGAACGA	CTGTGGCGCAAGGAGAGGTAG
<b>Kif1b</b>	CAGCAGAGACTGGACGCGGATT	ACTGCTGGGGAGGCCACACTTT
<b>Lgals1</b>	TCGGACGCCAAGAGCTTTGTGC	GAAGGCAGGTTCCCGGTGTTTCG
<b>Math3 (NeuroD4)</b>	TTGAAGGGAAGGGATTTGTAGAGA	GGGAGCCCTGGAGACTGATAG
<b>Meis1</b>	GGCATCAGAGCGCCAGGACCTA	CGGGCTACATACTCCCCTGGCA
<b>Ngn1</b>	CGAGCCCGGCCAGCGACAC	GGGCAGGCCAGGAAAGGAGAAAAG
<b>Pax6</b>	TCCCCGCGTTACTGTAATCGAGGCC	CGGGATCCATGCAGAACAGTCACAGC
<b>Prr15</b>	AGCCCTGGTGGAAATCTCTGAC	ATTGCGCCGACTATTGCCTGTTTT
<b>Rlbp1 (CRALBP)</b>	CCAAGAAAGAGCTGTCAGGGACGG	TTTGCTCTGCCCTGGTCTCTCCG
<b>Tmem58</b>	CCTTCTGCTGCGGGACCTGCTACC	TCCTGGCCTTCAAACGTGCTCTGG
<b>Tmem87a</b>	GCGGCCATCAGCAAATAACCAG	AGGCCGGAAGTGCTACATCAGTCA
<b>Zic1</b>	CAACAGCAGCGACCGCAAGA	GGTGGGTGGCGTGGACGAC
<b>Zic3</b>	AGCGAGCAGTGAGGTTGAGCC	ACTCAAGAGCGCGGAACCACGG

#### 4.1.8 General Buffers and Solutions

<i>Buffer / Solution</i>	<i>Composition</i>
LB- medium	20 g/l LB broth base in H <sub>2</sub> O
LB-Agar	40 g/l LB-Agar in H <sub>2</sub> O
PBS	1,3 M NaCl, 27 mM KCl, 15 mM KH <sub>2</sub> PO <sub>4</sub> , 83 mM Na <sub>2</sub> HPO <sub>4</sub>
PFA 20%	200 g/l PFA, 10 M NaOH, PBS, pH7
SSC 20x	NaCl 175.3g, sodium citrate 88.8g, add DEPC-H <sub>2</sub> O 1l, pH 9.5
TE- Buffer	10mM Tris, 1mM EDTA, pH8

## 4.2 Methods

### 4.2.1 Animals and genotyping

#### 4.2.1.1 Animals

All animals were kept in the animal facility of the Helmholtz Zentrum München. Experimental procedures were performed in accordance with German and European Union guidelines. Animals were maintained on a 12h light-dark cycle and the day of vaginal plug was considered as embryonic day 0 (E0). The Pax6<sup>Leca2</sup> and Pax6<sup>Leca4</sup> mouse lines (Thaung et al., 2002) were obtained from the GlaxoSmithKline Research & Development Limited (UK). Animals were crossed two generations with the CD1 wild type strain; afterwards maintained by interbreeding (original background: 129S6). Small-eye (Sey, designated Pax6<sup>Sey</sup>) mutant mice (Hill et al., 1991) were maintained by interbreeding on a mixed background (C57BL/6J×DBA/2J). Interbreeding between Gsx2EGFP (designated Gsx2; maintained on a mixed background) kockin (Wang et al., 2009a) and Pax6<sup>Sey</sup> heterozygote mice was performed to generate Gsx2;Pax6 double heterozygotes, which were subsequently crossed to generate Gsx2;Pax6 double homozygous mutants.

#### 4.2.1.2 Mouse tail DNA extraction

Parental animals were maintained in a heterozygote allelic state and crossed to obtain all three possible genotypes (WT/WT, WT/-, -/-) from the same litter. To sort out the different genotypes and maintain the colonies, Pax6<sup>Leca4</sup> and Pax6<sup>Sey</sup> mice were distinguished by their eye phenotypes. Gsx2 mice were genotyped for mutant and wild-type alleles by genomic PCR. In case of the Pax6<sup>Leca2</sup> mice, homozygote animals were also distinguished by their eye phenotype; wild-type and heterozygote animals were genotyped by PCR, followed by sequencing on tail DNA. Tail DNA Extraction was performed with the Gentra Puregene Mouse Tail Kit (Qiagen) according to the manufacturer's instructions. Briefly, 5mm long tail clips from ear marked mice (3-4 weeks old) were incubated overnight at 55°C in 0.3ml of lysis buffer supplemented with 1mg/ml of Proteinase K. The next day, samples were briefly cooled down on ice and 100µl protein precipitation solution was added. Next, samples were vortexed and hair and tissue residues were removed by centrifugation at 13.000 rpm for 3min. The supernatant was poured into 0.3ml isopropanol and mixed well. The precipitates were washed in 0.3ml 70% ethanol and dissolved in 50µl hydration buffer. To solve the DNA,

samples were incubated for 1h at 65°C and diluted 1:100 with H<sub>2</sub>O for the PCR reaction.

#### 4.2.1.3 PCR Genotyping

Genotyping of the Pax6<sup>Leca2</sup> and Gsx2 mice was performed with a standard PCR mix containing 0.2µM of each required primer, 0.2mM of each dNTP (dATP, dCTP, dGTP, dTTP), 0.5µl MgCl<sub>2</sub>, 1.5 U of Taq DNA polymerase (Qiagen), 2.5µl 10xPCR buffer and 2µl (~100ng) of genomic DNA in a final volume of 25µl per reaction. The DNA was amplified under the following cycling conditions:

For Pax6<sup>Leca2</sup>:

	94°C	2 min
30 x	94°C	50 sec
	57°C	50 sec
	72°C	50 sec
	72°C	5 min

The following primers were used:

Pax6Leca2\_for: TCCAGGATGGCTGGGAGCTT.  
 Pax6Leca2\_rev: TTGCGTGGGTTGCCCTGGTA  
 PCR product size: 295bp.



**Figure 4-1 Example of PCR products for Pax6<sup>Leca2</sup> genotyping**

For Leca2 genotyping, first a PCR was performed on gDNA from adult mice or embryos using primers to amplify a 295 bp product including the Leca2 mutation, followed by sequencing of this PCR product.

Abbreviations: bp, base pairs; M, DNA marker; pd, primer dimer.

For Gsx2:

	94°C	2 min
30 x	94°C	1 min
	58°C	1 min
	72°C	2 min
	72°C	5 min

The following primers were used:

Gsx2Int5B: CCACGGAGATTCCAAGTCC  
 Gsx2-1437: GCATCCACCCCAAATCTCAGTC  
 PCR product size specific for wild-type allele: 298bp  
 Gsx2Int2: CCTAGGAATGCTCGTCAAGAAG  
 Gsx2Int5A: CATCACCATCACCAGCCCC  
 PCR product size specific for knockin allele: 225bp

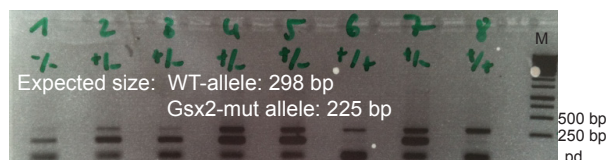


**Figure 4-2 Example of PCR products for Gsx2 genotyping**

Animals were genotyped according to the protocol by Wang et al., 2009: using a primer pair to detect the Gsx2EGFP allele (product: 225 bp) and using another pair of primers that include one sequence in the deleted region of the first exon (product: 298 bp). +/+, WT; +/-, hetero; -/-, mutant.

Abbreviations: bp, base pairs; M, DNA marker; pd, primer dimer.

#### 4.2.1.4 Sequencing

Prior to sequencing the PCR product was cleaned from the PCR reaction mix by gel extraction including clean up using the QIAquick Gel-Extraction Kit (Qiagen) according to the manufacturer's instructions. For the sequencing PCR reaction the following reagents were used:

0,5µl	Big Dye (contains polymerase)
2,0µl	Big Dye – buffer
10pM (0,5µl from 100µM stock)	primer (sense or antisense)
2µl	template-DNA

And the sequencing PCR was performed under the following cycling conditions:

	96°C	1 min
35 x	96°C	10 sec
	50°C	5 sec
	60°C	4 min
	4°C	∞

Finally the sequencing PCR was cleaned using DyeEX 2.0 Spin columns (Qiagen) according to the manufacturer's instructions and filled into the sequencing plate. The sequencing was then performed at the Sequencing Core Facility of the Helmholtz Zentrum München and for sequence analysis the Vector NTi program (Invitrogen) was applied.

#### 4.2.1.5 Fixation of mouse brains and cryosectioning

Mice used in this study were anesthetized by CO<sub>2</sub> and sacrificed by cervical dislocation. Embryos were immediately placed into Hanks Balanced Salt Solution (HBSS (Gibco); supplemented with 10mM Hepes (Gibco)) and dissected. Embryonic brains or heads were then fixed at 4°C in 4% PFA (paraformaldehyde) dissolved in PBS, under constant rotation. According to their age, fixation time lasted: 2h – E12 whole heads; 2h – E14 brains; 3.5h – E14 whole heads; 2.5h – E15 brains; 3h – E16 brains and 4h – E18 brains. After fixation, brains or heads were rinsed with PBS and cryoprotected in 30% sucrose/PBS at 4°C over night,

followed by freezing in Tissue Tek. Tissue was either stored at  $-20^{\circ}\text{C}$  or immediately cut in  $12\mu\text{m}$  to  $25\mu\text{m}$  thick sections on a Cryostat (Leica) and stored at  $-20^{\circ}\text{C}$ .

#### 4.2.2 Immunostainings

Immunostaining was performed either on fixed tissue culture samples (Immunocytochemistry) or cryosectioned brain slices (Immunohistochemistry). Prior to the staining procedure, coverslips stored in azide-PBS were washed in normal PBS and cryosections were shortly rehydrated by incubation in PBS at RT.

In general, antibodies were diluted in a solution containing 0.5% Triton-X100/PBS and 10% normal goat serum (NGS) as blocking agent. Under normal staining procedures primary antibodies were applied O/N at  $4^{\circ}\text{C}$ , followed by three washing steps in PBS and secondary antibody staining at RT for 2h. To visualize nuclei, Dapi (4', 6' Diamidino-2-phenylindole, Sigma) was included in the secondary antibody staining solution with a concentration of  $0.1\mu\text{g}/\text{ml}$ . Finally coverslips and sections were washed three times in PBS and mounted in Aqua Poly/Mount, a glycerol-based mounting medium that retains fluorescent stains.

As secondary antibodies, subclass specific antibodies conjugated to Alexa-488, Alexa-543, Alexa-633 (dilution: 1:1000, Invitrogen) or Cy2, Cy3, Cy5 (dilution: 1:400, Jackson Immuno Research) were applied. For signal amplification, Avidin-Biotin interactions were used. Thus, after primary antibody labelling, sections were incubated with a biotinylated secondary antibody (dilution: 1:400, Vector Laboratories) for 2h at RT, washed 3x in PBS and finally incubated with fluorochrome (Alexa-433,-543 or -633) conjugated Streptavidin (dilution 1:1000, Invitrogen) for 2h at RT.

Certain primary antibodies required one of the following specific pre-treatments to retrieve the antigen:

##### **Citrate-buffer pre-treatment:**

Coverslips were boiled for 30sec and sections for 8min in 0.01M sodium citrate (pH6) at 700V in a microwave, followed by brief PBS incubation prior to primary antibody staining.

##### **HCl pre-treatment:**

Sections were incubated in 2N HCl for 30min at RT, followed by 2x 15min incubation in 0.1M sodium-tetraborate (pH8.5).

If co-labelling with two different primary antibodies required pre-treatment for one antibody, normal staining was performed first, followed by post-fixation with 4% PFA for 15-30min at RT, before pre-treatment was applied for the second primary antibody.

All antibody used in the present study and their dilutions and treatment conditions are listed under 4.1.6.

#### 4.2.3 In situ hybridization - mRNA

In situ hybridization was performed on 12-25µm thick cryosections under semi-sterile conditions using sterile pipette tips and gloves. The procedure comprised two main steps: (a) generation of the digoxigenin (DIG)-labelled antisense RNA probe by in-vitro transcription and (b) hybridisation of the RNA probe followed by signal detection.

For in-vitro transcription the ISH-plasmid was first linearized over night using in general 1µl of the according enzyme for 20µg DNA and 5µl 10xbuffer in a final volume of 50µl. After digestions, the linearized plasmid was purified using phenol extraction. In vitro transcription was then performed with 1µg linearized plasmid and the following reaction mix: 2µl digoxigenin labelled dNTPs (Roche), 2µl 10x transcription buffer (Stratagene), 1µl RNase inhibitor (Roche) and 2.5µl of the appropriate RNA polymerase (T3, T7 or Sp6) (Roche). The reaction mix was incubated for 2h at 37°C followed by DNaseI treatment (addition of 2µl DNaseI) for 30-45min at 37°C. Then cleanup of the RNA was performed by adding 10µl LiCL, 80µl RNase-free water and 300µl 100%EtOH and incubation at -20°C for at least 2h or over night followed by EtOH precipitation (resuspension of pellet in 25µl RNase-free water). Finally the quality of the RNA probe was evaluated on a gel.

The hybridisation reaction on cryosections was performed in humidified chambers to avoid drying out of the sections. In general 1µl RNA probe per 150µl hybridisation buffer (50% formamide, 10xsalt, 50% dextransulfat, 50x Denhardt's Soutlion, 50 µg/mL yeast tRNA (Roche) in H<sub>2</sub>O) was used. The RNA probe / hybridisation buffer mixture was first heated up to 70°C for 4min in order to separate the RNA strands. After brief mixing, 150µl were applied per slide, covered with parafilm and incubated at 60-65°C overnight. The next day, the sections were placed into a sterile washing chamber and incubated once in pre-warmed washing solution (50% formamide, 4xSSC, 0.1% Tween20 in H<sub>2</sub>O) at 60-65°C for 10min followed by two washing steps for 30min at 60-65°C. Followed by two washing steps in 1x MABT (100mM maleic acid, 150mM NaCl, 0.1% Tween20, pH 7.5 in H<sub>2</sub>O) for 30min at RT. Then the sections were incubated in blocking buffer (5xMABT, 10% blocking reagent (Roche), 5% FCS) for 1h at RT, followed by antibody staining (antidigoxigenin fab fragments 1:2500 in ISH blocking buffer (Roche)) over night at 4°C. Antibody staining was again performed in a humidified chamber and slides were covered with parafilm. The next day, slides were washed 5 times in 1xMABT buffer and twice in freshly prepared AP staining buffer (100mM Tris (pH 9.5), 50mM MgCl<sub>2</sub>, 200mM NaCl, 0.1% Tween20 in H<sub>2</sub>O). Signal detection was performed by adding 3.5µl NBT (Roche) and 3.5µl BCIP (Roche) solutions

to 1ml AP staining buffer and incubation on the sections until the desired staining intensity was reached. The detection was stopped by washing the sections in autoclaved water and sections were mounted with Aqua Poly/Mount.

The ISH-Plasmid for Ngn2 was kindly provided by Francois Guillemot.

#### **4.2.4 In situ hybridization - microRNA**

MicroRNA in situ hybridization was performed on 12-25µm thick cryosections under semi-sterile conditions using sterile chambers, pipette tips, gloves and DEPC treated water for all solutions. DIG-labeled miRCURY LNA™ microRNA detection probes were used to detect the following miRNAs: miR-9 (TA: ~51°C; kind gift from G.Luxenhofer); miR-92b (TA: ~63°C); miR-124 (TA: ~60°C); miR-126-3p (TA: ~52°C).

Cryosections stored at -20°C were dried at RT for 30min and post-fixed for 12-15min in 4% PFA. Next, the sections were washed three times for 3min in PBS followed by incubation in acetylation solution (200ml H<sub>2</sub>O, 2ml TEA, 250µl glacial acetic acid) for 10min under stirring conditions. To permeabilize the tissue, sections were incubated with 5µg/ml Proteinase K (dissolved in PBS) for 5-10min. After two additional washing steps (in PBS for 3min), sections were placed into 1xSSC solution for 30min. Prior to hybridisation, sections were incubated for at least 2h in hybridisation buffer (5x Denhardt's solution, 205ug/ml baker yeast tRNA, 5x SSC, 20% formamide) without probe at the appropriate hybridisation temperature (see above). After the detection probe was diluted (generally 1:200-1:500) in hybridisation buffer, 150µl were applied per slide, covered with parafilm and incubated at the appropriate temperature overnight. Also, all washing buffers for the next day were incubated at the same temperature overnight. The next day, sections were placed into a washing chamber and washed: 4 x 15min in 1xSSC buffer (1xSSC + 0.1% Tx-100) followed by 4 x 15min in 0.2xSSC buffer (0,2xSSC + 0.1% Tx-100), both at 60°C and finally once for 15min in 0.2SSC buffer (0,2xSSC + 0.1% Tx-100; not pre-heated) at RT. For DIG staining, sections were incubated first in buffer 1 (100mM Tris, 150mM NaCl, pH 7.5) for 5min at RT, followed by blocking in 1% blocking reagent (Roche; prepared with buffer 1) for one hour. Then 200µl anti-DIG antibody (1:2000 in 1% blocking reagent) was applied per section and incubated for 2h at 37°C. Then sections were washed for 15min in buffer1 at RT, followed by an additional wash step of 10min in buffer 2 (100mM Tris, 100mM NaCl, pH 9.5). Signal detection was then performed by adding 3.5µl NBT (Roche) and 3.5µl BCIP (Roche) solutions to 1ml buffer 3 (buffer 2 +1M MgCl<sub>2</sub>), which was then incubated on the sections until the desired staining intensity was reached. The detection was stopped by washing the sections in TE

buffer or autoclaved water and sections were mounted with Aqua Poly/Mount.

#### 4.2.5 Molecular Biology

##### 4.2.5.1 Cloning of constructs

In order to overexpress the Pax6 Leca mutant forms in primary cell cultures, viral expression vector plasmids were constructed. The coding sequence of Pax6<sup>Leca4</sup> and Pax6<sup>Leca2</sup> mutant forms were obtained by PCR using isolated cDNA from E14 cortex tissue of the respective mouse mutant as template. The PCR was performed with the following primers: PDlessr1\_for: 5'-TCCCCGCGGTTACTGTAATCGAGGCC-3'; Delh3f1\_rev: 5'-CGGGATCCATGCAGAACAGTCACAGC-3'.

The PCR product was then cloned into the Stratagene PCR cloning vector by ligation and transformed, both according to the manufacturer's instructions. After confirmation of the correct sequence of this plasmid by sequencing, the Leca mutant forms were subcloned into the pENTRY1A vector (Invitrogen, Gateway System) by sequential digestion with XhoI and BamHI. Finally the Leca mutant cDNAs were shuttled into the pCAG-GFP destination vector (Invitrogen, Gateway System; kind gift by Paolo Malatesta) by LR reaction (Gateway, System). The resulting plasmid was checked by sequencing.

##### 4.2.5.2 Transformation into chemically competent *E.coli*

A 50 µl aliquot of the chemo-competent cells (bacterial strains see under 4.1.4) was thawed on ice. LB medium was preheated to 42°C. Then 5 µl of the ligation reaction (~5 µg) was added, mixed and incubated on ice for 20 min. Cells were then heat shocked for 45 s at 42°C, and cooled on ice for 2 min. 500 µl of the pre-heated LB medium was added and cells were incubated for 45-60 min at 37°C on a shaker. Afterwards, different volumes (50-500 µl) were plated on bacterial agar plates containing the appropriate antibiotic and incubated over night at 37°C.

##### 4.2.5.3 Bacterial liquid cultures and DNA purification

For small scale (4ml) or large scale (200ml) liquid cultures, a single colony was inoculated into 4ml or 200ml LB medium (supplemented with the appropriate antibiotic) respectively, and incubated over night at 37°C under vigorous shaking. Plasmid DNA was then isolated using Qiagen's Mini Prep or Maxi Prep kit following the manufacturer's instruction manuals.

#### 4.2.5.4 *Restriction digestion of DNA*

A typical reaction was prepared as follows:

1 µg	DNA plasmid
2 µl	10x reaction buffer (NEB)
0.5 – 3.0 µl	Restriction enzyme (5-10 U) (NEB)
ad 20 µl	H <sub>2</sub> O

The reaction was incubated at the appropriate temperature (depending on the enzyme) for 1 hour or overnight. Cleavage efficiency was investigated by gel electrophoresis.

#### 4.2.5.5 *Ligation*

For ligations, the insert DNA was generally used in a 5-10 fold excess of vector DNA. The ligation reaction was incubated at 16°C overnight and transformed the next day. Colonies were picked, DNA extracted and analyzed by digestions or for the final vectors by sequencing.

### 4.2.6 **Cell Culture**

#### 4.2.6.1 *Preparation of primary embryonic cerebral cortical cell culture*

Timed-pregnant mice were anesthetized by CO<sub>2</sub> and sacrificed by cervical dislocation. The embryos were removed by caesarean section and immediately placed into Hanks Balanced Salt Solution (HBSS (Gibco); supplemented with 10mM HEPES (Gibco)). The brains were dissected out, the telencephalic hemispheres were separated and the meninges, the hippocampus (anlage) and the olfactory bulbs were removed. Then the dorsal telencephalon (cortex) was separated from the ventral telencephalon and the cortex tissues of both hemispheres were transferred to a 15 ml falcon tube containing HBSS. The tissues were collected at the bottom of the falcon by centrifugation for 5 min at 1200 rpm. The tissue was incubated in 0.05% trypsin-EDTA for 15 min at 37°C. To stop the trypsin digestion and for dissociation, several ml DMEM (Gibco) with 10% fetal calf serum (FCS) were added and a fire polished Pasteur pipette (preincubated in DMEM/FCS to coat the glass) was used to mechanically disrupt the tissue. After two washing steps with DMEM/FCS 3x10<sup>5</sup> cortex cells were plated on poly-D-lysine coated glass coverslips in 24 well plates (NUNC) in 500µl DMEM/10%FCS/P/S. The following day 500µl of DMEM media without FCS supplemented with the B27 cocktail was added per well and each second day 500µl of the above DMEM/B27 medium were replaced.

### 4.2.6.2 *Clonal analysis in primary culture*

For clonal analysis of the Pax6<sup>Leca4</sup> and Pax6<sup>Leca2</sup> cortices the plated cells of the mutants and the corresponding wild-type controls were infected 2 hours after plating with the pMXIG retrovirus to obtain no more than 50 clones per coverslip. For overexpression experiments of the Pax6 Leca mutant forms in BL6 wild-type cultures, the appropriate retrovirus (based on the viral plasmids: pCAG-Leca2-/Leca4-/Pax6wt- or Ctrl-IRES-GFP; see also under 4.1.5) was added 2 hours after plating. The cells were fixed after one week and clone composition and size was analyzed using immunocytochemistry.

### 4.2.6.3 *Dual-luciferase reporter assay*

The reporter assays were performed in P19 carcinoma cells and Human Embryonic Kidney (HEK) cells, both cultured with DMEMGlutaMAX/10%FCS/P/S media. For all transfections, P19 or HEK cells were plated at a density of  $8 \times 10^5$  cells per 24-well, 20 hours prior to transfection in media without antibiotic. Transfections were performed with 1  $\mu$ g expression plasmid, 1  $\mu$ g of the promoter construct driving firefly (*Photinus pyralis*) luciferase and 0.1  $\mu$ g of Renilla-TK luciferase plasmid (Promega) for control of transfection efficiency. As transfection reagent Lipofectamine 2000 (Invitrogen) was used according to the manufacturer's instructions. After 4 hours, medium was changed and after 48 hours cell extracts were prepared for luciferase activity measurement with a luminometer (Berthold Centro LB 960) according to the manufacturer's instruction protocol (Promega). Relative light units were normalized to Renilla luciferase activity and then to the control transduced cells.

As promoter constructs, the pGL3-based promoter plasmids containing the Pax6 consensus sites P6CON-P3 (combination PD-binding site and HD-binding site) or P3 (HD-binding site) were analysed (see under 4.1.5). As expression plasmids, the retroviral vector constructs, expressing wild-type Pax6 or the Leca4 or Leca2 mutant form of Pax6 under the CAG promoter were used.

### 4.2.7 **Embryonic stem cell differentiation culture protocol**

Mouse embryonic stem cells (ESC; line J1) were cultured according to the Bibel et al., 2007 protocol. Briefly, ESC were thawed on a layer of mouse embryonic fibroblasts (MEFs or feeder cells were prepared from E13 embryos). Importantly the feeder layer (thawed on 6cm dishes coated with 0.2% gelatine) had to be very dense so that the ESC formed potatoe-shaped colonies on them. Before adding the ESCs, the feeder cells were inactivated with

Mitomycin C (Sigma) for 2h at 37°C and washed once with PBS. Feeder cells alone were grown in EB-Medium and with ESC in ES-Medium (see under 4.1.3.2). The density of the ESC cells grown on the feeder layer had to be adjusted so that the colonies, grown for two days on a feeder layer did not touch each other. After passaging the ESC 3-6 times on top of inactivated feeder cells, they were transferred to gelatine coated dishes (10cm) without feeders. On gelatine, ESC changed their morphology. They started to flatten, still forming colonies but rather in a monolayer. Importantly, the dish had to be 80% confluent after 48 hours, thus cells had to be highly proliferative. Normally, at the 4th-5th passage on gelatine, the ESC cultures contained no more feeder cells. From this point, 3 million cells were transferred to one 10cm bacterial dish and cultured in EB-Medium. This induced cellular aggregate formation (CA). 48h after plating, medium was changed by transferring the CAs to 50ml falcons. After they settled on the bottom of the tube, medium was exchanged. On day four and six, medium was replaced again and 5µM retinoic acid was added as inductive stimulus. On day eight cells were considered as neuronal progenitors. Then, cellular aggregates were dissociated with freshly prepared trypsin (0.05% dissolved in 0.04% EDTA/PBS) and  $1.3 \times 10^6$  cells were plated on Poly-Id-ornithine (PORN) and laminin coated 6-well plates in N2 medium. Media were exchanged 2 hours and 24 hours after plating; cells acquired radial glia elongated morphology. After two more days N2 medium was replaced by complete medium and the culture was kept up to five more days, leading to cultures with pure glutamatergic neurons.

#### **4.2.8 RNA isolation and microarray analysis**

For the analysis of the Pax6 mutant cerebral cortices total RNA was isolated from E12 or E14 cortical tissue using the RNeasy Micro kit (Qiagen) or RNeasy Mini kit (Qiagen) according to the manufacturer's instructions including digestion of remaining genomic DNA. RNA concentration was measured at the Nanodrop (260nm / 280nm ratio) and to assess the RNA quality for microarray analysis the Agilent 2100 Bioanalyzer was used. The Agilent software assigns a specific quality number to the RNA sample based on its electrophoretic profile. This RNA Integrity Number (RIN) ranges from 1 (reflecting totally degraded RNA) to 10 (reflecting completely intact RNA). For microarray analysis only high quality RNA (RIN>7) was used.

For each microarray chip total RNA (100 ng) was first amplified using the one-cycle MessageAmp Premier labeling kit (Ambion). And 10 µg of amplified aRNA were hybridized on Affymetrix Mouse Genome 430 2.0 arrays according to the manufacturer's instructions.

The statistic analysis of the microarrays was then performed by utilizing the statistical programming environment R (R Development Core Team (Team, 2006)) implemented in CARMAweb (Rainer et al., 2006). The probe set summaries were calculated with RMA (default settings including quantile normalization and application of the Tukey's median polish algorithm). Datasets were filtered for average expression >50 in at least one group (mutant or WT) and for linear ratios >1.1x (Mut/WT). Then, genewise testing for differential expression was done employing the limma t-test and Benjamini-Hochberg multiple testing correction (FDR < 10%). Heatmaps were generated with CARMAweb.

The mRNA transcriptome analysis of embryonic stem cell derived radial glia and neurons at different stages during differentiation (Bibel et al., 2004; Bibel et al., 2007) was performed on the total RNA samples that were extracted and used for the microRNA-array analysis (see below). Prior to microarray analysis these samples of total RNA were loaded again onto RNeasy Mini columns (Qiagen) and treated with DNase I to digest remaining DNA. Analysis was then performed the same way as described above for the cortical tissue arrays.

### **4.2.9 MicroRNA extraction and miRNA-array analysis**

For the miRNA array screen, RNA including miRNAs and total RNA was extracted from the following five different time points of the embryonic stem cell differentiation system (according to (Bibel et al., 2004; Bibel et al., 2007)):

- 1.) Cellular aggregate stage: day 4 (CA<sub>d4</sub>); not treated with retinoic acid (RA)
- 2.) Cellular aggregate stage: day 6 (CA<sub>d6</sub>); once treated with RA
- 3.) Cellular aggregate stage: day 8 (CA<sub>d8</sub>); twice treated with RA
- 4.) Radial glia progenitor stage: 14 hours past plating of CA<sub>d8</sub> cells (P14h)
- 5.) Neuronal stage: 7 days past plating of CA<sub>d8</sub> cells (N7d)

Cells from each time point were collected three times from three independent cultures to receive three biological replicates.

From the three cellular aggregate stages, one 10 cm dish of the floating CAs was collected by brief centrifugation. Media was removed; cells were washed once with PBS, resuspended in 350 µl RLT buffer and stored at -80°C. P14h radial glia and N7 neurons were plated in 6-well plates and 3x 6wells were combined and collected in 300 µl RLT and stored at -80°C. After collection of all biological replicates, total RNA was extracted of all samples. Samples were thawed on ice and 2 x more RLT buffer was added prior to homogenization with a 26 G

syringe and needle. 1.5 x volume of 100% ethanol was added and thoroughly mixed by vortexing. 700µl of the sample was then loaded onto a RNeasy Mini spin column (Qiagen) and centrifuged 15 s at 10.000 rpm (flow-through discarded); precipitations were omitted. This step was repeated until the whole sample had been pipetted onto the spin column. The spin column was then transferred into a new 2 ml collection tube and washed twice with 500 µl RPE by centrifugation for 15 s at 10.000 rpm. The spin column was placed again into a new collection tube and centrifuged for 1 min at full speed to remove remaining buffer. Finally the column was placed into a sterile 1.5 ml eppendorf tube and miRNAs and total RNA were eluted in 30 µl RNase-free water by centrifugation at 10.000 rpm for 1 min. Concentration was determined at the nanodrop. 3µg of each sample were sent to the company Exiqon who performed quality control with the Agilent Bioanalyzer 2100 and subsequent miRNA-array analysis. All samples from the stages 1-4 had a higher RIN value than 7, indicative of good quality RNA for array analysis. The RNA of the three replicates of the neuronal stage was of less good quality with RIN values of 3.6, 5.4 and 6.2. However this quality was still acceptable for array analysis. Array analysis performed by Exiqon included the labeling of the samples using the miRCURY™ Hy3™/Hy5™ power labeling kit, hybridization on the miRCURY™ Array (v.11.0) and data analysis of the arrays as described in their manual.

#### **4.2.10 CDNA synthesis and quantitative pcr analysis**

For qPCR, extracted RNA (500ng -1µg) was reverse transcribed to cDNA using the SuperScript II™ First-Strand Synthesis System (Invitrogen) according to the manufacturer's instructions. Real-time PCR was performed using gene-specific primers (list of primers see under 4.1.7) and the SYBRGreen mastermix (Biorad) on a DNA Engine Opticon™ machine (Biorad). The melting temperature of primer dimers was determined in order to exclude primer dimers from the analysis. As reference gene for normalization of the target gene's expression GAPDH was used. The relative expression of each mRNA was calculated using the delta CT method between the gene of interest and the reference gene (GAPDH) ( $E=1/2^{-(-\Delta Ct)}$ ).

#### **4.2.11 Data analysis**

Quantifications of cells in mitosis (PH3+) were performed at E12 across the entire dorsal wall from lateral to medial position and at E14 in 150 µm wide radial stripes covering the entire radial thickness with the ventricular surface. The radial length was measured in the

center and at lateral position of the cerebral cortex using ImageJ (NIH). All quantifications were performed on images from the dorsal telencephalon in rostral regions using level-matched sections of at least three stage-matched embryos of each genotype, from at least three different litters. For the clonal analysis in vitro, clone composition and clone size of each clone per coverslip was determined and the mean was calculated per coverslips (6-9 coverslips, 3 experiments). The number of activated-Caspase-3 positive cells was quantified in an average of 15 sections per animal in rostral regions of the cerebral cortex (3 animals per genotype).

#### 4.2.11.1 Statistics

Calculations of the arithmetic average:  $\bar{x} = \frac{1}{n} \sum_{i=1}^n x_i$

the standard deviation (SD):  $s = \sqrt{\frac{\sum_{i=1}^N (x_i - \bar{x})^2}{N-1}}$

and the standard error of the mean (SEM):  $SEM = \frac{s}{\sqrt{n}}$

were performed with Microsoft Excel. The one-way Anova test was used to examine whether data sets differed significantly. Data were considered as significant with  $p < 0.05$  (\*), very significant with  $p < 0.01$  (\*\*) and highly significant with  $p < 0.001$  (\*\*).

## 5 Appendix

### 5.1 Abbreviation

<b>%</b>	Percent
<b>°C</b>	Degree Celsius
<b>µg</b>	Microgram(s)
<b>µL</b>	Microlitre(s)
<b>A</b>	Absorption
<b>aa</b>	Amino acid
<b>bHLH</b>	Basic helix-loop-helix
<b>bp</b>	base pair
<b>BSA</b>	Bovine serum albumine
<b>CR</b>	Calretinin
<b>cDNA</b>	Complementary DeoxyriboNucleic Acid
<b>CGE</b>	Caudal ganglionic eminence
<b>cm</b>	Centimeter(s)
<b>CNS</b>	Central Nervous System
<b>CO<sub>2</sub></b>	Carbon Dioxide
<b>CP</b>	Cortical Plate
<b>CSF</b>	Cerebrospinal Fluid
<b>DAPI</b>	4,6-diamidine-2-pheylidolehydrochloride
<b>dd</b>	double distilled (ultrapure)
<b>DMEM</b>	Dulbecco's Modified Eagle Medium
<b>DNA</b>	Deoxyribonucleic acid
<b>dNTP</b>	DeoxyNucleoside TriPhosphate(s)
<b>e.g.</b>	For example (Latin 'exempli gratia')
<b>EDTA</b>	Ethylene-Diamine-tetra-Acetic-Acid
<b>EPL</b>	External Plexiform Layer
<b>FCS</b>	Fetal Calf Serum
<b>g</b>	Gram(s)
<b>GABA</b>	gamma-Amino Butyric Acid
<b>GAPDH</b>	GlycerAldehyde 3-Phosphate DeHydrogenase
<b>GCL</b>	Granule Cell Layer
<b>GE</b>	Ganglionic Eminence
<b>GFP</b>	Green Fluorescent Protein
<b>GL</b>	Glomerular Layer
<b>h</b>	Hour(s)
<b>HBSS</b>	Hank's balanced salt solution
<b>HCL</b>	Hydrochloric acid
<b>HEPES</b>	4-(2-Hydroxyethyl)-1-piperazineethanesulfonic acid
<b>INM</b>	Interkinetic Nuclear Migration
<b>IRES</b>	Internal Ribosomal Entry Site
<b>ISH</b>	In-Situ Hybridisation
<b>IZ</b>	Intermediate Zone
<b>kb</b>	Kilobase
<b>kDa</b>	Kilodalton
<b>kg</b>	Kilogram(s)
<b>LB</b>	Luria-Bertani medium

<b>Leca</b>	LEns Corneal Adhesion
<b>LGE</b>	Lateral Ganglionic Eminence
<b>LIF</b>	Leukemia Inhibitory Factor
<b>LTR</b>	Long Terminal Repeat
<b>MC</b>	Mitral Cells
<b>mg</b>	Milligram(s)
<b>MGE</b>	Medial ganglionic eminence
<b>min</b>	Minute(s)
<b>mL</b>	Millilitre(s)
<b>MLV</b>	Moloney Murine Leukemia Virus
<b>mRNA</b>	Messenger Ribonucleic Acid
<b>miRNA</b>	Micro Ribonucleic Acid
<b>NaCL</b>	Sodium chloride
<b>ng</b>	Nanogram(s)
<b>OB</b>	Olfactory Bulb
<b>OBLS</b>	Olfactory Bulb Like Structure
<b>PBS</b>	Phosphate buffered saline
<b>PCR</b>	Polymerase chain reaction
<b>PDL</b>	Poly-D-Lysine
<b>PFA</b>	Paraformaldehyde
<b>RA</b>	Retinoic Acid
<b>RMS</b>	Rostral Migratory Stream
<b>RNA</b>	Ribonucleic acid
<b>rpm</b>	Rotations per minute
<b>RT</b>	room temperature
<b>sec</b>	Second(s)
<b>SEM</b>	Standard Error of the Mean
<b>SVZ</b>	Sub Ventricular Zone

## 5.2 Tables

**Table 5-1:** Mean size of clones in cultures from Pax6<sup>Leca4</sup> and Pax6<sup>Leca2</sup> mutant mice and after overexpression of GFP control, Pax6 and Pax6 Leca mutant forms in primary culture.

Virus	Mean clone size	Mean clone size – Pure neuronal clones	Mean clone size – Mixed clones	Mean clone size – Pure non-neuronal clones
<b>GFP</b> - in WT cultures	4.9 ± 0.6	1.8 ± 0.28	7.7 ± 1.41	9.3 ± 1.35
- in Leca4 mutant cultures	7.5 ± 0.6	1.6 ± 0.09	7.2 ± 0.83	12.6 ± 0.88
<b>GFP</b> - in WT cultures	4.1 ± 0.3	1.3 ± 0.05	4.3 ± 0.68	7.0 ± 0.83
- in Leca2 mutant cultures	4.4 ± 0.5	1.5 ± 0.08	7.8 ± 2.44	6.9 ± 0.84
<i>Overexpression in WT cultures:</i>				
<b>GFP</b>	5.9 ± 1.4	1.7 ± 0.2	8.7 ± 2.9	7.4 ± 2.6
<b>Pax6-GFP</b>	3.6 ± 0.8	1.3 ± 0.05	4.7 ± 1.2	4.9 ± 1.8
<b>Leca4-GFP</b>	3.5 ± 0.7	1.4 ± 0.1	5.8 ± 1.6	3.6 ± 0.7
<b>Leca2-GFP</b>	5.9 ± 1.5	1.4 ± 0.1	8.9 ± 2.0	7.9 ± 3.4

**Table 5-2:** Probe sets differentially expressed between WT and Pax6<sup>Leca4</sup> cortices

Probe_set	Gene symbol or ID	Ratio, significant FDR<10%, ratio>1.4x, Av>50 (416)	Av Pax6 Leca4	Av WT	Pax6 Chip Binding sites (Ales Cvekl unpublished data)
<b>Up-regulated probe sets (237)</b>					
1434369_a_at	Cryab	8,89	255	29	cortex
1441778_at	Adcyap1	8,27	447	54	
1460412_at	Fbln7	7,47	348	47	lens
1457012_at	Dbx1	6,76	342	51	
1448326_a_at	Crabp1	6,19	796	129	
1434376_at	Cd44	6,04	243	40	
1416455_a_at	Cryab	5,62	154	27	cortex
1416953_at	Ctgf	5,41	430	79	lens
1423427_at	Adcyap1	5,28	1015	192	
1424131_at	Col6a3	5,15	490	95	
1442542_at	Eya4	5,03	776	154	lens
1445897_s_at	lfi35	5,00	181	36	lens
1455931_at	Chrna3	4,98	333	67	
1452106_at	Npnt	4,23	347	82	
1418424_at	Tnfaip6	4,10	120	29	
1449393_at	LOC100046930	3,97	51	13	
1455439_a_at	Lgals1	3,96	1346	340	cortex, lens, pancreas
1452010_at	Chrna3	3,86	470	122	
1419573_a_at	Lgals1	3,84	1262	328	cortex, lens, pancreas
1456238_at	LOC668917	3,78	82	22	
1456665_at	Eya4	3,70	181	49	lens
1430700_a_at	Pla2g7	3,64	499	137	
1457008_at	Chrn4	3,49	176	50	
1457048_at	Qrfpr	3,38	202	60	
1452107_s_at	Npnt	3,36	92	27	
1439795_at	Gpr64	3,27	88	27	lens
1451776_s_at	Hopx	3,26	2595	797	
1423760_at	Cd44	3,19	96	30	
1428662_a_at	Hopx	3,16	5099	1615	
1428891_at	Parm1	2,88	279	97	
1455451_at	Kctd14	2,86	153	54	
1460044_at	Onecut2	2,83	118	42	
1419633_at	Uncx	2,82	93	33	
1424404_at	0610040J01Rik	2,78	302	109	

1451415_at	1810011O10Rik	2,65	722	273	
1444980_at	Onecut2	2,59	70	27	
1424214_at	Parm1	2,57	111	43	
1449357_at	2310030G06Rik	2,55	130	51	
1438551_at	Neurog1	2,53	1491	590	cortex
1435595_at	1810011O10Rik	2,52	378	150	
1440564_at	Prokr2	2,50	399	160	
1453006_at	Fgfbp3	2,47	4461	1808	cortex
1454772_at	Snrnp200	2,43	402	166	
1436642_x_at	AW047730	2,40	1334	556	
1426622_a_at	Qpct	2,36	139	59	
1424127_at	Eya2	2,30	77	34	
1448713_at	Stat4	2,30	183	80	
1448162_at	Vcam1	2,28	1231	539	
1419215_at	Aox4	2,28	94	41	cortex
1424596_s_at	Lmcd1	2,25	584	259	
1451191_at	Crabp2	2,23	525	236	cortex
1423516_a_at	Nid2	2,23	256	115	
1417090_at	Rcn1	2,20	2041	927	pancreas, cortex
1416630_at	Id3	2,20	812	370	
1456509_at	1110032F04Rik	2,18	623	285	
1440374_at	Pde1c	2,14	554	258	cortex
1434449_at	Aqp4	2,13	77	36	
1437695_at	Prokr2	2,11	310	147	
1448390_a_at	Dhrs3	2,11	102	48	
1439774_at	Prrx1	2,08	156	75	
1415897_a_at	Mgst1	2,08	799	384	pancreas
1443998_at	Rassf2	2,06	65	32	cortex
1416776_at	Crym	2,04	489	239	
1432331_a_at	Prrx2	2,03	301	149	
1429856_at	Tspan18	2,01	102	51	
1448392_at	Sparc	1,99	1619	812	cortex
1440005_at	Onecut2	1,94	62	32	
1434572_at	Hdac9	1,93	570	295	
1436791_at	Wnt5a	1,93	414	215	lens
1425528_at	Prrx1	1,92	396	207	
1441499_at	Grid1	1,91	128	67	cortex
1420884_at	Sln	1,91	145	76	
1439483_at	Al506816	1,88	1170	621	
1450117_at	Tcf7l1	1,88	820	436	
1435363_at	Plekhg1	1,88	532	283	
1438571_at	Bub1	1,86	195	105	
1454985_at	Ambra1	1,85	956	516	lens

1437743_at	Aebp2	1,85	218	117	
1434070_at	Jag1	1,85	564	305	
1457587_at	Kcnq5	1,84	290	157	
1440323_at	Syt2	1,84	54	29	
1423306_at	2010002N04Rik	1,84	182	99	
1420418_at	Syt2	1,83	52	28	
1416589_at	Sparc	1,82	2095	1151	cortex
1424617_at	lfi35	1,81	91	50	lens
1429896_at	5830408B19Rik	1,79	196	110	
1424176_a_at	Anxa4	1,79	85	48	
1439019_at	Fras1	1,79	228	127	
1428990_at	2310047K21Rik	1,77	262	148	
1425811_a_at	Csrp1	1,77	415	235	
1429284_at	Mobkl2b	1,76	564	320	lens
1424695_at	2010011I20Rik	1,76	1906	1082	
1437930_at	Glt25d2	1,74	153	88	lens
1421141_a_at	Foxp1	1,73	786	454	
1452065_at	Vstm2a	1,73	253	146	
1435622_at	Hs3st3a1	1,73	129	74	
1420919_at	Sgk3	1,72	187	109	pancreas, lens
1449145_a_at	Cav1	1,72	541	314	
1459151_x_at	lfi35	1,71	112	65	lens
1417649_at	Cdkn1c	1,71	4180	2445	
1424659_at	Slit2	1,71	481	281	
1455123_at	St18	1,71	1481	867	
1449084_s_at	Sh3d19	1,71	423	248	
1423718_at	Ak3	1,70	730	429	
1440290_at	Gm10010	1,70	74	43	
1436590_at	Ppp1r3b	1,70	87	51	
1460248_at	Cpxm2	1,69	86	51	
1455512_at	Shisa6	1,69	172	102	
1421223_a_at	Anxa4	1,69	177	105	
1442434_at	D8Ertd82e	1,68	1705	1012	
1426642_at	Fn1	1,68	1058	631	
1454728_s_at	Atp8a1	1,67	660	394	cortex
1447992_s_at	Pcsk2	1,67	123	74	
1435828_at	Maf	1,67	295	177	lens
1440445_at	Pax6os1	1,67	95	57	
1422824_s_at	Eps8	1,66	260	156	
1427256_at	Vcan	1,66	2012	1212	
1435092_at	Arl4a	1,66	171	103	
1422823_at	Eps8	1,66	228	137	
1452217_at	Ahnak	1,66	153	92	cortex
1435208_at	Dtx3l	1,66	308	186	

1423717_at	Ak3	1,65	2128	1287	
1416897_at	Parp9	1,65	235	143	
1451450_at	2010011I20Rik	1,65	3520	2133	
1424694_at	2010011I20Rik	1,65	2445	1484	
1454984_at	Lifr	1,65	246	149	pancreas
1459702_at	1459702_at	1,64	86	52	
1447849_s_at	Maf	1,64	502	306	lens
1435222_at	Foxp1	1,64	1892	1155	
1421597_a_at	Msx3	1,64	130	80	
1424097_at	Elovl7	1,63	76	47	
1433827_at	Atp8a1	1,62	664	409	cortex
1434141_at	Gucy1a3	1,61	1145	711	
1455500_at	Rnf213	1,61	205	127	
1435070_at	Aebp2	1,61	471	292	
1417195_at	Wwc2	1,61	228	142	
1421694_a_at	Vcan	1,60	285	178	
1421142_s_at	Foxp1	1,60	636	398	
1451321_a_at	Rbm43	1,59	213	134	
1425526_a_at	Prrx1	1,59	130	82	
1426774_at	Parp12	1,58	113	71	
1427912_at	Cbr3	1,58	91	58	
1436346_at	Cd109	1,57	98	62	
1434666_at	LOC100048247	1,57	787	500	
1433617_s_at	B4galt5	1,57	1496	954	
1452008_at	Ttc39b	1,57	734	468	
1451440_at	Chodl	1,57	123	78	
1416498_at	Ppic	1,57	547	349	
1417196_s_at	Wwc2	1,56	198	127	
1420918_at	Sgk3	1,56	118	76	pancreas, lens
1450673_at	Col9a2	1,56	52	34	
1417694_at	Gab1	1,56	2388	1534	pancreas
1429830_a_at	Cd59a	1,56	121	78	
1437782_at	Cntnap2	1,55	457	294	
1429270_a_at	Syce2	1,55	1868	1207	
1429987_at	9930013L23Rik	1,55	298	193	
1449314_at	Zfpm2	1,55	2060	1332	lens
1440691_at	Cyp2j6	1,54	80	52	
1441972_at	6230424C14Rik	1,54	175	114	
1428804_at	Mfap3l	1,54	219	142	
1425810_a_at	Csrp1	1,53	214	140	
1451119_a_at	Fbln1	1,53	867	566	cortex
1435297_at	Gjd2	1,53	220	143	
1439874_at	9330102E08Rik	1,53	146	96	
1449773_s_at	Gadd45b	1,53	93	61	

1437927_at	Dlg2	1,53	544	356	
1460409_at	Cpt1a	1,52	830	544	
1452331_s_at	Qser1	1,52	1012	665	
1440192_at	Ttc39b	1,52	327	215	
1441657_at	1441657_at	1,52	328	216	
1456060_at	Maf	1,51	1066	706	lens
1417932_at	Il18	1,51	609	404	
1421811_at	LOC640441	1,50	485	322	
1420534_at	Gucy1a3	1,50	69	46	
1434866_x_at	Cpt1a	1,50	141	94	
1420500_at	Dnajc1	1,49	542	363	
1425974_a_at	Trim25	1,49	172	115	
1450971_at	Gadd45b	1,49	164	110	
1420984_at	Pctp	1,48	85	57	
1439825_at	Dtx3l	1,48	235	158	
1440355_at	Kctd12b	1,48	169	114	
1457157_at	Plch1	1,48	313	212	
1449933_a_at	Tsen15	1,48	1418	959	cortex
1453070_at	Pcdh17	1,47	415	282	
1431429_a_at	Arl4a	1,47	382	260	
1453795_at	Fahd2a	1,47	605	411	
1446179_at	1446179_at	1,47	411	280	
1417693_a_at	Gab1	1,46	1375	941	pancreas
1424191_a_at	Tmem41a	1,46	1837	1257	
1441053_at	ENSMUSG0000003774 0	1,46	155	106	
1416579_a_at	Epcam	1,46	82	56	
1437404_at	Mast4	1,46	170	117	
1451693_a_at	Fgf12	1,46	398	274	cortex
1433942_at	Myo6	1,45	261	179	
1438796_at	Nr4a3	1,45	1925	1324	
1435262_at	Pign	1,45	386	266	
1435596_at	Pion	1,45	264	182	
1455242_at	Foxp1	1,45	1448	1002	
1450036_at	Sgk3	1,44	278	192	pancreas, lens
1440454_at	Pion	1,44	87	60	
1450716_at	Adamts1	1,44	354	245	lens
1419367_at	Decr1	1,44	803	557	
1419493_a_at	Tpd52	1,44	715	497	
1427369_at	Nlrp6	1,44	69	48	cortex
1419093_at	Tdo2	1,44	53	37	pancreas
1455182_at	Kif1b	1,43	1194	832	pancreas, lens
1449401_at	C1qc	1,43	165	115	
1423258_at	Syt9	1,43	244	170	cortex

1455324_at	Plcx2	1,43	4521	3156	
1450241_a_at	Evi2a	1,43	80	56	
1417381_at	C1qa	1,43	253	177	
1435751_at	Abcc9	1,43	89	62	
1437442_at	Pcdh7	1,43	363	254	cortex
1420831_at	Qsox1	1,43	197	138	
1426440_at	Dhrs7	1,43	273	191	
1451046_at	LOC100047651	1,43	117	82	
1433501_at	Ctso	1,43	259	182	cortex
1449167_at	Epb4.1l4a	1,43	189	133	lens
1433643_at	Cacna2d1	1,43	2754	1932	lens
1449876_at	Prkg1	1,42	51	36	
1417130_s_at	Angptl4	1,42	166	116	cortex
1423596_at	Nek6	1,42	1593	1120	
1440527_at	1440527_at	1,42	461	325	
1418135_at	Aff1	1,42	250	176	
1417625_s_at	Cxcr7	1,42	1968	1388	
1416441_at	Pgcp	1,42	66	46	
1435285_at	Mpped2	1,42	4871	3438	
1429089_s_at	2900026A02Rik	1,42	1140	805	
1434775_at	Pard3	1,41	1011	715	lens
1435841_s_at	Suclg2	1,41	1065	753	
1417667_a_at	Pter	1,41	230	162	pancreas
1454656_at	Spata13	1,41	888	629	
1420981_a_at	Lmo4	1,41	2916	2065	lens
1425669_at	Mobkl2b	1,41	103	73	lens
1426581_at	Ptpmt1	1,41	836	594	
1436404_at	Tlcd1	1,41	108	76	
1457651_x_at	Rem2	1,41	217	154	
<b>Down-regulated probe sets (179)</b>					
1426037_a_at	Rgs16	0,70	372	528	
1428729_at	Krit1	0,70	108	154	
1449374_at	Pipox	0,70	102	144	
1438769_a_at	Thyn1	0,70	364	519	
1450936_a_at	Dnase1l2	0,70	54	77	
1455748_at	Dynlt1d	0,70	119	170	
1449420_at	Pde1b	0,70	1305	1861	
1427535_s_at	Obsl1	0,70	285	407	cortex
1451657_a_at	Enox2	0,70	46	66	
1421262_at	Lipg	0,70	308	440	lens
1425766_x_at	Gm6354	0,70	39	55	
1437650_at	C730026J16	0,70	224	321	
1420764_at	Scrg1	0,70	91	131	

1457243_at	Tmem219	0,70	58	83	
1423367_at	Wnt7a	0,70	515	739	
1448406_at	Eid1	0,69	2078	2990	
1456759_at	Lrrc4c	0,69	196	282	cortex
1450188_s_at	Lipg	0,69	166	239	lens
1436913_at	Cdc14a	0,69	133	192	
1453060_at	Rgs8	0,69	238	344	
1427293_a_at	Auts2	0,69	494	715	
1442353_at	Itpa	0,69	38	55	
1442800_x_at	Fam181b	0,69	96	140	
1429653_at	Gse1	0,69	90	132	
1439248_at	Rmi1	0,69	39	57	cortex
1451991_at	Epha7	0,69	362	528	
1455557_at	LOC553095	0,69	833	1215	
1421835_at	Mtap7	0,68	40	58	
1441690_at	Cdh8	0,68	54	79	lens
1416934_at	Mtm1	0,68	70	102	
1440443_at	E030016H06Rik	0,68	59	87	
1440108_at	Foxp2	0,68	268	395	
1426641_at	Trib2	0,68	41	61	
1422596_at	Nkain4	0,68	451	667	
1427271_at	Zbtb44	0,68	199	294	
1438231_at	Foxp2	0,67	338	502	
1458704_at	1458704_at	0,67	47	70	
1418495_at	Zc3h8	0,67	236	351	cortex
1420838_at	Ntrk2	0,67	413	615	lens
1440996_at	1440996_at	0,67	70	104	
1448943_at	Nrp1	0,67	1369	2046	
1457836_at	Mfsd11	0,67	71	106	pancreas
1418153_at	Lama1	0,67	62	93	lens
1444679_at	Phf21a	0,67	126	189	
1440770_at	Bcl2	0,67	36	54	cortex, lens
1428571_at	Col9a1	0,66	111	167	
1438232_at	Foxp2	0,66	544	826	
1425574_at	Epha3	0,66	280	427	
1450650_at	Myo10	0,65	272	417	
1453787_at	Tmx4	0,65	84	130	
1429360_at	Klf3	0,65	519	799	
1445443_at	1445443_at	0,65	79	122	
1436371_at	Recql	0,65	73	112	
1444424_at	1444424_at	0,65	40	61	
1450181_at	Cux2	0,65	249	385	cortex
1426340_at	Slc1a3	0,65	256	396	
1452114_s_at	Igfbp5	0,64	414	643	

1452731_x_at	100041874	0,64	841	1308	
1446321_at	B230208B08Rik	0,64	99	154	
1436854_at	Trpc2	0,64	94	147	
1458023_at	Gpkow	0,64	58	91	cortex
1456533_at	Dpy19l1	0,64	769	1200	
1444510_at	1444510_at	0,64	73	114	
1429345_at	Tubgcp4	0,64	67	105	
1436578_at	Ermn	0,64	37	59	
1421970_a_at	Gria2	0,64	2067	3247	cortex
1448977_at	Tcfap2c	0,63	326	514	
1448944_at	Nrp1	0,63	846	1337	
1450930_at	Hpca	0,63	290	458	cortex
1456901_at	Adamts20	0,63	142	225	lens
1428301_at	100041874	0,63	2313	3678	
1419291_x_at	Gas5	0,62	4712	7550	
1458408_at	Samd8	0,62	103	165	
1455044_at	Tmem44	0,62	387	625	
1456397_at	Cdh4	0,62	1096	1770	
1454720_at	Apba3	0,62	59	95	
1421836_at	Mtap7	0,62	151	244	
1437677_at	ENSMUSG0000003031 6	0,62	101	164	
1420799_at	Ntsr1	0,61	142	232	
1421604_a_at	Klf3	0,61	185	303	
1444104_at	1444104_at	0,61	31	51	
1426526_s_at	Ovgp1	0,61	89	147	
1457318_at	A330008L17Rik	0,61	84	138	
1435770_at	Tmx4	0,61	69	113	
1456138_at	Lypd6	0,61	105	173	
1450047_at	Hs6st2	0,60	1038	1716	cortex, lens
1417133_at	Pmp22	0,60	144	238	cortex, lens
1435494_s_at	Dsp	0,60	62	103	lens
1454768_at	Kcnf1	0,60	42	70	
1438296_at	Gm14462	0,60	144	239	
1421999_at	Tshr	0,60	38	63	
1439200_x_at	1439200_x_at	0,60	1521	2543	
1441136_at	1441136_at	0,60	41	69	
1450512_at	Ntn4	0,60	49	82	lens
1416846_a_at	Pdzrn3	0,59	989	1666	
1426341_at	Slc1a3	0,59	149	254	
1454969_at	Lypd6	0,59	458	779	lens
1425833_a_at	Hpca	0,59	59	101	cortex
1420660_at	Lrrc6	0,59	42	72	
1442019_at	1442019_at	0,59	106	180	

1419034_at	Csnk2a1	0,58	722	1235	
1444500_at	Ahsa1	0,58	85	146	
1452031_at	Slc1a3	0,58	351	604	
1456495_s_at	Osbpl6	0,58	53	91	
1431056_a_at	Lpl	0,58	172	297	
1449422_at	Cdh4	0,58	758	1309	
1452386_at	Sall3	0,58	237	411	
1415904_at	Lpl	0,57	1694	2951	
1457843_at	Lypd6	0,57	97	169	lens
1422164_at	Pou3f4	0,57	115	201	
1436010_at	Lrrc16b	0,57	546	966	
1456903_at	Ptx3	0,56	30	53	
1455636_at	Lsamp	0,56	74	131	cortex
1431057_a_at	Prss23	0,56	32	57	cortex
1453596_at	Id2	0,56	67	120	pancreas, lens
1418984_at	Inadl	0,56	125	224	
1416448_at	Itpa	0,56	672	1205	
1452728_at	Kirrel3	0,56	141	254	
1422428_at	Acsbg1	0,55	119	215	
1449865_at	Sema3a	0,55	100	182	
1442300_at	Tshr	0,55	47	84	
1449848_at	Gna14	0,55	76	138	
1422573_at	Ampd3	0,54	36	66	cortex
1450990_at	Gpc3	0,54	80	147	
1417520_at	Nfe2l3	0,53	267	499	
1415824_at	Scd2	0,53	852	1602	pancreas
1448754_at	Rbp1	0,53	934	1766	lens
1420938_at	Hs6st2	0,53	50	95	cortex, lens
1435196_at	Ntrk2	0,53	91	173	lens
1418983_at	Inadl	0,52	87	166	
1453595_at	2900064B18Rik	0,52	48	93	
1440273_at	1440273_at	0,50	167	332	
1421937_at	Dapp1	0,50	91	182	
1458112_at	Adarb2	0,50	29	57	
1417312_at	Dkk3	0,50	51	103	
1433989_at	Slc6a11	0,50	53	107	
1444543_at	1444543_at	0,49	350	713	
1429621_at	Cand2	0,49	289	592	
1448842_at	Cdo1	0,48	502	1043	cortex
1456970_at	1456970_at	0,48	73	152	
1455056_at	Lmo7	0,47	179	377	
1453245_at	9130024F11Rik	0,47	140	298	
1418376_at	Fgf15	0,46	32	69	
1438842_at	Mtch2	0,46	77	167	cortex, lens

## Appendix

1426584_a_at	Sord	0,46	105	229	
1418310_a_at	Rlbp1	0,46	665	1447	cortex
1455271_at	Gm13889	0,45	513	1127	
1415964_at	Scd1	0,45	123	273	
1449859_at	Golt1b	0,44	337	757	cortex, lens
1439870_at	A330008L17Rik	0,44	28	65	
1457151_at	ENSMUSG0000008649 5	0,44	30	69	
1419033_at	2610018G03Rik	0,44	71	162	
1441648_at	C1qtnf4	0,44	120	276	
1455365_at	Cdh8	0,43	58	133	lens
1422052_at	Cdh8	0,43	106	244	lens
1423478_at	Prkcb	0,43	88	203	
1449444_a_at	LOC100048499	0,43	436	1007	
1422165_at	Pou3f4	0,43	81	191	
1460419_a_at	Prkcb	0,42	443	1046	
1453465_x_at	Gm14057	0,42	70	166	
1424186_at	Ccdc80	0,41	110	267	cortex
1438824_at	Slc20a1	0,41	67	161	
1426063_a_at	Gem	0,41	43	106	
1416342_at	Tnc	0,40	182	452	cortex
1447640_s_at	Pbx3	0,39	329	839	
1439794_at	Ntn4	0,39	191	495	lens
1431491_at	9430087N24Rik	0,37	132	355	
1460045_at	Cdh7	0,36	30	84	
1425443_at	Tcfap2d	0,33	30	90	
1436222_at	Gas5	0,32	269	834	
1424843_a_at	Gas5	0,32	314	975	
1424400_a_at	Aldh1l1	0,30	73	239	
1418666_at	Ptx3	0,27	265	993	
1450992_a_at	Meis1	0,24	50	209	
1441579_at	Dmrta1	0,22	49	220	
1432088_at	Veph1	0,19	23	124	
1449445_x_at	Mfap1a	0,12	216	1747	
1428114_at	Slc14a1	0,12	14	116	
1419370_a_at	Mfap1a	0,03	31	908	

**Table 5-3:** Probe sets differentially expressed between WT and Pax6<sup>Leca2</sup> cortices

Probe_set	Gene symbol or ID	Significant FDR<10% ratio>1.4 (0.71)x (94)	Av Pax6 Leca2	Av WT	Pax6 Chip Binding sites (Ales Cvekl unpublished data)
<b>Up-regulated probe sets (35)</b>					
1433919_at	Asb4	3,54	255	72	cortex
1423422_at	Asb4	3,19	158	50	cortex
1440049_at	1440049_at	2,77	55	20	
1438194_at	Slc1a2	2,66	827	312	cortex
1438571_at	Bub1	2,53	185	73	
1454112_a_at	Haus2	2,41	291	121	
1454772_at	Snrnp200	2,25	533	237	
1434278_at	Mtm1	2,24	1804	806	
1428077_at	LOC100047091	1,95	490	251	
1419271_at	Pax6	1,90	4536	2386	cortex
1438737_at	Zic3	1,90	414	218	lens
1439627_at	Zic1	1,87	1758	941	pancreas
1452526_a_at	Pax6	1,81	506	279	cortex
1439854_at	Hrk	1,80	382	212	cortex
1428990_at	2310047K21Rik	1,74	226	130	
1433707_at	Gabra4	1,74	239	137	
1444139_at	Ddit4l	1,73	210	122	
1433685_a_at	6430706D22Rik	1,71	1914	1118	
1449571_at	Trhr	1,68	162	96	
1456005_a_at	Bcl2l11	1,67	912	546	lens
1437086_at	Ascl1	1,63	680	417	
1419719_at	Gabrb1	1,61	195	121	
1456006_at	Bcl2l11	1,61	121	75	lens
1439332_at	Ddit4l	1,61	189	117	
1416232_at	Olig2	1,59	156	98	
1458076_at	1458076_at	1,57	106	68	
1435449_at	Bcl2l11	1,56	135	87	lens
1432509_at	5033430I15Rik	1,54	210	136	
1457260_at	5730409E04Rik	1,54	54	35	
1419123_a_at	Pdgfc	1,52	637	419	
1450857_a_at	Col1a2	1,51	112	74	
1447628_x_at	Mrps5	1,50	143	95	lens
1448194_a_at	H19	1,48	1115	754	
1430798_x_at	Mrpl15	1,46	377	258	pancreas
1434327_at	2610020H08Rik	1,40	62	44	

Down-regulated probe sets (59)					
1423478_at	Prkcb	0,71	152	213	
1421836_at	Mtap7	0,71	132	186	
1453372_at	Dnajc1	0,70	121	171	
1435292_at	Tbc1d4	0,70	167	238	
1422243_at	Fgf7	0,70	37	52	
1418172_at	Hebp1	0,70	123	177	lens
1435246_at	Paqr8	0,69	173	251	
1442312_at	Tbl1xr1	0,69	49	71	cortex, lens
1417986_at	Nrarp	0,68	532	779	
1423259_at	Id4	0,68	6594	9739	cortex
1428580_at	Blvra	0,67	275	408	
1420501_at	Dnajc1	0,67	217	322	
1417574_at	Cxcl12	0,67	58	87	
1417872_at	Fhl1	0,67	1617	2423	cortex
1429273_at	Bmper	0,67	286	429	
1433782_at	Cldn12	0,67	212	319	cortex, pancreas
1421365_at	Fst	0,66	97	147	cortex
1450928_at	LOC100045546	0,66	3797	5732	
1448507_at	Efhd1	0,66	35	53	
1425474_a_at	Vps39	0,65	132	202	
1456543_at	Prokr1	0,65	90	138	
1434025_at	1434025_at	0,65	73	113	
1451461_a_at	Aldoc	0,64	5210	8093	
1439661_at	Slc16a14	0,64	254	397	
1437774_at	ENSMUSG0000008543 8	0,63	312	493	
1420500_at	Dnajc1	0,63	253	403	
1452398_at	Plce1	0,62	417	670	
1430629_at	Slc16a14	0,62	170	276	
1455298_at	1455298_at	0,60	485	810	
1428958_at	Paqr8	0,60	435	728	
1418157_at	LOC100046044	0,60	1197	2006	
1420459_at	Ripply3	0,59	65	110	lens
1421999_at	Tshr	0,59	45	76	
1423260_at	Id4	0,58	1352	2312	cortex
1438428_at	Jph1	0,58	124	214	
1426501_a_at	Tifa	0,57	179	317	
1444468_at	Paqr8	0,56	203	365	
1460607_at	Igsf11	0,55	113	205	
1450990_at	Gpc3	0,53	69	130	
1437872_at	Napepld	0,53	109	204	
1424186_at	Ccdc80	0,51	127	252	cortex

1453465_x_at	Gm14057	0,50	70	141	
1421937_at	Dapp1	0,49	81	165	
1449581_at	Emid1	0,49	215	443	
1429308_at	Prdm16	0,47	67	143	
1437095_at	Tspan18	0,44	81	185	
1440707_at	Dmrt3	0,42	190	449	
1452114_s_at	Igfbp5	0,41	278	671	
1438405_at	Fgf7	0,41	25	61	
1455056_at	Lmo7	0,39	130	338	
1438551_at	Neurog1	0,38	202	539	
1448823_at	Cxcl12	0,37	227	610	
1436694_s_at	Neurod4	0,36	99	277	cortex
1420385_at	Gna14	0,36	20	56	
1418054_at	Neurod4	0,28	64	225	cortex
1449848_at	Gna14	0,26	39	146	
1428114_at	Slc14a1	0,25	12	46	
1434202_a_at	Fam107a	0,24	24	102	
1418310_a_at	Rlbp1	0,12	122	1059	cortex

**Table 5-4:** Overlap of significantly altered probe sets between Pax6<sup>Leca4</sup> and Pax6<sup>Leca2</sup> cortices

Probe_set	Gene symbol or ID	Ratio Pax6 Leca2 vs. WT (94)	Ratio Pax6 Leca4 vs. WT (416)	Ratio Pax6 Sey vs. WT (1898)	Pax6 Chip Binding sites (Ales Cvekl unpublished data)
<b>17 probe sets</b>					
1418310_a_at	Rlbp1	0,12	0,46	0,02	cortex
1428114_at	Slc14a1	0,25	0,12	0,21	
1449848_at	Gna14	0,26	0,55	0,38	
1438551_at	Neurog1	0,38	2,53	0,16	cortex
1455056_at	Lmo7	0,39	0,47	0,31	
1452114_s_at	Igfbp5	0,41	0,64	0,38	
1421937_at	Dapp1	0,49	0,50	0,41	
1453465_x_at	Gm14057	0,50	0,42		
1424186_at	Ccdc80	0,51	0,41	0,55	cortex
1450990_at	Gpc3	0,53	0,54		
1421999_at	Tshr	0,59	0,60		
1420500_at	Dnajc1	0,63	1,49		
1423478_at	Prkcb	0,71	0,43	0,62	
1421836_at	Mtap7	0,71	0,62		
1428990_at	2310047K21Rik	1,74	1,77		
1454772_at	Snrnp200	2,25	2,43		
1438571_at	Bub1	2,53	1,86	2,19	

**Table 5-5:** Overlap of significantly altered probe sets between Pax6<sup>Leca4</sup> and Pax6<sup>Sey</sup> cortices

Probe_set	Gene symbol or ID	Ratio Pax6 Leca2 vs. WT (94)	Ratio Pax6 Leca4 vs. WT (416)	Ratio Pax6 Sey vs. WT (1898)	Pax6 Chip Binding sites (Ales Cvekl unpublished data)
<b>137 probe sets</b>					
1418310_a_at	Rlbp1	0,12	0,46	0,02	cortex
1441579_at	Dmrta1		0,22	0,08	
1438551_at	Neurog1	0,38	2,53	0,16	cortex
1453245_at	9130024F11Rik		0,47	0,16	
1425443_at	Tcfap2d		0,33	0,17	
1431491_at	9430087N24Rik		0,37	0,20	
1428114_at	Slc14a1	0,25	0,12	0,21	
1449420_at	Pde1b		0,70	0,23	
1432088_at	Veph1		0,19	0,25	
1457843_at	Lypd6		0,57	0,27	lens
1449422_at	Cdh4		0,58	0,30	
1456397_at	Cdh4		0,62	0,30	
1455056_at	Lmo7	0,39	0,47	0,31	
1426340_at	Slc1a3		0,65	0,32	
1439870_at	A330008L17Rik		0,44	0,32	
1454969_at	Lypd6		0,59	0,33	
1452031_at	Slc1a3		0,58	0,33	
1422052_at	Cdh8		0,43	0,34	lens
1455365_at	Cdh8		0,43	0,34	lens
1448944_at	Nrp1		0,63	0,36	
1448943_at	Nrp1		0,67	0,36	
1449848_at	Gna14	0,26	0,55	0,38	
1456495_s_at	Osbpl6		0,58	0,38	
1452114_s_at	Igfbp5	0,41	0,64	0,38	
1426063_a_at	Gem		0,41	0,40	
1426341_at	Slc1a3		0,59	0,41	
1454720_at	Apba3		0,62	0,41	
1421937_at	Dapp1	0,49	0,50	0,41	
1417520_at	Nfe2l3		0,53	0,43	
1417133_at	Pmp22		0,60	0,44	cortex, lens
1449865_at	Sema3a		0,55	0,45	
1456138_at	Lypd6		0,61	0,45	lens
61418983_at	Inadl		0,52	0,47	
1448977_at	Tcfap2c		0,63	0,47	
1450047_at	Hs6st2		0,60	0,51	cortex, lens
1436010_at	Lrrc16b		0,57	0,53	
1418984_at	Inadl		0,56	0,53	

1460419_a_at	Prkcb		0,42	0,54	
1424186_at	Ccdc80	0,51	0,41	0,55	cortex
1420938_at	Hs6st2		0,53	0,57	cortex, lens
125574_at	Epha3		0,66	0,57	
1452728_at	Kirrel3		0,56	0,57	
1437650_at	C730026J16		0,70	0,57	
1455636_at	Lsamp		0,56	0,58	cortex
1416342_at	Tnc		0,40	0,58	cortex
1450181_at	Cux2		0,65	0,58	cortex
1428571_at	Col9a1		0,66	0,58	
1433989_at	Slc6a11		0,50	0,58	
1418666_at	Ptx3		0,27	0,59	
1451991_at	Epha7		0,69	0,59	
1456533_at	Dpy19l1		0,64	0,59	
1416934_at	Mtm1		0,68	0,60	
1442019_at	1442019_at		0,59	0,61	
1419033_at	2610018G03Rik		0,44	0,61	
1423478_at	Prkcb	0,71	0,43	0,62	
1450930_at	Hpca		0,63	0,62	cortex
1457318_at	A330008L17Rik		0,61	0,63	
1424400_a_at	Aldh1l1		0,30	0,65	
1417312_at	Dkk3		0,50	0,65	
1421604_a_at	Klf3		0,61	0,66	
1440273_at	1440273_at		0,50	0,66	
1446321_at	B230208B08Rik		0,64	0,69	
1420799_at	Ntsr1		0,61	0,69	
1429270_a_at	Syce2		1,55	1,41	
1420981_a_at	Lmo4		1,41	1,43	lens
1440564_at	Prokr2		2,50	1,45	
1429284_at	Mobkl2b		1,76	1,47	lens
1457651_x_at	Rem2		1,41	1,50	
1428662_a_at	Hopx		3,16	1,50	
1424596_s_at	Lmcd1		2,25	1,50	
1448713_at	Stat4		2,30	1,52	
1451776_s_at	Hopx		3,26	1,52	
1447992_s_at	Pcsk2		1,67	1,52	
1457012_at	Dbx1		6,76	1,53	
1426774_at	Parp12		1,58	1,53	
1431429_a_at	Arl4a		1,47	1,57	
1449167_at	Epb4.114a		1,43	1,57	lens
1419573_a_at	Lgals1		3,84	1,57	cortex, lens, pancreas
1455439_a_at	Lgals1		3,96	1,58	cortex, lens, pancreas
1435092_at	Arl4a		1,66	1,59	
1437695_at	Prokr2		2,11	1,59	
1427256_at	Vcan		1,66	1,67	
1442542_at	Eya4		5,03	1,67	lens

1417649_at	Cdkn1c		1,71	1,71	
1421694_a_at	Vcan		1,60	1,71	
1424659_at	Slit2		1,71	1,73	
1423516_a_at	Nid2		2,23	1,74	
1425669_at	Mobkl2b		1,41	1,84	lens
1442434_at	D8Ert82e		1,68	2,03	
1425526_a_at	Prrx1		1,59	2,05	
1455123_at	St18		1,71	2,14	
1451119_a_at	Fbln1		1,53	2,17	cortex
1438571_at	Bub1	2,53	1,86	2,19	
1436791_at	Wnt5a		1,93	2,31	lens
1425528_at	Prrx1		1,92	2,75	
1428891_at	Parm1		2,88	2,76	
1439774_at	Prrx1		2,08	2,82	
1424214_at	Parm1		2,57	2,83	
1421597_a_at	Msx3		1,64	3,26	
1424127_at	Eya2		2,30	3,28	
1416630_at	Id3		2,20	3,36	
1451191_at	Crabp2		2,23	3,40	cortex
1448326_a_at	Crabp1		6,19	5,69	
1419633_at	Uncx		2,82	7,74	
1429987_at	9930013L23Rik		1,55	0,45	
1452065_at	Vstm2a		1,73	0,51	
1452008_at	Ttc39b		1,57	0,51	
1437442_at	Pcdh7		1,43	0,52	cortex
1435595_at	1810011O10Rik		2,52	0,55	
1457587_at	Kcnq5		1,84	0,59	
1440192_at	Ttc39b		1,52	0,60	
1424694_at	2010011I20Rik		1,65	0,60	
1451450_at	2010011I20Rik		1,65	0,62	
1456060_at	Maf		1,51	0,62	
1429896_at	5830408B19Rik		1,79	0,63	
1453006_at	Fgfbp3		2,47	0,63	cortex
1424695_at	2010011I20Rik		1,76	0,64	
1451415_at	1810011O10Rik		2,65	0,69	
1435222_at	Foxp1		1,64	0,69	
1434070_at	Jag1		1,85	0,70	
1435297_at	Gjd2		1,53	0,71	
1456970_at	1456970_at		0,48	1,45	
1449374_at	Pipox		0,70	1,51	
1436854_at	Trpc2		0,64	1,54	
1426584_a_at	Sord		0,46	1,58	
1429653_at	Gse1		0,69	1,64	
1460045_at	Cdh7		0,36	1,67	
1440108_at	Foxp2		0,68	1,73	
1438232_at	Foxp2		0,66	1,82	

1438231_at	Foxp2	0,67	1,86
1455271_at	Gm13889	0,45	2,18
1436578_at	Ernm	0,64	2,22
1458112_at	Adarb2	0,50	2,72
1444510_at	1444510_at	0,64	3,28
1422164_at	Pou3f4	0,57	4,06
1422165_at	Pou3f4	0,43	4,08
1447640_s_at	Pbx3	0,39	5,03

**Table 5-6:** Overlap of significantly altered probe sets between Pax6<sup>Leca2</sup> and Pax6<sup>Sey</sup> cortices

Probe_set	Gene symbol or ID	Ratio Pax6 Leca2 vs. WT (94)	Ratio Pax6 Leca4 vs. WT (416)	Ratio Pax6 Sey Vs. WT (1898)	Pax6 Chip Binding sites (Ales Cvekl unpublished data)
<b>55 probe sets</b>					
1418310_a_at	Rlbp1	0,12	0,46	0,02	cortex
1428114_at	Slc14a1	0,25	0,12	0,21	
1449848_at	Gna14	0,26	0,55	0,38	
1418054_at	Neurod4	0,28		0,10	cortex
1436694_s_at	Neurod4	0,36		0,16	cortex
1448823_at	Cxcl12	0,37		0,18	
1438551_at	Neurog1	0,38	2,53	0,16	cortex
1455056_at	Lmo7	0,39	0,47	0,31	
1452114_s_at	Igfbp5	0,41	0,64	0,38	
1440707_at	Dmrt3	0,42		0,58	
1429308_at	Prdm16	0,47		0,70	
1421937_at	Dapp1	0,49	0,50	0,41	
1449581_at	Emid1	0,49		0,58	
1424186_at	Ccdc80	0,51	0,41	0,55	cortex
1437872_at	Napepld	0,53		0,48	
1460607_at	Igsf11	0,55		0,56	
1444468_at	Paqr8	0,56		0,40	
1426501_a_at	Tifa	0,57		0,59	
1438428_at	Jph1	0,58		0,18	
1420459_at	Ripply3	0,59		0,69	lens
1428958_at	Paqr8	0,60		0,39	
1455298_at	1455298_at	0,60		0,62	
1430629_at	Slc16a14	0,62		0,56	
1452398_at	Plce1	0,62		0,58	
1439661_at	Slc16a14	0,64		0,52	
1451461_a_at	Aldoc	0,64		0,32	
1434025_at	1434025_at	0,65		0,63	
1456543_at	Prokr1	0,65		0,35	

1450928_at	LOC100045546	0,66		0,70	
1433782_at	Cldn12	0,67		0,63	cortex, pancreas
1417872_at	Fhl1	0,67		0,60	cortex
1417574_at	Cxcl12	0,67		0,69	
1435246_at	Paqr8	0,69		0,46	
1423478_at	Prkcb	0,71	0,43	0,62	
1448194_a_at	H19	1,48		1,82	
1457260_at	5730409E04Rik	1,54		1,56	
1435449_at	Bcl2l11	1,56		1,95	lens
1458076_at	1458076_at	1,57		1,67	
1416232_at	Olig2	1,59		6,47	
1456006_at	Bcl2l11	1,61		1,79	lens
1419719_at	Gabrb1	1,61		1,90	
1437086_at	Ascl1	1,63		5,40	
1456005_a_at	Bcl2l11	1,67		1,88	lens
1433707_at	Gabra4	1,74		1,77	
1439854_at	Hrk	1,80		2,00	cortex
1452526_a_at	Pax6	1,81		1,52	cortex
1439627_at	Zic1	1,87		2,73	pancreas
1438737_at	Zic3	1,90		2,83	lens
1419271_at	Pax6	1,90		1,48	cortex
1428077_at	LOC100047091	1,95		2,15	
1438571_at	Bub1	2,53	1,86	2,19	
1438194_at	Slc1a2	2,66		1,61	cortex
1440049_at	1440049_at	2,77		3,77	
1423422_at	Asb4	3,19		7,94	cortex
1433919_at	Asb4	3,54		12,29	cortex

**Table 5-7:** Comparison significantly altered probe sets between Pax6<sup>Leca4</sup>, Pax6<sup>Leca2</sup> and Pax6<sup>Sey</sup> cortices and Pax6 CHIP data (Ales Cvekl unpublished data)

Probe_set	Gene symbol or ID	Ratio Pax6 Leca2 vs. WT	Ratio Pax6 Leca4 vs. WT	Ratio Pax6 Sey vs. WT	Pax6 Chip Binding sites (Ales Cevkl unpublished data)
<b>3 probe sets Pax6Leca4 / Pax6Leca2 / Pax6Sey / Pax6 CHIP signal</b>					
1438551_at	Neurog1	0,38	2,53	0,16	cortex
1424186_at	Ccdc80	0,51	0,41	0,55	cortex
1418310_a_at	Rlbp1	0,12	0,46	0,02	cortex

23 probe sets Pax6Leca4 / Pax6Sey / Pax6 CHIP signal					
1457843_at	Lypd6		0,57	0,27	lens
1422052_at	Cdh8		0,43	0,34	lens
1455365_at	Cdh8		0,43	0,34	lens
1417133_at	Pmp22		0,6	0,44	cortex, lens
1456138_at	Lypd6		0,61	0,45	lens
1450047_at	Hs6st2		0,6	0,51	cortex, lens
1420938_at	Hs6st2		0,53	0,57	cortex, lens
1455636_at	Lsamp		0,56	0,58	cortex
1416342_at	Tnc		0,4	0,58	cortex
1450181_at	Cux2		0,65	0,58	cortex
1450930_at	Hpca		0,63	0,62	cortex
1420981_a_at	Lmo4		1,41	1,43	lens
1429284_at	Mobkl2b		1,76	1,47	lens
1449167_at	Epb4.1l4a		1,43	1,57	lens
1419573_a_at	Lgals1		3,84	1,57	cortex, lens, pancreas
1455439_a_at	Lgals1		3,96	1,58	cortex, lens, pancreas
1442542_at	Eya4		5,03	1,67	lens
1425669_at	Mobkl2b		1,41	1,84	lens
1451119_a_at	Fbln1		1,53	2,17	cortex
1436791_at	Wnt5a		1,93	2,31	lens
1451191_at	Crabp2		2,23	3,4	cortex
1437442_at	Pcdh7		1,43	0,52	cortex
1453006_at	Fgfbp3		2,47	0,63	cortex
16 probe sets Pax6Leca4 / Pax6Sey / Pax6 CHIP signal					
1418054_at	Neurod4	0,28		0,1	cortex
1436694_s_at	Neurod4	0,36		0,16	cortex
1420459_at	Ripply3	0,59		0,69	lens
1433782_at	Cldn12	0,67		0,63	cortex, pancreas
1417872_at	Fhl1	0,67		0,6	cortex
1435449_at	Bcl2l11	1,56		1,95	lens
1456006_at	Bcl2l11	1,61		1,79	lens
1456005_a_at	Bcl2l11	1,67		1,88	lens
1439854_at	Hrk	1,8		2	cortex
1452526_a_at	Pax6	1,81		1,52	cortex
1439627_at	Zic1	1,87		2,73	pancreas
1438737_at	Zic3	1,9		2,83	lens
1419271_at	Pax6	1,9		1,48	cortex
1438194_at	Slc1a2	2,66		1,61	cortex
1423422_at	Asb4	3,19		7,94	cortex
1433919_at	Asb4	3,54		12,29	cortex

3 + 23 + 16 = **42** probe sets overlap

**42** / total overlap **182** probe sets (see Venn diagram Fig.2-25) = **23%**

3 probe sets (labeled in grey) regulated in different directions

**39** / **42** regulated in the same direction = **93%**

## 6 References

- Aaku-Saraste E, Hellwig A, Huttner WB (1996) Loss of occludin and functional tight junctions, but not ZO-1, during neural tube closure--remodeling of the neuroepithelium prior to neurogenesis. *Dev Biol* 180:664-679.
- Agoston Z, Schulte D (2009) Meis2 competes with the Groucho co-repressor Tle4 for binding to Otx2 and specifies tectal fate without induction of a secondary midbrain-hindbrain boundary organizer. *Development* 136:3311-3322.
- Anchan RM, Drake DP, Haines CF, Gerwe EA, LaMantia AS (1997) Disruption of local retinoid-mediated gene expression accompanies abnormal development in the mammalian olfactory pathway. *J Comp Neurol* 379:171-184.
- Anderson TR, Hedlund E, Carpenter EM (2002) Differential Pax6 promoter activity and transcript expression during forebrain development. *Mech Dev* 114:171-175.
- Andrews GL, Mastick GS (2003) R-cadherin is a Pax6-regulated, growth-promoting cue for pioneer axons. *J Neurosci* 23:9873-9880.
- Arnold SJ, Huang G-J, Cheung AFP, Era T, Nishikawa S-I, Bikoff EK, Molnar Z, Robertson EJ, Groszer M (2008) The T-box transcription factor Eomes/Tbr2 regulates neurogenesis in the cortical subventricular zone. *Genes Dev* 22:2479-2484.
- Asami M, Pilz GA, Ninkovic J, Godinho L, Schroeder T, Huttner WB, Gotz M (2011) The role of Pax6 in regulating the orientation and mode of cell division of progenitors in the mouse cerebral cortex. *Development* 138:5067-5078.
- Ashery-Padan R, Gruss P (2001) Pax6 lights-up the way for eye development. *Curr Opin Cell Biol* 13:706-714.
- Ashery-Padan R, Marquardt T, Zhou X, Gruss P (2000) Pax6 activity in the lens primordium is required for lens formation and for correct placement of a single retina in the eye. *Genes Dev* 14:2701-2711.
- Astrom KE, Webster HD (1991) The early development of the neopallial wall and area choroidea in fetal rats. A light and electron microscopic study. *Advances in anatomy, embryology, and cell biology* 123:1-76.
- Azuma N, Nishina S, Yanagisawa H, Okuyama T, Yamada M (1996) PAX6 missense mutation in isolated foveal hypoplasia. *Nat Genet* 13:141-142.
- Bain G, Ray WJ, Yao M, Gottlieb DI (1996) Retinoic acid promotes neural and represses mesodermal gene expression in mouse embryonic stem cells in culture. *Biochem Biophys Res Commun* 223:691-694.
- Bain G, Kitchens D, Yao M, Huettnner JE, Gottlieb DI (1995) Embryonic stem cells express neuronal properties in vitro. *Dev Biol* 168:342-357.
- Bartel DP (2004) MicroRNAs: genomics, biogenesis, mechanism, and function. *Cell* 116:281-297.
- Bartel DP (2009) MicroRNAs: target recognition and regulatory functions. *Cell* 136:215-233.
- Benetti R, Gonzalo S, Jaco I, Munoz P, Gonzalez S, Schoeftner S, Murchison E, Andl T, Chen T, Klatt P, Li E, Serrano M, Millar S, Hannon G, Blasco MA (2008) A mammalian microRNA cluster controls DNA methylation and telomere recombination via Rbl2-dependent regulation of DNA methyltransferases. *Nat Struct Mol Biol* 15:268-279.
- Bernstein E, Caudy AA, Hammond SM, Hannon GJ (2001) Role for a bidentate ribonuclease in the initiation step of RNA interference. *Nature* 409:363-366.

- Bernstein E, Kim SY, Carmell MA, Murchison EP, Alcorn H, Li MZ, Mills AA, Elledge SJ, Anderson KV, Hannon GJ (2003) Dicer is essential for mouse development. *Nat Genet* 35:215-217.
- Bhide PG (1996) Cell cycle kinetics in the embryonic mouse corpus striatum. *J Comp Neurol* 374:506-522.
- Bibel M, Richter J, Lacroix E, Barde YA (2007) Generation of a defined and uniform population of CNS progenitors and neurons from mouse embryonic stem cells. *Nat Protoc* 2:1034-1043.
- Bibel M, Richter J, Schrenk K, Tucker KL, Staiger V, Korte M, Goetz M, Barde YA (2004) Differentiation of mouse embryonic stem cells into a defined neuronal lineage. *Nat Neurosci* 7:1003-1009.
- Bishop KM, Goudreau G, O'Leary DD (2000) Regulation of area identity in the mammalian neocortex by *Emx2* and *Pax6*. *Science* 288:344-349.
- Bishop KM, Rubenstein JL, O'Leary DD (2002) Distinct actions of *Emx1*, *Emx2*, and *Pax6* in regulating the specification of areas in the developing neocortex. *J Neurosci* 22:7627-7638.
- Boppana S, Scheglov A, Geffers R, Tarabykin V (2012) Cellular retinaldehyde-binding protein (CRALBP) is a direct downstream target of transcription factor *Pax6*. *Biochim Biophys Acta* 1820:151-156.
- Borchert GM, Lanier W, Davidson BL (2006) RNA polymerase III transcribes human microRNAs. *Nat Struct Mol Biol* 13:1097-1101.
- Bouchard M (2003) [Pax genes and cell specification]. *Medecine sciences : M/S* 19:535-537.
- Brantjes H, Barker N, van Es J, Clevers H (2002) TCF: Lady Justice casting the final verdict on the outcome of Wnt signalling. *Biological chemistry* 383:255-261.
- Brill E, Gobble R, Angeles C, Lagos-Quintana M, Crago A, Laxa B, Decarolis P, Zhang L, Antonescu C, Socci ND, Taylor BS, Sander C, Koff A, Singer S (2010) *ZIC1* overexpression is oncogenic in liposarcoma. *Cancer research* 70:6891-6901.
- Brill MS, Snappyan M, Wohlfrom H, Ninkovic J, Jawerka M, Mastick GS, Ashery-Padan R, Saghatelian A, Berninger B, Gotz M (2008) A *dlx2*- and *pax6*-dependent transcriptional code for periglomerular neuron specification in the adult olfactory bulb. *J Neurosci* 28:6439-6452.
- Brill MS, Ninkovic J, Winpenny E, Hodge RD, Ozen I, Yang R, Lepier A, Gascon S, Erdelyi F, Szabo G, Parras C, Guillemot F, Frotscher M, Berninger B, Hevner RF, Raineteau O, Gotz M (2009) Adult generation of glutamatergic olfactory bulb interneurons. *Nat Neurosci* 12(12):1524-1533.
- Britz O, Mattar P, Nguyen L, Langevin LM, Zimmer C, Alam S, Guillemot F, Schuurmans C (2006) A role for proneural genes in the maturation of cortical progenitor cells. *Cereb Cortex* 16 Suppl 1:i138-151.
- Bulfone A, Martinez S, Marigo V, Campanella M, Basile A, Quaderi N, Gattuso C, Rubenstein JL, Ballabio A (1999) Expression pattern of the *Tbr2* (*Eomesodermin*) gene during mouse and chick brain development. *Mech Dev* 84:133-138.
- Cai L, Morrow EM, Cepko CL (2000) Misexpression of basic helix-loop-helix genes in the murine cerebral cortex affects cell fate choices and neuronal survival. *Development* 127:3021-3030.
- Campbell K (2003) Dorsal-ventral patterning in the mammalian telencephalon. *Curr Opin Neurobiol* 13:50-56.

- Caric D, Gooday D, Hill RE, McConnell SK, Price DJ (1997) Determination of the migratory capacity of embryonic cortical cells lacking the transcription factor Pax-6. *Development* 124:5087-5096.
- Carriere C, Plaza S, Martin P, Quatannens B, Bailly M, Stehelin D, Saule S (1993) Characterization of quail Pax-6 (Pax-QNR) proteins expressed in the neuroretina. *Mol Cell Biol* 13:7257-7266.
- Casanova MF, Trippe J, 2nd (2006) Regulatory mechanisms of cortical laminar development. *Brain Res Rev* 51:72-84.
- Chalepakis G, Tremblay P, Gruss P (1992) Pax genes, mutants and molecular function. *Journal of cell science Supplement* 16:61-67.
- Chambon P (1996) A decade of molecular biology of retinoic acid receptors. *FASEB J* 10:940-954.
- Chapouton P, Gartner A, Gotz M (1999) The role of Pax6 in restricting cell migration between developing cortex and basal ganglia. *Development* 126:5569-5579.
- Chauhan BK, Yang Y, Cveklova K, Cvekl A (2004) Functional properties of natural human PAX6 and PAX6(5a) mutants. *Invest Ophthalmol Vis Sci* 45:385-392.
- Chen C, Ridzon D, Lee CT, Blake J, Sun Y, Strauss WM (2007) Defining embryonic stem cell identity using differentiation-related microRNAs and their potential targets. *Mammalian genome : official journal of the International Mammalian Genome Society* 18:316-327.
- Cheng TS, Hsiao YL, Lin CC, Hsu CM, Chang MS, Lee CI, Yu RC, Huang CY, Howng SL, Hong YR (2007) hNinein is required for targeting spindle-associated protein Astrin to the centrosome during the S and G2 phases. *Exp Cell Res* 313:1710-1721.
- Chenn A (2008) Wnt/beta-catenin signaling in cerebral cortical development. *Organogenesis* 4:76-80.
- Chenn A, Walsh CA (2002) Regulation of cerebral cortical size by control of cell cycle exit in neural precursors. *Science* 297:365-369.
- Cocas LA, Georgala PA, Mangin JM, Clegg JM, Kessarar N, Haydar TF, Gallo V, Price DJ, Corbin JG (2011) Pax6 is required at the telencephalic pallial-subpallial boundary for the generation of neuronal diversity in the postnatal limbic system. *J Neurosci* 31:5313-5324.
- Conti L, Pollard SM, Gorba T, Reitano E, Toselli M, Biella G, Sun Y, Sanzone S, Ying QL, Cattaneo E, Smith A (2005) Niche-independent symmetrical self-renewal of a mammalian tissue stem cell. *PLoS Biol* 3:e283.
- Corbin JG, Rutlin M, Gaiano N, Fishell G (2003) Combinatorial function of the homeodomain proteins Nkx2.1 and Gsh2 in ventral telencephalic patterning. *Development* 130:4895-4906.
- Coutinho P, Pavlou S, Bhatia S, Chalmers KJ, Kleinjan DA, van Heyningen V (2011) Discovery and assessment of conserved Pax6 target genes and enhancers. *Genome Res* 21:1349-1359.
- Cubelos B, Sebastian-Serrano A, Kim S, Moreno-Ortiz C, Redondo JM, Walsh CA, Nieto M (2008) Cux-2 controls the proliferation of neuronal intermediate precursors of the cortical subventricular zone. *Cereb Cortex* 18:1758-1770.
- Cubelos B, Sebastian-Serrano A, Beccari L, Calcagnotto ME, Cisneros E, Kim S, Dopazo A, Alvarez-Dolado M, Redondo JM, Bovolenta P, Walsh CA, Nieto M (2010) Cux1 and Cux2 regulate dendritic branching, spine morphology, and synapses of the upper layer neurons of the cortex. *Neuron* 66:523-535.

- Czerny T, Busslinger M (1995) DNA-binding and transactivation properties of Pax-6: three amino acids in the paired domain are responsible for the different sequence recognition of Pax-6 and BSAP (Pax-5). *Mol Cell Biol* 15:2858-2871.
- Czerny T, Schaffner G, Busslinger M (1993) DNA sequence recognition by Pax proteins: bipartite structure of the paired domain and its binding site. *Genes Dev* 7:2048-2061.
- D'Arcangelo G, Miao GG, Chen SC, Soares HD, Morgan JI, Curran T (1995) A protein related to extracellular matrix proteins deleted in the mouse mutant reeler. *Nature* 374:719-723.
- D'Arcangelo G, Nakajima K, Miyata T, Ogawa M, Mikoshiba K, Curran T (1997) Reelin is a secreted glycoprotein recognized by the CR-50 monoclonal antibody. *J Neurosci* 17:23-31.
- D'Sa-Eipper C, Roth KA (2000) Caspase regulation of neuronal progenitor cell apoptosis. *Dev Neurosci* 22:116-124.
- Dames P, Puff R, Weise M, Parhofer KG, Goke B, Gotz M, Graw J, Favor J, Lechner A (2010) Relative roles of the different Pax6 domains for pancreatic alpha cell development. *BMC developmental biology* 10:39.
- Damiani D, Alexander JJ, O'Rourke JR, McManus M, Jadhav AP, Cepko CL, Hauswirth WW, Harfe BD, Strettoi E (2008) Dicer inactivation leads to progressive functional and structural degeneration of the mouse retina. *J Neurosci* 28:4878-4887.
- Davis JA, Reed RR (1996) Role of Olf-1 and Pax-6 transcription factors in neurodevelopment. *J Neurosci* 16:5082-5094.
- De Carlos JA, Lopez-Mascaraque L, Valverde F (1995) The telencephalic vesicles are innervated by olfactory placode-derived cells: a possible mechanism to induce neocortical development. *Neuroscience* 68:1167-1178.
- de Faria O, Jr., Cui QL, Bin JM, Bull SJ, Kennedy TE, Bar-Or A, Antel JP, Colman DR, Dhaunchak AS (2012) Regulation of miRNA 219 and miRNA Clusters 338 and 17-92 in Oligodendrocytes. *Frontiers in genetics* 3:46.
- De Pietri Tonelli D, Pulvers JN, Haffner C, Murchison EP, Hannon GJ, Huttner WB (2008) miRNAs are essential for survival and differentiation of newborn neurons but not for expansion of neural progenitors during early neurogenesis in the mouse embryonic neocortex. *Development* 135:3911-3921.
- Dellovade TL, Pfaff DW, Schwanzel-Fukuda M (1998) Olfactory bulb development is altered in small-eye (Sey) mice. *J Comp Neurol* 402:402-418.
- Desai AR, McConnell SK (2000) Progressive restriction in fate potential by neural progenitors during cerebral cortical development. *Development* 127:2863-2872.
- Di Lullo E, Haton C, Le Poupon C, Volovitch M, Joliot A, Thomas JL, Prochiantz A (2011) Paracrine Pax6 activity regulates oligodendrocyte precursor cell migration in the chick embryonic neural tube. *Development* 138:4991-5001.
- Du T, Zamore PD (2005) microPrimer: the biogenesis and function of microRNA. *Development* 132:4645-4652.
- Dugas JC, Cuellar TL, Scholze A, Ason B, Ibrahim A, Emery B, Zamanian JL, Foo LC, McManus MT, Barres BA (2010) Dicer1 and miR-219 Are required for normal oligodendrocyte differentiation and myelination. *Neuron* 65:597-611.
- Elvenes J, Thomassen EI, Johnsen SS, Kaino K, Sjøttem E, Johansen T (2011) Pax6 represses androgen receptor-mediated transactivation by inhibiting recruitment of the coactivator SPBP. *PLoS One* 6:e24659.

## References

---

- Endo M, Doi R, Nishita M, Minami Y (2012) Ror-family receptor tyrosine kinases regulate maintenance of neural progenitor cells in the developing neocortex. *J Cell Sci*.
- Engelkamp D, Rashbass P, Seawright A, van Heyningen V (1999) Role of Pax6 in development of the cerebellar system. *Development* 126:3585-3596.
- Englund C, Fink A, Lau C, Pham D, Daza RA, Bulfone A, Kowalczyk T, Hevner RF (2005) Pax6, Tbr2, and Tbr1 are expressed sequentially by radial glia, intermediate progenitor cells, and postmitotic neurons in developing neocortex. *J Neurosci* 25:247-251.
- Epstein J, Cai J, Glaser T, Jepeal L, Maas R (1994a) Identification of a Pax paired domain recognition sequence and evidence for DNA-dependent conformational changes. *J Biol Chem* 269:8355-8361.
- Epstein JA, Glaser T, Cai J, Jepeal L, Walton DS, Maas RL (1994b) Two independent and interactive DNA-binding subdomains of the Pax6 paired domain are regulated by alternative splicing. *Genes Dev* 8:2022-2034.
- Estivill-Torrus G, Pearson H, van Heyningen V, Price DJ, Rashbass P (2002) Pax6 is required to regulate the cell cycle and the rate of progression from symmetrical to asymmetrical division in mammalian cortical progenitors. *Development* 129:455-466.
- Farh KK, Grimson A, Jan C, Lewis BP, Johnston WK, Lim LP, Burge CB, Bartel DP (2005) The widespread impact of mammalian MicroRNAs on mRNA repression and evolution. *Science* 310:1817-1821.
- Favor J, Peters H, Hermann T, Schmahl W, Chatterjee B, Neuhauser-Klaus A, Sandulache R (2001) Molecular characterization of Pax6(2Neu) through Pax6(10Neu): an extension of the Pax6 allelic series and the identification of two possible hypomorph alleles in the mouse *Mus musculus*. *Genetics* 159:1689-1700.
- Favor J, Gloeckner CJ, Neuhauser-Klaus A, Pretsch W, Sandulache R, Saule S, Zaus I (2008) Relationship of Pax6 activity levels to the extent of eye development in the mouse, *Mus musculus*. *Genetics* 179:1345-1355.
- Fietz SA, Huttner WB (2011) Cortical progenitor expansion, self-renewal and neurogenesis—a polarized perspective. *Curr Opin Neurobiol* 21:23-35.
- Fineberg SK, Kosik KS, Davidson BL (2009) MicroRNAs potentiate neural development. *Neuron* 64:303-309.
- Fish JE, Santoro MM, Morton SU, Yu S, Yeh RF, Wythe JD, Ivey KN, Bruneau BG, Stainier DY, Srivastava D (2008) miR-126 regulates angiogenic signaling and vascular integrity. *Dev Cell* 15:272-284.
- Fish JL, Kosodo Y, Enard W, Paabo S, Huttner WB (2006) *Aspm* specifically maintains symmetric proliferative divisions of neuroepithelial cells. *Proc Natl Acad Sci U S A* 103:10438-10443.
- Fode C, Ma Q, Casarosa S, Ang SL, Anderson DJ, Guillemot F (2000) A role for neural determination genes in specifying the dorsoventral identity of telencephalic neurons. *Genes Dev* 14:67-80.
- Fong AP, Yao Z, Zhong JW, Cao Y, Ruzzo WL, Gentleman RC, Tapscott SJ (2012) Genetic and epigenetic determinants of neurogenesis and myogenesis. *Dev Cell* 22:721-735.
- Frantz GD, McConnell SK (1996) Restriction of late cerebral cortical progenitors to an upper-layer fate. *Neuron* 17:55-61.
- Fukuda T, Kawano H, Osumi N, Eto K, Kawamura K (2000) Histogenesis of the cerebral cortex in rat fetuses with a mutation in the Pax-6 gene. *Brain Res Dev Brain Res* 120:65-75.

- Funatsu N, Inoue T, Nakamura S (2004) Gene expression analysis of the late embryonic mouse cerebral cortex using DNA microarray: identification of several region- and layer-specific genes. *Cereb Cortex* 14:1031-1044.
- Gal JS, Morozov YM, Ayoub AE, Chatterjee M, Rakic P, Haydar TF (2006) Molecular and morphological heterogeneity of neural precursors in the mouse neocortical proliferative zones. *J Neurosci* 26:1045-1056.
- Garcia-Moreno F, Lopez-Mascaraque L, De Carlos JA (2007) Origins and migratory routes of murine Cajal-Retzius cells. *J Comp Neurol* 500:419-432.
- Gaspard N, Bouschet T, Hourez R, Dimidschstein J, Naeije G, van den Aemele J, Espuny-Camacho I, Herpoel A, Passante L, Schiffmann SN, Gaillard A, Vanderhaeghen P (2008) An intrinsic mechanism of corticogenesis from embryonic stem cells. *Nature* 455:351-357.
- Georgala PA, Manuel M, Price DJ (2011a) The generation of superficial cortical layers is regulated by levels of the transcription factor Pax6. *Cereb Cortex* 21:81-94.
- Georgala PA, Carr CB, Price DJ (2011b) The role of Pax6 in forebrain development. *Dev Neurobiol* 71:690-709.
- Ghosh AP, Cape JD, Klocke BJ, Roth KA (2011) Deficiency of pro-apoptotic Hrk attenuates programmed cell death in the developing murine nervous system but does not affect Bcl-x deficiency-induced neuron apoptosis. *The journal of histochemistry and cytochemistry : official journal of the Histochemistry Society* 59:976-983.
- Giardino L, Bettelli C, Calza L (2000) In vivo regulation of precursor cells in the subventricular zone of adult rat brain by thyroid hormone and retinoids. *Neurosci Lett* 295:17-20.
- Giraldez AJ, Cinalli RM, Glasner ME, Enright AJ, Thomson JM, Baskerville S, Hammond SM, Bartel DP, Schier AF (2005) MicroRNAs regulate brain morphogenesis in zebrafish. *Science* 308:833-838.
- Glaser T, Walton DS, Maas RL (1992) Genomic structure, evolutionary conservation and aniridia mutations in the human PAX6 gene. *Nat Genet* 2:232-239.
- Gorski JA, Talley T, Qiu M, Puelles L, Rubenstein JL, Jones KR (2002) Cortical excitatory neurons and glia, but not GABAergic neurons, are produced in the Emx1-expressing lineage. *J Neurosci* 22:6309-6314.
- Gotz M, Sommer L (2005) Cortical development: the art of generating cell diversity. *Development* 132:3327-3332.
- Gotz M, Huttner WB (2005) The cell biology of neurogenesis. *Nat Rev Mol Cell Biol* 6:777-788.
- Gotz M, Stoykova A, Gruss P (1998) Pax6 controls radial glia differentiation in the cerebral cortex. *Neuron* 21:1031-1044.
- Graw J (2010) Eye development. *Current topics in developmental biology* 90:343-386.
- Graw J, Loster J, Puk O, Munster D, Haubst N, Soewarto D, Fuchs H, Meyer B, Nurnberg P, Pretsch W, Selby P, Favor J, Wolf E, Hrabe de Angelis M (2005) Three novel Pax6 alleles in the mouse leading to the same small-eye phenotype caused by different consequences at target promoters. *Invest Ophthalmol Vis Sci* 46:4671-4683.
- Gregory RI, Yan KP, Amuthan G, Chendrimada T, Doratotaj B, Cooch N, Shiekhattar R (2004) The Microprocessor complex mediates the genesis of microRNAs. *Nature* 432:235-240.
- Grishok A, Pasquinelli AE, Conte D, Li N, Parrish S, Ha I, Baillie DL, Fire A, Ruvkun G, Mello CC (2001) Genes and mechanisms related to RNA interference regulate expression of the small temporal RNAs that control *C. elegans* developmental timing. *Cell* 106:23-34.

## References

---

- Grove EA, Tole S, Limon J, Yip L, Ragsdale CW (1998) The hem of the embryonic cerebral cortex is defined by the expression of multiple Wnt genes and is compromised in Gli3-deficient mice. *Development* 125:2315-2325.
- Guan K, Chang H, Rolletschek A, Wobus AM (2001) Embryonic stem cell-derived neurogenesis. Retinoic acid induction and lineage selection of neuronal cells. *Cell Tissue Res* 305:171-176.
- Guillemot F (2005) Cellular and molecular control of neurogenesis in the mammalian telencephalon. *Curr Opin Cell Biol* 17:639-647.
- Guillemot F, Molnar Z, Tarabykin V, Stoykova A (2006) Molecular mechanisms of cortical differentiation. *Eur J Neurosci* 23:857-868.
- Habas R, Dawid IB, He X (2003) Coactivation of Rac and Rho by Wnt/Frizzled signaling is required for vertebrate gastrulation. *Genes Dev* 17:295-309.
- Hack MA, Sugimori M, Lundberg C, Nakafuku M, Götz M (2004a) Regionalization and fate specification in neurospheres: the role of Olig2 and Pax6. *Molecular and Cellular Neuroscience* 25:664-678.
- Hack MA, Sugimori M, Lundberg C, Nakafuku M, Gotz M (2004b) Regionalization and fate specification in neurospheres: the role of Olig2 and Pax6. *Mol Cell Neurosci* 25:664-678.
- Hack MA, Saghatelian A, de Chevigny A, Pfeifer A, Ashery-Padan R, Lledo PM, Gotz M (2005) Neuronal fate determinants of adult olfactory bulb neurogenesis. *Nat Neurosci* 8:865-872.
- Hammond SM, Bernstein E, Beach D, Hannon GJ (2000) An RNA-directed nuclease mediates post-transcriptional gene silencing in *Drosophila* cells. *Nature* 404:293-296.
- Harrison SJ, Parrish M, Monaghan AP (2008) Sall3 is required for the terminal maturation of olfactory glomerular interneurons. *J Comp Neurol* 507:1780-1794.
- Hartfuss E, Galli R, Heins N, Gotz M (2001) Characterization of CNS precursor subtypes and radial glia. *Dev Biol* 229:15-30.
- Haskell GT, LaMantia AS (2005) Retinoic acid signaling identifies a distinct precursor population in the developing and adult forebrain. *J Neurosci* 25:7636-7647.
- Haubensak W, Attardo A, Denk W, Huttner WB (2004) Neurons arise in the basal neuroepithelium of the early mammalian telencephalon: a major site of neurogenesis. *Proc Natl Acad Sci U S A* 101:3196-3201.
- Haubst N, Berger J, Radjendirane V, Graw J, Favor J, Saunders GF, Stoykova A, Gotz M (2004) Molecular dissection of Pax6 function: the specific roles of the paired domain and homeodomain in brain development. *Development* 131:6131-6140.
- He S, Purity MK, Wang WL, Wolf L, Chauhan BK, Cveklova K, Tamm ER, Ashery-Padan R, Metzger D, Nakai A, Chambon P, Zavadil J, Cvekl A (2010) Chromatin remodeling enzyme Brg1 is required for mouse lens fiber cell terminal differentiation and its denucleation. *Epigenetics & chromatin* 3:21.
- Hebert JM, Fishell G (2008) The genetics of early telencephalon patterning: some assembly required. *Nat Rev Neurosci* 9:678-685.
- Hebert SS, De Strooper B (2007) Molecular biology. miRNAs in neurodegeneration. *Science* 317:1179-1180.

- Heine P, Dohle E, Bumsted-O'Brien K, Engelkamp D, Schulte D (2008) Evidence for an evolutionary conserved role of homothorax/Meis1/2 during vertebrate retina development. *Development* 135:805-811.
- Heins N, Malatesta P, Cecconi F, Nakafuku M, Tucker KL, Hack MA, Chapouton P, Barde YA, Gotz M (2002) Glial cells generate neurons: the role of the transcription factor Pax6. *Nat Neurosci* 5:308-315.
- Hendzel MJ, Wei Y, Mancini MA, Van Hooser A, Ranalli T, Brinkley BR, Bazett-Jones DP, Allis CD (1997) Mitosis-specific phosphorylation of histone H3 initiates primarily within pericentromeric heterochromatin during G2 and spreads in an ordered fashion coincident with mitotic chromosome condensation. *Chromosoma* 106:348-360.
- Heng X, Breer H, Zhang X, Tang Y, Li J, Zhang S, Le W (2012) Sall3 Correlates with the Expression of TH in Mouse Olfactory Bulb. *Journal of molecular neuroscience : MN* 46:293-302.
- Hill RE, Favor J, Hogan BL, Ton CC, Saunders GF, Hanson IM, Prosser J, Jordan T, Hastie ND, van Heyningen V (1991) Mouse small eye results from mutations in a paired-like homeobox-containing gene. *Nature* 354:522-525.
- Hirabayashi Y, Itoh Y, Tabata H, Nakajima K, Akiyama T, Masuyama N, Gotoh Y (2004) The Wnt/beta-catenin pathway directs neuronal differentiation of cortical neural precursor cells. *Development* 131:2791-2801.
- Hirata T, Nomura T, Takagi Y, Sato Y, Tomioka N, Fujisawa H, Osumi N (2002) Mosaic development of the olfactory cortex with Pax6-dependent and -independent components. *Brain Res Dev Brain Res* 136:17-26.
- Hogan BL, Horsburgh G, Cohen J, Hetherington CM, Fisher G, Lyon MF (1986) Small eyes (Sey): a homozygous lethal mutation on chromosome 2 which affects the differentiation of both lens and nasal placodes in the mouse. *Journal of embryology and experimental morphology* 97:95-110.
- Holm PC, Mader MT, Haubst N, Wizenmann A, Sigvardsson M, Gotz M (2007) Loss- and gain-of-function analyses reveal targets of Pax6 in the developing mouse telencephalon. *Mol Cell Neurosci* 34:99-119.
- Houbaviy HB, Murray MF, Sharp PA (2003) Embryonic stem cell-specific MicroRNAs. *Dev Cell* 5:351-358.
- Huang B, Li W, Zhao B, Xia C, Liang R, Ruan K, Jing N, Jin Y (2009) MicroRNA expression profiling during neural differentiation of mouse embryonic carcinoma P19 cells. *Acta biochimica et biophysica Sinica* 41:231-236.
- Huang X, Hong CS, O'Donnell M, Saint-Jeannet JP (2005) The doublesex-related gene, XDmr4, is required for neurogenesis in the olfactory system. *Proc Natl Acad Sci U S A* 102:11349-11354.
- Huelsken J, Birchmeier W (2001) New aspects of Wnt signaling pathways in higher vertebrates. *Current opinion in genetics & development* 11:547-553.
- Huttner WB, Kosodo Y (2005) Symmetric versus asymmetric cell division during neurogenesis in the developing vertebrate central nervous system. *Curr Opin Cell Biol* 17:648-657.
- Hutvagner G, McLachlan J, Pasquinelli AE, Balint E, Tuschl T, Zamore PD (2001) A cellular function for the RNA-interference enzyme Dicer in the maturation of the let-7 small temporal RNA. *Science* 293:834-838.
- Inoue T, Nakamura S, Osumi N (2000) Fate mapping of the mouse prosencephalic neural plate. *Dev Biol* 219:373-383.

## References

---

- Inoue T, Ota M, Ogawa M, Mikoshiba K, Aruga J (2007) Zic1 and Zic3 regulate medial forebrain development through expansion of neuronal progenitors. *J Neurosci* 27:5461-5473.
- Iorio MV, Ferracin M, Liu CG, Veronese A, Spizzo R, Sabbioni S, Magri E, Pedriali M, Fabbri M, Campiglio M, Menard S, Palazzo JP, Rosenberg A, Musiani P, Volinia S, Nenci I, Calin GA, Querzoli P, Negrini M, Croce CM (2005) MicroRNA gene expression deregulation in human breast cancer. *Cancer research* 65:7065-7070.
- Israsena N, Hu M, Fu W, Kan L, Kessler JA (2004) The presence of FGF2 signaling determines whether beta-catenin exerts effects on proliferation or neuronal differentiation of neural stem cells. *Dev Biol* 268:220-231.
- Jacobson M (1991) *Developmental Biology*. New York: Plenum.
- Javaherian A, Kriegstein A (2009) A stem cell niche for intermediate progenitor cells of the embryonic cortex. *Cereb Cortex* 19 Suppl 1:i70-77.
- Jimenez D, Garcia C, de Castro F, Chedotal A, Sotelo C, de Carlos JA, Valverde F, Lopez-Mascaraque L (2000) Evidence for intrinsic development of olfactory structures in Pax-6 mutant mice. *J Comp Neurol* 428:511-526.
- Johansson PA, Cappello S, Gotz M (2010) Stem cells niches during development--lessons from the cerebral cortex. *Curr Opin Neurobiol* 20:400-407.
- Jun S, Desplan C (1996) Cooperative interactions between paired domain and homeodomain. *Development* 122:2639-2650.
- Jung S, Park RH, Kim S, Jeon YJ, Ham DS, Jung MY, Kim SS, Lee YD, Park CH, Suh-Kim H (2010) Id proteins facilitate self-renewal and proliferation of neural stem cells. *Stem Cells Dev* 19:831-841.
- Kamachi Y, Uchikawa M, Tanouchi A, Sekido R, Kondoh H (2001) Pax6 and SOX2 form a co-DNA-binding partner complex that regulates initiation of lens development. *Genes Dev* 15:1272-1286.
- Kanellopoulou C, Muljo SA, Kung AL, Ganesan S, Drapkin R, Jenuwein T, Livingston DM, Rajewsky K (2005) Dicer-deficient mouse embryonic stem cells are defective in differentiation and centromeric silencing. *Genes Dev* 19:489-501.
- Kapsimali M, Kloosterman WP, de Bruijn E, Rosa F, Plasterk RH, Wilson SW (2007) MicroRNAs show a wide diversity of expression profiles in the developing and mature central nervous system. *Genome biology* 8:R173.
- Kawahara H, Imai T, Okano H (2012) MicroRNAs in Neural Stem Cells and Neurogenesis. *Frontiers in neuroscience* 6:30.
- Kawase-Koga Y, Low R, Otaegi G, Pollock A, Deng H, Eisenhaber F, Maurer-Stroh S, Sun T (2010) RNAase-III enzyme Dicer maintains signaling pathways for differentiation and survival in mouse cortical neural stem cells. *J Cell Sci* 123:586-594.
- Kim AS, Lowenstein DH, Pleasure SJ (2001) Wnt receptors and Wnt inhibitors are expressed in gradients in the developing telencephalon. *Mech Dev* 103:167-172.
- Kim J, Lauderdale JD (2006) Analysis of Pax6 expression using a BAC transgene reveals the presence of a paired-less isoform of Pax6 in the eye and olfactory bulb. *Dev Biol* 292:486-505.
- Kim J, Inoue K, Ishii J, Vanti WB, Voronov SV, Murchison E, Hannon G, Abeliovich A (2007) A MicroRNA feedback circuit in midbrain dopamine neurons. *Science* 317:1220-1224.
- Kim VN, Han J, Siomi MC (2009) Biogenesis of small RNAs in animals. *Nat Rev Mol Cell Biol* 10:126-139.

- Knoepfler PS, Kamps MP (1997) The Pbx family of proteins is strongly upregulated by a post-transcriptional mechanism during retinoic acid-induced differentiation of P19 embryonal carcinoma cells. *Mech Dev* 63:5-14.
- Kohwi M, Osumi N, Rubenstein JL, Alvarez-Buylla A (2005) Pax6 is required for making specific subpopulations of granule and periglomerular neurons in the olfactory bulb. *J Neurosci* 25:6997-7003.
- Kohwi M, Petryniak MA, Long JE, Ekker M, Obata K, Yanagawa Y, Rubenstein JL, Alvarez-Buylla A (2007) A subpopulation of olfactory bulb GABAergic interneurons is derived from Emx1- and Dlx5/6-expressing progenitors. *J Neurosci* 27:6878-6891.
- Konno D, Shioi G, Shitamukai A, Mori A, Kiyonari H, Miyata T, Matsuzaki F (2008) Neuroepithelial progenitors undergo LGN-dependent planar divisions to maintain self-renewability during mammalian neurogenesis. *Nat Cell Biol* 10:93-101.
- Kosaka K, Aika Y, Toida K, Heizmann CW, Hunziker W, Jacobowitz DM, Nagatsu I, Streit P, Visser TJ, Kosaka T (1995) Chemically defined neuron groups and their subpopulations in the glomerular layer of the rat main olfactory bulb. *Neurosci Res* 23:73-88.
- Kowalczyk T, Pontious A, Englund C, Daza RA, Bedogni F, Hodge R, Attardo A, Bell C, Huttner WB, Hevner RF (2009) Intermediate neuronal progenitors (basal progenitors) produce pyramidal-projection neurons for all layers of cerebral cortex. *Cereb Cortex* 19:2439-2450.
- Kozmik Z (2005) Pax genes in eye development and evolution. *Current opinion in genetics & development* 15:430-438.
- Kozmik Z, Czerny T, Busslinger M (1997) Alternatively spliced insertions in the paired domain restrict the DNA sequence specificity of Pax6 and Pax8. *Embo J* 16:6793-6803.
- Krichevsky AM, Sonntag KC, Isacson O, Kosik KS (2006) Specific microRNAs modulate embryonic stem cell-derived neurogenesis. *STEM CELLS* 24:857-864.
- Kriegstein A, Alvarez-Buylla A (2009) The glial nature of embryonic and adult neural stem cells. *Annu Rev Neurosci* 32:149-184.
- Kroll TT, O'Leary DD (2005) Ventralized dorsal telencephalic progenitors in Pax6 mutant mice generate GABA interneurons of a lateral ganglionic eminence fate. *Proc Natl Acad Sci U S A* 102:7374-7379.
- Krubitzer L, Kaas J (2005) The evolution of the neocortex in mammals: how is phenotypic diversity generated? *Curr Opin Neurobiol* 15:444-453.
- Kuhl M, Sheldahl LC, Park M, Miller JR, Moon RT (2000) The Wnt/Ca2+ pathway: a new vertebrate Wnt signaling pathway takes shape. *Trends in genetics : TIG* 16:279-283.
- Kuwahara A, Hirabayashi Y, Knoepfler PS, Taketo MM, Sakai J, Kodama T, Gotoh Y (2010) Wnt signaling and its downstream target N-myc regulate basal progenitors in the developing neocortex. *Development* 137:1035-1044.
- Lau P, Hudson LD (2010) MicroRNAs in Neural Cell Differentiation. *Brain Res* 1338: 14-19.
- Lau P, Verrier JD, Nielsen JA, Johnson KR, Notterpek L, Hudson LD (2008) Identification of dynamically regulated microRNA and mRNA networks in developing oligodendrocytes. *J Neurosci* 28:11720-11730.
- Lee Y, Kim M, Han J, Yeom KH, Lee S, Baek SH, Kim VN (2004) MicroRNA genes are transcribed by RNA polymerase II. *Embo J* 23:4051-4060.
- Li X, Jin P (2010) Roles of small regulatory RNAs in determining neuronal identity. *Nat Rev Neurosci* 11:329-338.

## References

---

- Ling YH, Tornos C, Perez-Soler R (1998) Phosphorylation of Bcl-2 is a marker of M phase events and not a determinant of apoptosis. *J Biol Chem* 273:18984-18991.
- Liu J, Carmell MA, Rivas FV, Marsden CG, Thomson JM, Song JJ, Hammond SM, Joshua-Tor L, Hannon GJ (2004) Argonaute2 is the catalytic engine of mammalian RNAi. *Science* 305:1437-1441.
- Lopez-Mascaraque L, de Castro F (2002) The olfactory bulb as an independent developmental domain. *Cell Death Differ* 9:1279-1286.
- Lopez-Mascaraque L, Garcia C, Valverde F, de Carlos JA (1998) Central olfactory structures in Pax-6 mutant mice. *Annals of the New York Academy of Sciences* 855:83-94.
- Lopez-Mascaraque L, Garcia C, Blanchart A, De Carlos JA (2005) Olfactory epithelium influences the orientation of mitral cell dendrites during development. *Dev Dyn* 232:325-335.
- Lui JH, Hansen DV, Kriegstein AR (2011) Development and evolution of the human neocortex. *Cell* 146:18-36.
- Lumsden A, Krumlauf R (1996) Patterning the vertebrate neuraxis. *Science* 274:1109-1115.
- Lyden D, Young AZ, Zagzag D, Yan W, Gerald W, O'Reilly R, Bader BL, Hynes RO, Zhuang Y, Manova K, Benezra R (1999) Id1 and Id3 are required for neurogenesis, angiogenesis and vascularization of tumour xenografts. *Nature* 401:670-677.
- Mac Fhearraigh S, Mc Gee MM (2011) Cyclin B1 interacts with the BH3-only protein Bim and mediates its phosphorylation by Cdk1 during mitosis. *Cell Cycle* 10:3886-3896.
- Malatesta P, Hartfuss E, Gotz M (2000) Isolation of radial glial cells by fluorescent-activated cell sorting reveals a neuronal lineage. *Development* 127:5253 - 5263.
- Malatesta P, Hack MA, Hartfuss E, Kettenmann H, Klinkert W, Kirchhoff F, Götz M (2003a) Neuronal or Glial Progeny: Regional Differences in Radial Glia Fate. *Neuron* 37:751-764.
- Malatesta P, Hack MA, Hartfuss E, Kettenmann H, Klinkert W, Kirchhoff F, Gotz M (2003b) Neuronal or glial progeny: regional differences in radial glia fate. *Neuron* 37:751-764.
- Mangold O (1993) Ueber die Induktionsfaehigkeit der verschiedenen Bezirke der Neurula von Urodelen. *Naturwissenschaften* 21: 716-766.
- Manuel M, Georgala PA, Carr CB, Chanas S, Kleinjan DA, Martynoga B, Mason JO, Molinek M, Pinson J, Pratt T, Quinn JC, Simpson TI, Tyas DA, van Heyningen V, West JD, Price DJ (2007) Controlled overexpression of Pax6 in vivo negatively autoregulates the Pax6 locus, causing cell-autonomous defects of late cortical progenitor proliferation with little effect on cortical arealization. *Development* 134:545-555.
- Marquardt T, Ashery-Padan R, Andrejewski N, Scardigli R, Guillemot F, Gruss P (2001) Pax6 is required for the multipotent state of retinal progenitor cells. *Cell* 105:43-55.
- Marson A, Levine SS, Cole MF, Frampton GM, Brambrink T, Johnstone S, Guenther MG, Johnston WK, Wernig M, Newman J, Calabrese JM, Dennis LM, Volkert TL, Gupta S, Love J, Hannett N, Sharp PA, Bartel DP, Jaenisch R, Young RA (2008) Connecting microRNA genes to the core transcriptional regulatory circuitry of embryonic stem cells. *Cell* 134:521-533.
- Martinez J, Tuschl T (2004) RISC is a 5' phosphomonoester-producing RNA endonuclease. *Genes Dev* 18:975-980.
- Matsuo T, Osumi-Yamashita N, Noji S, Ohuchi H, Koyama E, Myokai F, Matsuo N, Taniguchi S, Doi H, Iseki S, et al. (1993) A mutation in the Pax-6 gene in rat small eye is associated with impaired migration of midbrain crest cells. *Nat Genet* 3:299-304.

- McConnell SK, Kaznowski CE (1991) Cell cycle dependence of laminar determination in developing neocortex. *Science* 254:282-285.
- Melton KR, Iulianella A, Trainor PA (2004) Gene expression and regulation of hindbrain and spinal cord development. *Frontiers in bioscience : a journal and virtual library* 9:117-138.
- Mikkola I, Bruun JA, Holm T, Johansen T (2001) Superactivation of Pax6-mediated transactivation from paired domain-binding sites by dna-independent recruitment of different homeodomain proteins. *J Biol Chem* 276:4109-4118.
- Mishra R, Gorlov IP, Chao LY, Singh S, Saunders GF (2002) PAX6, paired domain influences sequence recognition by the homeodomain. *J Biol Chem* 277:49488-49494.
- Misson JP, Austin CP, Takahashi T, Cepko CL, Caviness VS, Jr. (1991) The alignment of migrating neural cells in relation to the murine neopallial radial glial fiber system. *Cereb Cortex* 1:221-229.
- Miyata T, Kawaguchi A, Okano H, Ogawa M (2001) Asymmetric inheritance of radial glial fibers by cortical neurons. *Neuron* 31:727-741.
- Miyata T, Kawaguchi A, Saito K, Kawano M, Muto T, Ogawa M (2004) Asymmetric production of surface-dividing and non-surface-dividing cortical progenitor cells. *Development* 131:3133-3145.
- Molyneaux BJ, Arlotta P, Menezes JR, Macklis JD (2007) Neuronal subtype specification in the cerebral cortex. *Nat Rev Neurosci* 8:427-437.
- Mori T, Buffo A, Gotz M (2005) The novel roles of glial cells revisited: the contribution of radial glia and astrocytes to neurogenesis. *Current topics in developmental biology* 69:67-99.
- Mukherji S, Ebert MS, Zheng GX, Tsang JS, Sharp PA, van Oudenaarden A (2011) MicroRNAs can generate thresholds in target gene expression. *Nat Genet* 43:854-859.
- Munji RN, Choe Y, Li G, Siegenthaler JA, Pleasure SJ (2011) Wnt signaling regulates neuronal differentiation of cortical intermediate progenitors. *J Neurosci* 31:1676-1687.
- Murchison EP, Partridge JF, Tam OH, Cheloufi S, Hannon GJ (2005) Characterization of Dicer-deficient murine embryonic stem cells. *Proc Natl Acad Sci U S A* 102:12135-12140.
- Murciano A, Zamora J, Lopez-Sanchez J, Frade JM (2002) Interkinetic nuclear movement may provide spatial clues to the regulation of neurogenesis. *Mol Cell Neurosci* 21:285-300.
- Muzio L, Mallamaci A (2003) Emx1, emx2 and pax6 in specification, regionalization and arealization of the cerebral cortex. *Cereb Cortex* 13:641-647.
- Muzio L, DiBenedetto B, Stoykova A, Boncinelli E, Gruss P, Mallamaci A (2002a) Emx2 and Pax6 control regionalization of the pre-neuronogenic cortical primordium. *Cereb Cortex* 12:129-139.
- Muzio L, DiBenedetto B, Stoykova A, Boncinelli E, Gruss P, Mallamaci A (2002b) Conversion of cerebral cortex into basal ganglia in Emx2(-/-) Pax6(Sey/Sey) double-mutant mice. *Nat Neurosci* 5:737-745.
- Nakamura O, Toivonen S (1978) Organizer: A Milestone of a Half Century from Spemann. Elsevier / North-Holland Biomedical, Amsterdam.
- Napoli JL (1999) Interactions of retinoid binding proteins and enzymes in retinoid metabolism. *Biochim Biophys Acta* 1440:139-162.

- Neyt C, Welch M, Langston A, Kohtz J, Fishell G (1997) A short-range signal restricts cell movement between telencephalic proliferative zones. *J Neurosci* 17:9194-9203.
- Nieto M, Schuurmans C, Britz O, Guillemot F (2001) Neural bHLH genes control the neuronal versus glial fate decision in cortical progenitors. *Neuron* 29:401-413.
- Nieto M, Monuki ES, Tang H, Imitola J, Haubst N, Khoury SJ, Cunningham J, Gotz M, Walsh CA (2004) Expression of Cux-1 and Cux-2 in the subventricular zone and upper layers II-IV of the cerebral cortex. *J Comp Neurol* 479:168-180.
- Niimi T, Seimiya M, Kloter U, Flister S, Gehring WJ (1999) Direct regulatory interaction of the eyeless protein with an eye-specific enhancer in the sine oculis gene during eye induction in *Drosophila*. *Development* 126:2253-2260.
- Nikoletopoulou V, Plachta N, Allen ND, Pinto L, Gotz M, Barde YA (2007) Neurotrophin Receptor-Mediated Death of Misspecified Neurons Generated from Embryonic Stem Cells Lacking Pax6. *Cell Stem Cell* 1:529-540.
- Ninkovic J, Pinto L, Petricca S, Lepier A, Sun J, Rieger MA, Schroeder T, Cvekl A, Favor J, Gotz M (2010) The transcription factor Pax6 regulates survival of dopaminergic olfactory bulb neurons via crystallin alphaA. *Neuron* 68:682-694.
- Noctor S, Flint A, Weissman T, Dammerman R, Kriegstein A (2001a) Neurons derived from radial glial cells establish radial units in neocortex. *Nature* 409:714 - 720.
- Noctor SC, Martinez-Cerdeno V, Ivic L, Kriegstein AR (2004) Cortical neurons arise in symmetric and asymmetric division zones and migrate through specific phases. *Nat Neurosci* 7:136-144.
- Noctor SC, Flint AC, Weissman TA, Dammerman RS, Kriegstein AR (2001b) Neurons derived from radial glial cells establish radial units in neocortex. *Nature* 409:714-720.
- Nomura T, Osumi N (2004) Misrouting of mitral cell progenitors in the Pax6/small eye rat telencephalon. *Development* 131:787-796.
- Nomura T, Haba H, Osumi N (2007) Role of a transcription factor Pax6 in the developing vertebrate olfactory system. *Dev Growth Differ* 49:683-690.
- Nomura T, Holmberg J, Frisen J, Osumi N (2006) Pax6-dependent boundary defines alignment of migrating olfactory cortex neurons via the repulsive activity of ephrin A5. *Development* 133:1335-1345.
- Ogawa M, Miyata T, Nakajima K, Yagyu K, Seike M, Ikenaka K, Yamamoto H, Mikoshiba K (1995) The reeler gene-associated antigen on Cajal-Retzius neurons is a crucial molecule for laminar organization of cortical neurons. *Neuron* 14:899-912.
- Okamura K, Hagen JW, Duan H, Tyler DM, Lai EC (2007) The mirtron pathway generates microRNA-class regulatory RNAs in *Drosophila*. *Cell* 130:89-100.
- Osumi N, Shinohara H, Numayama-Tsuruta K, Maekawa M (2008) Concise review: Pax6 transcription factor contributes to both embryonic and adult neurogenesis as a multifunctional regulator. *Stem Cells* 26:1663-1672.
- Ozsolak F, Poling LL, Wang Z, Liu H, Liu XS, Roeder RG, Zhang X, Song JS, Fisher DE (2008) Chromatin structure analyses identify miRNA promoters. *Genes Dev* 22:3172-3183.
- Panzanelli P, Fritschy JM, Yanagawa Y, Obata K, Sassoe-Pognetto M (2007) GABAergic phenotype of periglomerular cells in the rodent olfactory bulb. *J Comp Neurol* 502:990-1002.

- Park D, Xiang AP, Zhang L, Mao FF, Walton NM, Choi SS, Lahn BT (2009) The radial glia antibody RC2 recognizes a protein encoded by Nestin. *Biochem Biophys Res Commun* 382:588-592.
- Parras CM, Schuurmans C, Scardigli R, Kim J, Anderson DJ, Guillemot F (2002) Divergent functions of the proneural genes Mash1 and Ngn2 in the specification of neuronal subtype identity. *Genes Dev* 16:324-338.
- Parrish-Aungst S, Shipley MT, Erdelyi F, Szabo G, Puche AC (2007) Quantitative analysis of neuronal diversity in the mouse olfactory bulb. *J Comp Neurol* 501:825-836.
- Perez-Garcia CG, Tissir F, Goffinet AM, Meyer G (2004) Reelin receptors in developing laminated brain structures of mouse and human. *Eur J Neurosci* 20:2827-2832.
- Piatigorsky J (1998) Multifunctional lens crystallins and corneal enzymes. More than meets the eye. *Annals of the New York Academy of Sciences* 842:7-15.
- Pinon MC, Tuoc TC, Ashery-Padan R, Molnar Z, Stoykova A (2008) Altered molecular regionalization and normal thalamocortical connections in cortex-specific Pax6 knock-out mice. *J Neurosci* 28:8724-8734.
- Pinto L, Gotz M (2007) Radial glial cell heterogeneity--the source of diverse progeny in the CNS. *Prog Neurobiol* 83:2-23.
- Pinto L, Drechsel D, Schmid MT, Ninkovic J, Irmeler M, Brill MS, Restani L, Gianfranceschi L, Cerri C, Weber SN, Tarabykin V, Baer K, Guillemot F, Beckers J, Zecevic N, Dehay C, Caleo M, Schorle H, Gotz M (2009) AP2gamma regulates basal progenitor fate in a region- and layer-specific manner in the developing cortex. *Nat Neurosci* 12:1229-1237.
- Planque N, Leconte L, Coquelle FM, Benkhalifa S, Martin P, Felder-Schmittbuhl MP, Saule S (2001) Interaction of Maf transcription factors with Pax-6 results in synergistic activation of the glucagon promoter. *J Biol Chem* 276:35751-35760.
- Pollard SM, Conti L, Sun Y, Goffredo D, Smith A (2006) Adherent neural stem (NS) cells from fetal and adult forebrain. *Cereb Cortex* 16 Suppl 1:i112-120.
- Pontious A, Kowalczyk T, Englund C, Hevner RF (2008) Role of intermediate progenitor cells in cerebral cortex development. *Dev Neurosci* 30:24-32.
- Pourebahim R, Van Dam K, Bauters M, De Wever I, Sciot R, Cassiman JJ, Tejpar S (2007) ZIC1 gene expression is controlled by DNA and histone methylation in mesenchymal proliferations. *FEBS Lett* 581:5122-5126.
- Puschel AW, Gruss P, Westerfield M (1992) Sequence and expression pattern of pax-6 are highly conserved between zebrafish and mice. *Development* 114:643-651.
- Putcha GV, Moulder KL, Golden JP, Bouillet P, Adams JA, Strasser A, Johnson EM (2001) Induction of BIM, a proapoptotic BH3-only BCL-2 family member, is critical for neuronal apoptosis. *Neuron* 29:615-628.
- Qian X, Shen Q, Goderie SK, He W, Capela A, Davis AA, Temple S (2000) Timing of CNS cell generation: a programmed sequence of neuron and glial cell production from isolated murine cortical stem cells. *Neuron* 28:69-80.
- Quinn JC, Molinek M, Martynoga BS, Zaki PA, Faedo A, Bulfone A, Hevner RF, West JD, Price DJ (2007) Pax6 controls cerebral cortical cell number by regulating exit from the cell cycle and specifies cortical cell identity by a cell autonomous mechanism. *Dev Biol* 302:50-65.
- Rainer J, Sanchez-Cabo F, Stocker G, Sturn A, Trajanoski Z (2006) CARMAweb: comprehensive R- and bioconductor-based web service for microarray data analysis. *Nucleic Acids Res* 34:W498-503.

## References

---

- Ramaesh T, Williams SE, Paul C, Ramaesh K, Dhillon B, West JD (2009) Histopathological characterisation of effects of the mouse Pax6Leca4 missense mutation on eye development. *Experimental Eye Research* 89:263-273.
- Rash BG, Grove EA (2007) Patterning the dorsal telencephalon: a role for sonic hedgehog? *J Neurosci* 27:11595-11603.
- Rubenstein JL, Shimamura K, Martinez S, Puelles L (1998) Regionalization of the prosencephalic neural plate. *Annu Rev Neurosci* 21:445-477.
- Rubenstein JL, Anderson S, Shi L, Miyashita-Lin E, Bulfone A, Hevner R (1999) Genetic control of cortical regionalization and connectivity. *Cereb Cortex* 9:524-532.
- Ruberte E, Friederich V, Chambon P, Morriss-Kay G (1993) Retinoic acid receptors and cellular retinoid binding proteins. III. Their differential transcript distribution during mouse nervous system development. *Development* 118:267-282.
- Ruby JG, Jan CH, Bartel DP (2007) Intronic microRNA precursors that bypass Drosha processing. *Nature* 448:83-86.
- Ruiz I, Altaba A (1993) Induction and axial patterning of the neural plate: Planar and vertical signals. *J Neurobiol* 24:1276-1304
- Sakurai K, Osumi N (2008) The neurogenesis-controlling factor, Pax6, inhibits proliferation and promotes maturation in murine astrocytes. *J Neurosci* 28:4604-4612.
- Sansom SN, Griffiths DS, Faedo A, Kleinjan DJ, Ruan Y, Smith J, van Heyningen V, Rubenstein JL, Livesey FJ (2009) The level of the transcription factor Pax6 is essential for controlling the balance between neural stem cell self-renewal and neurogenesis. *PLoS Genet* 5:e1000511.
- Sasai Y, DeRobertis EM (1997) Ectodermal patterning in vertebrate embryos. *Dev Biology* 182:5-20.
- Scardigli R, Schuurmans C, Gradwohl G, Guillemot F (2001) Crossregulation between Neurogenin2 and pathways specifying neuronal identity in the spinal cord. *Neuron* 31:203-217.
- Scardigli R, Baumer N, Gruss P, Guillemot F, Le Roux I (2003) Direct and concentration-dependent regulation of the proneural gene Neurogenin2 by Pax6. *Development* 130:3269-3281.
- Schaefer A, O'Carroll D, Tan CL, Hillman D, Sugimori M, Llinas R, Greengard P (2007) Cerebellar neurodegeneration in the absence of microRNAs. *The Journal of experimental medicine* 204:1553-1558.
- Schiffmann SN, Bernier B, Goffinet AM (1997) Reelin mRNA expression during mouse brain development. *Eur J Neurosci* 9:1055-1071.
- Schmahl W, Knoedlseder M, Favor J, Davidson D (1993) Defects of neuronal migration and the pathogenesis of cortical malformations are associated with Small eye (Sey) in the mouse, a point mutation at the Pax-6-locus. *Acta Neuropathol* 86:126-135.
- Schuurmans C, Guillemot F (2002) Molecular mechanisms underlying cell fate specification in the developing telencephalon. *Curr Opin Neurobiol* 12:26-34.
- Schuurmans C, Armant O, Nieto M, Stenman JM, Britz O, Klenin N, Brown C, Langevin LM, Seibt J, Tang H, Cunningham JM, Dyck R, Walsh C, Campbell K, Polleux F, Guillemot F (2004) Sequential phases of cortical specification involve Neurogenin-dependent and -independent pathways. *Embo J* 23:2892-2902.

- Schwarz DS, Hutvagner G, Du T, Xu Z, Aronin N, Zamore PD (2003) Asymmetry in the assembly of the RNAi enzyme complex. *Cell* 115:199-208.
- Sempere LF, Freemantle S, Pitha-Rowe I, Moss E, Dmitrovsky E, Ambros V (2004) Expression profiling of mammalian microRNAs uncovers a subset of brain-expressed microRNAs with possible roles in murine and human neuronal differentiation. *Genome biology* 5:R13.
- Sessa A, Mao CA, Hadjantonakis AK, Klein WH, Broccoli V (2008) Tbr2 directs conversion of radial glia into basal precursors and guides neuronal amplification by indirect neurogenesis in the developing neocortex. *Neuron* 60:56-69.
- Shen Q, Wang Y, Dimos JT, Fasano CA, Phoenix TN, Lemischka IR, Ivanova NB, Stifani S, Morrisey EE, Temple S (2006) The timing of cortical neurogenesis is encoded within lineages of individual progenitor cells. *Nat Neurosci* 9:743-751.
- Sheng G, Thouvenot E, Schmucker D, Wilson DS, Desplan C (1997) Direct regulation of rhodopsin 1 by Pax-6/eyeless in *Drosophila*: evidence for a conserved function in photoreceptors. *Genes Dev* 11:1122-1131.
- Shi Y, Zhao X, Hsieh J, Wichterle H, Impey S, Banerjee S, Neveu P, Kosik KS (2010) MicroRNA regulation of neural stem cells and neurogenesis. *J Neurosci* 30:14931-14936.
- Shibata M, Nakao H, Kiyonari H, Abe T, Aizawa S (2011) MicroRNA-9 regulates neurogenesis in mouse telencephalon by targeting multiple transcription factors. *J Neurosci* 31:3407-3422.
- Shimamura K, Rubenstein JL (1997) Inductive interactions direct early regionalization of the mouse forebrain. *Development* 124:2709-2718.
- Shimamura K, Martinez S, Puelles L, Rubenstein JL (1997) Patterns of gene expression in the neural plate and neural tube subdivide the embryonic forebrain into transverse and longitudinal domains. *Dev Neurosci* 19:88-96.
- Shimazaki T, Arsenijevic Y, Ryan AK, Rosenfeld MG, Weiss S (1999) A role for the POU-III transcription factor Brn-4 in the regulation of striatal neuron precursor differentiation. *Embo J* 18:444-456.
- Shimizu T, Nakazawa M, Kani S, Bae YK, Kageyama R, Hibi M (2010) Zinc finger genes Fezf1 and Fezf2 control neuronal differentiation by repressing Hes5 expression in the forebrain. *Development* 137:1875-1885.
- Shimoda Y, Tajima Y, Osanai T, Katsume A, Kohara M, Kudo T, Narimatsu H, Takashima N, Ishii Y, Nakamura S, Osumi N, Sanai Y (2002) Pax6 controls the expression of Lewis x epitope in the embryonic forebrain by regulating alpha 1,3-fucosyltransferase IX expression. *J Biol Chem* 277:2033-2039.
- Shitamukai A, Konno D, Matsuzaki F (2011) Oblique radial glial divisions in the developing mouse neocortex induce self-renewing progenitors outside the germinal zone that resemble primate outer subventricular zone progenitors. *J Neurosci* 31:3683-3695.
- Shoukimas GM, Hinds JW (1978) The development of the cerebral cortex in the embryonic mouse: an electron microscopic serial section analysis. *J Comp Neurol* 179:795-830.
- Shukla S, Mishra R (2012) Predictions on impact of missense mutations on structure function relationship of PAX6 and its alternatively spliced isoform PAX6(5a). *Interdisciplinary sciences, computational life sciences* 4:54-73.
- Siegenthaler JA, Ashique AM, Zarbalis K, Patterson KP, Hecht JH, Kane MA, Folias AE, Choe Y, May SR, Kume T, Napoli JL, Peterson AS, Pleasure SJ (2009) Retinoic acid from the meninges regulates cortical neuron generation. *Cell* 139:597-609.

## References

---

- Singh S, Stellrecht CM, Tang HK, Saunders GF (2000) Modulation of PAX6 homeodomain function by the paired domain. *J Biol Chem* 275:17306-17313.
- Sinkkonen L, Hugenschmidt T, Berninger P, Gaidatzis D, Mohn F, Artus-Revel CG, Zavolan M, Svoboda P, Filipowicz W (2008) MicroRNAs control de novo DNA methylation through regulation of transcriptional repressors in mouse embryonic stem cells. *Nat Struct Mol Biol* 15:259-267.
- Smith D, Wagner E, Koul O, McCaffery P, Drager UC (2001) Retinoic acid synthesis for the developing telencephalon. *Cereb Cortex* 11:894-905.
- Spemann H, Mangold H (1924) Ueber die Induktion Embryonalanlagen durch Implantation artfremder Organisatoren. *W Roux Arch f Entw d Organism u mikrosk Anat* 100: 599-638.
- Stancik EK, Navarro-Quiroga I, Sellke R, Haydar TF (2010) Heterogeneity in ventricular zone neural precursors contributes to neuronal fate diversity in the postnatal neocortex. *J Neurosci* 30:7028-7036.
- Stark A, Brennecke J, Bushati N, Russell RB, Cohen SM (2005) Animal MicroRNAs confer robustness to gene expression and have a significant impact on 3'UTR evolution. *Cell* 123:1133-1146.
- Stoykova A, Gruss P (1994) Roles of Pax-genes in developing and adult brain as suggested by expression patterns. *J Neurosci* 14:1395-1412.
- Stoykova A, Fritsch R, Walther C, Gruss P (1996) Forebrain patterning defects in Small eye mutant mice. *Development* 122:3453-3465.
- Stoykova A, Gotz M, Gruss P, Price J (1997) Pax6-dependent regulation of adhesive patterning, R-cadherin expression and boundary formation in developing forebrain. *Development* 124:3765-3777.
- Stoykova A, Treichel D, Hallonet M, Gruss P (2000) Pax6 modulates the dorsoventral patterning of the mammalian telencephalon. *J Neurosci* 20:8042-8050.
- Stubbs D, DeProto J, Nie K, Englund C, Mahmud I, Hevner R, Molnar Z (2009) Neurovascular congruence during cerebral cortical development. *Cereb Cortex* 19 Suppl 1:i32-41.
- Takahashi H, Liu FC (2006) Genetic patterning of the mammalian telencephalon by morphogenetic molecules and transcription factors. *Birth defects research Part C, Embryo today : reviews* 78:256-266.
- Takahashi T, Misson JP, Caviness VS, Jr. (1990) Glial process elongation and branching in the developing murine neocortex: a qualitative and quantitative immunohistochemical analysis. *J Comp Neurol* 302:15-28.
- Takahashi T, Nowakowski RS, Caviness VS, Jr. (1996) Interkinetic and migratory behavior of a cohort of neocortical neurons arising in the early embryonic murine cerebral wall. *J Neurosci* 16:5762-5776.
- Tarabykin V, Stoykova A, Usman N, Gruss P (2001) Cortical upper layer neurons derive from the subventricular zone as indicated by Svet1 gene expression. *Development* 128:1983-1993.
- Team RDC (2006) R: A language and environment for statistical computing, Available at R Foundation for Statistical Computing, Vienne, Austria.
- Teissier A, Griveau A, Vigier L, Piolot T, Borello U, Pierani A (2010) A novel transient glutamatergic population migrating from the pallial-subpallial boundary contributes to neocortical development. *J Neurosci* 30:10563-10574.

- Thaung C, West K, Clark BJ, McKie L, Morgan JE, Arnold K, Nolan PM, Peters J, Hunter AJ, Brown SDM, Jackson IJ, Cross SH (2002) Novel ENU-induced eye mutations in the mouse: models for human eye disease. *Human Molecular Genetics* 11:755-767.
- Thein KH, Kleylein-Sohn J, Nigg EA, Gruneberg U (2007) Astrin is required for the maintenance of sister chromatid cohesion and centrosome integrity. *J Cell Biol* 178:345-354.
- Tiberi L, Vanderhaeghen P, van den Aemele J (2012) Cortical neurogenesis and morphogens: diversity of cues, sources and functions. *Curr Opin Cell Biol* 24:269-276.
- Toida K, Kosaka K, Aika Y, Kosaka T (2000) Chemically defined neuron groups and their subpopulations in the glomerular layer of the rat main olfactory bulb--IV. Intraglomerular synapses of tyrosine hydroxylase-immunoreactive neurons. *Neuroscience* 101:11-17.
- Toresson H, Campbell K (2001) A role for Gsh1 in the developing striatum and olfactory bulb of Gsh2 mutant mice. *Development* 128:4769-4780.
- Toresson H, Potter SS, Campbell K (2000) Genetic control of dorsal-ventral identity in the telencephalon: opposing roles for Pax6 and Gsh2. *Development* 127:4361-4371.
- Tuoc TC, Radyushkin K, Tonchev AB, Pinon MC, Ashery-Padan R, Molnar Z, Davidoff MS, Stoykova A (2009) Selective cortical layering abnormalities and behavioral deficits in cortex-specific Pax6 knock-out mice. *J Neurosci* 29:8335-8349.
- Tzoulaki I, White IM, Hanson IM (2005) PAX6 mutations: genotype-phenotype correlations. *BMC genetics* 6:27.
- Uribe RA, Gross JM (2010) Id2a influences neuron and glia formation in the zebrafish retina by modulating retinoblast cell cycle kinetics. *Development* 137:3763-3774.
- Ventura RE, Goldman JE (2007) Dorsal radial glia generate olfactory bulb interneurons in the postnatal murine brain. *J Neurosci* 27:4297-4302.
- Virchow R (1846) Ueber das granulirte Ansehen der Wanderungen der Gehirnventrikel. *Allg Z Psychiatr* 3:424-450.
- Visel A, Carson J, Oldekamp J, Warnecke M, Jakubcakova V, Zhou X, Shaw CA, Alvarez-Bolado G, Eichele G (2007) Regulatory pathway analysis by high-throughput in situ hybridization. *PLoS Genet* 3:1867-1883.
- von Holst A, Egbers U, Prochiantz A, Faissner A (2007) Neural stem/progenitor cells express 20 tenascin C isoforms that are differentially regulated by Pax6. *J Biol Chem* 282:9172-9181.
- Walther C, Gruss P (1991) Pax-6, a murine paired box gene, is expressed in the developing CNS. *Development* 113:1435-1449.
- Walther C, Guenet JL, Simon D, Deutsch U, Jostes B, Goulding MD, Plachov D, Balling R, Gruss P (1991) Pax: a murine multigene family of paired box-containing genes. *Genomics* 11:424-434.
- Wang B, Waclaw RR, Allen ZJ, 2nd, Guillemot F, Campbell K (2009a) Ascl1 is a required downstream effector of Gsx gene function in the embryonic mouse telencephalon. *Neural Dev* 4:5.
- Wang J, Huang W, Wu Y, Hou J, Nie Y, Gu H, Li J, Hu S, Zhang H (2012) MicroRNA-193 Promotes Proliferation Effects for Bone Mesenchymal Stem Cells After Low-Level Laser Irradiation Treatment Through Inhibitor of Growth Family, Member 5. *Stem Cells Dev*.
- Wang L, Bluske KK, Dickel LK, Nakagawa Y (2011a) Basal progenitor cells in the embryonic mouse thalamus - their molecular characterization and the role of neurogenins and Pax6. *Neural Dev* 6:35.

## References

---

- Wang S, Aurora AB, Johnson BA, Qi X, McAnally J, Hill JA, Richardson JA, Bassel-Duby R, Olson EN (2008a) The endothelial-specific microRNA miR-126 governs vascular integrity and angiogenesis. *Dev Cell* 15:261-271.
- Wang SH, Bian CJ, Zhao CH (2008b) [Expression and function of microRNA in embryonic stem cell]. *Yi chuan = Hereditas / Zhongguo yi chuan xue hui bian ji* 30:1545-1549.
- Wang X, Tsai JW, LaMonica B, Kriegstein AR (2011b) A new subtype of progenitor cell in the mouse embryonic neocortex. *Nat Neurosci* 14:555-561.
- Wang Y, Keys DN, Au-Young JK, Chen C (2009b) MicroRNAs in embryonic stem cells. *Journal of cellular physiology* 218:251-255.
- Wang Y, Medvid R, Melton C, Jaenisch R, Blueloch R (2007) DGCR8 is essential for microRNA biogenesis and silencing of embryonic stem cell self-renewal. *Nat Genet* 39:380-385.
- Wang Y, Baskerville S, Shenoy A, Babiarz JE, Baehner L, Blueloch R (2008c) Embryonic stem cell-specific microRNAs regulate the G1-S transition and promote rapid proliferation. *Nat Genet* 40:1478-1483.
- Warren N, Price DJ (1997) Roles of Pax-6 in murine diencephalic development. *Development* 124:1573-1582.
- Warren N, Caric D, Pratt T, Clausen JA, Asavaritikrai P, Mason JO, Hill RE, Price DJ (1999) The transcription factor, Pax6, is required for cell proliferation and differentiation in the developing cerebral cortex. *Cereb Cortex* 9:627-635.
- Watabe Y, Baba Y, Nakauchi H, Mizota A, Watanabe S (2011) The role of Zic family zinc finger transcription factors in the proliferation and differentiation of retinal progenitor cells. *Biochem Biophys Res Commun* 415:42-47.
- Wichterle H, Turnbull DH, Nery S, Fishell G, Alvarez-Buylla A (2001) In utero fate mapping reveals distinct migratory pathways and fates of neurons born in the mammalian basal forebrain. *Development* 128:3759-3771.
- Willaime-Morawek S, Seaberg RM, Batista C, Labbe E, Attisano L, Gorski JA, Jones KR, Kam A, Morshead CM, van der Kooy D (2006) Embryonic cortical neural stem cells migrate ventrally and persist as postnatal striatal stem cells. *J Cell Biol* 175:159-168.
- Wilson D, Sheng G, Lecuit T, Dostatni N, Desplan C (1993) Cooperative dimerization of paired class homeo domains on DNA. *Genes Dev* 7:2120-2134.
- Wilson PA, Hemmati-Brivanlou A (1997) Vertebrate neural induction: Inducers, inhibitors and a new synthesis. *Neuron* 18:699-710.
- Wodarz A, Nusse R (1998) Mechanisms of Wnt signaling in development. *Annu Rev Cell Dev Biol* 14:59-88.
- Wolf LV, Yang Y, Wang J, Xie Q, Braunger B, Tamm ER, Zavadil J, Cvekl A (2009) Identification of pax6-dependent gene regulatory networks in the mouse lens. *PLoS ONE* 4:e4159.
- Wonders CP, Anderson SA (2006) The origin and specification of cortical interneurons. *Nat Rev Neurosci* 7:687-696.
- Woodhead GJ, Mutch CA, Olson EC, Chenn A (2006) Cell-autonomous beta-catenin signaling regulates cortical precursor proliferation. *J Neurosci* 26:12620-12630.
- Wu SX, Goebbels S, Nakamura K, Kometani K, Minato N, Kaneko T, Nave KA, Tamamaki N (2005) Pyramidal neurons of upper cortical layers generated by NEX-positive progenitor cells in the subventricular zone. *Proc Natl Acad Sci U S A* 102:17172-17177.

- Xie Q, Cvekl A (2011) The Orchestration of Mammalian Tissue Morphogenesis through a Series of Coherent Feed-forward Loops. *J Biol Chem* 286:43259-43271.
- Xu HE, Rould MA, Xu W, Epstein JA, Maas RL, Pabo CO (1999) Crystal structure of the human Pax6 paired domain-DNA complex reveals specific roles for the linker region and carboxy-terminal subdomain in DNA binding. *Genes Dev* 13:1263-1275.
- Yamaguchi Y, Sawada J, Yamada M, Handa H, Azuma N (1997) Autoregulation of Pax6 transcriptional activation by two distinct DNA-binding subdomains of the paired domain. *Genes to cells : devoted to molecular & cellular mechanisms* 2:255-261.
- Yang Z, Song L, Huang C (2009) Gadd45 proteins as critical signal transducers linking NF-kappaB to MAPK cascades. *Current cancer drug targets* 9:915-930.
- Yi R, Qin Y, Macara IG, Cullen BR (2003) Exportin-5 mediates the nuclear export of pre-microRNAs and short hairpin RNAs. *Genes Dev* 17:3011-3016.
- Ying SY, Lin SL (2005) Intronic microRNAs. *Biochem Biophys Res Commun* 326:515-520.
- Young KM, Fogarty M, Kessar N, Richardson WD (2007) Subventricular zone stem cells are heterogeneous with respect to their embryonic origins and neurogenic fates in the adult olfactory bulb. *J Neurosci* 27:8286-8296.
- Yun K, Potter S, Rubenstein JL (2001) Gsh2 and Pax6 play complementary roles in dorsoventral patterning of the mammalian telencephalon. *Development* 128:193-205.
- Zhang Y, Emmons SW (1995) Specification of sense-organ identity by a *Caenorhabditis elegans* Pax-6 homologue. *Nature* 377:55-59.
- Zhao C, Sun G, Li S, Shi Y (2009) A feedback regulatory loop involving microRNA-9 and nuclear receptor TLX in neural stem cell fate determination. *Nat Struct Mol Biol* 16:365-371.
- Zhao X, He X, Han X, Yu Y, Ye F, Chen Y, Hoang T, Xu X, Mi QS, Xin M, Wang F, Appel B, Lu QR (2010) MicroRNA-mediated control of oligodendrocyte differentiation. *Neuron* 65:612-626.
- Zhou CJ, Borello U, Rubenstein JL, Pleasure SJ (2006) Neuronal production and precursor proliferation defects in the neocortex of mice with loss of function in the canonical Wnt signaling pathway. *Neuroscience* 142:1119-1131.
- Zimmer C, Tiveron MC, Bodmer R, Cremer H (2004) Dynamics of Cux2 expression suggests that an early pool of SVZ precursors is fated to become upper cortical layer neurons. *Cereb Cortex* 14:1408-1420.

## 7 Acknowledgments

In the first place, I would like to thank **Magdalena Götz** for giving me the opportunity to work in her lab. I am very grateful for her continuous support within the last years. I thank her for sharing her knowledge - especially around Pax6 – and appreciate her many useful comments and advices on this work. I also would like to thank her for creating a great research environment with numerous visits of other great scientists, the exceptional research retreats every year and especially for the international working environment. To work with so many people from many different countries, has been a real pleasure with heaps of fun, excitement and interesting cultural discussions.

Very special thanks to **Jovica Ninkovic** for his advice, constructive criticism and the plentiful copious discussions around my work. Thank you!

Many thanks to **Andrea Steiner-Mezzadri** and **Timucin Öztürk** for a great deal of technical work, and also **Angelika Waiser** for her ever great technical help with the ESC culture and also thanks to **Emily Violette Baumgart** and **Detlef Franzen**.

I have been fortunate to interact with many awesome colleagues and want to thank all the people from the Götz lab. Many have influenced me greatly and have become very good friends. Especially I want to thank the whole bunch of people working at the Helmholtz, namely **Franziska Weinandy**, **Ruth Beckervordersandforth-Bonk**, **Silvia Cappello**, **Pia Johansson**, **Vidya Ramesh**, **Dilek Colak**, **Maki Asami**, **Stefania Petricca**, **Joana Barbosa**, **Melanie Lerch**, **Efil Bayam**, **Judith Fischer-Sternjak**, **Lana Sirko**, **Rossella Di Giacomo**, **Christian Böhringer**, **Gregor Pilz**, **Sven Falk**, **Ciro Petrone** and **Filippo Calzolari**. Thanks to all of you for the good atmosphere, advices, fruitful discussions and the many precious memories inside and outside the lab along the way; I'll never forget the retreat time we stayed up until the birds started singing. Special thanks also to **Francesca Vigano** for her friendship and **Felipe Ortega de la O** for so many funny “Shakespeare” moments and showing us the wonderful world of “Cacique”.

I would also like to thank **Laure Bally-Cuif** for joining my thesis committees, her great input and copious scientific discussions.

Thanks also go to the lovely **Elsa Melo** and **Donna Thomson** who made administrative life so easy.

I am most thankful to my parents for their support during my studies.

Last but definitely not least, I thank **Ronny Stahl** for staying by me during the happy and hard moments, for your constant scientific support and for much, much more.

**I am truly indebted to all of you for making the Ph.D.-time an unforgettable experience!**

---

**PUBLICATIONS****Part of this work will be published as follows:**

**Walcher T**, Xie Q, Sun J, Öztürk T, Beckers J, Niessing D, Irmeler M, Stoykova A, Cvekl A, Ninkovic J, Götz M. “Molecular mechanisms of coordinating neurogenesis and proliferation – functional dissection of the Paired domain of Pax6” – Manuskript akzeptiert bei Development

Stahl R, **Walcher T**, De Juan Romero C, Irmeler M, Blum R, Borrell V, Götz M. „TRNP1 regulates expansion and folding of the mammalian cerebral cortex by control of radial glial fate“- Manuskript in Revision bei Cell

Xie Q, Yang Y, Huang J, Ninkovic J, **Walcher T**, Wolf L, Vitenzon A, Zheng D, Götz M, Beebe D, Zavadil J and Cvekl A. “Pax6 interactions with chromatin and identification of its novel direct target genes in lens and forebrain” – PLoS One. 2013;8(1):e54507. doi: 10.1371/journal.pone.0054507. Epub 2013 Jan 14

Saulnier A, Keruzore M, De Clercq S, Bar I, Moers V, Magnani D, **Walcher T**, Filippis C, Kricha S, Parlier D, Viviani L, Matson C, Nakagawa Y, Theil T, Götz M, Mallamaci A, Marine J, Zarkower D, Bellefroid E. “The doublesex homolog Dmrt5 is required for the development of the caudomedial cerebral cortex in mammals” – Cereb Cortex. 2012 Aug 23. [Epub ahead of print]

Rose AJ, Diaz MB, Reimann A, Klement J, **Walcher T**, Krones-Herzig A, Strobel O, Werner J, Peters A, Kleyman A, Tuckermann JP, Vegiopoulos A and Herzig S (2011). “Molecular control of systemic bile acid homeostasis by the liver glucocorticoid receptor” Cell Metabolism. 14(1):123-30